A Thesis

entitled

PLANE ELASTO-PLASTIC ANALYSIS OF V-NOTCHED PLATE UNDER BENDING BY BOUNDARY INTEGRAL EQUATION METHOD

by

Walter Rzasnicki

as partial fulfillment of the requirements of
the Doctor of Philosophy Degree in
Engineering Science

The University of Toledo
March 1973

I

An Abstract of

PLANE ELASTO-PLASTIC ANALYSIS OF V-NOTCHED PLATE UNDER BENDING BY BOUNDARY INTEGRAL EQUATION METHOD

Walter Rzasnicki

Submitted in partial fulfillment
of the requirements of the
Doctor of Philosophy Degree in
Engineering Science

The University of Toledo
March 1973

A method of solution is presented, which, when applied to the elasto-plastic analysis of plates having a v-notch on one edge and subjected to pure bending, will produce stress and strain fields in much greater detail than presently available. Application of the boundary integral equation method results in two coupled Fredholm-type integral equations, subject to prescribed boundary conditions. These equations are replaced by a system of simultaneous algebraic equations and solved by a successive approximation method employing Prandtl-Reuss incremental plasticity relations. The method is first applied to number of elasto-static problems and the results compared with available solutions. Good agreement is obtained in all cases. The elasto-plastic analysis provides detailed stress and strain distributions for several cases of plates with various notch angles and notch depths. A strain hardening material is assumed and both plane strain and plane stress conditions are considered. The generalized stress intensity factor K_I^* is introduced. Rice's J integral is calculated and its relation to the generalized stress intensity factor is presented. Notch opening displacements are calculated and, for one case, are compared with the available experimental results showing very good agreement.

II

A Thesis

entitled

Plane Elasto-Plastic Analysis of V-notched Plate Under Bending by Boundary Integral Equation Method

by

Walter Rzasnicki

as partial fulfillment of the requirements of
the Doctor of Philosophy Degree in
Engineering Science

The University of Toledo
March 1973

Acknowledgments

The author is most grateful to Dr. A. Mendelson and Prof. D. D. Raftopoulos of the University of Toledo, his thesis advisors, for their assistance and guidance during the course of this study.

I would also like to express my sincere appreciation to Dr. L. U. Albers for his assistance in developing the computer program and for his valuable advice regarding the numerical procedures.

The help provided by Mr. G. Diedrich in obtaining computerized graphs is gratefully acknowledged.

Very special thanks are due my wife, Eugenia, for help and understanding during my doctoral studies.

Finally, I wish to thank the Lewis Research Center of the National Aeronautics and Space Administration for providing financial support for this work.

Table of Contents

List of Tables

List of Figures

List of Symbols

a	notch depth
a_{ij}, b_{ij}, c_{ij} d_{ij}, e_{ij}, f_{ij}	coefficients in the boundary equations
A	area of cell in the region R
$A_{ij}, B_{ij}, C_{ij}, D_{ij}$ $E_{ij}, F_{ij}, G_{ij}, H_{ij}$ I_{ij}, K_{ij}	coefficients in the stress equations
C, C', C_ε	boundary contours
E	Young's modulus of elasticity
g	function of plastic strain increments
J	value of Rice's contour integral
K_I, K_{II}, K_{III}	stress intensity factor at the notch tip for three characteristic crack opening displacements
K_I^*	generalized stress intensity factor for opening mode crack displacement
ℓ_j, m_j	directional cosines
L	half length of the plate
m	strain hardening parameter
n	order of stress singularity in the vicinity of tip of the notch
$\bar{n}, \bar{s}$	unit vectors normal and tangent to contour C
$P(x,y)$	point on contour C or in region R

$q(\xi,\eta)$	point on contour C
$\tilde{q}$	dimensionless load σ_{max}/σ_0
r	distance between two points having coordinates (x,y) and (ξ,η)
r,θ	polar coordinate directions
R	a planar region bounded by a closed contour C
s	length measured along contour C
T	convergence parameter
T_i	stress vector active along boundary
u_i	displacement vector
u_y	displacement in y direction
u(x,y), v(x,y)	arbitrary continuous functions
w	width of the plate
$W(\varepsilon)$	strain energy density
x,y,z	rectangular Cartesian coordinate directions
α	notch angle
Γ	arbitrary contour surrounding a crack tip
δ_{ij}	Kronecker delta
ε_{ij}	strain tensor
$\varepsilon_x,\varepsilon_y,\varepsilon_z,\varepsilon_{xy}$	components of strain tensor in Cartesian coordinates
ε'_{ij}	modified total strain tensor
$\varepsilon'_x,\varepsilon'_y,\varepsilon'_z,\varepsilon'_{xy}$	components of modified total strain tensor in Cartesian coordinates
$\Delta\varepsilon_p$	equivalent plastic strain increment
μ	Poisson's ratio

ξ,η	rectangular Cartesian coordinate directions
ρ	function of r $\quad \rho = r^2 \ell n\ r$
σ_{ij}	stress tensor
$\sigma_x,\sigma_y,\sigma_z,\sigma_{xy}$	components of stress tensor in Cartesian coordinates
σ_e	equivalent stress
σ_0	tensile yield stress
σ_{max}	maximum nominal bending stress
φ	Airy stress function
Φ	function of Airy stress function $\quad \Phi = \nabla^2\varphi$
∇^2	Laplace's operator, $\frac{\partial^2}{\partial x^2} + \frac{\partial^2}{\partial y^2}$
∇^4	biharmonic operator, $\frac{\partial^4}{\partial x^4} + 2\frac{\partial^4}{\partial x^2 \partial y^2} + \frac{\partial^4}{\partial y^4}$
Subscripts	
x,y,z	refer to rectangular Cartesian coordinates
i,j,k	integers
Superscripts	
~	dimensionless quantity
'	derivative in outward normal direction
e	elastic
p	plastic

Chapter 1

Introduction

The principal objective of fracture mechanics is the prediction of the load at which the structure, weakened by a crack, will fail. Knowledge of the stress distribution near the crack tip is of fundamental importance in evaluating this load at failure. Structures of high strength, normally ductile materials have failed in quasi-brittle fashion at loads well below design. The failures were traced to the presence of flaws or cracks.

The failures of T-class Liberty Ships in the Second World War, and losses of de Haviland "Comet" aircraft (1953-1954) stimulated a major research effort in fracture mechanics. In the past most of the theoretical analysis was based on planar elasticity.

The importance of the presence of a flaw or crack in stressed bodies was recognized by Griffith [1,2] who, using the solution for the elliptic cavity in an infinite plate as obtained by Inglis [3], formulated the problem in energy terms. Griffith proposed that crack propagation would take place when the elastic energy released due to crack extension was equal or greater than the energy absorbed by the

the fracture process. The value of fracture load σ_c, for a given crack length, was given as $\sigma_c = \sqrt{2ET/\pi a}$ for plane stress case and $\sigma_c = \sqrt{2ET/\pi a(1 - \mu^2)}$ for plane strain case, where a - one half of the crack length, E - Young's modulus, μ - Poisson's ratio, and T - surface tension of the material along the crack.

For the case of brittle materials, Griffith assumed that the effects of plastic behavior prior to fracture could be neglected. This assumption makes unrealistic use of this theory for quasi-brittle fractures, where small amounts of plastic deformation occur in the vicinity of the crack tip.

Irwin [4] and Orowan [5,6] suggested a modification to Griffith's theory, which would account for the limited amount of plastic deformation. They replaced the surface energy T in Griffith's equation by the energy spent in localized plastic deformation. This modification forms the basis for linear fracture mechanics.

The critical strain energy release rate was re-defined by Irwin [7,8,9] as a crack extension force G, and reaching a critical value G_c when the crack starts to propagate. The force G_c is frequently called the fracture toughness. Based on the analysis due to Westergaard [10] and Sneddon [11], Irwin [7,8] introduced the stress intensity factor K, which describes the stress distribution in the vicinity of the crack tip, and is dependent only on geometry and loading. He noted that the stress intensity factor K is proportional to the square root of the force G tending to cause crack extension, i.e.,

$K^2 = EG$ for plane stress and $K^2 = EG/(1 - \mu^2)$ for plane strain conditions.

The above analysis assumes that the plastic strains are confined to the zone in the vicinity of the crack tip, which is small in comparison to the crack size. Under this restriction the stress relaxation by plastic flow near the crack surfaces will have a relatively small influence upon the calculation of the force G.

Subsequent investigations by Williams [12,13], Wigglesworth [14], Erdogan [15], Irwin [16] and others demonstrated that, for identical values of stress intensity factors K, identical elastic stress fields are obtained in the immediate vicinity of the crack tip.

A summary of the results based on the plane theory of elasticity is presented by Paris and Sih [17].

Most of these results come from applications of eigenfunction expansions, complex variable formulation, and conformal mapping techniques.

Using boundary collocation technique, solutions to the single edge crack plate subjected to various type loads were obtained by Gross, Srawley and Brown [18] and by Gross and Srawley [19,20]. Applying the same method Gross [21] and Gross and Mendelson [22] obtained solutions to plane elastostatic problems of v-notched plates subjected to various types of loading. Bueckner [23] analyzed several crack problems, including the edge-notched strip in bending. His method of analysis was based on the representation of a crack by a

continuous distribution of dislocation singularities, leading to a regular Fredholm integral equation.

The method of potential was applied by Walker [24] in solving selected edge-notched plate problems. Hays [25] used finite element method combined with evaluation of Rice's contour integral [26] in determination of stress intensity factors for various cases of a cracked plate subjected to uniform tension or pure bending.

Elastic analysis is now widely accepted for cases where small scale yielding took place prior to fracture. However, when the plastic zone that develops prior to fracture is not small in comparison with the crack length and other geometrical parameters, elastic-plastic treatment of the problem is essential.

Mathematical theory of plasticity is most readily applied to elastic-plastic analysis of longitudinal cracks in cylindrical bars subjected to pure torsion. The limiting case of the edge-notched infinitely thick plate subjected to pure shear loading (anti-plane, tearing mode, III - see Section 4.3) was considered by Hult and McClintock [27]. Taking into account elastic-perfectly plastic behavior of the material, they obtained stress and strain distribution around the tip of the notch.

Using conformal mapping and relaxation techniques, Koskinen [28] provided the solution to grooved plate of finite thickness subjected to longitudinal shear. At low strain levels the shape of elastic-plastic boundary was found to be in good agreement with the one obtained by Hult and McClintock [27]. The singular behavior of the

environment near the crack tip was not eliminated by plastic behavior.

Based on the results of anti-plane elastic - perfectly plastic analysis McClintock and Irwin [29] confirmed the proposed correction by Irwin [30] that, for small scale yielding, the elastic field outside the plastic region was identical to that which would be predicted for an elastic body with a crack whose length is adjusted to $a = a_0 + r_y$. Here a_0 and a are initial and the adjusted crack half-lengths respectively and $r_y = K^2/2\pi\sigma_0^2$ where σ_0 is the uniaxial tensile yield stress. However, for larger amounts of yielding, McClintock and Irwin [29] concluded that more complete study of the stress and strain distribution near the tip of cracks under mode I loading is needed before fracture criteria for such cases could be formulated.

The influence of strain hardening on the size of the plastic zone for the case of anti-plane loading was discussed by Rice [31,32]. He found that the singular behavior of stresses and strains at the crack tip was influenced by the strain hardening properties of the material, the sum of stress and strain singularities remaining approximately constant and equal to unity. The size of the plastic zone was reduced with increasing values of the strain hardening parameter.

Swedlow et al [33] and Swedlow [35], using finite element technique and Prandtl-Reuss incremental plasticity relations, analyzed stress and strain distributions in work-hardening cracked plates subjected to uniaxial tension. The results [33,34,35] confirm the singular behavior of the stresses and strains in the vicinity of the

crack tip and, for the first time, give approximate information on the growth of the plastic enclave for the case of in-plane loading. Swedlow [35] pointed out that for a plane strain case the plastic enclave increases at a much lower rate than for a plane stress case.

Using the total deformation theory of plasticity in conjunction with hardening stress-strain relations, Rice and Rosengren [36] and Hutchison [37,38] produced near-tip solutions for cracked plates loaded in-plane in pure shear or in tension. As in the case of anti-plane loading, the product of stress and strain exhibits singularity varying inversely with distance from the tip of the crack in all cases considered. Also, these authors have shown that the stress and strain fields at a crack tip could be determined from the parameter characterizing loading and geometry, and that this parameter is a function of Rice's path-independent contour integral [39]. Hutchison [38] noted that, for perfectly plastic material, the plane strain case gives higher tensile stress ahead of the crack tip than plane stress by an approximate factor of 2.5.

From this brief survey of the results of elastic and elastic-plastic stress analysis of cracked bodies, it is apparent that the linear theory of elasticity provides solutions leading to computations of fracture toughness in terms of the stress intensity factor K.

To establish interaction between elasto-plastic deformations and the fracture process, knowledge of the stress and strain distributions near the crack tip is of fundamental importance. The most widely used

techniques of solution, such as finite difference or finite element methods, do not provide good enough resolution in the vicinity of the crack tip, but do give an indication of the shape and growth of the plastic zone. Therefore, further work is needed to improve the accuracy of the results, especially in the immediate vicinity of the crack tip.

The primary objective of this dissertation is to present a method of solution which, when applied to elasto-plastic analysis of the crack tip environment, will produce stress and strain fields in much greater detail than presently available.

The boundary integral equation method, whose development is discussed in references [40 to 43], seems to be a logical choice. This method of solution utilizes Green's second theorem to reduce the non-homogeneous biharmonic equation for the Airy stress function to two coupled Fredholm-type integral equations, which must satisfy specified boundary conditions. A numerical method is utilized in which two coupled integral equations of the Fredholm-type are replaced by a system of simultaneous algebraic equations and solved by a digital computer, yielding stresses and strains at any desired location throughout the interior of the region.

The integral equation method has been utilized in the solution of various plane elastostatic problems. A number of torsion problems have been solved by Jaswon and Ponter [44] for bars with selected cross-sections, such as hollow ellipse, hollow rectangle and circles

with curved [illegible] Rim and Henry [45] obtained solutions for a circular disk subjected to diametrally opposite concentrated forces and to an infinite plate with an elliptic hole under uniform internal pressure. They report an excellent agreement with the known analytical results. Segedin and Brickell [46] applied an integral equation method to the case of elastically loaded thin corner plate, and using this method, Walker [24] obtained solutions, yielding very good results for a number of plane problems, including edge-notched plate subjected to simple tension.

The boundary integral equation method has never been applied in the solution of any elasto-plastic problem. The objective of this study is to provide a general formulation of this method for plane problems where plastic deformation is occuring, and in particular to obtain a solution for a plane problem with a geometric singularity.

A single edge v-notched specimen subjected to pure bending load is particularily efficient for fracture toughness studies. It is widely recommended by ASTM Committee E24 on Fracture Testing of Metals. Since no solution of this problem has been published, the investigations of this thesis will be devoted to this geometry and loading.

Difficulties related to the singularity at the notch tip required special treatment of the neighboring boundary and interior field. The treatment of the boundary is presented in Chapter 4 and the interior field in Chapter 5.

The elastic case is considered first and results compared with those obtained by others. Then the method is extended to the elasto-plastic case. A strain hardening material is assumed, with strain hardening parameter $m = 0.05$ or $m = 0.10$. Detailed results are given for plates with various notch angles and notch depths for plane strain or plane stress conditions.

Chapter 2

Statement of the Problem

2.1 Physical Problem

Consider a rectangular plate with a single edge V-notch, subjected to pure bending load (Fig. 1). Determine:

(a) The elasto-plastic state of stress in the plate.

(b) Stress intensity factor and Rice's J integral in the vicinity of the tip of the notch.

(c) Displacement at the edge of the V-notch.

The cases of plane strain and plane stress conditions are to be considered.

The calculations will be performed for varying notch angles, notch depths, and strain hardening parameters.

2.2 Assumptions

The following assumptions are made:

(a) The deformations are infinitesimal, i.e., quadratic terms in strain tensor are set to zero.

(b) Body forces are neglected.

(c) The effect of inertia is small and can be neglected.

(d) The material is homogeneous and isotropic.

(e) The material strain hardens isotropically.

Chapter 3

Mathematical Problem

3.1 Biharmonic Equation

To determine the state of stress in a plane elasto-plastic problem, it is necessary to solve the differential equations of equilibrium, subject to prescribed boundary conditions. To assure the condition of continuity of the body the compatibility equation must also be satisfied.

For a plane strain or plane stress problem the equations of equilibrium in Cartesian coordinates are as follows:

$$\begin{aligned} \frac{\partial \sigma_x}{\partial x} + \frac{\partial \sigma_{xy}}{\partial y} &= 0 \\ \frac{\partial \sigma_{xy}}{\partial x} + \frac{\partial \sigma_y}{\partial y} &= 0 \end{aligned} \tag{1}$$

The compatibility equation is

$$\frac{\partial^2 \varepsilon_x}{\partial y^2} + \frac{\partial^2 \varepsilon_y}{\partial x^2} - 2 \frac{\partial^2 \varepsilon_{xy}}{\partial x \partial y} = 0 \tag{2}$$

The stress-strain relations for the plane strain condition, using incompressibility condition in plastic range [51], are

$$\left.\begin{aligned}
\varepsilon_x &= \frac{1}{E}[\sigma_x - \mu(\sigma_y + \sigma_z)] + \varepsilon_x^p + \Delta\varepsilon_x^p \\
\varepsilon_y &= \frac{1}{E}[\sigma_y - \mu(\sigma_x + \sigma_z)] + \varepsilon_y^p + \Delta\varepsilon_y^p \\
\varepsilon_z &= \frac{1}{E}[\sigma_z - \mu(\sigma_x + \sigma_y)] - \varepsilon_x^p - \varepsilon_y^p - \Delta\varepsilon_x^p - \Delta\varepsilon_y^p = 0 \\
\varepsilon_{xy} &= \frac{1+\mu}{E}\sigma_{xy} + \varepsilon_{xy}^p + \Delta\varepsilon_{xy}^p
\end{aligned}\right\} \qquad (3)$$

where ε_x^p, ε_y^p, and ε_{xy}^p represent the accumulation of plastic strain increments from the beginning of the loading history up to, but not including the current increment of the load, and $\Delta\varepsilon_x^p$, $\Delta\varepsilon_y^p$, and $\Delta\varepsilon_{xy}^p$ are the increments of plastic strain due to the current increment of load.

For the plane stress condition we have

$$\left.\begin{aligned}
\varepsilon_x &= \frac{1}{E}(\sigma_x - \mu\sigma_y) + \varepsilon_x^p + \Delta\varepsilon_x^p \\
\varepsilon_y &= \frac{1}{E}(\sigma_y - \mu\sigma_x) + \varepsilon_y^p + \Delta\varepsilon_y^p \\
\varepsilon_z &= -\frac{\mu}{E}(\sigma_x + \sigma_y) - \varepsilon_x^p - \varepsilon_y^p - \Delta\varepsilon_x^p - \Delta\varepsilon_y^p \\
\varepsilon_{xy} &= \frac{1+\mu}{E}\sigma_{xy} + \varepsilon_{xy}^p + \Delta\varepsilon_{xy}^p
\end{aligned}\right\} \qquad (4)$$

The incremental theory of plasticity, von Mises yield criterion and the flow rule associated with it result in the Prandtl-Reuss stress-strain relations [51], which for the plane strain case are

$$\left.\begin{aligned}
\Delta\varepsilon_x^p &= \frac{\Delta\varepsilon_p}{2\sigma_e}(2\sigma_x - \sigma_y - \sigma_z) \\
\Delta\varepsilon_y^p &= \frac{\Delta\varepsilon_p}{2\sigma_e}(2\sigma_y - \sigma_z - \sigma_x) \\
\Delta\varepsilon_z^p &= \frac{\Delta\varepsilon_p}{2\sigma_e}(2\sigma_z - \sigma_x - \sigma_y) = -\Delta\varepsilon_x^p - \Delta\varepsilon_y^p \\
\Delta\varepsilon_{xy}^p &= \frac{3}{2}\frac{\Delta\varepsilon_p}{\sigma_e}\sigma_{xy}
\end{aligned}\right\} \qquad (5)$$

where the equivalent plastic strain increment is

$$\Delta\varepsilon_p = \frac{2}{\sqrt{3}}\sqrt{(\Delta\varepsilon_x^p)^2 + (\Delta\varepsilon_y^p)^2 + \Delta\varepsilon_x^p \cdot \Delta\varepsilon_y^p + (\Delta\varepsilon_{xy}^p)^2} \qquad (6)$$

and the equivalent stress is

$$\sigma_e = \frac{1}{\sqrt{2}}\sqrt{(\sigma_x - \sigma_y)^2 + (\sigma_y - \sigma_z)^2 + (\sigma_z - \sigma_x)^2 + 6\sigma_{xy}^2} \qquad (7)$$

For the plane stress conditions

$$\left.\begin{aligned}
\Delta\varepsilon_x^p &= \frac{\Delta\varepsilon_p}{2\sigma_e}(2\sigma_x - \sigma_y) \\
\Delta\varepsilon_y^p &= \frac{\Delta\varepsilon_p}{2\sigma_e}(2\sigma_y - \sigma_x) \\
\Delta\varepsilon_z^p &= -\frac{\Delta\varepsilon_p}{2\sigma_e}(\sigma_x + \sigma_y) = -\Delta\varepsilon_x^p - \Delta\varepsilon_y^p \\
\Delta\varepsilon_{xy}^p &= \frac{3}{2}\frac{\Delta\varepsilon_p}{\sigma_e}\sigma_{xy}
\end{aligned}\right\} \qquad (8)$$

$$\sigma_e = \sqrt{\sigma_x^2 + \sigma_y^2 - \sigma_x\sigma_y + 3\sigma_{xy}^2} \qquad (9)$$

with equivalent plastic strain increment $\Delta\varepsilon_p$ defined by equation (6).

The equivalent plastic strain increment $\Delta\varepsilon_p$ and the equivalent stress σ_e are related thru the uniaxial tensile stress-strain curve. For a material with linear strain hardening parameter m this relationship is shown in Fig. 2.

The Prandtl-Reuss equations can be expressed in terms of strains only. This form, used in the iterative process of calculating plastic strains, improves the stability and speeds up the convergence process [52].

Using standard indicial notation, the total strains can be written

$$\varepsilon_{ij} = \varepsilon^e_{ij} + \varepsilon^p_{ij} + \Delta\varepsilon^p_{ij} \tag{10}$$

where, elastic component of the total strain is given by

$$\varepsilon^e_{ij} = \frac{1+\mu}{E}\sigma_{ij} - \delta_{ij}\frac{\mu}{E}\sigma_{ii} \tag{11}$$

and

ε^p_{ij} - is accumulated plastic strain up to, but not including, the current increment of load

$\Delta\varepsilon^p_{ij}$ - is the increment of plastic strain due to the current increment of load

We define the modified total strains as

$$\varepsilon'_{ij} \equiv \varepsilon_{ij} - \varepsilon^p_{ij} \tag{12}$$

Then

$$\varepsilon'_{ij} = \varepsilon^e_{ij} + \Delta\varepsilon^p_{ij} \tag{13}$$

The equivalent modified total strain is now defined as

$$\varepsilon_{et} = \frac{\sqrt{2}}{3}\sqrt{(\varepsilon_x' - \varepsilon_y')^2 + (\varepsilon_x' - \varepsilon_z')^2 + (\varepsilon_y' - \varepsilon_z')^2 + 6\varepsilon_{xy}'^2} \qquad (14)$$

The new plastic strain increment-total strain relations, an equivalent to Prandtl-Reuss equations, are

$$\left.\begin{aligned}
\Delta\varepsilon_x^p &= \frac{\Delta\varepsilon_p}{3\varepsilon_{et}}(2\varepsilon_x' - \varepsilon_y' - \varepsilon_z') \\
\Delta\varepsilon_y^p &= \frac{\Delta\varepsilon_p}{3\varepsilon_{et}}(2\varepsilon_y' - \varepsilon_z' - \varepsilon_x') \\
\Delta\varepsilon_z^p &= \frac{\Delta\varepsilon_p}{3\varepsilon_{et}}(2\varepsilon_z' - \varepsilon_x' - \varepsilon_y') = -(\Delta\varepsilon_x^p + \Delta\varepsilon_y^p) \\
\Delta\varepsilon_{xy}^p &= \frac{\Delta\varepsilon_p}{\varepsilon_{et}}\varepsilon_{xy}'
\end{aligned}\right\} \qquad (15)$$

The equivalent modified total strain can be related to the uniaxial stress-strain curve (Fig. 2) by the following expression

$$\Delta\varepsilon_p = \frac{\varepsilon_{et} - \frac{2}{3}\frac{1+\mu}{E}\sigma_{e,i-1}}{1 + \frac{2}{3}\frac{1+\mu}{E}\left(\frac{\Delta\sigma_e}{\Delta\varepsilon_p}\right)_{i-1}}$$

where the modified total strain ε_{et} is defined by equation (14), the equivalent stress $\sigma_{e,i-1}$ is defined by equations (7) or (9) and is evaluated at the end of the preceding current load increment, and μ is a Poisson's ratio.

For the material with the linear strain hardening parameter m the above relation becomes

$$\Delta\varepsilon_p = \frac{\varepsilon_{et} - \frac{2}{3}\frac{1+\mu}{E}\sigma_{e,i-1}}{1 + \frac{2}{3}(1+\mu)\frac{m}{1-m}} \tag{16}$$

The stresses are expressed in terms of Airy stress function $\varphi(x,y)$ [47] satisfying equilibrium equations (1)

$$\sigma_x = \frac{\partial^2\varphi}{\partial y^2} \qquad \sigma_y = \frac{\partial^2\varphi}{\partial x^2} \qquad \sigma_{xy} = -\frac{\partial^2\varphi}{\partial x\partial y} \tag{17}$$

Substituting stress-strain relations (3) or (4) into compatibility equation (2) we obtain compatibility relation in terms of stresses.

For plane strain, we have

$$(1-\mu^2)\left(\frac{\partial^2\sigma_x}{\partial y^2} + \frac{\partial^2\sigma_y}{\partial x^2} - 2\frac{\partial^2\sigma_{xy}}{\partial x\partial y}\right) + E\left[\frac{\partial^2}{\partial y^2}(\varepsilon_x^p + \Delta\varepsilon_x^p) + \frac{\partial^2}{\partial x^2}(\varepsilon_y^p + \Delta\varepsilon_y^p) - 2\frac{\partial^2}{\partial x\partial y}(\varepsilon_{xy}^p + \Delta\varepsilon_{xy}^p)\right] - \mu E\nabla^2(\varepsilon_x^p + \Delta\varepsilon_x^p + \varepsilon_y^p + \Delta\varepsilon_y^p)$$

$$= \mu(1+\mu)\left(\frac{\partial^2\sigma_x}{\partial x^2} + \frac{\partial^2\sigma_y}{\partial y^2} + 2\frac{\partial^2\sigma_{xy}}{\partial x\partial y}\right) \tag{18}$$

and for plane stress

$$\frac{\partial^2\sigma_x}{\partial y^2} + \frac{\partial^2\sigma_y}{\partial x^2} - 2\frac{\partial^2\sigma_{xy}}{\partial x\partial y} + E\left[\frac{\partial^2}{\partial y^2}(\varepsilon_x^p + \Delta\varepsilon_x^p) + \frac{\partial^2}{\partial x^2}(\varepsilon_y^p + \Delta\varepsilon_y^p) - 2\frac{\partial^2}{\partial x\partial y}(\varepsilon_{xy}^p + \Delta\varepsilon_{xy}^p)\right] = \mu\left(\frac{\partial^2\sigma_y}{\partial y^2} + \frac{\partial^2\sigma_x}{\partial x^2} + 2\frac{\partial^2\sigma_{xy}}{\partial x\partial y}\right) \tag{19}$$

Differentiating the first of the equilibrium equations (1) with respect to x, and second equation with respect to y and combining them, we obtain

$$\frac{\partial^2 \sigma_x}{\partial x^2} + \frac{\partial^2 \sigma_y}{\partial y^2} + 2 \frac{\partial^2 \sigma_{xy}}{\partial x \partial y} = 0 \tag{20}$$

Substituting equations (17) and (20) into equations (18) or (19) yields

$$\nabla^4 \varphi(x,y) = g(x,y) \tag{21}$$

where the Laplacian ∇^2, is

$$\nabla^2 = \frac{\partial^2}{\partial x^2} + \frac{\partial^2}{\partial y^2}$$

and

$$g(x,y) = -\frac{E}{1-\mu^2}\left[\frac{\partial^2}{\partial y^2}(\varepsilon_x^p + \Delta\varepsilon_x^p) + \frac{\partial^2}{\partial x^2}(\varepsilon_y^p + \Delta\varepsilon_y^p) - 2\frac{\partial^2}{\partial x \partial y}(\varepsilon_{xy}^p + \Delta\varepsilon_{xy}^p)\right] + \frac{\mu E}{1-\mu^2}\nabla^2(\varepsilon_x^p + \Delta\varepsilon_x^p + \varepsilon_y^p + \Delta\varepsilon_y^p) \tag{22}$$

for plane strain case and

$$g(x,y) = -E\left[\frac{\partial^2}{\partial y^2}(\varepsilon_x^p + \Delta\varepsilon_x^p) + \frac{\partial^2}{\partial x^2}(\varepsilon_y^p + \Delta\varepsilon_y^p) - 2\frac{\partial^2}{\partial x \partial y}(\varepsilon_{xy}^p + \Delta\varepsilon_{xy}^p)\right] \tag{23}$$

for plane stress case.

For convenience the following dimensionless quantities are introduced:

$$\left.\begin{aligned} \tilde{x} &\equiv \frac{x}{w} & \tilde{\varphi}(\tilde{x},\tilde{y}) &\equiv \frac{\varphi(x,y)}{\sigma_0 w^2} \\ \tilde{y} &\equiv \frac{y}{w} & \tilde{g}(\tilde{x},\tilde{y}) &\equiv \frac{g(x,y)w^2}{\sigma_0} \\ \tilde{\varepsilon} &\equiv \frac{\varepsilon E}{\sigma_0} & \tilde{q} &= \frac{\sigma_{max}}{\sigma_0} \end{aligned}\right\} \tag{24}$$

Equation (21) and associated with it equations (22) and (23) can now be written in dimensionless form

$$\tilde{\nabla}^4 \varphi(\tilde{x},\tilde{y}) = \tilde{g}(\tilde{x},\tilde{y}) \tag{25}$$

$$\left.\begin{aligned}\tilde{g}(\tilde{x},\tilde{y}) = -\frac{1}{1-\mu^2}\Bigg[&\frac{\partial^2}{\partial\tilde{y}^2}(\tilde{\varepsilon}^p_x + \Delta\tilde{\varepsilon}^p_x) + \frac{\partial^2}{\partial\tilde{x}^2}(\tilde{\varepsilon}^p_y + \Delta\tilde{\varepsilon}^p_y)\\ &- 2\frac{\partial^2}{\partial\tilde{x}\partial\tilde{y}}(\tilde{\varepsilon}^p_{xy} + \Delta\tilde{\varepsilon}^p_{xy})\Bigg] + \frac{\mu}{1-\mu^2}\tilde{\nabla}^2(\tilde{\varepsilon}^p_x + \Delta\tilde{\varepsilon}^p_x\\ &+ \tilde{\varepsilon}^p_y + \Delta\tilde{\varepsilon}^p_y)\end{aligned}\right\} \text{plane strain} \tag{26}$$

$$\left.\begin{aligned}\tilde{g}(\tilde{x},\tilde{y}) = -\Bigg[&\frac{\partial^2}{\partial\tilde{y}^2}(\tilde{\varepsilon}^p_x + \Delta\tilde{\varepsilon}^p_x) + \frac{\partial^2}{\partial\tilde{x}^2}(\tilde{\varepsilon}^p_y + \Delta\tilde{\varepsilon}^p_y)\\ &- 2\frac{\partial^2}{\partial\tilde{x}\partial\tilde{y}}(\tilde{\varepsilon}^p_{xy} + \Delta\tilde{\varepsilon}^p_{xy})\Bigg]\end{aligned}\right\} \text{plane stress} \tag{27}$$

The following are the boundary conditions to be satisfied by the stress function $\tilde{\varphi}(\tilde{x},\tilde{y})$, as derived in Appendix A (Fig. 1).

$$\left.\begin{aligned}&\text{along boundary OA and OA'} \quad \tilde{\varphi}(\tilde{x},\tilde{y}) = 0;\ \frac{\partial\tilde{\varphi}}{\partial\tilde{n}} = 0\\ &\text{along boundary AB and A'B'} \quad \tilde{\varphi}(\tilde{x},\tilde{y}) = 0;\ \frac{\partial\tilde{\varphi}}{\partial\tilde{n}} = 0\\ &\text{along boundary BC and B'C'}\\ &\qquad \tilde{\varphi}(\tilde{x},\tilde{y}) = -\tilde{q}\left(\frac{\tilde{x}^3}{3} + \tilde{a}\tilde{x}^2 + \tilde{a}^2\tilde{x} + \frac{\tilde{a}^3}{3}\right) + \tilde{q}\left(\frac{\tilde{x}^2}{2} + \tilde{a}\tilde{x} + \frac{\tilde{a}^2}{2}\right)\\ &\qquad \frac{\partial\tilde{\varphi}}{\partial\tilde{n}} = 0\\ &\text{along boundary CD and C'D} \quad \tilde{\varphi}(\tilde{x},\tilde{y}) = \frac{\tilde{q}}{6};\ \frac{\partial\tilde{\varphi}}{\partial\tilde{n}} = 0\end{aligned}\right\} \tag{28}$$

The plane elasto-plastic problem was reduced to a solution of the non-homogeneous biharmonic equation (25) subject to boundary conditions (28) and applicable plasticity relations.

3.2 Integral Equation Method

The method of solution used in this dissertation utilizes Green's second theorem to reduce the non-homogeneous biharmonic equation (25) to two coupled, Fredholm type, integral equations, which must satisfy specified boundary conditions (28).

The fundamental theory related to these integral equations, the question of existence and uniqueness of solutions are presented in work by Jaswon [40], Sym [41,42], and Rizzo F, J [43], and references [48,49,50].

Consider two functions $u(x,y)$ and $v(x,y)$ having continuous derivatives of first and second order in simply connected region R, bounded by a sectionally smooth curve C. The direction of the line integral and the positive outward normal is shown in Fig. 3.

Green's Second Theorem [48,49] states

$$\iint_R (u\nabla^2 v - v\nabla^2 u)\,dxdy = \int_C \left(u\frac{\partial v}{\partial n} - v\frac{\partial u}{\partial n}\right)ds \tag{29}$$

If we let

$$u = \nabla^2 \varphi \tag{30}$$

then it follows, that

$$\iint_R (\nabla^2\varphi\nabla^2 v - v\nabla^4\varphi)\,dxdy = \int_C \left[\nabla^2\varphi \frac{\partial v}{\partial n} - v \frac{\partial}{\partial n}(\nabla^2\varphi)\right] ds$$

or

$$\iint_R \nabla^2\varphi\nabla^2 v\,dxdy = \iint_R v\nabla^4\varphi\,dxdy + \int_C \left[\nabla^2\varphi \frac{\partial v}{\partial n} - v \frac{\partial}{\partial n}(\nabla^2\varphi)\right] ds \qquad (31)$$

Since the left hand side of equation (31) is symmetric with respect to functions $\varphi(x,y)$ and $v(x,y)$ we can also write

$$\iint_R \nabla^2\varphi\nabla^2 v\,dxdy = \iint_R \varphi\nabla^4 v\,dxdy + \int_C \left[\nabla^2 v \frac{\partial\varphi}{\partial n} - \varphi\frac{\partial}{\partial n}(\nabla^2 v)\right] ds \qquad (32)$$

Subtracting equation (32) from equation (31) yields

$$\iint_R (\varphi\nabla^4 v - v\nabla^4\varphi)\,dxdy = \int_C \left[\varphi \frac{\partial}{\partial n}(\nabla^2 v) - \frac{\partial\varphi}{\partial n}\nabla^2 v + \nabla^2\varphi \frac{\partial v}{\partial n} - v \frac{\partial}{\partial n}(\nabla^2\varphi)\right] ds \qquad (33)$$

3.2.1. Solution of Harmonic Problem

Let us introduce function $\Phi(x,y)$ such that

$$\Phi \equiv \nabla^2\varphi \qquad (34)$$

Substituting equation (34) into equation (21) yields

$$\nabla^2\Phi(x,y) = g(x,y) \qquad (35)$$

Let $r(x,y,\xi,\eta)$ be the distance between any two points $P(x,y)$ and $q(\xi,\eta)$ in region R, as shown in Fig. 3, such that $P \subset R + C$ and $q \subset C$.

Substituting relations (30), (34), and (35) into Green's Second Theorem, equation (29), choosing for v, fundamental solution, $v = \ell n\ r$ yields

$$\iint_R - g(\xi,\eta)\ell n\ r\ d\xi d\eta = \int_C \left[\Phi \frac{\partial}{\partial n} (\ell n\ r) - \frac{\partial \Phi}{\partial n} \ell n\ r \right] ds \qquad (36)$$

and taking into account the singularity at $r = 0$, as shown in Appendix B, results in

$$2\pi\Phi(x,y) - \iint_R g(\xi,\eta)\ell n\ r\ d\xi d\eta = \int_C \left[\Phi \frac{\partial}{\partial n} (\ell n\ r) - \frac{\partial \Phi}{\partial n} \ell n\ r \right] ds \quad \text{for } P \subset R \qquad (37)$$

and

$$\pi\Phi(x,y) - \iint_R g(\xi,\eta)\ell n\ r\ d\xi d\eta = \int_C \left[\Phi \frac{\partial}{\partial n} (\ell n\ r) - \frac{\partial \Phi}{\partial n} \ell n\ r \right] ds \quad \text{for } P \subset C \qquad (38)$$

Equation (38) is similar to Green's Boundary Formula derived by Jaswon [40], except for the term describing the effect of plastic deformations.

3.2.2 Solution of Biharmonic Problem

Combining equation (33) with equations (21) and (34) and choosing this time $v \equiv \rho = r^2 \ell n\ r$ we have

$$\iint_R - \rho g(\xi,\eta) d\xi d\eta = \int_C \left[\varphi \frac{\partial}{\partial n} (\nabla^2 \rho) - \frac{\partial \varphi}{\partial n} \nabla^2 \rho + \Phi \frac{\partial \rho}{\partial n} - \frac{\partial \Phi}{\partial n} \rho \right] ds \qquad (39)$$

Taking into account the singularity at $r = 0$, we obtain, as shown in Appendix B,

$$8\pi\varphi(x,y) - \iint_R \rho g(\xi,\eta)\,d\xi d\eta = \int_C \left[\varphi \frac{\partial}{\partial n}(\nabla^2\rho) - \frac{\partial\varphi}{\partial n}\nabla^2\rho + \Phi\frac{\partial\rho}{\partial n} - \frac{\partial\Phi}{\partial n}\rho\right] ds \qquad \text{for } P \subset R \quad (40)$$

and

$$4\pi\varphi(x,y) - \iint_R \rho g(\xi,\eta)\,d\xi d\eta = \int_C \left[\varphi \frac{\partial}{\partial n}(\nabla^2\rho) - \frac{\partial\varphi}{\partial n}\nabla^2\rho + \Phi\frac{\partial\rho}{\partial n} - \frac{\partial\Phi}{\partial n}\rho\right] ds \qquad \text{for } P \subset C \quad (41)$$

Equation (40) would, for a known function $g(x,y)$, give us directly a solution to the biharmonic equation (21) provided the stress function $\varphi(x,y)$, $\frac{\partial\varphi(x,y)}{\partial n}$, $\nabla^2\varphi(x,y)$, and $\frac{\partial}{\partial n}(\nabla^2\varphi(x,y))$ were known on the boundary C.

However, only stress function φ and its outward normal derivative $\frac{\partial\varphi}{\partial n}$ are specified. The values of $\nabla^2\varphi \equiv \Phi$ and $\frac{\partial}{\partial n}(\nabla^2\varphi) \equiv \frac{\partial\Phi}{\partial n}$ must be compatible with the specified values of φ and $\frac{\partial\varphi}{\partial n}$ on the boundary. To assure this compatibility, we have to solve a system of coupled integral equations (38) and (41), which contain the unknown functions Φ and $\frac{\partial\Phi}{\partial n}$.

Once the values of Φ and $\frac{\partial\Phi}{\partial n}$ on the boundary C of region R are known we can proceed with the calculation of the stress field in the region R utilizing equations (40) and (17), and appropriate stress-strain relations.

3.3 Numerical Analysis

Since it is generally impossible to solve the system of coupled integral equations analytically, a numerical method is utilized in which the integral equations (38) and (41) are replaced by a system of $2n$ simultaneous algebraic equations with $2n$ unknowns, i.e., Φ_i and $\frac{\partial \Phi_i}{\partial n}$ where $i = 1, 2, \ldots n$.

For simplicity of notation let us denote the normal derivatives by prime superscripts.

Let us assume that the function Φ and its normal derivative Φ' are piece-wise constant on the boundary C. We can divide the boundary into n intervals, not necessarily equal, numbered consecutively in the direction of increasing s. The center of each interval is designated as a node and assigned constant values of Φ_i and Φ'_i.

In a similar manner the interior of region R can be covered by a grid, containing m cells, with assigned constant values of the function $g(\xi,\eta)$ and $\gamma(x,y,\xi,\eta)$. The cells do not have to have equal areas. Their nodal points are located at the centroids.

The arrangement of boundary and interior region subdivisions is shown in Fig. 4.

Using the above assumptions, equations (38) and (41) can be written

$$\left.\begin{aligned}
\pi\Phi_i - \sum_{k=1}^{m} (g\ \ell n\ r)_k \iint_k d\xi d\eta &= \sum_{j=1}^{n} \Phi_j \int_j (\ell n\ r)'\, ds \\
&\quad - \sum_{j=1}^{n} \Phi_j' \int_j \ell n\ r\, ds \\
4\pi\varphi_i - \sum_{k=1}^{m} (g\rho)_k \iint_k d\xi d\eta &= \sum_{j=1}^{n} \varphi_j \int_j (\nabla^2\rho)'\, ds \\
&\quad - \sum_{j=1}^{n} \varphi_j' \int_j \nabla^2\rho\, ds + \sum_{j=1}^{n} \Phi_j \int_j \rho'\, ds \\
&\quad - \sum_{j=1}^{n} \Phi_j' \int_j \rho\, ds
\end{aligned}\right\} \qquad (42)$$

$$i = 1,2,\ldots\ n$$

where $\int_j$ means the integral over the j^{th} segment and $\int_k\int$ means means the integral over the k^{th} cell.

The stress function φ is not a constant on loaded boundaries BC and B'C' as shown by equation (28). The assumption that it is piecewise constant may lead to appreciable errors in numerical results. To overcome this difficulty the summations given by equation (42) for intervals lying on the loaded boundaries and involving stress function are replaced by direct integration.

Again, for convenience we non-dimensionalize all the distances with respect to the width of the plate w and introduce the following dimensionless quantities

$$\tilde{\Phi} = \frac{\Phi}{\sigma_0} \qquad \tilde{\Phi}' = \frac{\Phi' w}{\sigma_0} \tag{43}$$

To simplify calculations we introduce the following notations. Let

$\tilde{r}_{ij}$ - dimensionless distance from the i^{th} node to <u>any</u> point in the j^{th} interval

$\tilde{r}_{ik}$ - dimensionless distance from the i^{th} node to <u>centroid</u> of the k^{th} cell

and

$$\tilde{\rho}_{ij} = (\tilde{r}^2 \ell n\ \tilde{r})_{ij}$$

$$\tilde{\rho}_{ik} = (\tilde{r}^2 \ell n\ \tilde{r})_{ik}$$

Define coefficients

$$\left.\begin{aligned}
\tilde{a}_{ij} &= \int_j (\ell n\ \tilde{r}_{ij})' d\tilde{s} \\
\tilde{b}_{ij} &= -\int_j \ell n\ \tilde{r}_{ij}\ d\tilde{s} \\
\tilde{c}_{ij} &= \int_j \tilde{\rho}'_{ij}\ d\tilde{s} \\
\tilde{d}_{ij} &= -\int_j \tilde{\rho}_{ij}\ d\tilde{s} \\
\tilde{e}_{ij} &= \int_j (\tilde{\nabla}^2 \tilde{\rho}_{ij})' d\tilde{s} \\
\tilde{f}_{ij} &= -\int_j \tilde{\nabla}^2 \tilde{\rho}_{ij}\, d\tilde{s}
\end{aligned}\right\} \tag{44}$$

Equations (42) can now be written as

$$\pi\tilde{\Phi}_i - \ell n\ \tilde{r}_{ik}(\tilde{g}\tilde{A})_k = \tilde{a}_{ij}\tilde{\Phi}_j + \tilde{b}_{ij}\tilde{\Phi}'_j$$

$$4\pi\tilde{\varphi}_i - \tilde{\rho}_{ik}(\tilde{g}\tilde{A})_k = \tilde{c}_{ij}\tilde{\Phi}_j + \tilde{d}_{ij}\tilde{\Phi}'_j + \tilde{e}_{ij}\tilde{\varphi}_j + \tilde{f}_{ij}\tilde{\varphi}'_j \tag{45}$$

with

$$i = 1,2,\ldots n; \qquad j = 1,2,\ldots n; \qquad k = 1,2,\ldots m$$

which we will call boundary equations. For the segments on the loaded boundary, where stress function $\tilde{\varphi}$ is not a constant, the summation $\tilde{e}_{ij}\varphi_j$ is replaced by direct integration.

The coefficients given by equation (44) can be evaluated by Simpson's rule for $i \neq j$, and analytically for $i = j$. For the boundary segments which can be represented by straight lines the analytical solution is possible. The evaluation of the coefficients (44) is given in Appendix C.

Equation (45) expressed in matrix form becomes

$$\begin{bmatrix} [\tilde{a}_{ij} - \delta_{ij}\pi] & [\tilde{b}_{ij}] \\ nxn & nxn \\ [\tilde{c}_{ij}] & [\tilde{d}_{ij}] \\ nxn & nxn \end{bmatrix} \begin{Bmatrix} [\tilde{\Phi}_j] \\ nx1 \\ [\tilde{\Phi}'_j] \\ nx1 \end{Bmatrix} = - \begin{bmatrix} [\ell n\ \tilde{r}_{ik}] & [0] & [0] \\ nxm & nxn & nxn \\ [\tilde{\rho}_{ik}] & [\tilde{e}_{ij} - \delta_{ij}4\pi] & [\tilde{f}_{ij}] \\ nxm & nxn & nxn \end{bmatrix} \begin{Bmatrix} [(\tilde{g}\tilde{A})_k] \\ mx1 \\ [\tilde{\varphi}_j] \\ nx1 \\ [\tilde{\varphi}'_j] \\ nx1 \end{Bmatrix} \tag{46}$$

The problem reduced to the solution of the following matrix system

$$[\tilde{B}]\{\tilde{X}\} = \{\tilde{R}\} \tag{47}$$

where $[\tilde{B}]$ is 2nx2n matrix and $\{\tilde{X}\}$ and $\{\tilde{R}\}$ are 2nx1 column matrices.

Matrix $[\tilde{B}]$ is dependent only on geometry, i.e., number of nodes and their distribution on the boundary. Since matrix $\{\tilde{R}\}$ contains non-linear function $\tilde{g}(\tilde{\xi},\tilde{\eta})$, which depends on the stress field and therefore on matrix $\{\tilde{X}\}$, we choose to use an iterative process to obtain the solution.

In this dissertation the method of successive elastic solutions [51,52,53] is utilized. Application of this method will be discussed in Chapter 5.

To calculate stresses from the stress function (40) we need not perform any numerical differentiation of the stress function. We can differentiate under the integral sign in this equation and then obtain stresses by the same type of numerical integration as in equations (45), once $\tilde{\Phi}$ and $\tilde{\Phi}'$ are known on the boundary.

Using notations of equation (44), equation (40) can be written in the following form

$$8\pi\tilde{\varphi}_i = \tilde{\rho}_{ik}(\tilde{g}\tilde{A})_k + \tilde{c}_{ij}\tilde{\Phi}_j + \tilde{d}_{ij}\tilde{\Phi}'_j + \tilde{e}_{ij}\tilde{\varphi}_j + \tilde{f}_{ij}\tilde{\varphi}'_j \qquad (48)$$

with

$i = 1, 2, 3, \ldots m \qquad j = 1, 2, 3, \ldots n \qquad k = 1, 2, 3, \ldots m$

where indexes i and k refer to the centroids of ith and kth cells and j- to jth boundary segment as shown in Fig. 5.

Applying equations (17) to equation (48) yields the stress equations

$$
\left.
\begin{aligned}
8\pi\tilde{\sigma}_x(\tilde{x},\tilde{y})_i &= \left\{ \ell n[(\tilde{x}-\tilde{\xi})^2 + (\tilde{y}-\tilde{\eta})^2] + \frac{2(\tilde{y}-\tilde{\eta})^2}{(\tilde{x}-\tilde{\xi})^2 + (\tilde{y}-\tilde{\eta})^2} + 1 \right\}_{ik} (\tilde{g}\tilde{A})_k \\
&\quad + \tilde{A}_{ij}\tilde{\varphi}_j + \tilde{B}_{ij}\tilde{\varphi}'_j + \tilde{C}_{ij}\tilde{\Phi}_j + \tilde{D}_{ij}\tilde{\Phi}'_j \\
8\pi\tilde{\sigma}_y(\tilde{x},\tilde{y})_i &= \left\{ \ell n[(\tilde{x}-\tilde{\xi})^2 + (\tilde{y}-\tilde{\eta})^2] + \frac{2(\tilde{x}-\tilde{\xi})^2}{(\tilde{x}-\tilde{\xi})^2 + (\tilde{y}-\tilde{\eta})^2} + 1 \right\}_{ik} (gA)_k \\
&\quad - \tilde{A}_{ij}\tilde{\varphi}_j - \tilde{B}_{ij}\tilde{\varphi}'_j + \tilde{E}_{ij}\tilde{\Phi}_j + \tilde{F}_{ij}\tilde{\Phi}'_j \\
-8\pi\tilde{\sigma}_{xy}(\tilde{x},\tilde{y})_i &= \left[\frac{2(\tilde{x}-\tilde{\xi})(\tilde{y}-\tilde{\eta})}{(\tilde{x}-\tilde{\xi})^2 + (\tilde{y}-\tilde{\eta})^2} \right]_{ik} (\tilde{g}\tilde{A})_k \\
&\quad + \tilde{G}_{ij}\tilde{\varphi}_j + \tilde{H}_{ij}\tilde{\varphi}'_j + \tilde{I}_{ij}\tilde{\Phi}_j + \tilde{K}_{ij}\tilde{\Phi}'_j \\
&\qquad \text{for } i \neq k \\
&\qquad i = 1,2\ldots m \qquad j = 1,2\ldots n \qquad k = 1,2\ldots m
\end{aligned}
\right\} \tag{49}
$$

The case of $i = k$ will be discussed in Chapter 5.

The coefficients $\tilde{A}_{ij}$, $\tilde{B}_{ij}$, $\tilde{C}_{ij}$, $\tilde{D}_{ij}$, $\tilde{E}_{ij}$, $\tilde{F}_{ij}$, $\tilde{G}_{ij}$, $\tilde{H}_{ij}$, $\tilde{I}_{ij}$, and $\tilde{K}_{ij}$ are obtained by appropriate differentiation under the integral sign of the coefficients given by equation (44)

Therefore, we have

$$
\left.
\begin{aligned}
\tilde{A}_{ij} &= \frac{\partial^2}{\partial \tilde{y}^2}\,(\tilde{e}_{ij}) = \int_j \frac{\partial}{\partial n}\left[\frac{(\tilde{x}_i-\tilde{\xi})^2-(\tilde{y}_i-\tilde{\eta})^2}{[(\tilde{x}_i-\tilde{\xi})^2+(\tilde{y}_i-\tilde{\eta})^2]^2}\right] d\tilde{s}\\
\tilde{B}_{ij} &= \frac{\partial^2}{\partial \tilde{y}^2}\,(\tilde{f}_{ij}) - 4\int_j \frac{(\tilde{y}_i-\tilde{\eta})^2-(\tilde{x}_i-\tilde{\xi})^2}{[(\tilde{x}_i-\tilde{\xi})^2+(\tilde{y}_i-\tilde{\eta})^2]^2}\, d\tilde{s}\\
\tilde{C}_{ij} &= \frac{\partial^2}{\partial \tilde{y}^2}\,(\tilde{c}_{ij}) = \int_j \frac{\partial}{\partial \tilde{n}}\left\{\ell n[(\tilde{x}_i-\tilde{\xi})^2+(\tilde{y}_i-\tilde{\eta})^2]+\frac{2(\tilde{y}_i-\tilde{\eta})^2}{(\tilde{x}_i-\tilde{\xi})^2+(\tilde{y}_i-\tilde{\eta})^2}\right\} d\tilde{s}\\
\tilde{D}_{ij} &= \frac{\partial^2}{\partial \tilde{y}^2}\,(\tilde{d}_{ij}) = -\int_j \left\{\ell n[(\tilde{x}_i-\tilde{\xi})^2+(\tilde{y}_i-\tilde{\eta})^2]+\frac{2(\tilde{y}_i-\tilde{\eta})^2}{(\tilde{x}_i-\tilde{\xi})^2+(\tilde{y}_i-\tilde{\eta})^2}+1\right\} d\tilde{s}\\
\tilde{E}_{ij} &= \frac{\partial^2}{\partial \tilde{x}^2}\,(\tilde{c}_{ij}) = \int_j \frac{\partial}{\partial \tilde{n}}\left\{\ell n[(\tilde{x}_i-\tilde{\xi})^2+(\tilde{y}_i-\tilde{\eta})^2]+\frac{2(\tilde{x}_i-\tilde{\xi})^2}{(\tilde{x}_i-\tilde{\xi})^2+(\tilde{y}_i-\tilde{\eta})^2}\right\} d\tilde{s}\\
\tilde{F}_{ij} &= \frac{\partial^2}{\partial \tilde{x}^2}\,(\tilde{d}_{ij}) = -\int_j \left\{\ell n[(\tilde{x}_i-\tilde{\xi})^2+(\tilde{y}_i-\tilde{\eta})^2]+\frac{2(\tilde{x}_i-\tilde{\xi})^2}{(\tilde{x}_i-\tilde{\xi})^2+(\tilde{y}_i-\tilde{\eta})^2}+1\right\} d\tilde{s}\\
\tilde{G}_{ij} &= \frac{\partial^2}{\partial \tilde{x}\partial \tilde{y}}\,(\tilde{e}_{ij}) = -8\int_j \frac{\partial}{\partial \tilde{n}}\left\{\frac{(\tilde{x}_i-\tilde{\xi})(\tilde{y}_i-\tilde{\eta})}{[(\tilde{x}_i-\tilde{\xi})^2+(\tilde{y}_i-\tilde{\eta})^2]^2}\right\} d\tilde{s}\\
\tilde{H}_{ij} &= \frac{\partial^2}{\partial \tilde{x}\partial \tilde{y}}\,(\tilde{f}_{ij}) = 8\int_j \frac{(\tilde{x}_i-\tilde{\xi})(\tilde{y}_i-\tilde{\eta})}{[(\tilde{x}_i-\tilde{\xi})^2+(\tilde{y}_i-\tilde{\eta})^2]^2}\, d\tilde{s}\\
\tilde{I}_{ij} &= \frac{\partial^2}{\partial \tilde{x}\partial \tilde{y}}\,(\tilde{c}_{ij}) = 2\int_j \frac{\partial}{\partial \tilde{n}}\left\{\frac{(\tilde{x}_i-\tilde{\xi})(\tilde{y}_i-\tilde{\eta})}{(\tilde{x}_i-\tilde{\xi})^2+(\tilde{y}_i-\tilde{\eta})^2}\right\} d\tilde{s}\\
\tilde{K}_{ij} &= \frac{\partial^2}{\partial \tilde{x}\partial \tilde{y}}\,(\tilde{d}_{ij}) = -2\int_j \frac{(\tilde{x}_i-\tilde{\xi})(\tilde{y}_i-\tilde{\eta})}{(\tilde{x}_i-\tilde{\xi})^2+(\tilde{y}_i-\tilde{\eta})^2}\, d\tilde{s}
\end{aligned}
\right\} \quad (50)
$$

For segments on the loaded boundary the summations $\tilde{A}_{ij}\tilde{\varphi}_j$ and $\tilde{G}_{ij}\tilde{\varphi}_j$ are replaced by direct integration.

The evaluation of the coefficients (50) is given in Appendix C.

As stated previously the problem solution is obtained by solving a set of $2n$ simultaneous linear equations, where n is equal to the number of nodal points prescribed along the boundary, utilizing method of successive elastic solutions. The number of nodal points is limited only by the computer storage capacity. The numerical calculations were performed on IBM 7094 digital computer using single precision arithmetic. Matrix system given by equation (47) was solved using the modified Gauss elimination method, which utilizes pivoting and backward and forward substitutions.

Because of the complexity of the problem, the elastostatic case will be solved first. The results will be compared with known solutions and used as a guidance in the numerical treatment of the elastoplastic case.

Chapter 4

Solution of the Elastostatic Problem

4.1 Method of Solution

The plane strain or generalized plane stress elastostatic problems are defined in the terms of the Airy stress function $\tilde{\varphi}(\tilde{x},\tilde{y})$ satisfying the homogeneous biharmonic equation

$$\nabla^4\tilde{\varphi} = 0 \tag{51}$$

subject to boundary conditions (28), with stresses defined by equation (17) and stress-strain relations by equations (3) or (4), with the plastic components of the strains set to zero.

The integral equation method, outlined in Chapter 3 is utilized in the solution of the elastostatic problem. Since the plastic strains are equal to zero throughout the plate, we set $\tilde{g}(\tilde{x},\tilde{y}) = 0$ in the boundary equations (45), thus obtaining the system of $2n$ simultaneous modified boundary equations

$$\left.\begin{aligned} \pi\tilde{\Phi}_i &= \tilde{a}_{ij}\tilde{\Phi}_j + \tilde{b}_{ij}\tilde{\Phi}'_j \\ 4\pi\tilde{\varphi}_i &= \tilde{c}_{ij}\tilde{\Phi}_j + \tilde{d}_{ij}\tilde{\Phi}'_j + \tilde{e}_{ij}\tilde{\varphi}_j + \tilde{f}_{ij}\tilde{\varphi}'_j \\ i &= 1, 2, 3,\ldots n \\ j &= 1, 2, 3,\ldots n \end{aligned}\right\} \tag{52}$$

subject to boundary conditions (28). Once the values of $\tilde{\Phi}_j$ and $\tilde{\Phi}'_j$ are found for the boundary nodal points, the stress field can be calculated from modified stress equations

$$\left.\begin{aligned} 8\pi\tilde{\sigma}_x(\tilde{x},\tilde{y})_i &= \tilde{A}_{ij}\tilde{\varphi}_j + \tilde{B}_{ij}\tilde{\varphi}'_j + \tilde{C}_{ij}\tilde{\Phi}_j + \tilde{D}_{ij}\tilde{\Phi}'_j \\ 8\pi\tilde{\sigma}_y(\tilde{x},\tilde{y})_i &= -\tilde{A}_{ij}\tilde{\varphi}_j - \tilde{B}_{ij}\tilde{\varphi}'_j + \tilde{E}_{ij}\tilde{\Phi}_j + \tilde{F}_{ij}\tilde{\Phi}'_j \\ -8\pi\tilde{\sigma}_{xy}(\tilde{x},\tilde{y})_i &= \tilde{G}_{ij}\tilde{\varphi}_j + \tilde{H}_{ij}\tilde{\varphi}'_j + \tilde{I}_{ij}\tilde{\Phi}_j + \tilde{K}_{ij}\tilde{\Phi}'_j \\ i &- \text{refers to any point in the stress field} \\ & j = 1, 2, 3, \ldots n \end{aligned}\right\} \quad (53)$$

The coefficient appearing in equations (52) and (53) are given in Appendix C.

4.2 Numerical Procedures

The number of nodal points prescribed for the boundary is theoretically unlimited. However, computer storage capacity and difficulty associated with inversion of large matrices limited the size of the coefficient matrix $[\tilde{B}]$ of equation (47) to 140x140.

Because of geometric and loading symmetry about x axis it is possible to reduce the number of unknowns. For 2n total number of nodal points the number of equations and unknowns, Φ_i and Φ'_i, is reduced from 4n to 2n. Additional reduction in the number of unknowns is accomplished by taking into consideration St. Venant's effect at the loaded boundaries. To establish the St. Venant effect, the length of the plate must be sufficiently large and is given by Gross [21] to be $\tilde{L} = 1.2$. By definition

$$\Phi_j \equiv \nabla^2\varphi_j$$

and

$$\nabla^2 \varphi_j = \sigma_{x_j} + \sigma_{y_j}$$

Since, near the loaded boundaries BC and B'C', σ_{x_j} can be assumed to be essentially zero, then it follows

and

$$\left.\begin{aligned} \Phi_j &= \sigma_{y_j} \\ \Phi_j' &\equiv \frac{\partial \sigma_{y_j}}{\partial y} = 0 \end{aligned}\right\} \qquad (54)$$

The arrangement of boundary subdivisions and nodal points is shown in Fig. 6. Note that the corner points are always designated as interval points, never as nodal points, thus eliminating discontinuous functions from the numerical analysis.

Since the vicinity of the crack tip is of greatest interest a fine nodal spacing along the notch was chosen. To minimize the effect of the non-uniform spacing at the boundary points A and A' and to obtain fine resolution at the crack tip, 60 uniformly decreasing in length intervals were taken along the notch. The rate of change in the interval length was optimized for each case by examination of the results and comparison with available solutions. The resulting stress field in the vicinity of the tip of the notch proved to be very sensitive to the length of the boundary segments along the notch. The rate of change in the interval length varied from case to case between 8% to 10%, the smallest interval at the tip of the notch $\tilde{s} \approx 0.00015$.

Each of the boundaries AB, A'B', DC, and DC' was divided into 5 intervals of equal length. Boundaries BC and B'C' with 15

uniformly spaced nodal points and assigned to them values of Φ_j and Φ'_j from equation (54) complete the boundary nodal arrangement.

The above nodal arrangement was used for all the elastostatic and elasto-plastic cases considered in this dissertation. The original set of 340 simultaneous equations was reduced to the set of 140 equations containing 140 unknown, i.e., Φ_i and Φ'_i, i = 1, 2, 3...70.

4.3 Stress Intensity Factor and Rice's J-Integral

It is recognized in linear fracture mechanics that a stress intensity factor is a scaling factor for the stress field in the vicinity of the crack tip where fracture takes place. Following Paris and Sih [17] three distinct singular fields are defined based on resulting crack opening displacements. The first mode (mode I) defines an opening mode where the crack surfaces are displaced normal to the crack plane. The second mode (mode II) is described by displacements in which crack surfaces slide over one another perpendicular to the leading edge of the crack. The third mode (mode III) defines anti-plane sliding where the crack surfaces slide with respect to one another parallel to the leading edge of the crack (Fig. 7). The stress intensity factors associated with the three displacement modes, are designated as K_I, K_{II}, and K_{III}, respectively. For the case of pure bending only mode I displacement and stress intensity factor K_I are obtained.

Stress intensity factor K_I under mode I notch displacement is defined [21, 24], in terms of coordinate system shown in Fig. 1, as follows

$$K_I = \lim_{r\to 0} \sqrt{2\pi}\, r^n \sigma_y(r,\theta)\Big|_{\theta=0} \tag{55}$$

From the known stress field in the vicinity of the tip of the notch the order of singularity n in equation (55) can be determined by plotting $\ell n\, \sigma_y$ versus $\ell n\, r$, and least squares fit of a straight line thru the plotted points.

Once the order of singularity is found, a plot of relation (55) as $r\to 0$ yields the stress intensity factor K_I.

By considering the behavior of elastic body containing a crack Rice [39] developed a relationship associated with the change in energy of the body due to growth of the crack. This relationship is expressed in terms of the path independent integral, which is given the symbol J. The integral J is defined as

$$J = \int_\Gamma \left(W(\varepsilon)dy - T_i \frac{\partial u_i}{\partial x}\, ds \right) \tag{56}$$

Here Γ is a curve surrounding the notch tip (Fig. 8(a)). The integral is evaluated in a counterclockwise sense, starting from the notch surface. Strain energy density is defined as

$$W(\varepsilon_{mn}) = \int_0^{\varepsilon_{mn}} \sigma_{ij} d\varepsilon_{ij} \tag{57}$$

the traction vector as

$$T_i = \sigma_{ij} n_j \tag{58}$$

and u_i is a displacement vector defined in terms of strain tensor as

$$\varepsilon_{ij} = \frac{1}{2} (u_{i,j} + u_{j,i}) \tag{59}$$

By considering the singular terms associated with the stress environment near the crack tip in linearly elastic body and evaluating equation (56) Rice obtained the following relations

$$\left.\begin{aligned} J &= \frac{1-\mu^2}{E} K_I^2 \qquad \text{(for plane strain)} \\ J &= \frac{1}{E} K_I^2 \qquad \text{(for plane stress)} \end{aligned}\right\} \tag{60}$$

Equations (60) allow to evaluate the stress intensity factors without detailed knowledge of the stress field very near the crack tip.

Choosing a rectangular path (Fig. 8(b)), and taking advantage of geometric and loading symmetry about x axis the contour integral J may be written as

$$\left.\begin{aligned} J = 2 &\int_1^2 \left[W(\varepsilon) - \sigma_x \varepsilon_x - \sigma_{xy} \frac{\partial u_y}{\partial x}\right] dy \\ &+ 2 \int_2^3 \left(\sigma_{xy} \varepsilon_x + \sigma_y \frac{\partial u_y}{\partial x}\right) dx \\ &+ 2 \int_3^4 \left[W(\varepsilon) - \sigma_x \varepsilon_x - \sigma_{xy} \frac{\partial u_y}{\partial x}\right] dy \end{aligned}\right\} \tag{61}$$

where

$$W(\varepsilon) = \int_0^{\varepsilon_{mn}} (\sigma_x d\varepsilon_x + 2\sigma_{xy} d\varepsilon_{xy} + \sigma_y d\varepsilon_y) \tag{62}$$

The limits of integration in equation (61) refer to the coordinates of the points indicated in Fig. 8(b).

4.4 Results and Discussion

In order to establish the validity of the potential method in the solution of the case of a single edge notched plate subjected to pure bending, various geometrical configurations were considered, and the results compared with solutions obtained by other investigators using different analytical methods.

The computations were performed for cases of 3, 10, 30, and 60 degrees notch angles and varying notch depths. Figures 9 through 11 show x-directional and y-directional stress distribution as a function of distance from the tip of the notch. The results are compared with stress values obtained by the boundary collocation technique reported by Gross [21] and are found to be in excellent agreement. Tables 1 through 5 contain selected results of these stress computations.

As expected, the stresses approach infinity near the tip of the notch. The square root signularity associated with the crack changes from 0.500 to approximately 0.488 for a 60 degree notch angle as shown in Table 6. The order of singularity computed herein is compared with results given by Gross and Mendelson [22] and excellent agreement is obtained.

Table 7 shows the dimensionless stress intensity factor $\tilde{K}_I$ for various notch angles, obtained by plotting of the relation (55), as compared to the analytical solution obtained by Gross and Mendelson [22]. Analytical results give values higher by approximately 1 percent.

Table 8 gives the dimensionless elastic plane stress displacements at the edge of the notch for various cases considered herein. The displacements were obtained by numerical integration of relation (59) along straight line paths. The comparison is made with available results by Gross [21] and are found to be in very good agreement.

Finally, the relationship between path independent Rice's integral J and the stress intensity factor K_I given by equation (60) was checked. For plane stress case, the comparison between J values obtained by numerical integration of relation (61) and by use of the second equation (60) is shown in Table 9.

The results obtained for various elastic cases compare very well with existing solutions, thus building up the confidence to applicability of the potential method to the elasto-plastic case.

Chapter 5

Solution of the Elasto-Plastic Problem

5.1 Method of Solution

The plane elasto-plastic problem is defined in terms of the Airy stress function $\tilde{\varphi}(\tilde{x},\tilde{y})$ by the non-homogeneous biharmonic equation (25)

$$\tilde{\nabla}^4\tilde{\varphi} = \tilde{g}(\tilde{x},\tilde{y})$$

subject to boundary conditions (28). The stress strain relations are given by equations (3) for plane strain case and by equations (4) for plane stress case, function $\tilde{g}(\tilde{x},\tilde{y})$ by equations (26) or (27) and plasticity relations by modified Prandtl-Reuss equations (15).

As shown in Section 3.3 the elasto-plastic problem could be reduced to the solution of the system of 2n simultaneous boundary equations (45), containing a non-zero function $\tilde{g}(\tilde{x},\tilde{y})$. This function is dependent on the stress field, which is defined by the stress equations (49). The stress equations (49) are signular for $i = k$, i.e., when $\tilde{x}_i = \tilde{\xi}_k$ and $\tilde{y}_i = \tilde{\eta}_k$ and plastic flow occurres. For the case of a rectangular grid the coefficients of $(\tilde{g}\tilde{A})_{i=k}$ in these equations can be evaluated by direct integration, yielding the following relations:

$$
\left.
\begin{aligned}
8\pi\tilde{\sigma}_x(\tilde{x},\tilde{y})_i = &\left\{\left[\ell n\left(\frac{\tilde{\delta}_x^2+\tilde{\delta}_y^2}{4}\right)+\frac{2\tilde{\delta}_y}{\tilde{\delta}_x}\tan^{-1}\frac{\tilde{\delta}_x}{\tilde{\delta}_y}-1\right](\tilde{g}\tilde{A})\right\}_{i=k}\\
&+\left\{\ell n\left[(\tilde{x}-\tilde{\xi})^2+(\tilde{y}-\tilde{\eta})^2\right]+\frac{2(\tilde{y}-\tilde{\eta})^2}{(\tilde{x}-\tilde{\xi})^2+(\tilde{y}-\tilde{\eta})^2}+1\right\}_{\substack{ik\\ i\neq k}}(\tilde{g}\tilde{A})_k\\
&+\tilde{A}_{ij}\tilde{\varphi}_j+\tilde{B}_{ij}\tilde{\varphi}'_j+\tilde{C}_{ij}\tilde{\Phi}_j+\tilde{D}_{ij}\tilde{\Phi}'_j\\
8\pi\tilde{\sigma}_y(\tilde{x},\tilde{y})_i = &\left\{\left[\ell n\left(\frac{\tilde{\delta}_x^2+\tilde{\delta}_y^2}{4}\right)+\frac{2\tilde{\delta}_x}{\tilde{\delta}_y}\tan^{-1}\frac{\tilde{\delta}_y}{\tilde{\delta}_x}-1\right](\tilde{g}\tilde{A})\right\}_{i=k}\\
&+\left\{\ell n\left[(\tilde{x}-\tilde{\xi})^2+(\tilde{y}-\tilde{\eta})^2\right]+\frac{2(\tilde{x}-\tilde{\xi})^2}{(\tilde{x}-\tilde{\xi})^2+(\tilde{y}-\tilde{\eta})^2}+1\right\}_{\substack{ik\\ i\neq k}}(\tilde{g}\tilde{A})_k\\
&-\tilde{A}_{ij}\tilde{\varphi}_j-\tilde{B}_{ij}\tilde{\varphi}'_j+\tilde{E}_{ij}\tilde{\Phi}_j+F_{ij}\tilde{\Phi}'_j\\
-8\pi\tilde{\sigma}_{xy}(\tilde{x},\tilde{y})_i = &\left[\frac{2(\tilde{x}-\tilde{\xi})(\tilde{y}-\tilde{\eta})}{(\tilde{x}-\tilde{\xi})^2+(\tilde{y}-\tilde{\eta})^2}\right]_{\substack{ik\\ i\neq k}}(\tilde{g}\tilde{A})_k\\
&+\tilde{G}_{ij}\tilde{\varphi}_j+\tilde{H}_{ij}\tilde{\varphi}'_j+\tilde{I}_{ij}\tilde{\Phi}_j+\tilde{K}_{ij}\tilde{\Phi}'_j
\end{aligned}
\right\} \tag{63}
$$

$$i = 1,2,3\cdots m; \qquad j = 1,2,3\cdots n; \qquad k = 1,2,3\cdots m$$

where $\tilde{\delta}_x$ and $\tilde{\delta}_y$ represent, respectively, x-directional and y-directional dimension of the cell.

The solution to this boundary value problem is obtained by an iterative process, known as the method of successive elastic solutions [51,52]. This method, applied to the present problem, proceeds as follows. The loading path is divided into a number of sufficiently small increments, $\Delta\tilde{q}_i$. The $\tilde{g}$ function in the inhomogeneous equation (25) is thought of as a sum of $\Delta\tilde{g}_i$ functions, each corresponding to its load increment, $\Delta\tilde{q}_i$. Each $\Delta\tilde{g}_i$ is defined in terms of derivatives of the current plastic strain increments, $\Delta\tilde{\varepsilon}^p_x$, $\Delta\tilde{\varepsilon}^p_y$ and $\Delta\tilde{\varepsilon}^p_{xy}$, which in turn depend, through equivalent plastic strain increment $\Delta\tilde{\varepsilon}_p$, on the equivalent stress $\tilde{\sigma}_{e,i-1}$ associated with the previous load. The current plastic strain increments change iteratively as changing $\Delta\tilde{g}_i$ affects the stress field.

The iterative procedure for determining plastic strain increments for each load increment is as follows:

(1) Select a value of load, $\tilde{q}_i$.

(2) Guess initial values of plastic strain increments. For the first load increment, assume all values to be equal to zero. Otherwise, use the converged values from the previous load increment.

(3) Calculate $\tilde{g}_i = \tilde{g}_{i-1} + \Delta\tilde{g}_i$.

(4) Calculate $\tilde{\Phi}_i$ and $\tilde{\Phi}'_i$ from boundary equations (45).

(5) Calculate the stresses from stress equations (63).

(6) Calculate the modified total strains from equation (13) and evaluate the equivalent modified total strain $\tilde{\varepsilon}_{et}$ from equation (14).

(7) Find the equivalent plastic strain increment $\Delta\tilde{\varepsilon}_p$ from equation (16), which, in dimensionless form, is

$$\Delta\tilde{\varepsilon}_p = \frac{\tilde{\varepsilon}_{et} - \frac{2}{3}(1+\mu)\tilde{\sigma}_{e,i-1}}{1 + \frac{2}{3}(1+\mu)\frac{m}{1-m}} \tag{64}$$

where $\tilde{\sigma}_{e,i-1}$ is the dimensionless value of the equivalent stress at the end of the previous increment of loading. For the first load increment and also for the case where there was no plastic flow under previous loading, $\tilde{\sigma}_{e,i-1}$ is equal to the dimensionless yield stress $\tilde{\sigma}_0$, i.e., unity.

(8) Calculate new set of plastic strain increments from equations (15), and new $\Delta\tilde{g}_i$ from equations (26) or (27).

(9) Repeat steps 3 to 8 until the plastic strain increments converge.

(10) Sum the plastic strain increments and return to step 1.

It should be noted at this point that the above procedure can be applied only where there is no unloading. Once the successive approximation procedure has converged, the stresses and strains can be obtained at any desired point in the interior of the plate.

The iterative process is illustrated by the flow diagram of Fig. 12.

5.2 Numerical Procedures

The choice of the size of the grid, which has to cover the plate in the area, where plastic flow is expected to occur, is of utmost importance. A too coarse grid will not detect changes in the values of plastic-strain for small loading increments. A too fine mesh size may result in distorted values of second order derivatives of plastic

strains, which appear in the function $\tilde{g}(\tilde{x},\tilde{y})$. The loading increment and the grid size are related to each other. A bad choice of either of them could result in the divergence of the iterative process. To allow the maximum of grid points to be within the expected plastic zone, a variable grid spacing was chosen. The grid used for plane strain conditions was finer, in general, than the one used for plane stress case. The arrangement of boundary subdivisions, similar to the one used in the solution of the elastostatic problem, and a typical interior grid are shown in Fig. 13.

The interior area of the plate, where plastic flow is expected, was divided into r x s rectangular cells. Due to symmetry about the x axis, the number of unknown functions $\tilde{g}$, appearing in the boundary equations (45) and stress equations (63), was reduced from r x s to $m = r \times \frac{s + 1}{2}$, where now the coefficients of these functions represent the sum of the effect of left-hand and right-hand sides of the plastic field. Because of computation time limitations, the grid was arranged in 27x23 cell pattern, resulting in the number of unknowns ($\tilde{g}$) to be equal to 324. By increasing the number of unknowns to 400, the computation time for one iteration almost doubled. The smallest cells, located in the vicinity of the tip of the notch, have dimensions $\tilde{\delta}_x = 0.004$, $\tilde{\delta}_y = 0.008$ for plane strain cases, and $\tilde{\delta}_x = 0.004$, $\tilde{\delta}_y = 0.016$ for plane stress case.

Cells with centroids outside the plate above the tip of the notch were discarded and corresponding values of $\tilde{g}$ were set to equal zero.

Before we can proceed with the numerical solution, it is necessary to represent the function of plastic strains, $\tilde{g}(\tilde{x},\tilde{y})$, given by partial differential equations (26) or (27), by corresponding finite-difference equations.

The finite difference net for grid station (r,s) is shown in Fig. 14. For a given function $f = f(x,y)$, by use of central differences, we can obtain the following expressions for derivatives of this function

$$\left.\begin{aligned}
f_x &= \beta_{r-1,s}(f_{r-1,s} - f_{r,s}) + \beta_{r+1,s}(f_{r+1,s} - f_{r,s}) \\
f_y &= \beta_{r,s-1}(f_{r,s-1} - f_{r,s}) + \beta_{r,s+1}(f_{r,s+1} - f_{r,s}) \\
f_{xx} &= \alpha_{r-1,s}(f_{r-1,s} - f_{r,s}) + \alpha_{r+1,s}(f_{r+1,s} - f_{r,s}) \\
f_{yy} &= \alpha_{r,s-1}(f_{r,s-1} - f_{r,s}) + \alpha_{r,s+1}(f_{r,s+1} - f_{r,s}) \\
f_{xy} &= \gamma_{r-1,s-1}f_{r-1,s-1} + \gamma_{r-1,s}f_{r-1,s} + \gamma_{r-1,s+1}f_{r-1,s+1} \\
&\quad + \gamma_{r,s-1}f_{r,s-1} + \gamma_{r,s}f_{r,s} + \gamma_{r,s+1}f_{r,s+1} + \gamma_{r+1,s-1}f_{r+1,s-1} \\
&\quad + \gamma_{r+1,s}f_{r+1,s} + \gamma_{r+1,s+1}f_{r+1,s+1}
\end{aligned}\right\} \qquad (65)$$

The subscripts x,y denote differentiation with respect to variables x or y, r is a row index, s is a column index and the coefficients are given by the following relations

$$
\left.
\begin{aligned}
\alpha_{r-1,s} &= \frac{2}{\Delta\tilde{x}\Delta\tilde{x}_T} \\
\alpha_{r+1,s} &= \frac{2}{\Delta\tilde{x}\Delta\tilde{x}_B} \\
\alpha_{r,s-1} &= \frac{2}{\Delta\tilde{y}\Delta\tilde{y}_L} \\
\alpha_{r,s+1} &= \frac{2}{\Delta\tilde{y}\Delta\tilde{y}_R} \\
\beta_{r-1,s} &= -\frac{\Delta\tilde{x}_B}{\Delta\tilde{x}\Delta\tilde{x}_T} \\
\beta_{r+1,s} &= \frac{\Delta\tilde{x}_T}{\Delta\tilde{x}\Delta\tilde{x}_B} \\
\beta_{r,s-1} &= -\frac{\Delta\tilde{y}_R}{\Delta\tilde{y}\Delta\tilde{y}_L} \\
\beta_{r,s+1} &= \frac{\Delta\tilde{y}_L}{\Delta\tilde{y}\Delta\tilde{y}_R} \\
\gamma_{r-1,s-1} &= \beta_{r-1,s}\beta_{r,s-1} \\
\gamma_{r-1,s+1} &= \beta_{r-1,s}\beta_{r,s+1} \\
\gamma_{r+1,s-1} &= \beta_{r,s-1}\beta_{r+1,s} \\
\gamma_{r+1,s+1} &= \beta_{r,s+1}\beta_{r+1,s} \\
\gamma_{r-1,s} &= -\gamma_{r-1,s-1} - \gamma_{r-1,s+1} \\
\gamma_{r,s-1} &= -\gamma_{r-1,s-1} - \gamma_{r+1,s-1} \\
\gamma_{r,s+1} &= -\gamma_{r-1,s+1} - \gamma_{r+1,s+1} \\
\gamma_{r+1,s} &= -\gamma_{r+1,s-1} - \gamma_{r+1,s+1} \\
\gamma_{r,s} &= \gamma_{r-1,s-1} + \gamma_{r-1,s+1} + \gamma_{r+1,s-1} + \gamma_{r+1,s+1}
\end{aligned}
\right\} \qquad (66)
$$

where $\Delta\tilde{x}$, $\Delta\tilde{y}$, $\Delta\tilde{x}_T$, $\Delta\tilde{x}_B$, $\Delta\tilde{y}_L$ and $\Delta\tilde{y}_R$ are distances as defined in Fig. 13.

When relations (65) and (66) are used the function $\tilde{g}(\tilde{x},\tilde{y})$

can be expressed by following finite-difference expressions

$$\tilde{g}(\tilde{x},\tilde{y}) = \frac{\mu}{1-\mu^2}\Bigg\{\alpha_{r-1,s}\left(\tilde{\varepsilon}_x^p + \Delta\tilde{\varepsilon}_x^p\right)_{r-1,s} - (\alpha_{r-1,s} + \alpha_{r+1,s})\left(\tilde{\varepsilon}_x^p + \Delta\tilde{\varepsilon}_x^p\right)_{r,s}$$

$$+ \alpha_{r+1,s}\left(\tilde{\varepsilon}_x^p + \Delta\tilde{\varepsilon}_x^p\right)_{r+1,s} + \alpha_{r,s-1}\left(\tilde{\varepsilon}_y^p + \Delta\tilde{\varepsilon}_y^p\right)_{r,s-1}$$

$$- (\alpha_{r,s-1} + \alpha_{r,s+1})\left(\tilde{\varepsilon}_y^p + \Delta\tilde{\varepsilon}_y^p\right)_{r,s} + \alpha_{r,s+1}\left(\tilde{\varepsilon}_y^p + \Delta\tilde{\varepsilon}_y^p\right)_{r,s+1}\Bigg\}$$

$$- \frac{1}{1+\mu}\Bigg\{\alpha_{r,s-1}\left(\tilde{\varepsilon}_x^p + \Delta\tilde{\varepsilon}_x^p\right)_{r,s-1} - (\alpha_{r,s-1} + \alpha_{r,s+1})\left(\tilde{\varepsilon}_x^p + \Delta\tilde{\varepsilon}_x^p\right)_{r,s}$$

$$+ \alpha_{r,s+1}\left(\tilde{\varepsilon}_x^p + \Delta\tilde{\varepsilon}_x^p\right)_{r,s+1} + \alpha_{r-1,s}\left(\tilde{\varepsilon}_y^p + \Delta\tilde{\varepsilon}_y^p\right)_{r-1,s}$$

$$- (\alpha_{r-1,s} + \alpha_{r+1,s})\left(\tilde{\varepsilon}_y^p + \Delta\tilde{\varepsilon}_y^p\right)_{r,s} + \alpha_{r+1,s}\left(\tilde{\varepsilon}_y^p + \Delta\tilde{\varepsilon}_y^p\right)_{r+1,s}\Bigg\}$$

$$+ \frac{2}{1-\mu^2}\Bigg\{\gamma_{r-1,s-1}\left(\tilde{\varepsilon}_{xy}^p + \Delta\tilde{\varepsilon}_{xy}^p\right)_{r-1,s-1} + \gamma_{r-1,s}\left(\tilde{\varepsilon}_{xy}^p + \Delta\tilde{\varepsilon}_{xy}^p\right)_{r-1,s}$$

$$+ \gamma_{r-1,s+1}\left(\tilde{\varepsilon}_{xy}^p + \Delta\tilde{\varepsilon}_{xy}^p\right)_{r-1,s+1} + \gamma_{r,s-1}\left(\tilde{\varepsilon}_{xy}^p + \Delta\tilde{\varepsilon}_{xy}^p\right)_{r,s-1}$$

$$+ \gamma_{r,s}\left(\tilde{\varepsilon}_{xy}^p + \Delta\tilde{\varepsilon}_{xy}^p\right)_{r,s} + \gamma_{r,s+1}\left(\tilde{\varepsilon}_{xy}^p + \Delta\tilde{\varepsilon}_{xy}^p\right)_{r,s+1}$$

$$+ \gamma_{r+1,s-1}\left(\tilde{\varepsilon}_{xy}^p + \Delta\tilde{\varepsilon}_{xy}^p\right)_{r+1,s-1} + \gamma_{r+1,s}\left(\tilde{\varepsilon}_{xy}^p + \Delta\tilde{\varepsilon}_{xy}^p\right)_{r+1,s}$$

$$+ \gamma_{r+1,s+1}\left(\tilde{\varepsilon}_{xy}^p + \Delta\tilde{\varepsilon}_{xy}^p\right)_{r+1,s+1}\Bigg\}\Bigg\}$$

Plane Strain (67)

and

$$\tilde{g}(\tilde{x},\tilde{y}) = -\Bigg\{\Bigg[\alpha_{r,s-1}\left(\tilde{\varepsilon}_x^p + \Delta\tilde{\varepsilon}_x^p\right)_{r,s-1} - (\alpha_{r,s-1} + \alpha_{r,s+1})\left(\tilde{\varepsilon}_x^p + \Delta\tilde{\varepsilon}_x^p\right)_{r,s}$$

$$+ \alpha_{r,s+1}\left(\tilde{\varepsilon}_x^p + \Delta\tilde{\varepsilon}_x^p\right)_{r,s+1} + \alpha_{r-1,s}\left(\tilde{\varepsilon}_y^p + \Delta\tilde{\varepsilon}_y^p\right)_{r-1,s}$$

$$- (\alpha_{r-1,s} + \alpha_{r+1,s})\left(\tilde{\varepsilon}_y^p + \Delta\tilde{\varepsilon}_y^p\right)_{r,s} + \alpha_{r+1,s}\left(\tilde{\varepsilon}_y^p + \Delta\tilde{\varepsilon}_y^p\right)_{r+1,s}$$

$$- 2\Bigg[\gamma_{r-1,s-1}\left(\tilde{\varepsilon}_{xy}^p + \Delta\tilde{\varepsilon}_{xy}^p\right)_{r-1,s-1} + \gamma_{r-1,s}\left(\tilde{\varepsilon}_{xy}^p + \Delta\tilde{\varepsilon}_{xy}^p\right)_{r-1,s}$$

$$+ \gamma_{r-1,s+1}\left(\tilde{\varepsilon}_{xy}^p + \Delta\tilde{\varepsilon}_{xy}^p\right)_{r-1,s+1} + \gamma_{r,s-1}\left(\tilde{\varepsilon}_{xy}^p + \Delta\tilde{\varepsilon}_{xy}^p\right)_{r,s-1}$$

$$+ \gamma_{r,s}\left(\tilde{\varepsilon}_{xy}^p + \Delta\tilde{\varepsilon}_{xy}^p\right)_{r,s} + \gamma_{r,s+1}\left(\tilde{\varepsilon}_{xy}^p + \Delta\tilde{\varepsilon}_{xy}^p\right)_{r,s+1}$$

$$+ \gamma_{r+1,s-1}\left(\tilde{\varepsilon}_{xy}^p + \Delta\tilde{\varepsilon}_{xy}^p\right)_{r+1,s-1} + \gamma_{r+1,s}\left(\tilde{\varepsilon}_{xy}^p + \Delta\tilde{\varepsilon}_{xy}^p\right)_{r+1,s}$$

$$+ \gamma_{r+1,s+1}\left(\tilde{\varepsilon}_{xy}^p + \Delta\tilde{\varepsilon}_{xy}^p\right)_{r+1,s+1}\Bigg]\Bigg\}\Bigg] \qquad \text{Plane Stress} \qquad (68)$$

Central difference equations (67) or (68) were used to evaluate $\tilde{g}(\tilde{x},\tilde{y})$ only for interior plastic cells, where there was plastic flow at all eight adjacent cells. For non-interior cells the function was taken as an average of values of $\tilde{g}$ at neighboring plastic cells. Other methods of dealing with $\tilde{g}$ at centroids of non-interior plastic cells, such as backward differences or extrapolation, led to oscillation or divergence of the iterative process.

The convergence criterion is defined as an arbitrary maximum difference between successive values of one or more iterants. For the plastic field containing many points at which convergence is required, it is reasonable to set the convergence criterion based on an average value of the change in plastic strain increments. For the problems considered in this disertation, the convergence criterion was based on the convergence of plastic strain increments $\Delta\tilde{\varepsilon}^p_y$ and was defined as

$$\frac{\sum_{j=1}^{n} \left| \Delta\tilde{\varepsilon}^p_{y,k} - \Delta\tilde{\varepsilon}^p_{y,k-1} \right|_j}{n} < T \qquad (69)$$

where k - referes to current iteration

n - referes to number of plastic grid points for current iteration

T - is an arbitrary convergence parameter.

The computations were performed on an IBM 7094/7044 DCS digital computer using a Fortran IV program with single precision arithmetic. A brief description and listing of this program is given in Appendix D.

The convergence parameter T was set to 0.005 for all cases to be considered. Decreasing the convergence parameter T to 0.001 resulted in change in plastic strain increment values of approximately one in the third or fourth significant figure. For higher order accuracy, which does not appear to be necessary from a practical point of view, the computation time would be prohibitively long. The fact that the method of successive elastic solutions converges to the right answer has been shown by many examples in references [51,57].

Chapter 6

Results and Discussion

The problems selected for analysis were limited to the following geometries and strain hardening parameters for plane strain and plane stress conditions.

Plane strain conditions:

Case (a) Notch depth $\tilde{a} = 0.5$, notch angle $\alpha = 10^{o}$, strain hardening parameter $m = 0.05$

(b) Notch depth $\tilde{a} = 0.5$, notch angle $\alpha = 10^{o}$, strain hardening parameter $m = 0.10$

(c) Notch depth $\tilde{a} = 0.3$, notch angle $\alpha = 3^{o}$, strain hardening parameter $m = 0.10$

(d) Notch depth $\tilde{a} = 0.3$, notch angle $\alpha = 10^{o}$, strain hardening parameter $m = 0.10$

Plane stress conditions:

Case (e) Notch depth $\tilde{a} = 0.3$, notch angle $\alpha = 10^{o}$, strain hardening parameter $m = 0.10$

The load increment size was found to be dependent on the strain hardening parameter m. For $m = 0.05$ it was necessary to limit the load increment size to $\Delta\tilde{q} = 0.05$, while for $m = 0.10$ the load was incremented by $\Delta\tilde{q} = 0.10$. For the plate with notch depth $\tilde{a} = 0.5$ the minimum load required to produce plastic flow in the most highly

stressed grid points was found to be $\tilde{q} = 0.35$, and for $\tilde{a} = 0.3$ the initial load was found to be $\tilde{q} = 0.50$. The maximum load considered was $\tilde{q}$ [illegible] $\tilde{a} = 0.5$ cases, and $\tilde{q} = 0.9$ for the $\tilde{a} = 0.3$ cases. In the process of solving the above listed problems, the case with strain hardening parameter $m = 0.05$ required approximately 50 iterations for each increment of load (i.e., $\Delta\tilde{q} = 0.05$) to produce a converged solution. For cases where the strain hardening parameter $m = 0.1$ the average number of iterations needed for each increment of load (i.e., $\Delta\tilde{q} = 0.10$) was reduced to 40.

It would be only proper at this time to call attention to the magnitude of the task of carrying out the computations for a single case. The computation time required to perform one iteration regardless of the number of plastic grid points was approximately 5 minutes. The total computation time for case (a) was approximately 2000 minutes, and for other cases 1000 minutes each. These times could have been reduced by an order of magnitude or more if the program were run on a faster computer or one with greater available memory and better organization. Such third generations computers as IBM 360/65 and CDC 6600 are examples.

While the development of the program and the method of solution was easier to implement on the slower computer used (the IBM 7094/7044 DCS), future work could be adapted to run on the above mentioned faster computers.

Additional computation time could be saved by use of a somewhat different solution technique, known as the tangent modulus method [33].

In this method, an equation similar to equation (25) is derived in terms of the rate of change of the stress function. Assuming the stresses and strains are known at a given time, the increment in stress function and therefore increments in stresses and strains can be computed using the stress-strain curve.

The results of computations are presented in Figs. 15 through 70 and Tables 10 through 113.

The growth of plastic zone size with a load is shown in Figs. 15 through 24. It is seen that the shapes of the elasto-plastic boundaries remain similar to each other as the load increases. As expected, plastic flow starts around the tip of the notch and as the load increases appears also at the boundary opposite the notch. Comparison of Figs. 16 and 18 shows that the size and shape of the plastic zone is a function of strain hardening parameter m, the difference being most noticeable along the x axis. Comparison of Figs. 21 and 22 with Figs. 23 and 24 shows that for the same loads the size of plastic zones for plane strain are considerably smaller than those for plane stress. This has been indicated in the results obtained by Swedlow [35] for a cracked plate loaded in uniaxial tension.

The equivalent stress contours in the vicinity of the notch for maximum applied loads are plotted in Figs. 25 through 29. The curves are the loci of all points of constant equivalent stress. The curves corresponding to $\tilde{\sigma}_e = 1$ indicate the boundary of the plastic zone. In addition, an elastic yield locus representing the elasto-plastic boundary based on the elastic solution is shown in each case. Since

this is commonly assumed to be the boundary of the plastic zone, we can see that for plane strain cases this assumption introduces considerable error. Along the x axis the lengths of plastic zones obtained by elasto-plastic and elastic solutions vary by the factor of less than two, which is in a good agreement with predictions made by Irwin [30]. For the plane stress case the shape of the plastic boundary for both methods of solution is almost identical.

Stresses and strains were calculated in all cases for interior grid points. Selected results of these calculations are given in Figs. 30 through 58 and Tables 10 through 111.

In Figs. 30 and 31 x-directional and y-directional stress is plotted as a function of load and of the distance from the tip of the notch for two different strain hardening parameters under plain strain conditions. The increase of strain hardening parameter m from 0.05 to 0.10 caused reduction in these stresses by a very small percentage.

Figures 32 through 45 show the stress distributions along the x axis for all cases investigated in this study. To check the validity of the results, the bending moments with respect to the neutral axis at $\tilde{y} = 0$ were calculated and compared with the respective loading moments. For the specimen with a notch depth $\tilde{a} = 0.5$ the variation between computed moment and loading moment was less than 1%; for the specimen with $\tilde{a} = 0.3$ the error was approximately 5%.

For selected cases the sum of forces acting in the y-direction along the x axis was calculated. The results show very good agreement with the theoretical value of zero.

The order of the stress singularity n was determined for each case. The results are given in Tables 112 and 113. In case of plane strain conditions, the stress singularity decreases slowly as loading increases. In the case of the plane stress condition we have a sudden drop in n from its elastic value as plastic flow appears. Subsequently n slowly increases approaching a limit as the load increases.

Tables 10 through 16 contain selected stress data.

The behavior of the total strain components in the vicinity of the notch is shown in Figs. 46 through 51 for a case of $\tilde{a} = 0.5$, $\alpha = 10^{o}$, $m = 0.05$ and plane strain condition. The strains were plotted along $\tilde{x}$ = constant and $\tilde{y}$ = constant lines for load $\tilde{q} = 0.7$. It is worth noting the magnitudes of strain gradients present throughout the plastic zone. These high gradients account for difficulty in obtaining dependable values for function of plastic strain increments, $\tilde{g}$ (eqs. (26) or (27)). In Figs. 52 through 55, the dimensionless x-directional and y-directional total strains are plotted along the x axis for all plane strain cases. Figures 56 through 58 show the distribution of dimensionless total strain components $\tilde{\varepsilon}_x$, $\tilde{\varepsilon}_y$, $\tilde{\varepsilon}_z$ along the x axis for a case of $\tilde{a} = 0.3$, $\alpha = 10^{o}$, $m = 0.10$ and plane stress condition. As expected, in all cases, the strains approach infinity near the tip of the notch.

The product of y-directional stress and total strain was calculated for various cases. The order of singularity of that product was determined by plotting $\ell n(\tilde{\sigma}_y \tilde{\varepsilon}_y)$ versus $\ell n\, \tilde{r}$ and by making a

least squares fit of a straight line through the plotted points. It was found to be very close to unity for all cases considered.

Dimensionless total plastic strains are listed in Tables 67 through 111 for all cases considered for selected loads. The coordinates $(\tilde{x},\tilde{y})$ correspond to centroids of cells where plastic flow occurred.

In the case of an elasto-plastic problem the stress intensity factor, as defined by equation (55), must be generalized to the form

$$K_I^*(\sigma_{max}) = \lim_{r\to 0} \sqrt{2\pi}\, r^{n(\sigma_{max})} \sigma_y(r,\theta)\Big|_{\theta=0} \tag{70}$$

or in terms of dimensionless quantities

$$\tilde{K}_I^*(\tilde{q}) = \lim_{\tilde{r}\to 0} \sqrt{2\pi}\, \tilde{r}^{n(\tilde{q})} \tilde{\sigma}_y(\tilde{r},\theta)\Big|_{\theta=0} \tag{71}$$

For linear elastic behavior $\tilde{K}_I^*$ is identical with $\tilde{K}_I$.

The generalized stress intensity factor is obtained by plotting the relation (71). The results are shown in Figs. 59 through 61. Figure 59 shows the effect of strain hardening parameter m on the dimensionless generalized stress intensity factor for the case of a specimen with notch depth of $\tilde{a} = 0.5$ and $\alpha = 10^o$, under plane strain condition. The stress intensity factor shows no significant increase over the linear elastic value up to an applied load of $\tilde{q} = 0.40$. Above this load $\tilde{K}_I^*$ increases progressively for both m's, at the faster rate for lower strain hardening parameter. Similar behavior of

the stress intensity factor can be observed for the case of $\tilde{a} = 0.3$, $\alpha = 3^{o}$ and $m = 0.10$ shown in Fig. 60. The effect of plane stress or plane strain conditions on $\tilde{K}_I^*$ is shown in Fig. 61 for a case of $\tilde{a} = 0.3$, $\alpha = 10^{o}$ and $m = 0.10$. Here the stress intensity factor increases more rapidly for the plane strain case than for the plane stress condition.

The dimensionless y-directional notch opening displacements are plotted in Figs. 62, 64, and 65 for various cases. They were obtained by numerical integration of relation (59) along straight line paths. For each case a number of paths were chosen through the plastic region near the notch, and the resulting displacements were averaged. In general, the notch opening displacement varies linearly with the load until the plastic zone is established at the boundary opposite the notch. Then it increases rapidly, reaching values several times that which would be calculated from the elastic solution.

In order to verify in part, the numerically computed results, the notch opening displacements for a specimen with a 10^{o} edge notch, notch depth $\tilde{a} = 0.5$ and strain hardening parameter $m = 0.05$ were compared with experimental results obtained by Bubsey, R. T. and Jones, M. [54]. The specimen used in this experiment, made of Al 5083-0 with length to width ratio of 4:1, crack length $\tilde{a} = 0.5$ was subjected to three point bending. The stress-strain curve for this specimen is shown in Fig. 63. The strain hardening parameter can be approximated as $m \approx 0.055$. The stress-strain curve was idealized by assuming yield point at $\sigma_0 = 20000$ lb/in.^{2} as shown in Fig. 63

and the dimensionless notch opening displacements were calculated from experimental data. The results are shown in Fig. 62 and are in very good agreement with numerical results obtained herein. As could be expected the pure bending of the specimen with a 10^{o} edge notch results in slightly higher displacements than those obtained for a specimen with a crack and subjected to three point bending.

Finally, Rice's J integral was evaluated for several cases by using relations given by equations (61) and (62). As in notch opening displacement calculations, straight line paths were chosen through the plastic zone near the tip of the notch. The integral was evaluated using values of stresses, strains and displacements at cells centroids for a number of paths. The path-independence of J was not conclusive, since the results varied up to 15% from the averaged value. Since the results obtained by Hayes [25] for the bodies deforming in accordance with the Prandtl-Reuss equations indicate path-independence of J integral, it is possible that the results obtained herein do not indicate that the path independent property is lost but rather than the field values, particularily strains, are not as accurate as one may desire.

The average values of the dimensionless $\tilde{J}$ integral as a function of load are plotted in Fig. 66 for a case of a specimen with a 10^{o} edge notch, $\tilde{a} = 0.5$, $m = 0.05$ and plain strain condition. At the start of plastic flow $\tilde{J}$ increases rapidly with load. This is followed by almost linear variation with additional load. Similar behavior is indicated in Figs. 67 and 68 for a case of a specimen with a

10^{o} edge notch, $\tilde{a} = 0.3$, $m = 0.10$ and plane strain or plane stress conditions.

The relations between Rice's $\tilde{J}$ integral and stress intensity factor $\tilde{K}_I$ developed for linear elasticity (60) are obviously not applicable for the elasto-plastic problem. By plotting the $\tilde{J}/\tilde{K}_I^{*2}$ ratios as a function of load $\tilde{q}$, the relation between Rice's $\tilde{J}$ integral and the dimensionless generalized stress intensity factor $\tilde{K}_I^{*}$ is obtained for the above three cases. The plots are shown in Figs. 69 and 70. In all cases, the ratio $\tilde{J}/\tilde{K}_I^{*2}$ remains almost equal to elastic value of 0.89 for plane strain or 1.0 for plane stress and increases sharply at the load corresponding to the appearnace of the plastic zone at the boundary opposite the notch. Once the transition occurs the ratio increases approximately proportionally to the load increment.

Chapter 7

Summary and Conclusions

The boundary integral equation method was applied in the solution of the plane elasto-plastic problems. The use of this method was illustrated by obtaining stress and strain distributions for a number of specimens with a single edge notch and subjected to pure bending. The boundary integral equation method reduced the non-homogenious biharmonic equation to two coupled Fredholm-type integral equations. These integral equations were replaced by a system of simultaneous algebraic equations and solved numerically in conjunction with a method of successive elastic solutions.

In order to check the validity of this method, several elasto-static problems were solved. To improve the accuracy of the solution in the region of interest, i.e., in the vicinity of the notch, nodal spacing along the notch was taken as uniformaly decreasing in length toward the tip of the notch. The results proved to be very sensitive to the minimum segment length. The comparison of calculated stress distributions, stress intensity factors and displacements with available solutions obtained by others showed very good agreement.

This method, applied to elasto-plastic problems, proved to be capable of giving very detailed results such as stress and strain

distributions around the tip of the notch and, related to them, the shapes of plastic zones. A need for such detailed stress and strain distributions existed for some time in the field of fracture mechanics.

The obtained results also provide the information on the effect of strain hardening and on the differences that occur between plane stress and plane strain solutions. The singular nature of stresses and strains in the vicinity of the tip of the notch was confirmed. The order of singularity for the strain energy density was found to be unity, which is consistent with results previously obtained by other investigators.

To verify in part the numerically computed results, the notch opening displacement for one case was checked with the experimental results obtained for three point bending of an edge cracked specimen. Allowing for the difference in the notch angle and the loading method, the results were in good agreement.

The generalized stress intensity factor was introduced and calculated for several cases. Once the plastic zone was established around the tip of the notch, this parameter increased progressively over its elastic value. For cases considered it increased more rapidly for the plane strain condition than for the corresponding plane stress condition.

Rice's $\tilde{J}$ integral was calculated for several cases. Its path independence property has been qualitatively confirmed and the relation

between $\tilde{J}$ and the generalized stress intensity factor was graphically extended to the materials deforming according to the Prandtl-Reuss theory of plasticity.

The presence of a singularity at the tip of the notch makes accurate answers very difficult to obtain. Some improvement in the solution techniques and further investigation of the influence of the boundary nodal spacing and interior grid size on the resulting stress and strain fields, and therefore, on the notch opening displacements and J integrals, may be desirable. As a further check of the validity of the results obtained herein, an experimental program to measure notch opening displacements and to evaluate Rice's J integrals would be of great value.

Appendix A

Stress Function and Its Derivative Along the Boundaries of V-Notched Plate

The boundary conditions to be satisfied by the stress function $\varphi(x,y)$ [55] are

$$\left.\begin{aligned} \frac{\partial \varphi}{\partial y} &= \int^{s} T_x ds + C_1 \\ \frac{\partial \varphi}{\partial x} &= -\int^{s} T_y ds + C_2 \end{aligned}\right\} \qquad (A.1)$$

where

$$T_i = \sigma_{ij} \eta_j$$

are the boundary tractions. The integrations are performed along boundary.

Equations (A.1) permit to express the boundary value problem in terms of stress function $\varphi(x,y)$ and its normal derivative $\frac{\partial \varphi(x,y)}{\partial n}$ on the boundary.

Since the total differential is given by

$$d\varphi = \frac{\partial \varphi}{\partial x} dx + \frac{\partial \varphi}{\partial y} dy$$

we have by applying the chain rule

$$\left.\begin{aligned} \frac{\partial \varphi}{\partial s} &= \frac{\partial \varphi}{\partial x}\frac{dx}{ds} + \frac{\partial \varphi}{\partial y}\frac{dy}{ds} \\ \frac{\partial \varphi}{\partial n} &= \frac{\partial \varphi}{\partial x}\frac{dx}{dn} + \frac{\partial \varphi}{\partial y}\frac{dy}{dn} \end{aligned}\right\} \qquad (A.2)$$

Introducing direction cosines ℓ and m of the angles the outward normal n makes with the x and y axis, respectively, we have the following relations (Fig. 71)

$$\left.\begin{aligned} \ell &= \cos(x,n) = \frac{dx}{dn} = \frac{dy}{ds} \\ m &= \cos(y,n) = \frac{dy}{dn} = -\frac{dx}{ds} \end{aligned}\right\} \tag{A.3}$$

Substituting relations (A.3) into the first of equations (A.2) and integrating, we obtain

$$\varphi = \int^{s} \left(\frac{\partial \varphi}{\partial y}\,\ell - \frac{\partial \varphi}{\partial x}\,m\right) ds + C_3 \tag{A.4}$$

The second equation (A.2) combined with equations (A.3) yields

$$\frac{\partial \varphi}{\partial n} = \frac{\partial \varphi}{\partial x}\,\ell + \frac{\partial \varphi}{\partial y}\,m \tag{A.5}$$

Consider boundary along the notch OA (Fig. 1). For the unloaded boundary, tractions $T_x = T_y = 0$.

Since the stresses depend on the second derivatives of the stress function φ, we can arbitrarily set constants C_1, C_2, and C_3 in equations (A.1) and (A.4) equal to zero.

Combining equations (A.1), (A.4), and (A.5), we obtain that the stress function φ and its normal derivative $\frac{\partial \varphi}{\partial n}$ has to satisfy the following conditions along boundary OA

$$\varphi = 0; \qquad \frac{\partial \varphi}{\partial n} = 0 \tag{A.6}$$

Along the boundary AB, since $T_x = T_y = 0$, we have

$$\varphi = 0; \qquad \frac{\partial \varphi}{\partial n} = 0 \tag{A.7}$$

Along boundary BC, direction cosines are $\ell = 0$, $m = 1$, and the boundary tractions are

$$\left.\begin{aligned} T_x &= 0 \\ T_y &= \sigma_y = \frac{2\sigma_{max}}{w}\left(\frac{w}{2} - a - x\right) \end{aligned}\right\} \tag{A.8}$$

Substituting these tractions into equations (A.1) we have

$$\left.\begin{aligned} \frac{\partial \varphi}{\partial y} &= C_1 \\ \frac{\partial \varphi}{\partial x} &= \int \frac{2\sigma_{max}}{w}\left(\frac{w}{2} - a - x\right) dx + C_2 \end{aligned}\right\} \tag{A.9}$$

Since the derivatives of stress function at point B on the boundary must be continuous, we have the following conditions

$$\left.\frac{\partial \varphi}{\partial y}\right|_{B(-a,L)} = 0 \qquad \left.\frac{\partial \varphi}{\partial x}\right|_{B(-a,L)} = 0 \tag{A.10}$$

Therefore, it follows from equation (A.9)

$$\left.\begin{aligned} \frac{\partial \varphi}{\partial y} &\equiv \frac{\partial \varphi}{\partial n} = 0 \\ \text{and} \qquad \frac{\partial \varphi}{\partial x} &= \frac{2\sigma_{max}}{w}\left(\frac{w}{2}x - ax - \frac{x^2}{2}\right) + \sigma_{max}\frac{a}{w}(w - a) \end{aligned}\right\} \tag{A.11}$$

Substituting relations from equation (A.11) into equation (A.4), integrate, noting that $ds = -dx$ and at $B(-a,L)$ the stress function $\varphi = 0$, we obtain

$$\left.\begin{aligned} \varphi = &-\frac{\sigma_{max}}{w}\left(\frac{x^3}{3} + ax^2 + a^2x + \frac{a^3}{3}\right) \\ &+ \sigma_{max}\left(\frac{x^2}{2} + ax + \frac{a^2}{2}\right) \end{aligned}\right\} \tag{A.12}$$

Along boundary CD the tractions $T_x = T_y = 0$. Due to the continuity of stress function and its derivatives we have

$$\left.\begin{aligned} \varphi &= \varphi_{C(w-a,L)} = \frac{\sigma_{max} w^2}{6} \\ \frac{\partial \varphi}{\partial n} &= \frac{\partial \varphi}{\partial x} = \left.\frac{\partial \varphi}{\partial x}\right|_{C(w-a,L)} = 0 \end{aligned}\right\} \tag{A.13}$$

Using dimensionless relations (24), making all distances dimensionless with respect to the width of the plate w and making use of geometrical and loading symmetry about x axis, the boundary conditions can be summarized as follows:

$$\left.\begin{aligned} &\text{along boundary OA and OA'} \quad \tilde{\varphi} = 0; \qquad \frac{\partial \tilde{\varphi}}{\partial \tilde{n}} = 0 \\ &\text{along boundary AB and A'B'} \quad \tilde{\varphi} = 0; \qquad \frac{\partial \tilde{\varphi}}{\partial \tilde{n}} = 0 \\ &\text{along boundary BC and B'C'} \\ &\qquad \tilde{\varphi} = -\tilde{q}\left(\frac{\tilde{x}^3}{3} + \tilde{a}\tilde{x}^2 + \tilde{a}^2\tilde{x} + \frac{\tilde{a}^3}{3}\right) + \tilde{q}\left(\frac{\tilde{x}^2}{2} + \tilde{a}\tilde{x} + \frac{\tilde{a}^2}{2}\right) \\ &\qquad \frac{\partial \tilde{\varphi}}{\partial \tilde{n}} = 0 \\ &\text{along boundary CD and C'D} \quad \tilde{\varphi} = \frac{\tilde{q}}{6}; \qquad \frac{\partial \tilde{\varphi}}{\partial \tilde{n}} = 0 \end{aligned}\right\} \tag{A.14}$$

Appendix B

Green's Boundary Formula for Interior Points and Boundary Points

The integrals over boundary C appearing in equations (36) and (39) are singular at points $P(x,y) \subset C$ when $r(x,y,\xi,\eta) = 0$.

In order to perform integration we must exclude singular point by drawing a small semi-circle of radius ε about point P, as shown in Fig. 72. We now perform the integration along the new path and let ε go to zero.

Let contour

$$C' = C - C_{AB}$$

Then line integral from equation (36) can be written as

$$\lim_{\varepsilon \to 0} \int_{C'+C_\varepsilon} \left[\Phi \frac{\partial}{\partial n} (\ell n\ r) - \frac{\partial \Phi}{\partial n} \ell n\ r \right] ds =$$

$$= \int_{C'} \Phi \frac{\partial}{\partial n} (\ell n\ r) ds - \lim_{\varepsilon \to 0} \int_{C_\varepsilon} \Phi \frac{\partial}{\partial n} (\ell n\ r) ds - \int_{C'} \frac{\partial \Phi}{\partial n} \ell n\ r\ ds$$

$$+ \lim_{\varepsilon \to 0} \int_{C_\varepsilon} \frac{\partial \Phi}{\partial n} \ell n\ r\ ds \qquad \text{(B.1)}$$

Evaluating integrals, with $\frac{\partial}{\partial n} \equiv \frac{\partial}{\partial r}$, we have

$$\left.\begin{aligned} \lim_{\varepsilon\to 0} \int_{C_\varepsilon} \Phi \frac{\partial}{\partial n} (\ell n\ r) ds &= \lim_{\varepsilon\to 0} \int_0^{\pi} \Phi \frac{1}{\varepsilon} \varepsilon d\theta = \pi\Phi \\ \lim_{\varepsilon\to 0} \int_{C_\varepsilon} \frac{\partial \Phi}{\partial n} \ell n\ r\ ds &= \lim_{\varepsilon\to 0} \int_0^{\pi} \frac{\partial \Phi}{\partial n} \varepsilon\ \ell n\ \varepsilon d\theta = 0 \end{aligned}\right\} \quad (B.2)$$

Substitution of relations (B.2) into equation (B.1) yields

$$\lim_{\varepsilon\to 0} \int_{C'+C_\varepsilon} \left[\Phi \frac{\partial}{\partial n} (\ell n\ r) - \frac{\partial \Phi}{\partial n} \ell n\ r\right] ds = \int_{C-I(P)} \Phi \frac{\partial}{\partial n} (\ell n\ r) ds$$

$$- \int_C \frac{\partial \Phi}{\partial n} \ell n\ r\ ds - \pi\Phi \qquad \text{for } P \subset C \quad (B.3)$$

where $\int_{C-I(P)}$ means the integral along the boundary C excluding integral about singularity.

The line integral from equation (39) will be evaluated in the similar way

$$\lim_{\varepsilon\to 0} \int_{C'+C_\varepsilon} \left[\varphi \frac{\partial}{\partial n} (\nabla^2\rho) - \frac{\partial \varphi}{\partial n} \nabla^2\rho + \Phi \frac{\partial \rho}{\partial n} - \frac{\partial \Phi}{\partial n} \rho\right] ds = \int_{C'} \varphi \frac{\partial}{\partial n} (\nabla^2\rho) ds$$

$$- \lim_{\varepsilon\to 0} \int_{C_\varepsilon} \varphi \frac{\partial}{\partial n} (\nabla^2\rho) ds - \int_{C'} \frac{\partial \varphi}{\partial n} \nabla^2\rho ds + \lim_{\varepsilon\to 0} \int_{C_\varepsilon} \frac{\partial \varphi}{\partial n} \nabla^2\rho ds$$

$$+ \int_{C'} \Phi \frac{\partial \rho}{\partial n} ds - \lim_{\varepsilon\to 0} \int_{C_\varepsilon} \Phi \frac{\partial \rho}{\partial n} ds - \int_{C'} \frac{\partial \Phi}{\partial n} \rho ds$$

$$+ \lim_{\varepsilon\to 0} \int_{C_\varepsilon} \frac{\partial \Phi}{\partial n} \rho ds \quad (B.4)$$

Since

$$\rho = r^2 \ln r \quad \text{and} \quad \frac{\partial}{\partial n} \equiv \frac{\partial}{\partial r}$$

we have

$$\left.\begin{aligned} &\frac{\partial \rho}{\partial n} \equiv \frac{\partial \rho}{\partial r} = r(2\ln r + 1) \\ &\nabla^2 \rho \equiv \frac{\partial^2 \rho}{\partial r^2} + \frac{1}{r}\frac{\partial \rho}{\partial r} = 4(\ln r + 1) \\ &\frac{\partial}{\partial n}(\nabla^2 \rho) \equiv \frac{\partial}{\partial r}(\nabla^2 \rho) = \frac{4}{r} \\ &\nabla^4 \rho = 0 \end{aligned}\right\} \qquad (B.5)$$

Evaluating integrals from equation (B.4) using relations (B.5)

$$\left.\begin{aligned} &\lim_{\varepsilon\to 0} \int_{C_\varepsilon} \varphi \frac{\partial}{\partial n}(\nabla^2 \rho) ds = \lim_{\varepsilon\to 0} \int_0^{\pi} \varphi \frac{4}{\varepsilon} \varepsilon d\theta = 4\pi\varphi \\ &\lim_{\varepsilon\to 0} \int_{C_\varepsilon} \frac{\partial \varphi}{\partial n} \nabla^2 \rho ds = \lim_{\varepsilon\to 0} 4 \int_0^{\pi} \frac{d\varphi}{\partial r} \varepsilon(\ln \varepsilon + 1) d\theta = 0 \\ &\lim_{\varepsilon\to 0} \int_{C_\varepsilon} \Phi \frac{\partial \rho}{\partial n} ds = \lim_{\varepsilon\to 0} \int_0^{\pi} \Phi \varepsilon (2\ln \varepsilon + 1) \varepsilon d\theta = 0 \\ &\lim_{\varepsilon\to 0} \int_{C_\varepsilon} \frac{\partial \Phi}{\partial n} \rho ds = \lim_{\varepsilon\to 0} \int_0^{\pi} \frac{\partial \Phi}{\partial r} \varepsilon^2 \ln \varepsilon d\theta = 0 \end{aligned}\right\} \qquad (B.6)$$

and substituting them into equation (B.4) yields

$$\lim_{\varepsilon\to 0} \int_{C'+C_\varepsilon} \left[\varphi \frac{\partial}{\partial n}(\nabla^2 \rho) - \frac{\partial \varphi}{\partial n} \nabla^2 \rho + \Phi \frac{\partial \rho}{\partial n} - \frac{\partial \Phi}{\partial n} \rho\right] ds = \int_{C-I(P)} \varphi \frac{\partial}{\partial n}(\nabla^2 \rho) ds$$

$$+ \int_C \left[-\frac{\partial \varphi}{\partial n} \nabla^2 \rho + \Phi \frac{\partial \rho}{\partial n} - \frac{\partial \Phi}{\partial n} \rho\right] ds - 4\pi\varphi \qquad \text{for } P \subset C \qquad (B.7)$$

In order to derive the corresponding relationship for $P \subset R$ we introduce a new boundary contour.

The singular point is excluded by drawing a small circle of radius ε about point P and introducing a slit in region R between points A on contour C and B on contour C_ε, forming a new boundary $C + C_L + C_\varepsilon$, as shown in Fig. 73. The arrows on the contour refer to the direction of integration. Since $\int_A^B = -\int_B^A$, line integral from equation (36) can be written as

$$\lim_{\varepsilon\to 0} \int_{C+C_\varepsilon} \left[\Phi \frac{\partial}{\partial n}(\ell n\ r) - \frac{\partial \Phi}{\partial n} \ell n\ r\right] ds = \int_C \Phi \frac{\partial}{\partial n}(\ell n\ r) ds$$

$$- \lim_{\varepsilon\to 0} \int_{C_\varepsilon} \Phi \frac{\partial}{\partial n}(\ell n\ r) ds - \int_C \frac{\partial \Phi}{\partial n} \ell n\ r\ ds + \lim_{\varepsilon\to 0} \int_{C_\varepsilon} \frac{\partial \Phi}{\partial n} \ell n\ r\ ds \qquad (B.8)$$

Since the limits of integration over contour C_ε are 0 and 2π, equation (B.8) yields

$$\lim_{\varepsilon\to 0} \int_{C+C_\varepsilon} \left[\Phi \frac{\partial}{\partial n}(\ell n\ r) - \frac{\partial \Phi}{\partial n} \ell n\ r\right] ds = \int_{C-I(P)} \Phi \frac{\partial}{\partial n}(\ell n\ r) ds$$

$$- \int_C \frac{\partial \Phi}{\partial n} \ell n\ r\ ds - 2\pi\Phi \qquad \text{for } P \subset R \qquad (B.9)$$

Line integral from equation (39) yields

$$\lim_{\varepsilon \to 0} \int_{C+C_\varepsilon} \left[\varphi \frac{\partial}{\partial n} (\nabla^2 \rho) - \frac{\partial \varphi}{\partial n} \nabla^2 \rho + \Phi \frac{\partial \rho}{\partial n} - \frac{\partial \Phi}{\partial n} \rho \right] ds = \int_{C-I(P)} \varphi \frac{\partial}{\partial n} (\nabla^2 \rho) ds$$

$$+ \int_C \left[- \frac{\partial \varphi}{\partial n} \nabla^2 \rho + \Phi \frac{\partial \rho}{\partial n} - \frac{\partial \Phi}{\partial n} \rho \right] ds - 8\pi\varphi \qquad \text{for } P \subset R \qquad (B.10)$$

Appendix C

Evaluation of the Coefficients in the Boundary and Stress Equations

The coefficients to be evaluated can be expressed in general dimensionless form as

$$\int_{(\tilde{\xi}_j, \tilde{\eta}_j)}^{(\tilde{\xi}_{j+1}, \tilde{\eta}_{j+1})} f(\tilde{r})\, d\tilde{s}$$

or

$$\int_{(\tilde{\xi}_j, \tilde{\eta}_j)}^{(\tilde{\xi}_{j+1}, \tilde{\eta}_{j+1})} f(\tilde{\rho})\, d\tilde{s}$$

with

$$\left.\begin{aligned} \tilde{r} &= \sqrt{(\tilde{x}_i - \tilde{\xi})^2 + (\tilde{y}_i - \tilde{\eta})^2} \\ \text{and} \qquad \tilde{\rho} &= \tilde{r}^2 \ln \tilde{r} \end{aligned}\right\} \qquad (C.1)$$

where $\tilde{x}_i, \tilde{y}_i$ are the coordinates of the point $P \subset C$ for the boundary equations (45) and point $P \subset R$ for the stress equations (49).

For the boundary, which consists of straight lines, the coefficients can be evaluated analytically. Let us divide the boundary into straight line intervals. Let $\tilde{x}_i$ and $\tilde{y}_i$ designate the coordinates of the i^{th} node and let $\tilde{\xi}_j$ and $\tilde{\eta}_j$ designate coordinates of the

starting point of j^{th} interval, and $\tilde{\xi},\tilde{\eta}$ represent variable coordinates in the j^{th} interval.

Also, let ℓ_j and m_j be direction cosines the outward normal to the j^{th} segment makes respectively with $\tilde{x}$ and $\tilde{y}$ axes (Fig. 74). Since

$$\ell_j = \cos(\tilde{n},\tilde{x}) = \cos\theta$$

$$m_j = \cos(\tilde{n},\tilde{y}) = -\sin\theta$$

we have

$$d\tilde{s} = \sin\theta\ d\tilde{\xi} + \cos\theta\ d\tilde{\eta}$$

or

$$d\tilde{s} = -m_j d\tilde{\xi} + \ell_j d\tilde{\eta} \tag{C.2}$$

Normal derivative, designated by prime superscripts, is given by

$$\frac{\partial}{\partial\tilde{n}} = \ell_j \frac{\partial}{\partial\tilde{\xi}} + m_j \frac{\partial}{\partial\tilde{\eta}} \tag{C.3}$$

C.1 Coefficients of the Boundary Equations

The boundary coefficients, given by equation (44) are

$$\left.\begin{aligned}
\tilde{a}_{ij} &= \int_j (\ell n\ \tilde{r}_{ij})'\, d\tilde{s} \\
\tilde{b}_{ij} &= -\int_j \ell n\ \tilde{r}_{ij}\, d\tilde{s} \\
\tilde{c}_{ij} &= \int_j \tilde{\rho}'_{ij}\, d\tilde{s} \\
\tilde{d}_{ij} &= -\int_j \tilde{\rho}_{ij}\, d\tilde{s} \\
\tilde{e}_{ij} &= \int_j (\tilde{\nabla}^2\tilde{\rho}_{ij})'\, d\tilde{s} \\
\tilde{f}_{ij} &= -\int_j \tilde{\nabla}^2\tilde{\rho}_{ij}\, d\tilde{s}
\end{aligned}\right\} \tag{C.4}$$

Let us transform expressions given by equation (C.4) by use of equations (C.1), (C.2), and (C.3) into the following form

$$\left.\begin{aligned}
\tilde{a}_{ij} &= -\int_j \left[\frac{\tilde{x}_i - \tilde{\xi}}{\tilde{r}_{ij}^2}\ell_j + \frac{\tilde{y}_i - \tilde{\eta}}{\tilde{r}_{ij}^2} m_j\right][-m_j d\tilde{\xi} + \ell_j d\tilde{\eta}] \\
\tilde{b}_{ij} &= -\int_j \ell n\ \tilde{r}_{ij}(-m_j d\tilde{\xi} + \ell_j d\tilde{\eta}) \\
\tilde{c}_{ij} &= -\int_j (1 + \ell n\ \tilde{r}_{ij}^2)[(\tilde{x}_i - \tilde{\xi})\ell_j + (\tilde{y}_i - \tilde{\eta})m_j][-m_j d\tilde{\xi} + \ell_j d\tilde{\eta}] \\
\tilde{d}_{ij} &= -\int_j \tilde{r}_{ij}^2 \ell n\ \tilde{r}_{ij}[-m_j d\tilde{\xi} + \ell_j d\tilde{\eta}] \\
\tilde{e}_{ij} &= 4\tilde{a}_{ij} \\
\tilde{f}_{ij} &= -4\int_j (1 + \ell n\ \tilde{r}_{ij})(-m_j d\tilde{\xi} + \ell_j d\tilde{\eta}) \\
&= -4\int_j (-m_j d\tilde{\xi} + \ell_j d\tilde{\eta}) + 4\tilde{b}_{ij}
\end{aligned}\right\} \qquad \text{(C.5)}$$

For the j^{th} segment we have the following relations (Fig. 74)

where

$$\left.\begin{aligned}
\tilde{\eta} &= b_j\tilde{\xi} + \tilde{a}_j \\
\tilde{a}_j &= \tilde{\eta}_j - b_j\tilde{\xi}_j \\
b_j &= -\frac{\ell_j}{m_j}
\end{aligned}\right\} \qquad \text{(C.6)}$$

Inversely

$$\left.\begin{aligned} \tilde{\xi} &= d_j \tilde{\eta} + c_j \\ \text{where} \\ \tilde{c}_j &= -\frac{\tilde{a}_j}{b_j} \\ d_j &= \frac{1}{b_j} = -\frac{m_j}{\ell_j} \end{aligned}\right\} \qquad (C.7)$$

Since the boundary segments parallel to x axis have $m_j = \pm 1$, $\ell_j = 0$ relations given by equation (C.6) must be used. For segments parallel to y axis, where $m_j = 0$, $\ell_j = \pm 1$, equation (C.7) will apply. For the boundary along the notch either of these relations could be used.

C.1.1 Boundary segments on the notch and segments parallel to x axis

Combining first of equations (C.5) with equation (C.1) and equation (C.6) and using $m_j^2 + \ell_j^2 = 1$ yields

$$\tilde{a}_{ij} = (\tilde{y}_i - b_j \tilde{x}_i - \tilde{a}_j) \int_{\tilde{\xi}_j}^{\tilde{\xi}_{j+1}} \frac{d\tilde{\xi}}{(\tilde{x}_i - \tilde{\xi})^2 + (\tilde{y}_i - \tilde{a}_j - b_j \tilde{\xi})^2}$$

Evaluating the integral [56] results in

$$\left.\begin{aligned} \tilde{a}_{ij} = &\tan^{-1} \frac{\frac{\tilde{\xi}_{j+1}}{m_j^2} - \left(\tilde{x}_i + \frac{\ell_j^2}{m_j^2}\tilde{\xi}_j\right) + \frac{\ell_j}{m_j}(\tilde{y}_i - \tilde{\eta}_j)}{(\tilde{y}_i - \tilde{\eta}_j) + \frac{\ell_j}{m_j}(\tilde{x}_i - \tilde{\xi}_j)} \\ &- \tan^{-1} \frac{\frac{\tilde{\xi}_j}{m_j^2} - \left(\tilde{x}_i + \frac{\ell_j^2}{m_j^2}\tilde{\xi}_j\right) + \frac{\ell_j}{m_j}(\tilde{y}_i - \tilde{\eta}_j)}{(\tilde{y}_i - \tilde{\eta}_j) + \frac{\ell_j}{m_j}(\tilde{x}_i - \tilde{\xi}_j)} \\ &\text{for } i \neq j; \\ &\text{for } i = j \text{ limiting process gives } a_{ii} = 0 \end{aligned}\right\} \qquad (C.8)$$

In a similar way we evaluate the rest of coefficients given by equation (C.5)

$$\tilde{b}_{ij} = \frac{1}{2m_j} \int_{\tilde{\xi}_j}^{\tilde{\xi}_{j+1}} \ell n[(\tilde{x}_i - \tilde{\xi})^2 + (\tilde{y}_i - \tilde{a}_j - b_j\tilde{\xi})^2]d\tilde{\xi}$$

$$= \frac{1}{2m_j}\left\{\int_{\tilde{\xi}_j}^{\tilde{\xi}_{j+1}} \ell n[(\tilde{x}_i - \tilde{\xi}) + i(\tilde{y}_i - \tilde{a}_j - b_j\tilde{\xi})]d\tilde{\xi}\right.$$

$$\left. + \int_{\tilde{\xi}_j}^{\tilde{\xi}_{j+1}} \ell n[(\tilde{x}_i - \tilde{\xi}) - i(\tilde{y}_i - \tilde{a}_j - \ _j\tilde{\xi})]d\tilde{\xi}\right\}$$

or

$$\tilde{b}_{ij} = -\frac{\Delta\tilde{\xi}_j}{m_j} + \frac{m_j}{2}\left[\frac{\ell_j}{m_j}(\tilde{y}_i - \tilde{\eta}_{j+1}) - (\tilde{x}_i - \tilde{\xi}_{j+1})\right] \ell n\left[(\tilde{x}_i - \tilde{\xi}_{j+1})^2\right.$$

$$\left. + (\tilde{y}_i - \tilde{\eta}_{j+1})^2\right] - \frac{m_j}{2}\left[\frac{\ell_j}{m_j}(\tilde{y}_i - \tilde{\eta}_j) - (\tilde{x}_i - \tilde{\xi}_j)\right] \ell n\left[(\tilde{x}_i - \tilde{\xi}_j)^2\right.$$

$$\left. + (\tilde{y}_i - \tilde{\eta}_j)^2\right] + m_j\left[(\tilde{y}_i - \tilde{\eta}_j) + \frac{\ell_j}{m_j}(\tilde{x}_i - \tilde{\xi}_j)\right]$$

$$\left[\tan^{-1}\frac{\frac{\tilde{\xi}_{j+1}}{2} - \left(\tilde{x}_i + \frac{\ell_j^2}{m_j^2}\tilde{\xi}_j\right) + \frac{\ell_j}{m_j}(\tilde{y}_i - \tilde{\eta}_j)}{(\tilde{y}_i - \tilde{\eta}_j) + \frac{\ell_j}{m_j}(\tilde{x}_i - \tilde{\xi}_j)}\right.$$

$$\left. - \tan^{-1}\frac{\frac{\tilde{\xi}_j}{2} - \left(\tilde{x}_i + \frac{\ell_j^2}{m_j^2}\tilde{\xi}_j\right) + \frac{\ell_j}{m_j}(\tilde{y}_i - \tilde{\eta}_j)}{(\tilde{y}_i - \tilde{\eta}_j) + \frac{\ell_j}{m_j}(\tilde{x}_i - \tilde{\xi}_j)}\right] \qquad (C.9)$$

where $\Delta\tilde{\xi}_j = \tilde{\xi}_{j+1} - \tilde{\xi}_j$

For the next coefficient, we have

$$\tilde{c}_{ij} = \int_{\tilde{\xi}_j}^{\tilde{\xi}_{j+1}} (\tilde{y}_i - \tilde{a}_j - b_j\tilde{x}_i)(1 + \ell n \ \tilde{r}_{ij}^2)d\tilde{\xi}$$

or

$$\tilde{c}_{ij} = (\tilde{y}_i - \tilde{a}_j - b_j\tilde{x}_i)\Delta\tilde{\xi}_j + (\tilde{y}_i - \tilde{a}_j - b_j\tilde{x}_i) \int_{\tilde{\xi}_j}^{\tilde{\xi}_{j+1}} \ell n \ \tilde{r}_{ij}^2 d\tilde{\xi}$$

but from the second of equations (C.5) and equations (C.6) we have

$$\tilde{b}_{ij} = \frac{1}{2m_j} \int_{\tilde{\xi}_j}^{\tilde{\xi}_{j+1}} \ell n \ \tilde{r}_{ij}^2 d\tilde{\xi}$$

therefore

$$\tilde{c}_{ij} = (\tilde{y}_i - \tilde{a}_j - b_j\tilde{x}_i)\Delta\tilde{\xi}_j + 2m_j(\tilde{y}_i - \tilde{a}_j - b_j\tilde{x}_i)\tilde{b}_{ij}$$

or after some algebraic manipulations

$$\tilde{c}_{ij} = \left[(\tilde{y}_i - \tilde{\eta}_j) + \frac{\ell_j}{m_j}(\tilde{x}_i - \tilde{\xi}_j)\right]\left[\Delta\tilde{\xi}_j + 2m_j\tilde{b}_{ij}\right] \qquad \text{(C.10)}$$

The coefficient $\tilde{d}_{ij}$ is given by

$$\tilde{d}_{ij} = \frac{1}{2m_j} \int_{\tilde{\xi}_j}^{\tilde{\xi}_{j+1}} \tilde{r}_{ij}^2 \ell n \ \tilde{r}_{ij}^2 d\tilde{\xi} \qquad \text{(C.11)}$$

Integrating equation (C.11) by parts yields

$$\tilde{d}_{ij} = \frac{1}{6m_j}\left\{\left(A\tilde{\xi}_{j+1}^3 - 3\tilde{B}\tilde{\xi}_{j+1}^2 + 3\tilde{C}\tilde{\xi}_{j+1} - \tilde{D}\right)\ell n\left(A\tilde{\xi}_{j+1}^2 - 2\tilde{B}\tilde{\xi}_{j+1} + \tilde{C}\right)\right.$$

$$- \left(A\tilde{\xi}_j^3 - 3\tilde{B}\tilde{\xi}_j^2 + 3\tilde{C}\tilde{\xi}_j - \tilde{D}\right)\ell n\left(A\tilde{\xi}_j^2 - 2\tilde{B}\tilde{\xi}_j + \tilde{C}\right)$$

$$- 2\left(\frac{A}{3}\,\tilde{\xi}_{j+1}^3 - \tilde{B}\tilde{\xi}_{j+1}^2 + \frac{2A\tilde{C} - \tilde{B}^2}{A}\,\tilde{\xi}_{j+1}\right)$$

$$+ 2\left(\frac{A}{3}\,\tilde{\xi}_j^3 - \tilde{B}\tilde{\xi}_j^2 + \frac{2A\tilde{C} - \tilde{B}^2}{A}\,\tilde{\xi}_j\right)$$

$$- \frac{3A\tilde{B}\tilde{C} - A^2\tilde{D} - 2\tilde{B}^3}{A^2}\,\ell n\,\frac{A\tilde{\xi}_{j+1}^2 - 2\tilde{B}\tilde{\xi}_{j+1} + \tilde{C}}{A\tilde{\xi}_j^2 - 2\tilde{B}\tilde{\xi}_j + \tilde{C}}$$

$$\left.+ \frac{4}{A^2}\,(A\tilde{C} - \tilde{B}^2)^{3/2}\left[\tan^{-1}\frac{A\tilde{\xi}_{j+1} - \tilde{B}}{\sqrt{A\tilde{C} - \tilde{B}^2}} - \tan^{-1}\frac{A\tilde{\xi}_j - \tilde{B}}{\sqrt{A\tilde{C} - \tilde{B}^2}}\right]\right\} \qquad \text{(C.12)}$$

where

$$\left.\begin{aligned} A &= 1 + b_j^2 = \frac{1}{m_j^2} \\ \tilde{B} &= \tilde{x}_i + b_j(\tilde{y}_i - \tilde{a}_j) \\ \tilde{C} &= \tilde{x}_i^2 + (\tilde{y}_i - \tilde{a}_j)^2 \\ \tilde{D} &= \tilde{x}_i^3 + \frac{1}{b_j}\,(\tilde{y}_i - \tilde{a}_j)^3 \end{aligned}\right\} \qquad \text{(C.13)}$$

Finally the coefficient

$$\tilde{f}_{ij} = \frac{4}{m_j}\int_{\tilde{\xi}_j}^{\tilde{\xi}_{j+1}} d\tilde{\xi} + 4\tilde{b}_{ij}$$

or

$$\tilde{f}_{ij} = 4\left(\frac{\Delta\tilde{\xi}_j}{m_j} + \tilde{b}_{ij}\right) \qquad \text{(C.14)}$$

On the loaded boundaries BC and B'C' (Fig. 1) the stress function $\tilde{\varphi}$ is given in dimensionless form by equation (28) and it can be written in terms of $\tilde{\xi}$ and $\tilde{\eta}$ as

$$\tilde{\varphi}(\tilde{\xi},\tilde{\eta}) = -\frac{\tilde{q}}{3}\tilde{\xi}^3 + \frac{\tilde{q}(1-2\tilde{a})}{2}\tilde{\xi}^2 + \tilde{q}\tilde{a}(1-\tilde{a})\tilde{\xi} + \frac{\tilde{q}\tilde{a}^2}{6}(3-2\tilde{a}) \qquad (C.15)$$

Since the assumption that the stress function $\tilde{\varphi}$ on these boundaries is piecewise constant may lead to errors, the summation $\tilde{e}_{ij}\tilde{\varphi}_j$ in the boundary equation (45) is replaced for the boundary BC by the integral

$$\int_C^B \tilde{\varphi}_j \frac{\partial}{\partial\tilde{n}}(\tilde{\nabla}^2\tilde{\rho}_{ij})d\tilde{s} \qquad (C.16)$$

which can be evaluated in closed form. For this boundary $\ell_j = 0$ and therefore

$$\frac{\partial}{\partial\tilde{n}}(\tilde{\nabla}^2\tilde{\rho}_{ij}) = -4m_j\frac{\tilde{y}_i - \tilde{n}}{(\tilde{x}_i - \tilde{\xi})^2 + (\tilde{y}_i - \tilde{n})^2}$$

Since $\tilde{\eta} \equiv \tilde{n}_j = \tilde{L}$ for all segments on BC and $d\tilde{s} = -m_j d\tilde{\xi}$, the integral given by equation (C.16) becomes

$$\tilde{I}_{i_{(CB)}} = 4m_j^2(\tilde{y}_i - \tilde{n}_j)\int_{1-\tilde{a}}^{-\tilde{a}} \frac{\tilde{\varphi}d\tilde{\xi}}{(\tilde{x}_i - \tilde{\xi})^2 + (y_i - \eta_j)^2} \qquad (C.17)$$

which can be evaluated to give

$$\tilde{I}_{i_{(CB)}} = \frac{2\tilde{q}}{3}(\tilde{y}_i - \tilde{\eta}_j)\Bigg\{ 4\tilde{x}_i - 2(1-2\tilde{a})$$

$$+ \Big[(\tilde{y}_i - \tilde{\eta}_j)^2 - 3\tilde{x}_i^2 + 3(1-2\tilde{a})\tilde{x}_i + 3\tilde{a}(1-\tilde{a})\Big] \ln \frac{(\tilde{x}_i + \tilde{a})^2 + (\tilde{y}_i - \tilde{\eta}_j)^2}{(\tilde{x}_i + \tilde{a} - 1)^2 + (\tilde{y}_i - \tilde{\eta}_j)^2}$$

$$+ \frac{-2\tilde{x}_i\Big[\tilde{x}_i^2 - 3(\tilde{y}_i - \tilde{\eta}_j)^2\Big] + 3(1-2\tilde{a})\Big[\tilde{x}_i^2 - (\tilde{y}_i - \tilde{\eta}_j)^2\Big] + 6\tilde{a}(1-\tilde{a})\tilde{x}_i + \tilde{a}^2(3-2\tilde{a})}{|\tilde{y}_i - \tilde{\eta}_j|}$$

$$\Big[\tan^{-1}\frac{\tilde{x}_i + \tilde{a} - 1}{|\tilde{y}_i - \tilde{\eta}_j|} - \tan^{-1}\frac{\tilde{x}_i + \tilde{a}}{|\tilde{y}_i - \tilde{\eta}_j|}\Big]\Bigg\} \qquad (C.18)$$

For the segments located on boundary B'C' $\tilde{\eta} \equiv \tilde{\eta}_j = -\tilde{L}$. Reversing limits of integration in equation (C.17) yields

$$\tilde{I}_{i_{(B'C')}} = -\frac{2q}{3}(\tilde{y}_i - \tilde{\eta}_j)\Bigg\{ 4\tilde{x}_i - 2(1-2\tilde{a})$$

$$+ \Big[(\tilde{y}_i - \tilde{\eta}_j)^2 - 3\tilde{x}_i^2 + 3(1-2\tilde{a})\tilde{x}_i + 3\tilde{a}(1-\tilde{a})\Big] \ln \frac{(\tilde{x}_i + \tilde{a})^2 + (\tilde{y}_i - \tilde{\eta}_j)^2}{(\tilde{x}_i + \tilde{a} - 1)^2 + (\tilde{y}_i - \tilde{\eta}_j)^2}$$

$$+ \frac{-2\tilde{x}_i\Big[\tilde{x}_i^2 - 3(\tilde{y}_i - \tilde{\eta}_j)^2\Big] + 3(1-2\tilde{a})\Big[\tilde{x}_i^2 - (\tilde{y}_i - \tilde{\eta}_j)^2\Big] + 6\tilde{a}(1-\tilde{a})\tilde{x}_i + \tilde{a}^2(3-2\tilde{a})}{|\tilde{y}_i - \tilde{\eta}_j|}$$

$$\Big[\tan^{-1}\frac{\tilde{x}_i + \tilde{a} - 1}{|\tilde{y}_i - \tilde{\eta}_j|} - \tan^{-1}\frac{\tilde{x}_i + \tilde{a}}{|\tilde{y}_i - \tilde{\eta}_j|}\Big]\Bigg\} \qquad (C.19)$$

C.1.2 Boundary segments parallel to y axis

The coefficients for the segments on the boundary sections parallel to y axis can be evaluated in a similar manner.

Combining equations (C.5) with (C.6) and (C.7), setting $m_j = 0$, $\Delta\tilde{\eta}_j = \tilde{\eta}_{j+1} - \tilde{\eta}_j$ and performing indicated integrations, we obtain the

following expressions

$$\tilde{a}_{ij} = -\left[\tan^{-1}\frac{\tilde{\eta}_{j+1} - \tilde{y}_i}{\tilde{x}_i - \tilde{\xi}_j} - \tan^{-1}\frac{\tilde{\eta}_j - \tilde{y}_i}{\tilde{x}_i - \tilde{\xi}_j}\right]$$

for $i \neq j$

for $i = j$ limiting process gives $a_{ii} = 0$

$$\tilde{b}_{ij} = \ell_j \Delta\tilde{\eta}_j + \frac{\ell_j}{2}(\tilde{y}_i - \tilde{\eta}_{j+1})\ell n\left[(\tilde{y}_i - \tilde{\eta}_{j+1})^2 + (\tilde{x}_i - \tilde{\xi}_j)^2\right]$$
$$- \frac{\ell_j}{2}(\tilde{y}_i - \tilde{\eta}_j)\ell n\left[(\tilde{y}_i - \tilde{\eta}_j)^2 + (\tilde{x}_i - \tilde{\xi}_j)^2\right]$$
$$- \ell_j(\tilde{x}_i - \tilde{\xi}_j)\left[\tan^{-1}\frac{\tilde{\eta}_{j+1} - \tilde{y}_i}{\tilde{x}_i - \tilde{\xi}_j} - \tan^{-1}\frac{\tilde{\eta}_j - \tilde{y}_i}{\tilde{x}_i - \tilde{\xi}_j}\right]$$

$$\tilde{c}_{ij} = -(\tilde{x}_i - \tilde{\xi}_j)[\Delta\tilde{\eta}_j - 2\ell_j\tilde{b}_{ij}]$$

$$\tilde{d}_{ij} = \frac{\ell_j}{2}\left\{\left[\frac{1}{3}(\tilde{y}_i - \tilde{\eta}_{j+1})^3 + (\tilde{x}_i - \tilde{\xi}_j)^2(\tilde{y}_i - \tilde{\eta}_{j+1})\right]\ell n\left[(\tilde{y}_i - \tilde{\eta}_{j+1})^2\right.\right.$$
$$\left. + (\tilde{x}_i - \tilde{\xi}_j)^2\right] - \left[\frac{1}{3}(\tilde{y}_i - \tilde{\eta}_j)^3 + (\tilde{x}_i - \tilde{\xi}_j)^2(\tilde{y}_i - \tilde{\eta}_j)\right]\ell n\left[(\tilde{y}_i\right.$$
$$\left. - \tilde{\eta}_j)^2 + (\tilde{x}_i - \tilde{\xi}_j)^2\right] + \frac{4}{3}(\tilde{x}_i - \tilde{\xi}_j)^2\Delta\tilde{\eta}_j$$
$$- \frac{4}{3}(\tilde{x}_i - \tilde{\xi}_j)^3\left[\tan^{-1}\frac{\tilde{\eta}_{j+1} - \tilde{y}_i}{\tilde{x}_i - \tilde{\xi}_j} - \tan^{-1}\frac{\tilde{\eta}_j - \tilde{y}_i}{\tilde{x}_i - \tilde{\xi}_j}\right]$$
$$\left. - \frac{2}{9}\left[(\tilde{y}_i - \tilde{\eta}_{j+1})^3 - (\tilde{y}_i - \tilde{\eta}_j)^3\right]\right\}$$

$$\tilde{e}_{ij} = 4\tilde{a}_{ij}$$

$$\tilde{f}_{ij} = -4\left(\frac{\Delta\tilde{\eta}_j}{\ell_j} - \tilde{b}_{ij}\right)$$

(C.20)

C.2 Coefficients of the Stress Equation

The stress coefficients to be evaluated, given by equation (50), are

$$\tilde{A}_{ij} = 4 \int_j \frac{\partial}{\partial \tilde{n}} \left[\frac{(\tilde{x}_i - \tilde{\xi})^2 - (\tilde{y}_i - \tilde{n})^2}{\left[(\tilde{x}_i - \tilde{\xi})^2 + (\tilde{y}_i - \tilde{n})^2\right]^2} \right] d\tilde{s}$$

$$\tilde{B}_{ij} = 4 \int_j \frac{(\tilde{y}_i - \tilde{n})^2 - (\tilde{x}_i - \tilde{\xi})^2}{\left[(\tilde{x}_i - \tilde{\xi})^2 + (\tilde{y}_i - \tilde{n})^2\right]^2} d\tilde{s}$$

$$\tilde{C}_{ij} = \int_j \frac{\partial}{\partial \tilde{n}} \left\{ \ell n \left[(\tilde{x}_i - \tilde{\xi})^2 + (\tilde{y}_i - \tilde{n})^2\right] + \frac{2(\tilde{y}_i - \tilde{n})^2}{(\tilde{x}_i - \tilde{\xi})^2 + (\tilde{y}_i - \tilde{n})^2} \right\} d\tilde{s}$$

$$\tilde{D}_{ij} = - \int_j \left\{ \ell n \left[(\tilde{x}_i - \tilde{\xi})^2 + (\tilde{y}_i - \tilde{n})^2\right] + \frac{2(\tilde{y}_i - \tilde{n})^2}{(\tilde{x}_i - \tilde{\xi})^2 + (\tilde{y}_i - \tilde{n})^2} + 1 \right\} d\tilde{s}$$

$$\tilde{E}_{ij} = \int_j \frac{\partial}{\partial \tilde{n}} \left\{ \ell n \left[(\tilde{x}_i - \tilde{\xi})^2 + (\tilde{y}_i - \tilde{n})^2\right] + \frac{2(\tilde{x}_i - \tilde{\xi})^2}{(\tilde{x}_i - \tilde{\xi})^2 + (\tilde{y}_i - \tilde{n})^2} \right\} d\tilde{s}$$

$$\tilde{F}_{ij} = - \int_j \left\{ \ell n \left[(\tilde{x}_i - \tilde{\xi})^2 + (\tilde{y}_i - \tilde{n})^2\right] + \frac{2(\tilde{x}_i - \tilde{\xi})^2}{(\tilde{x}_i - \tilde{\xi})^2 + (\tilde{y}_i - \tilde{n})^2} + 1 \right\} d\tilde{s}$$

$$\tilde{G}_{ij} = - 8 \int_j \frac{\partial}{\partial \tilde{n}} \left\{ \frac{(\tilde{x}_i - \tilde{\xi})(\tilde{y}_i - \tilde{n})}{\left[(\tilde{x}_i - \tilde{\xi})^2 + (\tilde{y}_i - \tilde{n})^2\right]^2} \right\} d\tilde{s}$$

$$\tilde{H}_{ij} = 8 \int_j \frac{(\tilde{x}_i - \tilde{\xi})(\tilde{y}_i - \tilde{n})}{\left[(\tilde{x}_i - \tilde{\xi})^2 + (\tilde{y}_i - \tilde{n})^2\right]^2} d\tilde{s}$$

(Eq. (C.21) continued on next page)

$$\tilde{I}_{ij} = 2 \int_j \frac{\partial}{\partial \tilde{n}} \left\{ \frac{(\tilde{x}_i - \tilde{\xi})(\tilde{y}_i - \tilde{\eta})}{(\tilde{x}_i - \tilde{\xi})^2 + (\tilde{y}_i - \tilde{\eta})^2} \right\} d\tilde{s}$$

$$\tilde{K}_{ij} = -2 \int_j \frac{(\tilde{x}_i - \tilde{\xi})(\tilde{y}_i - \tilde{\eta})}{(\tilde{x}_i - \tilde{\xi})^2 + (\tilde{y}_i - \tilde{\eta})^2} d\tilde{s} \qquad \text{(C.21)}$$

C.2.1 Boundary segments on the notch and segments parallel to x axis

Let

$$\left.\begin{aligned} \tilde{d} &= \tilde{x}_i^2 + (\tilde{y}_i - \tilde{a}_j)^2 \\ \tilde{b} &= -2[\tilde{x}_i + b_j(\tilde{y}_i - \tilde{a}_j)] \\ c &= 1 + b_j^2 = \frac{1}{m_j^2} \\ \tilde{h} &= \tilde{x}_i^2 - (\tilde{y}_i - \tilde{a}_j)^2 \\ \tilde{e} &= -2[\tilde{x}_i - b_j(\tilde{y}_i - \tilde{a}_j)] \\ f &= 1 - b_j^2 \end{aligned}\right\} \qquad \text{(C.22)}$$

Combining equations (C.2), (C.3), (C.6), and (C.22) with expressions given by equation (C.21) yields

$$\tilde{A}_{ij} = \frac{8}{m_j}[\tilde{x}_i \ell_j - (\tilde{y}_i - \tilde{a}_j)m_j] \int_{\tilde{\xi}_j}^{\tilde{\xi}_{j+1}} \frac{d\tilde{\xi}}{(\tilde{d} + \tilde{b}\tilde{\xi} + c\tilde{\xi}^2)^2}$$

$$- \frac{16\ell_j}{m_j} \int_{\tilde{\xi}_j}^{\tilde{\xi}_{j+1}} \frac{\tilde{\xi} d\tilde{\xi}}{(\tilde{d} + \tilde{b}\tilde{\xi} + c\tilde{\xi}^2)^2}$$

(Eq. (C.23) continued on next page)

$$- \frac{16}{m_j} [\tilde{x}_i \ell_j + (\tilde{y}_i - \tilde{a}_j) m_j] \left[\tilde{h} \int_{\tilde{\xi}_j}^{\tilde{\xi}_{j+1}} \frac{d\tilde{\xi}}{(\tilde{d} + \tilde{b}\tilde{\xi} + \tilde{c}\tilde{\xi}^2)^3} \right.$$

$$\left. + \tilde{e} \int_{\tilde{\xi}_j}^{\tilde{\xi}_{j+1}} \frac{\tilde{\xi} d\tilde{\xi}}{(\tilde{d} + \tilde{b}\tilde{\xi} + \tilde{c}\tilde{\xi}^2)^3} + f \int_{\tilde{\xi}_j}^{\tilde{\xi}_{j+1}} \frac{\tilde{\xi}^2 d\tilde{\xi}}{(\tilde{d} + \tilde{b}\tilde{\xi} + \tilde{c}\tilde{\xi}^2)^3} \right]$$

$$\tilde{B}_{ij} = \frac{4}{m_j} \left[\tilde{h} \int_{\tilde{\xi}_j}^{\tilde{\xi}_{j+1}} \frac{d\tilde{\xi}}{(\tilde{d} + \tilde{b}\tilde{\xi} + c\tilde{\xi}^2)^2} + \tilde{e} \int_{\tilde{\xi}_j}^{\tilde{\xi}_{j+1}} \frac{\tilde{\xi} d\tilde{\xi}}{(\tilde{d} + \tilde{b}\tilde{\xi} + c\tilde{\xi}^2)^2} \right.$$

$$\left. + f \int_{\tilde{\xi}_j}^{\tilde{\xi}_{j+1}} \frac{\tilde{\xi}^2 d\tilde{\xi}}{(\tilde{d} + \tilde{b}\tilde{\xi} + \tilde{c}\tilde{\xi}^2)^2} \right]$$

$$\tilde{C}_{ij} = \frac{2}{m_j} [\tilde{x}_i \ell_j + (\tilde{y}_i - \tilde{a}_j) m_j] \int_{\tilde{\xi}_j}^{\tilde{\xi}_{j+1}} \frac{d\tilde{\xi}}{\tilde{d} + \tilde{b}\tilde{\xi} + c\tilde{\xi}^2}$$

$$+ \frac{4}{m_j} \tilde{x}_i (\tilde{y}_i - \tilde{a}_j) [\tilde{x}_i m_j - (\tilde{y}_i - \tilde{a}_j) \ell_j] \int_{\tilde{\xi}_j}^{\tilde{\xi}_{j+1}} \frac{d\tilde{\xi}}{(\tilde{d} + \tilde{b}\tilde{\xi} + c\tilde{\xi}^2)^2}$$

$$+ \frac{4}{m_j} \left\{ \left[\tilde{x}_i^2 + (\tilde{y}_i - \tilde{a}_j)^2 \right] \ell_j - \frac{2}{m_j} \tilde{x}_i (\tilde{y}_i - \tilde{a}_j) \right\} \int_{\tilde{\xi}_j}^{\tilde{\xi}_{j+1}} \frac{\tilde{\xi} d\tilde{\xi}}{(\tilde{d} + \tilde{b}\tilde{\xi} + c\tilde{\xi}^2)^2}$$

$$- 4 \left\{ \frac{2\ell_j}{m_j^2} [\tilde{x}_i m_j - (\tilde{y}_i - \tilde{a}_j) \ell_j] + \left[\tilde{x}_i \frac{\ell_j^3}{m_j^3} - (\tilde{y}_i - \tilde{a}_j) \right] \right\}$$

$$\int_{\tilde{\xi}_j}^{\tilde{\xi}_{j+1}} \frac{\tilde{\xi}^2 d\tilde{\xi}}{(\tilde{d} + \tilde{b}\tilde{\xi} + c\tilde{\xi}^2)^2} + \frac{4\ell_j}{m_j^3} \int_{\tilde{\xi}_j}^{\tilde{\xi}_{j+1}} \frac{\tilde{\xi}^3 d\tilde{\xi}}{(\tilde{d} + \tilde{b}\tilde{\xi} + c\tilde{\xi}^2)^2}$$

(Eq. (C.23) continued on next page)

$$\tilde{D}_{ij} = \frac{1}{m_j}\left\{\int_{\tilde{\xi}_j}^{\tilde{\xi}_{j+1}} \ell n(\tilde{d} + \tilde{b}\tilde{\xi} + c\tilde{\xi}^2)d\tilde{\xi} + 2\left[(\tilde{y}_i - \tilde{a}_j)^2 \int_{\tilde{\xi}_j}^{\tilde{\xi}_{j+1}} \frac{d\tilde{\xi}}{\tilde{d}+\tilde{b}\tilde{\xi}+c\tilde{\xi}^2}\right.\right.$$

$$\left.\left. - 2b_j(\tilde{y}_i - \tilde{a}_j) \int_{\tilde{\xi}_j}^{\tilde{\xi}_{j+1}} \frac{\tilde{\xi}d\tilde{\xi}}{\tilde{d}+\tilde{b}\tilde{\xi}+c\tilde{\xi}^2} + b_j^2 \int_{\tilde{\xi}_j}^{\tilde{\xi}_{j+1}} \frac{\tilde{\xi}^2 d\tilde{\xi}}{\tilde{d}+\tilde{b}\tilde{\xi}+c\tilde{\xi}^2}\right] + \Delta\tilde{\xi}_j\right\}$$

$$\tilde{E}_{ij} = \frac{2}{m_j}[\tilde{x}_i \ell_j + (\tilde{y}_i - \tilde{a}_j)m_j] \int_{\tilde{\xi}_j}^{\tilde{\xi}_{j+1}} \frac{d\tilde{\xi}}{\tilde{d} + \tilde{b}\tilde{\xi} + c\tilde{\xi}^2}$$

$$- \frac{4}{m_j}\tilde{x}_i(\tilde{y}_i - \tilde{a}_j)[\tilde{x}_i m_j - (\tilde{y}_i - \tilde{a}_j)\ell_j] \int_{\tilde{\xi}_j}^{\tilde{\xi}_{j+1}} \frac{d\tilde{\xi}}{(\tilde{d} + \tilde{b}\tilde{\xi} + c\tilde{\xi}^2)^2}$$

$$- \frac{4}{m_j}\left\{\left[\tilde{x}_i^2 + (\tilde{y}_i - \tilde{a}_j)^2\right]\ell_j - \frac{2}{m_j}\tilde{x}_i(\tilde{y}_i - \tilde{a}_j)\right\} \int_{\tilde{\xi}_j}^{\tilde{\xi}_{j+1}} \frac{\tilde{\xi}d\tilde{\xi}}{(\tilde{d}+\tilde{b}\tilde{\xi}+c\tilde{\xi}^2)^2}$$

$$+ 4\left\{\frac{2\ell_j}{m_j^2}[\tilde{x}_i m_j - (\tilde{y}_i - \tilde{a}_j)\ell_j] + \left[\tilde{x}_i \frac{\ell_j^3}{m_j^3}\right.\right.$$

$$\left.\left. - (\tilde{y}_i - \tilde{a}_j)\right]\right\} \int_{\tilde{\xi}_j}^{\tilde{\xi}_{j+1}} \frac{\tilde{\xi}^2 d\tilde{\xi}}{(\tilde{d}+\tilde{b}\tilde{\xi}+c\tilde{\xi}^2)^2} - \frac{4\ell_j}{m_j^3} \int_{\tilde{\xi}_j}^{\tilde{\xi}_{j+1}} \frac{\tilde{\xi}^3 d\tilde{\xi}}{(\tilde{d}+\tilde{b}\tilde{\xi}+c\tilde{\xi}^2)^2}$$

$$\tilde{F}_{ij} = \frac{1}{m_j}\left\{\int_{\tilde{\xi}_j}^{\tilde{\xi}_{j+1}} \ell n(\tilde{d}+\tilde{b}\tilde{\xi}+c\tilde{\xi}^2)d\tilde{\xi} + 2\left[\tilde{x}_i^2 \int_{\tilde{\xi}_j}^{\tilde{\xi}_{j+1}} \frac{d\tilde{\xi}}{\tilde{d}+\tilde{b}\tilde{\xi}+c\tilde{\xi}^2}\right.\right.$$

$$\left.\left. - 2\tilde{x}_i \int_{\tilde{\xi}_j}^{\tilde{\xi}_{j+1}} \frac{\tilde{\xi}d\tilde{\xi}}{\tilde{d}+\tilde{b}\tilde{\xi}+c\tilde{\xi}^2} + \int_{\tilde{\xi}_j}^{\tilde{\xi}_{j+1}} \frac{\tilde{\xi}^2 d\tilde{\xi}}{\tilde{d}+\tilde{b}\tilde{\xi}+c\tilde{\xi}^2}\right] + \Delta\tilde{\xi}_j\right\}$$

(Eq. (C.23) continued on next page)

$$\tilde{G}_{ij} = -\frac{8}{m_j}\left[\tilde{x}_i m_j + (\tilde{y}_i - \tilde{a}_j)\ell_j\right]\int_{\tilde{\xi}_j}^{\tilde{\xi}_{j+1}} \frac{d\tilde{\xi}}{(\tilde{d} + \tilde{b}\tilde{\xi} + c\tilde{\xi}^2)^2}$$

$$+ 8\left(1 - \frac{\ell_j^2}{m_j^2}\right)\int_{\tilde{\xi}_j}^{\tilde{\xi}_{j+1}} \frac{\tilde{\xi}d\tilde{\xi}}{(\tilde{d} + \tilde{b}\tilde{\xi} + c\tilde{\xi}^2)^2}$$

$$+ \frac{32\tilde{x}_i(\tilde{y}_i - \tilde{a}_j)}{m_j}\left[\tilde{x}_i\ell_j + (\tilde{y}_i - \tilde{a}_j)m_j\right]\int_{\tilde{\xi}_j}^{\tilde{\xi}_{j+1}} \frac{d\tilde{\xi}}{(\tilde{d} + \tilde{b}\tilde{\xi} + c\tilde{\xi}^2)^3}$$

$$+ \frac{32}{m_j^2}\left[\tilde{x}_i^2\ell_j^2 - (\tilde{y}_i - \tilde{a}_j)^2 m_j^2\right]\int_{\tilde{\xi}_j}^{\tilde{\xi}_{j+1}} \frac{\tilde{\xi}d\tilde{\xi}}{(\tilde{d} + \tilde{b}\tilde{\xi} + c\tilde{\xi}^2)^3}$$

$$- \frac{32\ell_j}{m_j^2}\left[\tilde{x}_i\ell_j + (\tilde{y}_i - \tilde{a}_j)m_j\right]\int_{\tilde{\xi}_j}^{\tilde{\xi}_{j+1}} \frac{\tilde{\xi}^2 d\tilde{\xi}}{(\tilde{d} + \tilde{b}\tilde{\xi} + c\tilde{\xi}^2)^3}$$

$$\tilde{H}_{ij} = -\frac{8}{m_j}\tilde{x}_i(\tilde{y}_i - \tilde{a}_j)\int_{\tilde{\xi}_j}^{\tilde{\xi}_{j+1}} \frac{d\tilde{\xi}}{(\tilde{d} + \tilde{b}\tilde{\xi} + c\tilde{\xi}^2)^2}$$

$$- \frac{8}{m_j^2}\left[\tilde{x}_i\ell_j - (\tilde{y}_i - \tilde{a}_j)m_j\right]\int_{\tilde{\xi}_j}^{\tilde{\xi}_{j+1}} \frac{\tilde{\xi}d\tilde{\xi}}{(\tilde{d} + \tilde{b}\tilde{\xi} + c\tilde{\xi}^2)^2}$$

$$+ \frac{8\ell_j}{m_j^2}\int_{\tilde{\xi}_j}^{\tilde{\xi}_{j+1}} \frac{\tilde{\xi}^2 d\tilde{\xi}}{(\tilde{d} + \tilde{b}\tilde{\xi} + c\tilde{\xi}^2)^2}$$

(Eq. (C.23) continued on next page)

$$\tilde{I}_{ij} = \frac{2}{m_j}\left[\tilde{x}_i m_j + (\tilde{y}_i - \tilde{a}_j)\ell_j\right] \int_{\tilde{\xi}_j}^{\tilde{\xi}_{j+1}} \frac{d\tilde{\xi}}{\tilde{d} + \tilde{b}\tilde{\xi} + c\tilde{\xi}^2}$$

$$-2\left(1 - \frac{\ell_j^2}{m_j^2}\right) \int_{\tilde{\xi}_j}^{\tilde{\xi}_{j+1}} \frac{\tilde{\xi} d\tilde{\xi}}{\tilde{d} + \tilde{b}\tilde{\xi} + c\tilde{\xi}^2}$$

$$-\frac{4\tilde{x}_i(\tilde{y}_i - \tilde{a}_j)}{m_j}\left[\tilde{x}_i \ell_j + (\tilde{y}_i - \tilde{a}_j)m_j\right] \int_{\tilde{\xi}_j}^{\tilde{\xi}_{j+1}} \frac{d\tilde{\xi}}{(\tilde{d} + \tilde{b}\tilde{\xi} + c\tilde{\xi}^2)^2}$$

$$-\frac{4}{m_j^2}\left[\tilde{x}_i^2 \ell_j^2 - (\tilde{y}_i - \tilde{a}_j)^2 m_j^2\right] \int_{\tilde{\xi}_j}^{\tilde{\xi}_{j+1}} \frac{\tilde{\xi} d\tilde{\xi}}{(\tilde{d} + \tilde{b}\tilde{\xi} + c\tilde{\xi}^2)^2}$$

$$+\frac{4\ell_j}{m_j^2}\left[\tilde{x}_i \ell_j + (\tilde{y}_i - \tilde{a}_j)m_j\right] \int_{\tilde{\xi}_j}^{\tilde{\xi}_{j+1}} \frac{\tilde{\xi}^2 d\tilde{\xi}}{(\tilde{d} + \tilde{b}\tilde{\xi} + c\tilde{\xi}^2)^2}$$

$$\tilde{K}_{ij} = \frac{2}{m_j}\tilde{x}_i(\tilde{y}_i - \tilde{a}_j) \int_{\tilde{\xi}_j}^{\tilde{\xi}_{j+1}} \frac{d\tilde{\xi}}{\tilde{d} + \tilde{b}\tilde{\xi} + c\tilde{\xi}^2}$$

$$+\frac{2}{m_j^2}\left[\tilde{x}_i \ell_j - (\tilde{y}_i - \tilde{a}_j)m_j\right] \int_{\tilde{\xi}_j}^{\tilde{\xi}_{j+1}} \frac{\tilde{\xi} d\tilde{\xi}}{\tilde{d} + \tilde{b}\tilde{\xi} + c\tilde{\xi}^2}$$

$$-\frac{2\ell_j}{m_j^2} \int_{\tilde{\xi}_j}^{\tilde{\xi}_{j+1}} \frac{\tilde{\xi}^2 d\tilde{\xi}}{\tilde{d} + \tilde{b}\tilde{\xi} + c\tilde{\xi}^2} \qquad (C.23)$$

To calculate the coefficients given by equations (C.23) the following integrals are required

$$\tilde{I}_1 = \int \frac{d\tilde{\xi}}{\tilde{d} + \tilde{b}\tilde{\xi} + c\tilde{\xi}^2} = \frac{2}{\sqrt{4\tilde{d}c - \tilde{b}^2}} \tan^{-1} \frac{2c\tilde{\xi} + \tilde{b}}{\sqrt{4\tilde{d}c - \tilde{b}^2}}$$

$$\tilde{I}_2 = \int \frac{\tilde{\xi} d\tilde{\xi}}{\tilde{d} + \tilde{b}\tilde{\xi} + c\tilde{\xi}^2} = \frac{1}{2c} \ln(\tilde{d} + \tilde{b}\tilde{\xi} + c\tilde{\xi}^2) - \frac{\tilde{b}}{c\sqrt{4\tilde{d}c - \tilde{b}^2}} \tan^{-1} \frac{2c\tilde{\xi} + \tilde{b}}{\sqrt{4\tilde{d}c - \tilde{b}^2}}$$

$$\tilde{I}_3 = \int \frac{\tilde{\xi}^2 d\tilde{\xi}}{\tilde{d} + \tilde{b}\tilde{\xi} + c\tilde{\xi}^2} = \frac{\tilde{\xi}}{c} - \frac{\tilde{b}}{2c^2} \ln(\tilde{d} + \tilde{b}\tilde{\xi} + c\tilde{\xi}^2) + \frac{\tilde{b}^2 - 2\tilde{d}c}{c^2\sqrt{4\tilde{d}c - \tilde{b}^2}} \tan^{-1} \frac{2c\tilde{\xi} + \tilde{b}}{\sqrt{4\tilde{d}c - \tilde{b}^2}}$$

$$\tilde{I}_4 = \int \frac{d\tilde{\xi}}{(\tilde{d} + \tilde{b}\tilde{\xi} + c\tilde{\xi}^2)^2} = \frac{1}{4\tilde{d}c - \tilde{b}^2} \left(\frac{2c\tilde{\xi} + \tilde{b}}{\tilde{d} + \tilde{b}\tilde{\xi} + c\tilde{\xi}^2} + \frac{4c}{\sqrt{4\tilde{d}c - \tilde{b}^2}} \tan^{-1} \frac{2c\tilde{\xi} + \tilde{b}}{\sqrt{4\tilde{d}c - \tilde{b}^2}} \right)$$

$$\tilde{I}_5 = \int \frac{\tilde{\xi} d\tilde{\xi}}{(\tilde{d} + \tilde{b}\tilde{\xi} + c\tilde{\xi}^2)^2} = -\frac{1}{4\tilde{d}c - \tilde{b}^2} \left(\frac{\tilde{b}\tilde{\xi} + 2\tilde{d}}{\tilde{d} + \tilde{b}\tilde{\xi} + c\tilde{\xi}^2} + \frac{2\tilde{b}}{\sqrt{4\tilde{d}c - \tilde{b}^2}} \tan^{-1} \frac{2c\tilde{\xi} + \tilde{b}}{\sqrt{4\tilde{d}c - \tilde{b}^2}} \right)$$

$$\tilde{I}_6 = \int \frac{\tilde{\xi}^2 d\tilde{\xi}}{(\tilde{d} + \tilde{b}\tilde{\xi} + c\tilde{\xi}^2)^2} = \frac{1}{4\tilde{d}c - \tilde{b}^2} \left[\frac{(\tilde{b}^2 - 2\tilde{d}c)\tilde{\xi} + \tilde{b}\tilde{d}}{c(\tilde{d} + \tilde{b}\tilde{\xi} + c\tilde{\xi}^2)} + \frac{4\tilde{d}}{\sqrt{4\tilde{d}c - \tilde{b}^2}} \tan^{-1} \frac{2c\tilde{\xi} + \tilde{b}}{\sqrt{4\tilde{d}c - \tilde{b}^2}} \right]$$

(Eq. (C.24 continued on next page)

$$\tilde{I}_7 = \int \frac{\tilde{\xi}^3 d\tilde{\xi}}{(\tilde{d} + \tilde{b}\tilde{\xi} + c\tilde{\xi}^2)^2} = \frac{1}{2c^2} \ell n(\tilde{d} + \tilde{b}\tilde{\xi} + c\tilde{\xi}^2)$$

$$+ \frac{\tilde{b}(\tilde{b}^2 - 6\tilde{d}c)}{c^2(4\tilde{d}c - \tilde{b}^2)^{3/2}} \tan^{-1} \frac{2c\tilde{\xi} + \tilde{b}}{\sqrt{4\tilde{d}c - \tilde{b}^2}} - \frac{\tilde{b}(\tilde{b}^2 - 3\tilde{d}c)\tilde{\xi} + \tilde{d}(\tilde{b}^2 - 2\tilde{d}c)}{c^2(4\tilde{d}c - \tilde{b}^2)(\tilde{d} + \tilde{b}\tilde{\xi} + c\tilde{\xi}^2)}$$

$$\tilde{I}_8 = \int \frac{d\tilde{\xi}}{(\tilde{d} + \tilde{b}\tilde{\xi} + c\tilde{\xi}^2)^3} = \frac{1}{4\tilde{d}c - \tilde{b}^2} \left[\frac{2c\tilde{\xi} + \tilde{b}}{2(\tilde{d} + \tilde{b}\tilde{\xi} + c\tilde{\xi}^2)^2} \right.$$

$$\left. + \frac{3c(2c\tilde{\xi} + \tilde{b})}{(4\tilde{d}c - \tilde{b}^2)(\tilde{d} + \tilde{b}\tilde{\xi} + c\tilde{\xi}^2)} + \frac{12c^2}{(4\tilde{d}c - \tilde{b}^2)^{3/2}} \tan^{-1} \frac{2c\tilde{\xi} + \tilde{b}}{\sqrt{4\tilde{d}c - \tilde{b}^2}} \right]$$

$$\tilde{I}_9 = \int \frac{\tilde{\xi} d\tilde{\xi}}{(\tilde{d} + \tilde{b}\tilde{\xi} + c\tilde{\xi}^2)^3} = - \frac{1}{2(4\tilde{d}c - \tilde{b}^2)} \left[\frac{\tilde{b}\tilde{\xi} + 2\tilde{d}}{(\tilde{d} + \tilde{b}\tilde{\xi} + c\tilde{\xi}^2)^2} + 3\tilde{b}\tilde{I}_4 \right]$$

$$\tilde{I}_{10} = \int \frac{\tilde{\xi}^2 d\tilde{\xi}}{(\tilde{d} + \tilde{b}\tilde{\xi} + c\tilde{\xi}^2)^3} = - \frac{1}{3c} \left[\frac{\tilde{\xi}}{(\tilde{d} + \tilde{b}\tilde{\xi} + c\tilde{\xi}^2)^2} - \tilde{d}\tilde{I}_8 + \tilde{b}\tilde{I}_9 \right]$$

$$\tilde{I}_{11} = \int \ell n(\tilde{d} + \tilde{b}\tilde{\xi} + c\tilde{\xi}^2) d\tilde{\xi} = \frac{2c\tilde{\xi} + \tilde{b}}{2c} [\ell n(\tilde{d} + \tilde{b}\tilde{\xi} + c\tilde{\xi}^2) - 2]$$

$$+ \frac{\sqrt{4\tilde{d}c - \tilde{b}^2}}{c} \tan^{-1} \frac{2c\tilde{\xi} + \tilde{b}}{\sqrt{4\tilde{d}c - \tilde{b}^2}}$$

$$\tilde{I}_{12} = \int \frac{\tilde{\xi}^3 d\tilde{\xi}}{(\tilde{d} + \tilde{b}\tilde{\xi} + c\tilde{\xi}^2)^3} = - \frac{\tilde{\xi}^2}{2(\tilde{d} + \tilde{b}\tilde{\xi} + c\tilde{\xi}^2)^2} + \tilde{d}\tilde{I}_9$$

(Eq. (C.24 continued on next page)

$$\tilde{I}_{13} = \int \frac{\tilde{\xi}^4 d\tilde{\xi}}{(\tilde{d} + \tilde{b}\tilde{\xi} + c\tilde{\xi}^2)^2} = \frac{\tilde{\xi}^3}{\tilde{d} + \tilde{b}\tilde{\xi} + c\tilde{\xi}^2} - 3\tilde{d}\tilde{I}_6 - 2\tilde{b}\tilde{I}_7$$

$$\tilde{I}_{14} = \int \frac{\tilde{\xi}^4 d\tilde{\xi}}{(\tilde{d} + \tilde{b}\tilde{\xi} + c\tilde{\xi}^2)^3} = -\frac{\tilde{\xi}^3}{(\tilde{d} + \tilde{b}\tilde{\xi} + c\tilde{\xi}^2)^2} + 3\tilde{d}\tilde{I}_{10} + \tilde{b}\tilde{I}_{12} \qquad \text{(C.24)}$$

Combining equations (C.23) and (C.24) we obtain

$$\tilde{A}_{ij} = \frac{8}{m_j}\left\{[\tilde{x}_i \ell_j - (\tilde{y}_i - \tilde{a}_j)m_j]\,\tilde{I}_4 - 2\ell_j\tilde{I}_5 \right.$$

$$\left. - 2[\tilde{x}_i \ell_j + (\tilde{y}_i - \tilde{a}_j)m_j](\tilde{h}\tilde{I}_8 + \tilde{e}\tilde{I}_9 + f\tilde{I}_{10})\right\}\Bigg|_{\tilde{\xi}_j}^{\tilde{\xi}_{j+1}}$$

$$\tilde{B}_{ij} = \frac{4}{m_j}(\tilde{h}\tilde{I}_4 + \tilde{e}\tilde{I}_5 + f\tilde{I}_6)\Big|_{\tilde{\xi}_j}^{\tilde{\xi}_{j+1}}$$

$$\tilde{C}_{ij} = \left\{\frac{2}{m_j}[\tilde{x}_i \ell_j + (\tilde{y}_i - \tilde{a}_j)m_j]\tilde{I}_1 + \frac{4}{m_j}\tilde{x}_i(\tilde{y}_i - \tilde{a}_j)[\tilde{x}_i m_j - (\tilde{y}_i - \tilde{a}_j)\ell_j]\tilde{I}_4 \right.$$

$$+ \frac{4}{m_j}\left[(\tilde{x}_i^2 + (\tilde{y}_i - \tilde{a}_j)^2)\ell_j - \frac{2}{m_j}\tilde{x}_i(\tilde{y}_i - \tilde{a}_j)\right]\tilde{I}_5 - 4\left[\frac{2\ell_j}{m_j^2}(\tilde{x}_i m_j\right.$$

$$\left.\left. - (\tilde{y}_i - \tilde{a}_j)\ell_j) + \left(\tilde{x}_i\frac{\ell_j^3}{m_j^3} - (\tilde{y}_i - \tilde{a}_j)\right)\right]\tilde{I}_6 + \frac{4\ell_j}{m_j^3}\tilde{I}_7\right\}\Bigg|_{\tilde{\xi}_j}^{\tilde{\xi}_{j+1}}$$

$$\tilde{D}_{ij} = \frac{1}{m_j}\left\{\tilde{I}_{11} + 2\left[(\tilde{y}_i - \tilde{a}_j)^2\tilde{I}_1 - 2b_j(\tilde{y}_i - \tilde{a}_j)\tilde{I}_2 + b_j^2\tilde{I}_3\right] + \tilde{\xi}\right\}\Bigg|_{\tilde{\xi}_j}^{\tilde{\xi}_{j+1}}$$

(Eq. (C.25) continued on next page)

$$\tilde{E}_{ij} = \left\{ \frac{2}{m_j} [\tilde{x}_i \ell_j + (\tilde{y}_i - \tilde{a}_j) m_j] \tilde{I}_1 - \frac{4}{m_j} \tilde{x}_i (\tilde{y}_i - \tilde{a}_j) [\tilde{x}_i m_j - (\tilde{y}_i - \tilde{a}_j) \ell_j] \tilde{I}_4 \right.$$

$$- \frac{4}{m_j} \left[(\tilde{x}_i^2 + (\tilde{y}_i - \tilde{a}_j)^2) \ell_j - \frac{2}{m_j} \tilde{x}_i (\tilde{y}_i - \tilde{a}_j) \right] \tilde{I}_5$$

$$\left. + 4 \left[\frac{2\ell_j}{m_j^2} (\tilde{x}_i m_j - (\tilde{y}_i - \tilde{a}_j) \ell_j) + \left(\tilde{x}_i \frac{\ell_j^3}{m_j^3} - (\tilde{y}_i - \tilde{a}_j) \right) \right] \tilde{I}_6 - \frac{4\ell_j}{m_j^3} \tilde{I}_7 \right\} \Bigg|_{\tilde{\xi}_j}^{\tilde{\xi}_{j+1}}$$

$$\tilde{F}_{ij} = \frac{1}{m_j} \left\{ \tilde{I}_{11} + 2 \left[\tilde{x}_i^2 \tilde{I}_1 - 2\tilde{x}_i \tilde{I}_2 + \tilde{I}_3 \right] + \tilde{\xi} \right\} \Bigg|_{\tilde{\xi}_j}^{\tilde{\xi}_{j+1}}$$

$$\tilde{G}_{ij} = \frac{8}{m_j} \left\{ - [\tilde{x}_i m_j + (\tilde{y}_i - \tilde{a}_j) \ell_j] \tilde{I}_4 + \frac{m_j^2 - \ell_j^2}{m_j} \tilde{I}_5 \right.$$

$$+ 4\tilde{x}_i (\tilde{y}_i - \tilde{a}_j) [\tilde{x}_i \ell_j + (\tilde{y}_i - \tilde{a}_j) m_j] \tilde{I}_8 + \frac{4}{m_j} \left[\tilde{x}_i^2 \ell_j^2 - (\tilde{y}_i - \tilde{a}_j)^2 m_j^2 \right] \tilde{I}_9$$

$$\left. - \frac{4\ell_j}{m_j} [\tilde{x}_i \ell_j + (\tilde{y}_i - \tilde{a}_j) m_j] \tilde{I}_{10} \right\} \Bigg|_{\tilde{\xi}_j}^{\tilde{\xi}_{j+1}}$$

$$\tilde{H}_{ij} = \frac{8}{m_j} \left\{ - \tilde{x}_i (\tilde{y}_i - \tilde{a}_j) \tilde{I}_4 - \frac{1}{m_j} [\tilde{x}_i \ell_j - (\tilde{y}_i - \tilde{a}_j) m_j] \tilde{I}_5 + \frac{\ell_j}{m_j} \tilde{I}_6 \right\} \Bigg|_{\tilde{\xi}_j}^{\tilde{\xi}_{j+1}}$$

(Eq. (C.25) continued on next page)

$$\tilde{I}_{ij} = \frac{2}{m_j}\left\{ [\tilde{x}_i m_j + (\tilde{y}_i - \tilde{a}_j)\ell_j]\tilde{I}_1 - \frac{m_j^2 - \ell_j^2}{m_j}\tilde{I}_2 \right.$$

$$- 2\tilde{x}_i(\tilde{y}_i - \tilde{a}_j)[\tilde{x}_i\ell_j + (\tilde{y}_i - \tilde{a}_j)m_j]\tilde{I}_4 - \frac{2}{m_j}[\tilde{x}_i^2\ell_j^2 - (\tilde{y}_i - \tilde{a}_j)^2 m_j^2]\tilde{I}_5$$

$$\left. + \frac{2\ell_j}{m_j}[\tilde{x}_i\ell_j + (\tilde{y}_i - \tilde{a}_j)m_j]\tilde{I}_6 \right\} \Bigg|_{\tilde{\xi}_j}^{\tilde{\xi}_{j+1}}$$

$$\tilde{K}_{ij} = \frac{2}{m_j}\left\{ \tilde{x}_i(\tilde{y}_i - \tilde{a}_j)\tilde{I}_1 + \frac{1}{m_j}[\tilde{x}_i\ell_j - (\tilde{y}_i - \tilde{a}_j)m_j]\tilde{I}_2 - \frac{\ell_j}{m_j}\tilde{I}_3 \right\} \Bigg|_{\tilde{\xi}_j}^{\tilde{\xi}_{j+1}} \tag{C.25}$$

For the boundaries BC and B'C' the summations $\tilde{A}_{ij}\tilde{\varphi}_j$ and $\tilde{G}_{ij}\tilde{\varphi}_j$ in the stress equations (49) have to be replaced by direct integration.

For the segments on the boundary BC summation $\tilde{A}_{ij}\tilde{\varphi}_j$ is replaced by

$$\frac{\partial^2}{\partial\tilde{y}^2}\int_C^B \tilde{\varphi}_j \frac{\partial}{\partial\tilde{n}}(\tilde{\nabla}^2\tilde{\rho}_{ij})d\tilde{s} \equiv \frac{\partial^2}{\partial\tilde{y}^2}\tilde{I}_{i(CB)} \tag{C.26}$$

and summation $\tilde{G}_{ij}\tilde{\varphi}_j$ by

$$\frac{\partial^2}{\partial\tilde{x}\partial\tilde{y}}\int_C^B \tilde{\varphi}_j \frac{\partial}{\partial\tilde{n}}(\nabla^2\tilde{\rho}_{ij})d\tilde{s} \equiv \frac{\partial^2}{\partial\tilde{x}\partial\tilde{y}}\tilde{I}_{i(CB)} \tag{C.27}$$

where the stress function $\tilde{\varphi}$ is given by equation (C.15), and integral $\tilde{I}_{i(CB)}$ by equation (C.18).

Differentiating $\tilde{I}_{i(CB)}$ twice with respect to $\tilde{y}$ under the integral sign, and using relations (C.24) yields

$$\tilde{I}_{i,\tilde{y}\tilde{y}_{(CB)}} = -24(\tilde{y}_i - \tilde{\eta}_j) \int_{1-\tilde{a}}^{-\tilde{a}} \frac{\tilde{\varphi} d\tilde{\xi}}{\left[(\tilde{x}_i - \tilde{\xi})^2 + (\tilde{y}_i - \tilde{\eta}_j)^2\right]^2}$$

$$+ 32(\tilde{y}_i - \tilde{\eta}_j)^3 \int_{1-\tilde{a}}^{-\tilde{a}} \frac{\tilde{\varphi} d\tilde{\xi}}{\left[(\tilde{x}_i - \tilde{\xi})^2 + (\tilde{y}_i - \tilde{\eta}_j)^2\right]^3}$$

$$= \Bigg\{ -4\tilde{q}(\tilde{y}_i - \tilde{\eta}_j) \left[-2\tilde{I}_7 + 3(1 - 2\tilde{a})\tilde{I}_6 + 6\tilde{a}(1 - \tilde{a})\tilde{I}_5 \right.$$

$$\left. + \tilde{a}^2(3 - 2\tilde{a})\tilde{I}_4 \right] + \frac{16\tilde{q}}{3} (\tilde{y}_i - \tilde{\eta}_j)^3 \left[-2\tilde{I}_{12} + 3(1 - 2\tilde{a})\tilde{I}_{10} \right.$$

$$\left. + 6\tilde{a}(1 - \tilde{a})\tilde{I}_9 + \tilde{a}^2(1 - 2\tilde{a})\tilde{I}_8 \right] \Bigg\} \Bigg|_{\tilde{\xi}=1-\tilde{a}}^{\tilde{\xi}=-\tilde{a}} \qquad \text{(C.28)}$$

The expression (C.27) replaces the summation $\tilde{G}_{ij}\tilde{\varphi}_j$, on boundary BC. Differentiating $\tilde{I}_{i(CB)}$ with respect to $\tilde{x}$ and $\tilde{y}$ under the integral sign and applying relations (C.24) we obtain

$$\tilde{I}_{i,\tilde{x}\tilde{y}_{(CB)}} = -8 \int_{1-\tilde{a}}^{-\tilde{a}} \frac{\tilde{\varphi}(\tilde{x}_i - \tilde{\xi}) d\tilde{\xi}}{\left[(\tilde{x}_i - \tilde{\xi})^2 + (\tilde{y}_i - \tilde{\eta}_j)^2\right]^2}$$

$$+ 32(\tilde{y}_i - \tilde{\eta}_j)^2 \int_{1-\tilde{a}}^{-\tilde{a}} \frac{\tilde{\varphi}(\tilde{x}_i - \tilde{\xi}) d\tilde{\xi}}{\left[(\tilde{x}_i - \tilde{\xi})^2 + (\tilde{y}_i - \tilde{\eta}_j)^2\right]^3}$$

(Eq. (C.29) continued on next page)

$$= \frac{4\tilde{q}}{3}\Bigg\{\Big\{-2\tilde{I}_{13} + [3(1 - 2\tilde{a}) + 2\tilde{x}_i]\tilde{I}_7 + [6\tilde{a}(1 - \tilde{a})$$

$$- 3(1 - 2\tilde{a})\tilde{x}_i]\tilde{I}_6 + [\tilde{a}^2(3 - 2\tilde{a}) - 6\tilde{a}(1 - \tilde{a})\tilde{x}_i]\tilde{I}_5$$

$$- \tilde{a}^2(3 - 2\tilde{a})\tilde{x}_i\tilde{I}_4\Big\} + 4(\tilde{y}_i - \tilde{\eta}_j)^2\Big\{2\tilde{I}_{14} - [3(1 - 2\tilde{a})$$

$$+ 2\tilde{x}_i]\tilde{I}_{12} - [6\tilde{a}(1 - \tilde{a}) - 3(1 - 2\tilde{a})\tilde{x}_i]\tilde{I}_{10} - \Big[\tilde{a}^2(3 - 2\tilde{a})$$

$$- 6\tilde{a}(1 - \tilde{a})\tilde{x}_i\Big]\tilde{I}_9 + \tilde{a}^2(3 - 2\tilde{a})\tilde{x}_i\tilde{I}_8\Big\}\Bigg\}\Bigg|_{\tilde{\xi}=1-\tilde{a}}^{\tilde{\xi}=-\tilde{a}} \qquad (C.29)$$

The necessary integrals for B'C' boundary are obtained by interchanging limits of integration in equations (C.28) and (C.29).

C.2.2 Boundary segments parallel to y axis

The coefficients for the segments on the boundary sections parallel to y-axis can be evaluated by integration of expressions given by equations (C.21) using relations given by equations (C.2), (C.3), (C.6), and (C.7) with $m_j = 0$, $\ell_j = \pm 1$.

We obtain

$$\tilde{A}_{ij} = -8(\tilde{x}_i - \tilde{\xi}_j)\left\{\frac{\tilde{y}_i - \tilde{\eta}_{j+1}}{\left[(\tilde{x}_i - \tilde{\xi}_j)^2 + (\tilde{y}_i - \tilde{\eta}_{j+1})^2\right]^2} - \frac{\tilde{y}_i - \tilde{\eta}_j}{\left[(x_i - \tilde{\xi}_j)^2 + (y_i - \tilde{\eta}_j)^2\right]^2}\right\}$$

(Eq. (C.30) continued on next page)

$$\tilde{B}_{ij} = \frac{4}{\ell_j}\left\{\frac{\tilde{y}_i - \tilde{\eta}_{j+1}}{(\tilde{x}_i - \tilde{\xi}_j)^2 + (\tilde{y}_i - \tilde{\eta}_{j+1})^2} - \frac{\tilde{y}_i - \tilde{\eta}_j}{(\tilde{x}_i - \tilde{\xi}_j)^2 + (\tilde{y}_i - \tilde{\eta}_j)^2}\right\}$$

$$\tilde{C}_{ij} = 2(\tilde{x}_i - \tilde{\xi}_j)\left\{\frac{\tilde{y}_i - \tilde{\eta}_{j+1}}{(\tilde{x}_i - \tilde{\xi}_j)^2 + (\tilde{y}_i - \tilde{\eta}_{j+1})^2} - \frac{\tilde{y}_i - \tilde{\eta}_j}{(\tilde{x}_i - \tilde{\xi}_j)^2 + (\tilde{y}_i - \tilde{\eta}_j)^2}\right\}$$

$$\tilde{D}_{ij} = \frac{1}{\ell_j}\left\{(\tilde{y}_i - \tilde{\eta}_{j+1})\ell n\left[(\tilde{x}_i - \tilde{\xi}_j)^2 + (\tilde{y}_i - \tilde{\eta}_{j+1})^2\right]\right.$$

$$\left. - (\tilde{y}_i - \tilde{\eta}_j)\ell n\left[(\tilde{x}_i - \tilde{\xi}_j)^2 + (\tilde{y}_i - \tilde{\eta}_j)^2\right] - \Delta\tilde{\eta}_j\right\}$$

$$\tilde{E}_{ij} = 4\left[\tan^{-1}\frac{\tilde{y}_i - \tilde{\eta}_{j+1}}{\tilde{x}_i - \tilde{\xi}_j} - \tan^{-1}\frac{\tilde{y}_i - \tilde{\eta}_j}{\tilde{x}_i - \tilde{\xi}_j}\right] - \tilde{C}_{ij}$$

$$\tilde{F}_{ij} = \tilde{D}_{ij} + \frac{2}{\ell_j}\left\{2(\tilde{x}_i - \tilde{\xi}_j)\left[\tan^{-1}\frac{\tilde{y}_i - \tilde{\eta}_{j+1}}{\tilde{x}_i - \tilde{\xi}_j} - \tan^{-1}\frac{\tilde{y}_i - \tilde{\eta}_j}{\tilde{x}_i - \tilde{\xi}_j}\right] + \Delta\tilde{\eta}_j\right\}$$

$$\tilde{G}_{ij} = 4\left[\frac{1}{(\tilde{x}_i - \tilde{\xi}_j)^2 + (\tilde{y}_i - \tilde{\eta}_{j+1})^2} - \frac{1}{(\tilde{x}_i - \tilde{\xi}_j)^2 + (\tilde{y}_i - \tilde{\eta}_j)^2}\right]$$

$$- 8(\tilde{x}_i - \tilde{\xi}_j)^2\left[\frac{1}{\left[(\tilde{x}_i - \tilde{\xi}_j)^2 + (\tilde{y}_i - \tilde{\eta}_{j+1})^2\right]^2} - \frac{1}{\left[(\tilde{x}_i - \tilde{\xi}_j)^2 + (\tilde{y}_i - \tilde{\eta}_j)^2\right]^2}\right]$$

(Eq. (C.30) continued on next page)

$$\tilde{H}_{ij} = \frac{4(\tilde{x}_i - \tilde{\xi}_j)}{\ell_j}\left[\frac{1}{(\tilde{x}_i - \tilde{\xi}_j)^2 + (\tilde{y}_i - \tilde{\eta}_{j+1})^2} - \frac{1}{(\tilde{x}_i - \tilde{\xi}_j)^2 + (\tilde{y}_i - \tilde{\eta}_j)^2}\right]$$

$$\tilde{I}_{ij} = \ell n \frac{(\tilde{x}_i - \tilde{\xi}_j)^2 + (\tilde{y}_i - \tilde{\eta}_{j+1})^2}{(\tilde{x}_i - \tilde{\xi}_j)^2 + (\tilde{y}_i - \tilde{\eta}_j)^2}$$

$$+ 2(\tilde{x}_i - \tilde{\xi}_j)^2\left[\frac{1}{(\tilde{x}_i - \tilde{\xi}_j)^2 + (\tilde{y}_i - \tilde{\eta}_{j+1})^2} - \frac{1}{(\tilde{x}_i - \tilde{\xi}_j)^2 + (\tilde{y}_i - \tilde{\eta}_j)^2}\right]$$

$$\tilde{K}_{ij} = \frac{\tilde{x}_i - \tilde{\xi}_j}{\ell_j} \ell n \frac{(\tilde{x}_i - \tilde{\xi}_j)^2 + (\tilde{y}_i - \tilde{\eta}_{j+1})^2}{(\tilde{x}_i - \tilde{\xi}_j)^2 + (\tilde{y}_i - \tilde{\eta}_j)^2} \qquad \text{(C.30)}$$

Appendix D

A listing of the digital computer program developed to perform numerical calculations for the problems considered in this dissertation is presented in this Appendix. The program uses Fortran IV algebraic type language and was used on an IBM 7094 digital computer.

The program consists of the main program designated as PNOTCH and 18 subroutines. The schematic flow diagram of this program is shown in Fig. 75.

The program makes use of overlay with the PNOTCH executive program in the parent link, and the 18 subroutines in 10 core loads. The first four core loads are associted with the initialization section, the remaining six with the load dependent loop. This large number of core loads was necessary because of the limitation of available storage. Of the 32,768 words of total storage, only approximately 25,000 are available for the program and its data. The program uses two physical tapes and three virtual tapes (disc storage) for large tables of data that are needed repetitively throughout the iterative process. Single precision floating point arithmetic was found to be sufficient for and consistent with the mathematical model of the problem.

The program is designed to operate on different cases by changing data cards which specify such things as specimen geometry (notch depth and angle), strain hardening parameter m, the location of nodal points

(boundary nodes, interior grid) and the load. This data is read in by subroutines GRID and ELASTIC (1).

The coefficient matrix $[\tilde{B}]$ for the simultaneous equations (47)

$$[\tilde{B}]\{\tilde{x}\} = \{\tilde{R}\}$$

is computed in subroutines VCAL and PARTC and is stored on tape. The $\{\tilde{R}\}$ vector has terms that are load dependent (computed in RHCAL) and terms that are $\tilde{g}$ dependent (computed in PHICAL using TABLE). The solution of these equations is carried out in SOLVE, using modified Gauss elimination method (Crout process with pivoting).

The stress equations (49) have terms that are load dependent (i.e., $\tilde{\varphi}_i$ dependent), terms that are dependent on boundary values of $\tilde{\Phi}_i$ and $\tilde{\Phi}_i'$, and terms that are dependent on $\tilde{g}$, which is a function of plastic strains. The load dependent part is computed in ELASTC(2). The coefficients of $\tilde{\Phi}_i$ and $\tilde{\Phi}_i'$ are computed in STCCAL and CDCAL and stored on tape. The $\tilde{\Phi}$-dependent part of the stresses is computed in GCALP. The $\tilde{g}$-dependent part is computed in GCAL using TABLEC.

The $\tilde{g}$ function, defined at cell centroids, is a combination of derivatives of plastic strains (eqs. (26) or (27)). The coefficients needed to compute these derivatives are computed in DRCAL and stored on tape. The current plastic strain increments are computed in GCALG. The current increment of the $\tilde{g}$ function (i.e., $\Delta\tilde{g}$) is computed in GDERIV.

Convergence is tested after each iteration of the $\tilde{g}$-dependent loop in GCALG, and is noted if it occurs. Because the convergence

process for even a single load increment may take hours and be interrupted by random hardware failure, GCALG causes a restart card deck to be punched every third iteration.

Subroutine TRMNL causes such a deck to be punched whenever there is insufficient time left to complete another iteration. The same subroutine lists and punches final results (stresses, strains, etc.) at all cell centroids whenever convergence has occured. It also sets up the necessary arrays for the next load increment.

```
$IBFTC PNCTCH  DECK
C MAIN PROGRAM FOR SOLUTION OF PLASTIC PROBLEM
      COMMON AA,CONTST,C2,CSM,C1M,CGM,CGB,CGC,CRFP,DAY,DNMM,FMM,
     2  ITER,KL,KM,KLOAD,N,N2,NP,N2P,N7,N8,NMW,NMWP,NXCL,NYCL,NCELL,
     3  NMWH,NMAX,PI,PI4,PI8,PLM,Q,QBG,Q1,R(140),TIMA,TIMB,TMTGOF,
     4  ISTC,XMIN,XMEW
      COMMON FX(220),PHIB(220),L(220),XB(220),YB(220)
      REAL KLOAD
C CHOOSE GRID,READ PROBLEM PARAMETERS,SET UP G FIELDS ETC.IN EITHER
C INITIAL OR RESTART MODE
      WRITE (6,11)
 11   FORMAT (11H INTO GRID )
      CALL GRID
C ELASTC (1) DOES THE FOLLOWING
C READS IN PROBLEM DATA
      NN=1
      WRITE (6,13)
 13   FORMAT (29H OUT OF GRID ,INTO ELASTC(1) )
      CALL ELASTC (NN)
C COMPUTE V MATRIX A,B,C,D
      WRITE (6,14)
 14   FORMAT (29H OUT OF ELASTC(1) ,INTO VCAL )
      CALL VCAL
C COMPUTES COEFFICIENT MATRIX V(140,140) AND STORES IT ON SCRATCH TAPE
      WRITE (6,15)
 15   FORMAT (26H OUT OF VCAL ,INTO PART C )
      CALL PART C
C COMPUTES GEOMETRY-DEPENDENT STRESS COEFFICIENTS AJ,CJ,.....KJ
C FOR ALL CELLS
C COMPUTE STCF MATRIX
      WRITE (6,16)
 16   FORMAT (28H OUT OF PART C ,INTO STCCAL )
      CALL STCCAL
C COMPUTE COEFFICIENTS FOR DERIVATIVE CALCULATION NEEDED IN GDERIV
      WRITE (6,17)
 17   FORMAT (27H OUT OF STCCAL ,INTO DRCAL )
      CALL DRCAL
      NN=2
      WRITE (6,18)
 18   FORMAT (30H OUT OF DRCAL ,INTO ELASTC(2) )
 37   CALL ELASTC (NN)
C ELASTC (2) COMPUTES THE PART OF THE RIGHT HAND SIDE THAT IS
C NOT G DEPENDENT
C COMPUTE PART OF RIGHT HAND SIDE THAT IS LOAD DEPENDENT
      WRITE (6,19)
 19   FORMAT (30H OUT OF ELAST(2) , INTO RHCAL )
      CALL RHCAL
C RESTORE ABC ARRAY
```

```
          WRITE (6,20)
 20       FORMAT (25H OUT OF RHCAL ,INTO RABC )
          CALL RABC
C COMPUTE G DEPENDENT PART OF RIGHT HAND SIDES
C SOLVE FOR NEW PHI AND PHI PRIME
          WRITE (6,21)
 21       FORMAT (26H OUT OF RABC ,INTO PHICAL )
 36       CALL PHICAL
          WRITE (6,22)
 22       FORMAT (27H OUT OF PHICAL ,INTO SOLVE )
          CALL SOLVE
          CALL TIME1(TIMB)
          IF (TIMB.LT.TIMA) TIMB=TIMB+DAY
          TIME=(TIMB-TIMA)/XMIN
          TIML=TMTGOF-TIMB
          WRITE (6,12) TIME,TIMA,TIML,TMTGOF
 12       FORMAT (21H TIME AFTER PHI CALC F8.3,1P3E14.5)
C CALCULATE NEW G (GNEW)
C COMPUTE NEW G FIELD BY DOING THE FOLLOWING
C COMPUTE STRESSES FOR ALL CELLS USING
C NEW CAP PHI
          CONTST=0.
          WRITE (6,23)
 23       FORMAT (26H OUT OF SOLVE ,INTO GCALP )
          CALL GCALP
C OLD G FIELD
          WRITE (6,24)
 24       FORMAT (25H OUT OF GCALP ,INTO GCAL )
          CALL GCAL
          WRITE (6,25)
 25       FORMAT (25H OUT OF GCAL ,INTO GCALG )
          CALL GCALG
          WRITE (6,26)
 26       FORMAT (27H OUT OF GCALG ,INTO GDERIV )
          CALL GDERIV
C OLD PLASTIC STRAINS
          WRITE (6,27)
 27       FORMAT (27H OUT OF GDERIV ,INTO GCALG )
          CALL GCALG
          REWIND 4
          IF (CONTST.LE.0.) WRITE (6,30)
 30       FORMAT (27H OUT OF GCALG ,INTO PHICAL )
          IF (CONTST.LE.0.) GO TO 36
C MAKE TERMINAL CALCULATIONS
C DUMP GNEW FOR RESTART
C COMPUTE AND DUMP TOTAL PLASTIC STRAIN
C DUMP SIGE FOR RESTART
          WRITE (6,28)
 28       FORMAT (26H OUT OF GCALG ,INTO TRMNL )
          CALL TRMNL
          WRITE (6,29)
 29       FORMAT (30H OUT OF TRMNL ,INTO ELASTC(2) )
          GO TO 37
          END
$ORIGIN         WALT
$IBFTC GRIDR    DECK
          SUBROUTINE GRID
          COMMON AA,CONTST,C2,CSM,C1M,CGM,CGB,CGC,CREP,DAY,DNMM,FMM,
     2    ITER,KL,KM,KLOAD,N,N2,NP,N2P,N7,N8,NMW,NMWP,NXCL,NYCL,NCELL,
     3    NMWH,NMAX,PI,PI4,PI8,PLM,Q,QBG,Q1,R(140),TIMA,TIMB,TMTGOF,
```

```
     4    ISTC,XMIN,XMEW
          COMMON FX(220),PHIB(220),L(220),XB(220),YB(220)
          COMMON /ABCOM/ ABC(1),AREA(400),AGSUM(2,400),COSW(400),
     2    COIT(800),CLX(400),CLY(400),CGSW(400),DEPX(400),DEPY(400),
     3    DEPXY(400),DEPYN(400),DELG(400),ETAB(221),EPX(400),EPY(400),
     4    EPXY(400),GBAS(400),GOLD(400),M(220),TYPE(400),
     5    RS(140),RH(140),RSAV(140),SIGE(400),WDR(140),XIB(221)
          REAL KLOAD
          REAL L,M
          DIMENSION GRX(30),GRY(30),CTRX(30),CTRY(30)
          NAME LIST /PLAST/ GRX,GRY,NGRX,NGRY,NRSTRT,EMM,TMIN,KLOAD,
     2    ISTC,NMAX
C INITIALIZE GRID FOR PLASTIC ZONE
          XMEW=.33
          READ (5,PLAST)
          XMIN=3600.
          C2=XMEW/(1.-XMEW**2)
          CSM=-1./(1.+XMEW)
          C1M=-2.*(CSM-C2)
C EMM IS TANGENT MODULUS-RELATED TO STRAIN HARDENING
          ENMM=1.+2.*(1.+XMEW)/3.*EMM/(1.-EMM)
          CGM=2.*(1.+XMEW)/3.
          CGB=(1.-XMEW**2)
          CGC=XMEW/CGB
          DAY=86400.*60.
          CALL TIME1(TIMA)
          TMTGOF=TIMA+TMIN*XMIN
          NXCL=NGRX-1
          NYCL=NGRY-1
C COMPUTE CELL CENTERS-LOOPS 11 AND 12
          DO 11 J=2,NGRX
 11       CTRX(J-1)=.5*(GRX(J-1)+GRX(J))
          DO 12 J=2,NGRY
 12       CTRY(J-1)=.5*(GRY(J-1)+GRY(J))
          WRITE (6,13) (CTRX(J), J=1,NXCL)
 13       FORMAT (18H CENTER OF X CELL 10F10.5)
          WRITE (6,14) (CTRY(J), J=1,NYCL)
 14       FORMAT (18H CENTER OF Y CELL 10F10.5)
          NCELL=NXCL*NYCL
          JC=1
C COMPUTE CLX,CLY,AREA FOR ALL CELLS-LOOP 15
          DO 15 J=1,NXCL
          CXC=CTRX(J)
          WDX=GRX(J+1)-GRX(J)
          K=JC
          DO 16 KK=1,NYCL
          CLX(K)=CXC
          CGSW(K)=0.
          COSW(K)=0.
          CLY(K)=CTRY(KK)
          IF (CLY(K).LT.1.E-5) CLY(K)=0.
          WDY=GRY(KK+1)-GRY(KK)
          IF (K.LE.264)   GO TO 41
          WDY=.05
          IF (CLY(K).EQ.0.)  GO TO 41
          CLY(K)=CLY(K-1)+WDY
 41       AW=.5*WDX
          BW=.5*WDY
          AL=ALOG(AW**2+BW**2)-1.
          AB=AW*BW
```

```
          AREA(K)=4.*AB
          ASB=AW/BW
          ATN=ATAN(ASB)
          COIT(K)=AL+2.*ATN/ASB
          COIT(K+400)=AL-2.*ATN*ASB+ASB*PI
 16       K=K+1
 15       JC=JC+NYCL
          K=NCELL
C  NSTART  +N  RESTART IN MIDDLE OF NTH LOAD
C  NSTART  -N  FIRST TIME NTH LOAD
          NLCD=IABS(NRSTRT)
C INITIALIZE LOAD DEPENDENT VECTORS GBAS,EPX,EPY,EPXY,SIGE
          IF (NLOD.GT.1) GO TO 22
C GBAS IS THE PART THAT DEPENDS ON SUM OF PREVIOUS
C PLASTIC STRAINS (EPX,....
          DO 23 J=1,NCELL
          GBAS(J)=0.
          EPX(J)=0.
          EPY(J)=0.
          EPXY(J)=0.
          SIGE(J)=1.
 23       CONTINUE
          GO TO 24
 22       CALL BCREAD (GBAS(1),GBAS(K))
          CALL BCREAD (EPX(1),EPX(K))
          CALL BCREAD (EPY(1),EPY(K))
          CALL BCREAD (EPXY(1),EPXY(K))
          CALL BCREAD (SIGE(1),SIGE(K))
          DO 35 J=1,K
          Y=SIGE(J)
          IF (Y.GE.1.) GO TO 35
          SIGE(J)=1.
 35       CONTINUE
          WRITE (6,25) (GBAS(J),J=1,K)
 25       FORMAT (7H GBASE 1P10E11.4)
          WRITE (6,26) (EPX(J),J=1,K)
 26       FORMAT (7H EPX   1P10E11.4)
          WRITE (6,27) (EPY(J),J=1,K)
 27       FORMAT (7H EPY   1P10E11.4)
 28       FORMAT (7H EPXY  1P10E11.4)
          WRITE (6,28) (EPXY(J),J=1,K)
          WRITE (6,29) (SIGE(J),J=1,K)
 29       FORMAT (7H SIGE  1P10E11.4)
C INITIALIZE G DEPENDENT VECTORS GOLD,DEPX,DEPY,DEPXY
 24       IF (NRSTRT.GT.0) GO TO 17
          DO 18 J=1,NCELL
          DEPX(J)=0.
          DEPY(J)=0.
          DEPXY(J)=0.
 18       GOLD(J)=GBAS(J)
          GO TO 19
 17       CALL BCREAD (GOLD(1),GOLD(K))
          CALL BCREAD (DEPX(1),DEPX(K))
          CALL BCREAD (DEPY(1),DEPY(K))
          CALL BCREAD (DEPXY(1),DEPXY(K))
          WRITE (6,31) (GOLD(J),J=1,K)
 31       FORMAT (7H G OLD 1P1CE11.4)
          WRITE (6,32) (DEPX(J),J=1,K)
 32       FORMAT (7H DEPX  1P1CE11.4)
          WRITE (6,33) (DEPY(J),J=1,K)
```

```
 33       FORMAT (7H DEPY  1P10E11.4)
         WRITE (6,34) (DEPXY(J),J=1,K)
 34       FORMAT (7H DEPXY 1P10E11.4)
 19       RETURN
          END
$IBFTC ELASTR  DECK
          SUBROUTINE ELASTC (NN)
          COMMON AA,CONTST,C2,CSM,C1M,CGM,CGB,CGC,CREP,DAY,DNMM,EMM,
     2    ITER,KL,KM,KLOAD,N,N2,NP,N2P,N7,N8,NMW,NMWP,NXCL,NYCL,NCELL,
     3    NMWH,NMAX,PI,PI4,PI8,PLM,Q,QBG,Q1,R(140),TIMA,TIMB,TMTCOF,
     4    ISTC,XMIN,XMEW
          COMMON FX(220),PHIB(220),L(220),XB(220),YB(220)
          COMMON /ABCOM/ ABC(1),AREA(400),AGSUM(2,400),COSW(400),
     2    COIT(800),CLX(400),CLY(400),CGSW(400),DEPX(400),DEPY(400),
     3    DEPXY(400),DEPYN(400),DELG(400),ETAB(221),EPX(400),EPY(400),
     4    EPXY(400),GBAS(400),GOLD(400),M(220),TYPE(400),
     5    RS(140),RH(140),RSAV(140),SIGE(400),WDR(140),XIB(221)
          REAL KLOAD
          REAL L,M
          NAME LIST /INPUT/ N,L,M,XIB,ETAB,PHIB,       FX,AA
          NAME LIST /PLAST/ GRX,GRY,NGRX,NGRY,NRSTRT,EMM,TMIN,KLOAD,
     2    ISTC,NMAX
          IF (NN.GT.1) GO TO 21
C GEOMETRY DEPENDENT SECTION
          READ (5,INPUT)
C COUNT UNKNOWNS
          NMW=0
          DO 551 J=1,N
          IF (FX(J).EQ.0.) NMW=NMW+1
 551      CONTINUE
          X=NMW
          WRITE (6,552) NMW
 552      FORMAT (10H UNKNOWNS I5)
          NMWH=NMW/2
          NMWP=NMW/2+1
          REWIND 2
          N2=N/2
          N2P=N2+1
C GENERATE XIB AND ETAB
          DO 1 J=1,60
 1        RS(J)=XIB(J)
          NSEC=RS(1)
          JA=2
          XIB(1)=RS(2)
          ETAB(1)=RS(3)
          K=2
          DO 3 JJ=1,NSEC
          XW=RS(JA)
          YW=RS(JA+1)
          NSTEP=RS(JA+2)
          XE=RS(JA+3)
          YE=RS(JA+4)
          XNS=NSTEP
          DX=XE-XW
          DY=YE-YW
          IF (JJ.LT.NSEC) GO TO 11
          RAT=RS(JA+5)
          IF (RAT.EQ.1.) GO TO 11
          RP=RAT**NSTEP
          XI=RAT-1.
```

```
      AL=XI/(RP-1.)*DX
      YSX=DY/DX
      DO 12 KK=2,NSTEP
      RP=RP/RAT
      AW=(RP-1.)/XI
      DXV=-AW*AL
      XIB(K)=DXV
      ETAB(K)=DXV*YSX
12    K=K+1
      GO TO 13
11    DX=DX/XNS
      DY=DY/XNS
      DO 14 KK=2,NSTEP
      XIB(K)=XIB(K-1)+DX
      ETAB(K)=ETAB(K-1)+DY
14    K=K+1
13    XIB(K)=XE
      ETAB(K)=YE
      KM=K-1
      K=K+1
3     JA=JA+3
      DO 4 KK=1,N2
      XIB(K)=XIB(KM)
      ETAB(K)=-ETAB(KM)
      KM=KM-1
4     K=K+1
      N7=NMW
      N8=140
      NP=N+1
C BASIC CONSTANTS
      PI=3.1415926
      PI4=4.*PI
      PI8=8.*PI
      C=1.E-12
      CBG=1.E-8
      C1=1.-C
      CA=-2.
      CB=3.-6.*AA
      CC=6.*AA*(1.-AA)
      CD=AA**2*(3.-2.*AA)
      DO 10 J=1,N
      XB(J)=.5*(XIB(J)+XIB(J+1))
      YB(J)=.5*(ETAB(J)+ETAB(J+1))
      PHIB(J)=0.
      PLM=L(J)*M(J)
      IF (PLM.NE.0.) GO TO 10
      PHIB(J)=((CA*XB(J)+CB)*XB(J)+CC)*XB(J)+CD
10    CONTINUE
      WRITE (6,15) (XB(J),YB(J), J=1,N2)
15    FORMAT (7H XB YB 10F10.5)
C SET AREA TO ZERO IF CELL CENTER OUTSIDE PLATE
      ELW=L(N2)
      EMW=M(N2)
      DO 75 K=1,NCELL
      IF (CLX(K).GT.0.) GO TO 75
      DSC=EMW*CLY(K)+ELW*CLX(K)+.0001
      IF (DSC.LT.0.) GO TO 75
      WRITE (6,76) K,CLX(K),CLY(K),AREA(K)
76    FORMAT (16H DISCARDED CELL I5,3F12.5)
      AREA(K)=0.
```

```
 75       CONTINUE
          CRFP=1.
          RETURN
C LOAD DEPENDENT SECTION
C ELASTC (2) DOES THE FOLLOWING
C COMPUTES SMALL PHI FROM KLOAD
C COMPUTES THE PART OF THE RIGHT HAND SIDETHAT IS NOT G DEPEND IN R(140)
C COMPUTES THE PART OF THE STRESSES THAT DEPENDS ON SMALL PHI AJ,GJSUM
C (2,NCELL)
 21       WRITE (6,22) KLOAD,AA
 22       FORMAT (7H KLOAD 2F10.4)
          ITER=0
          REWIND 8
          READ (8) (ABC(K),K=1,NMAX)
          IF (CRFP.NE.1.) READ (5,PLAST)
          WRITE (6,22) KLOAD
          CRF=KLOAD/6.
C COMPUTE SMALL PHI AND AGSUM
C REMOVE OLD CRF FACTOR
          DO 43 J=1,N
          PHIB(J)=PHIB(J)/CRFP
 43       FX(J)=FX(J)/CRFP
          DO 44 J=1,NCELL
          DO 44 K=1,2
 44       AGSUM(K,J)=AGSUM(K,J)/CRFP
C USE NEW CRF FACTOR
          DO 41 J=1,N
          FX(J)=FX(J)*CRF
          PHIB(J)=PHIB(J)*CRF
 41       CONTINUE
C COMPUTE AGSUM VECTOR
          DO 42 J=1,NCELL
          DO 42 K=1,2
 42       AGSUM(K,J)=AGSUM(K,J)*CRF
          WRITE (6,INPUT)
          DO 134 J=1,NMW
 134      R(J)=WDR(J)*CRF
          CRFP=CRF
          REWIND 8
          WRITE (8) (ABC(K),K=1,NMAX)
          END FILE 8
          RETURN
          END
$IBFTC VCALR
          SUBROUTINE VCAL
          COMMON AQ,CONTST,C2,CSM,C1M,CGM,CGB,CGC,CRFP,DAY,DNMW,EMM,
     2    ITER,KL,KM,KLOAD,N,N2,NP,N2P,N7,N8,NMW,NMWP,NXCL,NYCL,NCELL,
     3    NMWH,NMAX,PI,PI4,PI8,PLM,Q,QBG,Q1,R(140),TIMA,TIMB,TMTGOF,
     4    TSTC,XMIN,XMEW
          COMMON FX(220),PHIB(220),L(220),XB(220),YB(220)
          REAL KLOAD
          COMMON /ABCOM/ ABC(1),AREA(400),AGSUM(2,400),COSW(400),
     2    COIT(800),CLX(400),CLY(400),CGSW(400),DEPX(400),DEPY(400),
     3    DEPXY(400),DEPYN(400),DELG(400),ETAB(221),EPX(400),EPY(400),
     4    EPXY(400),GBAS(400),GOLD(400),M(220),TYPE(400),
     5    RS(140),RH(140),RSAV(140),SIGE(400),WDR(140),XIB(221)
          REAL L,M
          DIMENSION V(2,222)
C CALCULATE V MATRIX-SMALL A,B,C,D
C STORE ON TAPE 2
```

```
      DO 11 J=1,N
      DO 11 KK=1,2
11    V(KK,J)=0.
      N2M=N2-1
    DO 201 II=1,N2
      I=II
      PLI=L(I)*M(I)
      L1=2
      DO 20 J=1,N
      XIJ=100*I+J
      IF (J.LE.N2) GO TO 121
      JJ=NP-J
      GO TO 122
121   JJ=J
122   K=JJ+N2
132   IF (M(J))12,16,12
12    PLM=L(J)*M(J)
41    A1=YB(I)-ETAB(J)
      B1=YB(I)-ETAB(J+1)
      A2=XB(I)-XIB(J)
      A3=XB(I)-XIB(J+1)
      A4=XIB(J+1)-XIB(J)
      BJ=-L(J)/M(J)
      A5=ALOG(A3**2+B1**2)
      A6=ALOG(A2**2+A1**2)
      A71=XB(I)+BJ**2*XIB(J)+BJ*A1
      A72=A1-BJ*A2
      A73=M(J)**2
C     CALCULATION OF A(I,J) STORED IN FIRST QUADRANT OF V(I,J),L(J)=0.
      DA=0.
      IF (I.EQ.J) GO TO 124
      IF (ABS(A72).LT.Q) GO TO 124
      DA=ATAN((XIB(J+1)/A73-A71)/A72)
      DA=DA-ATAN((XIB(J)/A73-A71)/A72)
124   I=1
      V(I,JJ)=V(I,JJ)+DA
C     CALCULATION OF B(I,J) STORED IN SECOND QUADRANT OF V(I,J)
      DB=-A4/M(J)-.5*M(J)*((BJ*B1+A3)*A5-(BJ*A1+A2)*A6)+M(J)*(A1-
     2  BJ*A2)*DA
      V(I,K)=V(I,K)+DB
C     CALCULATION OF C(I,J) STORED IN THIRD QUADRANT OF V(I,J)
      V(L1,JJ)=V(L1,JJ)+(A1-BJ*A2)*(A4+2.*M(J)*DB)
C     CALCULATION OF D(I,J) STORED IN FOURTH QUADRANT OF V(I,J)
      IF (PLM.EQ.0.) GO TO 123
C    D(I,J) ALONG NOTCH
      AA=1./M(J)**2
      AJ=ETAB(J)-BJ*XIB(J)
      I=II
      YD=YB(I)-AJ
      BB=XB(I)+BJ*YD
      CC=XB(I)**2+YD**2
      DD=XB(I)**3+YD**3/BJ
      AS=AA**2
      CA=(2.*AA*CC-BB**2)/AA
      AM=AA*CC-BB**2
      AM=ABS(AM)
      IF (AM.LT.Q) AM=0.
      IF (I.EQ.J) AM=0.
      SA=SQRT(AM)
      AN=3.*AA*BB*CC-AS*DD-2.*BB**3
```

```
      X=XIB(J)
      P1=CC-X*(2.*BB-X*AA)
      P3=-DD+X*(3.*CC+X*(-3.*BB+X*AA))
      P5=X*(QA+X*(-BB+X*AA/3.))
      P7=AA*X-BB
      X=XIB(J+1)
      P2=CC-X*(2.*BB-X*AA)
      P4=-DD+X*(3.*CC+X*(-3.*BB+X*AA))
      P6=X*(QA+X*(-BB+X*AA/3.))
      P8=AA*X-BB
      A7C=0.
      IF (AM.LE.0.) GO TO 113
      A7C=ATAN(P8/SA)-ATAN(P7/SA)
 113  V(L1,K)=V(L1,K)+(P4*ALOG(P2)-P3*ALOG(P1)+2.*(P5-P6)-AN*ALOG
     2 (P2/P1)/AS+4.*AM*SA*A7C/AS)/(6.*M(J))
 432  FORMAT (5H 432 1P8E14.4)
      GO TO 20
 123  V(L1,K)=V(L1,K) -.5*M(J)*((A3**3/3.+A3*A1**2)*A5-(A2**3/3.+A2
     2 *A1**2)*A6-4.*A1**3*DA/3.+4.*A1**2*A4/3.-2.*(A3**3-A2**3)/9.)
      GO TO 20
C     M(J)=0.
 16   A1=XB(I)-XIB(J)
      A2=YB(I)-ETAB(J)
      A3=YB(I)-ETAB(J+1)
      A4=ETAB(J+1)-ETAB(J)
      A5=ALOG(A3**2+A1**2)
      A6=ALOG(A2**2+A1**2)
      A7=A1*A4/(A1**2+A2*A3)
      DA=-ATAN(A7)
      I=1
      V(I,JJ)=V(I,JJ)+DA
      DB=L(J)*(A4+.5*A3*A5-.5*A2*A6+A1*DA)
      V(I,K)=V(I,K)+DB
      V(L1,JJ)=-A1*A4+2.*L(J)*A1*DB    +V(L1,JJ)
      V(L1,K)=V(L1,K)+.5*L(J)*((A3**3/3.+A3*A1**2)*A5-(A2**3/3.+
     2 A2*A1**2)*A6+4.*A1**3*DA/3.+4.*A1**2*A4/3.-2.*(A3**3-A2**3)/9.)
 20   I=II
      WRITE (2) ((V(I,J), I=1,2), J=1,N)
      DO 202 I=1,2
      DO 202 J=1,N
 202  V(I,J)=0.
 201  CONTINUE
      END FILE 2
      REWIND 2
      REWIND 8
      WRITE (8) (ABC(K),K=1,NMAX)
      END FILE 8
      RETURN
      END
$ORIGIN        WALT
$IBFTC PARC    DECK
      SUBROUTINE PART C
      COMMON AA,CONTST,C2,CSM,C1M,CGM,CGB,CGC,CRFP,DAY,DNMM,EMM,
     2 ITER,KL,KM,KLOAD,N,N2,NP,N2P,N7,N8,NMW,NMWP,NXCL,NYCL,NCELL,
     3 NMWH,NMAX,PI,PI4,PI8,PLM,Q,QBG,Q1,R(140),TIMA,TIMB,TMTGOF,
     4 TSTC,XMIN,XMEW
      COMMON FX(220),PHIB(220),L(220),XB(220),YB(220)
      REAL L,M
      REAL KLOAD
      DIMENSION V(140,140)
```

```
      DIMENSION DRW (440)
      N8=140
      NDB=2*N
      NMW2=NMW/2
      I=1
      L1=NMWP
      DO 11 KK=1,N2
      READ (2) (DRW(K), K=1,NDB)
      IF (FX(KK).NE.0.) GO TO 11
      R(I)=0.
      R(L1)=0.
      J=1
      JJ=1
      DO 12 JW=1,NDB,2
      IF (FX(J).NE.0.) GO TO 51
      V(I,JJ)=DRW(JW)
      V(L1,JJ)=DRW(JW+1)
      GO TO 52
 51   R(I)=R(I)-DRW(JW)*FX(J)
      R(L1)=R(L1)-DRW(JW+1)*FX(J)
      GO TO 12
 52   JJ=JJ+1
 12   J=J+1
      L1=L1+1
      I=I+1
 11   CONTINUE
      DO 22 I=1,NMW2
 22   V(I,I)=V(I,I)-PI
      REWIND 2
      WRITE (2) ((V(J,K),J=1,N8),K=1,N8)
      END FILE 2
      REWIND 2
      WRITE (6,13) N8,N8
 13   FORMAT (24H WRITE V ON 2 IN PART C 2I5)
      RETURN
      END
$ORIGIN      WALT
$IBFTC STCALR  DECK
      SUBROUTINE STCCAL
      COMMON AA,CONTST,C2,CSM,C1M,CGM,CGB,CGC,CRFP,DAY,DNMM,FMM,
     2  ITER,KL,KM,KLOAD,N,N2,NP,N2P,N7,N8,NMW,NMWP,NXCL,NYCL,NCELL,
     3  NMWH,NMAX,PI,PI4,PI8,PLM,Q,QBG,Q1,R(140),TIMA,TIMB,TMTGOF,
     4  ISTC,XMIN,XMEW
      COMMON FX(220),PHIB(220),L(220),XB(220),YB(220)
      REAL KLOAD
C COMPUTES STRESS COEFFICIENTS MATRIX STCF(8XNCELLXN2),AJ,CJ,EJ,..... AND
C STORES IT ON TAPE
      DIMENSION STA(20)
      COMMON /STCOM/ ABC(1),AREA(400),AGSUM(2,400),COSW(400),
     2  COIT(800),CLX(400),CLY(400),CGSW(400),DEPX(400),DEPY(400),
     3  DEPXY(400),DEPYN(400),DELG(400),ETAB(221),EPX(400),EPY(400),
     4  EPXY(400),GBAS(400),GOLD(400),M(220),TYPE(400),
     5  RS(140),RH(140),RSAV(140),SIGE(400),WDR(140),XIB(221)
      REAL L,M
      DIMENSION TAS(20,510)
C RESTORE ABC ARRAY
      REWIND 8
      READ (8) (ABC(K),K=1,NMAX)
      DO 13 J=1,NMW
 13   WDR(J)=R(J)
```

```
          JR=1
          KL=20
          REWIND 4
          DO 1 JCL=1,NCELL
          IF (JR.LE.20) GO TO 41
          WRITE (4) ((TAS(J,K),J=1,KL),K=1,510)
          JCD=JCL-1
          JCB=JCL-KL
          WRITE (6,42) JCB,JCD
 42       FORMAT (13H TAPE 4 DUMP 2I5)
 21       JR=1
 41       DO 4 K=1,510
 4        TAS(JR,K)=0.
          STA(2)=CLX(JCL)
          STA(3)=CLY(JCL)
          ASB=0.
          GSB=0.
          STA (17)=ASB
          STA(18)=GSB
          DO 2 J=1,N
          IF (J.LE.N2) GO TO 55
          JJ=NP-J
          GO TO 56
 55       JJ=J
 56       K=JJ+N2
          STA(1)=J
          STA(4)=JJ
C CELL CENTER AT (S2,S3)
C J AND JJ AT S1 AND S4
          CALL CDCAL (STA)
C CJ,DJ,EJ,FJ,IJ,KJ,AJ,GJ AT S11-S18
          JC=(JJ-1)*6+1
          DO 3 K=11,16
          TAS(JR,JC)=STA(K)+TAS(JR,JC)
 3        JC=JC+1
          IF (J.LT.N) GO TO 2
          AGSUM (1,JCL)=STA(17)
          AGSUM(2,JCL)=STA(18)
 2        CONTINUE
 1        JR=JR+1
          JR=JR-1
          JQ=NCELL
          WRITE (6,43) JR,JQ
 43       FORMAT (10H LAST ROW 2I5)
          WRITE (6,44) (AGSUM (1,K),K=1,JQ)
          WRITE (6,45)
 45       FORMAT (25H ASUM ABOVE , GSUM BELOW )
          WRITE (6,44) (AGSUM (2,K),K=1,JQ)
 44       FORMAT (7H AGSUM 1P10E12.4)
          JCB=JCB+KL
          JCD=JCD+KL
          WRITE (6,42) JCB,JCD
          WRITE (4) ((TAS(J,K),J=1,KL),K=1,510)
          REWIND 8
          WRITE (8) (ABC(K),K=1,NMAX)
          END FILE 8
          RETURN
          END
$IBFTC CDCALR  DECK
          SUBROUTINE CDCAL(STW)
```

```
      DIMENSION STW(1),STA(20),VXW(8)
      COMMON AA,CONTST,C2,CSM,C1M,CGM,CGB,CGC,CRFP,DAY,DNMM,EMM,
     2  ITER,KL,KM,KLOAD,N,N2,NP,N2P,N7,N8,NMW,NMWP,NXCL,NYCL,NCELL,
     3  NMWH,NMAX,PI,PI4,PI8,PLM,Q,QBG,Q1,R(140),TIMA,TIMB,TMTGOF,
     4  TSTC,XMIN,XMEW
      COMMON FX(220),PHIB(220),L(220),XB(220),YB(220)
      REAL KLOAD
      COMMON /STCOM/ ABC(1),AREA(400),AGSUM(2,400),COSW(400),
     2  COIT(800),CLX(400),CLY(400),CGSW(400),DEPX(400),DEPY(400),
     3  DEPXY(400),DEPYN(400),DELG(400),ETAB(221),EPX(400),EPY(400),
     4  EPXY(400),GBAS(400),GOLD(400),M(220),TYPE(400),
     5  RS(140),RH(140),RSAV(140),SIGE(400),WDR(140),XIB(221)
      REAL L,M
      REAL IJ,KJ
      DO 1 K=1,18
1     STA(K)=STW(K)
      IF (NR.EQ.5) GO TO 41
      NR=5
      J19=0
      DO 21 J=1,N
      IF (L(J).NE.0.) GO TO 21
      J19=J
      WRITE (6,24) J19
24    FORMAT (5H J19 I5)
      GO TO 41
21    CONTINUE
41    X=STA(2)
      Y=STA(3)
      SXA=STA(17)
      SXG=STA(18)
      J=STA(1)
      JJ=STA(4)
      JSW=1
      IF (L(JJ).EQ.0.) JSW=-1
      A1=X-XIB(J)
      A2=X-XIB(J+1)
      A3=Y-ETAB(J)
      A4=Y-ETAB(J+1)
      IF (ABS(A1).LT.Q) GO TO 72
      A5=ATAN(A4/A1)-ATAN(A3/A1)
      GO TO 73
72    A5=0.
73    IF (ABS(A3).LT.Q) GO TO 74
      A6=ATAN(A2/A3)-ATAN(A1/A3)
      GO TO 75
74    A6=0.
75    A7=A1**2+A3**2
      A8=A2**2+A4**2
      A9=ALOG(A7)
      A10=ALOG(A8)
      IF (M(J)) 80,90,80
C     IF M(J)=0.
90    B1=A7*A8
      B2=B1**2
      AJ=8.*A1*(A3*A8**2-A4*A7**2)/B2
      BJ=4.*L(J)*(A4*A7-A3*A8)/B1
      CJ=.5*A1*BJ/L(J)
      DJ=L(J)*(A4*A10-A3*A9-ETAB(J+1)+ETAB(J))
      EJ=4.*A5-CJ
      FJ=L(J)*(4.*A1*A5+A4*(A10-2.)-A3*(A9-2.)-ETAB(J+1)+ETAB(J))
```

```
      CJ=4.*(A7-A8)/B1+8.*A1**2*(A8**2-A7**2)/B2
      HJ=4.*L(J)*A1*(A7-A8)/B1
      IJ=2.*A1**2*(A7-A8)/B1+A10-A9
      KJ=L(J)*A1*(A10-A9)
      GO TO 95
80    BJJ=-L(J)/M(J)
      AJJ=ETAB(J)-BJJ*XIB(J)
      YD=Y-AJJ
      AW=X*X+YD**2
      BW=-2.*(X+BJJ*YD)
      CW=1.+BJJ**2
      DW=X*X-YD**2
      EW=-2.*(X-BJJ*YD)
      DSS=4.*AW*CW-BW**2
      DS2=BW**2-2.*AW*CW
      FW=1.-BJJ**2
      CS=CW**2
57    FORMAT (8H DSZERO 1P4E14.5)
      IF (DSS.LT.0) DSS=.01
      DS=SQRT(DSS)
      XX=XIB(J+1)
      XS=XX**2
      P2=2.*CW*XX+BW
      P3=AW+BW*XX+CW*XS
      P4=BW*XX+2.*AW
      P5=ATAN(P2/DS)
      P3S=P3**2
      P6=DS2*XX+BW*AW
      XX=XIB(J)
      XS=XX**2
      P2X=2.*CW*XX+BW
      P3X=AW+BW*XX+CW*XS
      P4X=BW*XX+2.*AW
      P5X=ATAN(P2X/DS)
      P3SX=P3X**2
      P5D=P5-P5X
      P6X=DS2*XX+BW*AW
      AL=ALOG(P3/P3X)
      XLD=X*L(J)-YD*M(J)
      XLS=X*L(J)+YD*M(J)
      XMD=X*M(J)-YD*L(J)
      XL3=-BJJ**3*X-YD
      EM2=M(J)**2
      EM3=M(J)*EM2
      XMS=X*M(J)+YD*L(J)
      XI1=(P2/P3+4.*CW/DS*P5D-P2X/P3X)/DSS
      XI2=-(P4/P3-P4X/P3X+2.*BW/DS* P5D)/DSS
      XI3=(.5*(P2/P3S-P2X/P3SX)+3.*CW/DSS*(P2/P3-P2X/P3X)+12.
     2*(CW/DSS)**2*DS*P5D)/DSS
      XI4=-.5*(P4/P3S-P4X/P3SX+3.*BW*XI1)/DSS
      XI5=-(XIB(J+1)/P3S-XIB(J)/P3SX-AW*XI3+BW*XI4)/(3.*CW)
      XI6=((P6/P3-P6X/P3X)/CW+4.*AW/DS*P5D)/DSS
      XI7=2.*P5D/DS
      XI8=.5*AL/CS+BW*(BW**2-6.*AW*CW)*P5D*DS/(CS*DSS**2)-BW*(BW**2
     2-3.*AW*CW)/(CS*DSS)*(XIB(J+1)/P3-XIB(J)/P3X)-AW*(BW**2-2.*AW
     3*CW)/(CS*DSS)*(1./P3-1./P3X)
      XI9=(.5*(P2*ALOG(P3)-P2X*ALOG(P3X))-P2+P2X+DS*P5D)/CW
      XI10=(.5*AL-BW/DS*P5D)/CW
      XI11=(CW*(XIB(J+1)-XIB(J))-.5*BW*AL+DS2/DS*P5D)/CS
C     REMEMBER BJ AND HJ MULTIPLY ZEROS
```

```
      CJ=2./M(J)*XLS*XI7+4./M(J)*X*YD*XMD*XI1+4./M(J)*(AW*L(J)-2.*
     2 )*YD/M(J))*XI2-4.*(2.*L(J)/EM2*XMD+XL3)*XI6+4.*L(J)/EM3*XI8
      CJ=(XI9+2.*(YD**2*XI7-2.*BJJ*YD*XI10+BJJ**2*XI11)+XIB(J+1)
     2   -XIB(J))/M(J)
      EJ=4.*XLS*XI7/M(J)-CJ
      FJ=(XI9+2.*(X*X*XI7-2.*X*XI10+XI11)+XIB(J+1)-XIB(J))/M(J)
      IJ=2.*XMS*XI7/M(J)-2.*FW*XI10-4.*X*YD*XLS*XI1/M(J)-4.*XLS*XLD
     2 *XI2/EM2+4.*L(J)*XLS*XI6/EM2
      KJ=2.*X*YD*XI7/M(J)+2.*XLD*XI10/EM2+2.*BJJ*XI11/M(J)
      AJ=16.*(.5*XLD*XI1-L(J)*XI2-XLS/(3.*CW)*((3.*CW*DW+AW*FW)*XI3
     2 +(3.*CW*EW-BW*FW)*XI4-FW*(XIB(J+1)/P3S-XIB(J)/P3SX)))/M(J)
      GJ=-8.*XMS*XI1/M(J)+8.*FW*XI2+32.*X*YD*XLS*XI3/M(J)+32.*XLS
     2 *XLD*XI4/EM2-32.*L(J)*XLS*XI5/EM2
      IF (JSW) 96,96,95
 96   IF (J.NE.J19) GO TO 195
      VXW(1)=1.2
      XS=X*X
      AM=AA-1.
      XA=X+AA
      XM=X+AM
      XAS=XA**2
      XMS=XM**2
      VXW(2)=-1.2
      DO 97 JK=1,2
      ET=VXW(JK)
      YA=Y-ET
      YAS=YA**2
      YAB=ABS(YA)
      XAY=XAS+YAS
      XMY=XMS+YAS
      XAYS=XAY**2
      XMYS=XMY**2
      AL=ALOG(XAY/XMY)
      ATD=ATAN(XM/YAB)-ATAN(XA/YAB)
      SET=YA/YAB
      XAD=(XMS-XAS)/(XAY*XMY)
      XY=24.*YA*AL+48.*YA*(YAS-XS+(1.-2.*AA)*X-AA*AM)*XAD+8.*YA*(YAS
     2 -3.*XS+3.*(1.-2.*AA)*X-3.*AA*AM)*((XAS-YAS)/XAYS-(XMS-YAS)/XMYS)
     3 +48.*SET*(X-.5*(1.-2.*AA))*ATD+96.*YA*(X-.5*(1.-2.*AA))*(XA/
     4 XAY-XM/XMY)+16.*YA*(1.5*(1.-2.*AA)*(XS-YAS)-X*(XS-3.*YAS)-
     5 3.*AA*AM*X+.5*AA**2*(3.-2.*AA))*(XM/XMYS-XA/XAYS)
      VXW(JK+2)=XY
      XY=16.-24.*(X-.5*(1.-2.*AA))*AL+24.*(YAS-XS+(1.-2.*AA)*X+AA*
     2 (1.-AA))*(XA/XAY-XM/XMY)+48.*YAS*(.5*(1.-2.*AA)-X)*XAD+16.*YAS*
     3 (YAS-3.*XS+3.*(1.-2.*AA)*X+3.*AA*(1.-AA))*(XM/XMYS-XA/XAYS)
     4 +48.*YAB*ATD+48.*YAS*(X-.5*(1.-2.*AA))*(1./XMY-1./XAY)+24.*(YAS
     5 -XS+(1.-2.*AA)*X+AA*(1.-AA))*(XA/XAY-XM/XMY)+8.*(1.5*(1.-2.*AA)
     6 *(XS-YAS)-X*(XS-3.*YAS)+3.*AA*(1.-AA)*X+.5*AA**2*(3.-2.*AA))
     7 *((XMS-YAS)/XMYS-(XAS-YAS)/XAYS)
      VXW(JK+4)=XY
 97   CONTINUE
      AJ=VXW(3)-VXW(4)
      GJ=VXW(5)-VXW(6)
      SXA=SXA+AJ*CREP
      TXG=TXG+GJ*CREP
      GO TO 98
 195  AJ=0.
      GJ=0.
C     STRESSES
 95   SXA=SXA+AJ*PHIB(JJ)
```

```
          TXG=TXG+GJ*PHIB(JJ)
 98       STA(11)=CJ
          STA(12)=DJ
          STA(13)=EJ
          STA(14)=FJ
          STA(15)=IJ
          STA(16)=KJ
          STA(17)=SXA
          STA(18)=TXG
          DO 2 K=11,18
 2        STW(K)=STA(K)
          RETURN
          END
$ORIGIN         WALT
$IBFTC DRCALR  DECK
          SUBROUTINE DRCAL
C COMPUTE DERVATIVE COEFFICIENT (DRV) NEEDED IN GDERIV
          COMMON AA,CONTST,C2,CSM,C1M,CGM,CGB,CGC,CRFP,DAY,DNMM,EMM,
     2    ITER,KL,KM,KLOAD,N,N2,NP,N2P,N7,N8,NMW,NMWP,NXCL,NYCL,NCELL,
     3    NMWH,NMAX,PI,PI4,PI8,PLM,Q,QBG,Q1,R(140),TIMA,TIMB,TMTGOF,
     4    ISTC,XMIN,XMEW
          COMMON FX(220),PHIB(220),L(220),XB(220),YB(220)
          REAL KLOAD
          DIMENSION DRV (20,400)
          COMMON /DRCOM/ ABC(1),AREA(400),AGSUM(2,400),COSW(400),
     2    COIT(800),CLX(400),CLY(400),CGSW(400),DEPX(400),DEPY(400),
     3    DEPXY(400),DEPYN(400),DELG(400),ETAB(221),EPX(400),EPY(400),
     4    EPXY(400),GBAS(400),GOLD(400),M(220),TYPE(400),
     5    RS(140),RH(140),RSAV(140),SIGE(400),WDR(140),XIB(221)
          REAL L,M
          REWIND 8
          READ (8) (ABC(K),K=1,NMAX)
          NYCS=NYCL
          C2=0.
          CSM=-1.
          C1M=2.
          DO 41 J=1,NCELL
          KREM=(J/NYCL)*NYCL-J
          JB=J+NYCL
          JT=J-NYCL
          DRV(2,J)=0.
          DRV(5,J)=0.
          DRV(6,J)=0.
          DRV(7,J)=J
          DRV(8,J)=J
          DRV(4,J)=J
          IF (J.GT.NYCL) GO TO 42
C SECTION FOR TOP BORDER CELLS
          IF (AREA(J).GT.0.) GO TO 43
C SECTION FOR POINTS OUTSIDE PLATE
 47       DRV(1,J)=0.
          TYPE(J)=9.
          GO TO 41
 43       IF (KREM.GE.C ) GO TO 44
          TYPE(J)=10.
          GO TO 41
 44       TYPE(J)=8.
          GO TO 41
 42       IF (AREA(J).LE.0.) GO TO 47
          AXY=1.
```

```
          IF (CLY(J).GT.0.) GO TO 45
C CENTER LINE SECTION
          WXY=-1.
          IF (AREA(JT).GT.0.) GO TO 46
C SECTION FOR FIRST CELL BELOW NOTCH
          TYPE(J)=6.
          GO TO 41
 46       IF (JB.LT.NCELL) GO TO 48
          TYPE(J)=3.
          GO TO 41
C SECTION FOR BOTTOM BORDER CELLS
 45       IF (KREM.LT.0 ) GO TO 50
C SECTION FOR RIGHT BORDER CELLS
          TYPE(J)=7.
          IF (JB.GT.NCELL) TYPE(J)=11.
          GO TO 41
 50       JB=J+NYCL
          IF (JB.GT.NCELL) GO TO 49
          JUL=J-NYCL-1
          IF (AREA(JUL).GT.0.) GO TO 51
C POSTPONE TREATMENT OF CELLS BORDERING ON NOTCH
          TYPE(J)=4.
          GO TO 41
 49       TYPE(J)=5.
          GO TO 41
 48       TYPE(J)=2.
          DYL=CLY(J+1)-CLY(J)
          GO TO 52
 51       DYL=CLY(J)-CLY(J-1)
          TYPE(J)=1.
 52       DYR=CLY(J+1)-CLY(J)
          DXT=CLX(J)-CLX(JT)
          DXB=CLX(JB)-CLX(J)
          SUMX=DXB+DXT
          SUMY=DYR+DYL
          RAX=DXB/DXT
          RAY=DYR/DYL
          BET4=-RAY/SUMY
          BET6=1./(SUMY*RAY)
          TSY=2./SUMY
          TSX=2./SUMX
          ALF4=TSY/DYL
          ALF6=TSY/DYR
          BET2=-RAX/SUMX
          BET8=1./(RAX*SUMX)
          ALF2=TSX/DXT
          ALF8=TSX/DXB
          CRV(1,J)=C2*ALF2
          CRV(2,J)=CSM*ALF4
          CRV(3,J)=-C2*(ALF2+ALF8)-CSM*(ALF4+ALF6)
          CRV(4,J)=CSM*ALF6
          CRV(5,J)=C2*ALF8
          CRV(6,J)=CSM*ALF2
          CRV(7,J)=C2*ALF4
          CRV(8,J)=-CSM*(ALF2+ALF8)-C2*(ALF4+ALF6)
          CRV(9,J)=C2*ALF6
          CRV(10,J)=CSM*ALF8
          CEL1=BET2*BET4*C1M
          CEL3=BET2*BET6*C1M
          CEL7=BET4*BET8*C1M
```

```
          DEL9=BET6*BET8*C1M
          DRV(11,J)=DEL1*WXY
          DRV(12,J)=-DEL1-DEL3
          DRV(13,J)=DEL3
          DRV(14,J)=-(DEL1+DEL7)*WXY
          DRV(15,J)=DEL1+DEL3+DEL7+DEL9
          DRV(16,J)=-DEL3-DEL9
          DRV(17,J)=DEL7*WXY
          DRV(18,J)=-DEL7-DEL9
          DRV(19,J)=DEL9
 41       CONTINUE
          NYCL=NYCS
C SECTION FOR NOTCH BORDER CELLS
          DO 53 J=1,NCELL
          TYPW=TYPE(J)
          IF (TYPW.NE.4.) GO TO 53
          JB=J+NYCL
 55       TYPB=TYPE(JB)
          IF (TYPB.EQ.1.) GO TO 54
          JB=JB+NYCL
          GO TO 55
 54       JBB=JB+NYCL
          DJB=(CLX(J)-CLX(JB))/(CLX(JBB)-CLX(JB))
          DRV(1,J)=.5*DJB
          DRV(2,J)=.5*(1.-DJB)
          DRV(3,J)=JBB
          DRV(4,J)=JB
          JR=J+1
 56       TYPR=TYPE(JR)
          IF (TYPR.EQ.1.) GO TO 57
          JR=JR+1
          GO TO 56
 57       DJR=(CLY(J)-CLY(JR))/(CLY(JR+1)-CLY(JR))
          DRV(5,J)=.5*DJR
          DRV(6,J)=.5*(1.-DJR)
          DRV(7,J)=JR+1
          DRV(8,J)=JR
 53       CONTINUE
          WRITE (4) ((DRV(J,K),J=1,20),K=1,400)
          WRITE (6,11) ABC(1)
 11       FORMAT (33H WRITE DRV(20,400) ON 4 IN DRCAL F6.1)
          END FILE 4
          REWIND 4
          REWIND 8
          WRITE (8) (ABC(K),K=1,NMAX)
          END FILE 8
          RETURN
          END
$ORIGIN         WALT
$IBFTC RHCALR  DECK
          SUBROUTINE RHCAL
C         CALCULATION OF RIGHT HAND SIDE
          COMMON AA,CONTST,C2,CSM,C1M,CGM,CGB,CGC,CRFP,DAY,DNMM,EMM,
     2    ITER,KL,KM,KLOAD,N,N2,NP,N2P,N7,N8,NMW,NMWP,NXCL,NYCL,NCELL,
     3    NMWH,NMAX,PI,PI4,PI8,PLM,Q,QBG,Q1,R(140),TIMA,TIMB,TMTGOF,
     4    TSTC,XMIN,XMEW
          COMMON FX(220),PHIB(220),L(220),XB(220),YB(220)
          REAL L,M
          REAL KLOAD
          DIMENSION V(140,140)
```

```
      CRF=KLOAD/6.
      N8=140
      REWIND 2
      WRITE (6,11) CRF,N8
11    FORMAT (24H READ V FROM 2 IN RHCAL F6.1,I5)
      READ (2) ((V(J,K),J=1,N8),K=1,N8)
      REWIND 2
      A1=1.-AA
      A2=1.-2.*AA
      A5=2.*A2
      A6=3.*A2
      A7=3.*AA*A1
      B2=AA**2*(3.-2.*AA)
      JJ=1
      L1=NMWP
      DO 25 I=1,N2
      IF (FX(I).NE.0.) GO TO 25
      JP=1
      DO 26 J=1,N2
      IF (FX(J).NE.0.) GO TO 26
      IF (L(J).NE.0.) GO TO 54
      IF (I.NE.J) GO TO 53
      R(L1)=R(L1)+PI4*PHIB(I)
      GO TO 53
54    IF (L(J).NE.1.) GO TO 53
      R(L1)=R(L1)-4.*V(JJ,JP)*PHIB(J)
53    JP=JP+1
26    CONTINUE
      A3=XB(I)+AA
      A4=XB(I)-A1
      YD=YB(I)-1.20
      YS=YD**2
      XS=XB(I)**2
      C=ALOG((A3**2+YS)/(A4**2+YS))
      AY=ABS(YD)
      IF (AY.GT.QBG) GO TO 35
34    E=0.
      GO TO 39
35    E=(ATAN(A3/AY)-ATAN(A4/AY))/AY
39    R(L1)=R(L1)-4.*YD*(4.*XB(I)-A5+(YS-3.*XB(I)**2+A6*XB(I)+A7)*C
     2  -(-2.*XB(I)*(XS-3.*YS)+A6*(XS-YS)+2.*A7*XB(I)+B2)*E)*CRF
      YD=-YB(I)-1.20
      YS=YD**2
      C=ALOG((A3**2+YS)/(A4**2+YS))
      AY=ABS(YD)
      E=(ATAN(A3/AY)-ATAN(A4/AY))/AY
      R(L1)=R(L1)-4.*YD*(4.*XB(I)-A5+(YS-3.*XB(I)**2+A6*XB(I)+A7)*C
     2  -(-2.*XB(I)*(XS-3.*YS)+A6*(XS-YS)+2.*A7*XB(I)+B2)*E)*CRF
      L1=L1+1
      JJ=JJ+1
25    CONTINUE
      RETURN
      END
$ORIGIN       WALT
$IBFTC RABCR   DECK
      SUBROUTINE RABC
C RESTORE ABC ARRAY
      COMMON AA,CONTST,C2,CSM,C1M,CGM,CGB,CGC,CRFP,DAY,DNMM,EMM,
     2  ITER,KL,KM,KLOAD,N,N2,NP,N2P,N7,N8,NMW,NMWP,NXCL,NYCL,NCELL,
     3  NMWH,NMAX,PI,PI4,PI8,PLM,Q,QBG,Q1,R(140),TIMA,TIMB,TMTGOF,
```

```
     4    ISTC,XMIN,XMEW
          COMMON FX(220),PHIB(220),L(220),XB(220),YB(220)
          COMMON /PHCOM/ ABC(1),AREA(400),AGSUM(2,400),COSW(400),
     2    COIT(800),CLX(400),CLY(400),CGSW(400),DEPX(400),DEPY(400),
     3    DEPXY(400),DEPYN(400),DELG(400),ETAB(221),EPX(400),EPY(400),
     4    EPXY(400),GBAS(400),GOLD(400),M(220),TYPE(400),
     5    RS(140),RH(140),RSAV(140),SIGE(400),WDR(140),XIB(221)
          TNMAX=NMAX
          WRITE (6,12) PI,TNMAX
          CALL TIME1(TIMB)
          IF (TIMB.LT.TIMA) TIMB=TIMB+DAY
          TIME=(TIMB-TIMA)/XMIN
          WRITE (6,12) TIME,TIMA,TIMB,TMTGOF
 12       FORMAT (19H TIME TO GET READY F8.3,1P3E14.5)
C SAVE BASE RIGHT HAND SIDES IN RSAV
          REWIND 8
          READ (8) (ABC(K),K=1,NMAX)
          DO 35 J=1,NMW
 35       RSAV(J)=R(J)
          RETURN
          END
$IBFTC PHCALR  DECK
          SUBROUTINE PHICAL
C CALCULATE NEW CAP PHI AND PHIP R(140)
          DIMENSION CRH(140)
          COMMON AA,CONTST,C2,CSM,C1M,CGM,CGB,CGC,CRFP,DAY,DNMM,EMM,
     2    ITER,KL,KM,KLOAD,N,N2,NP,N2P,N7,N8,NMW,NMWP,NXCL,NYCL,NCELL,
     3    NMWH,NMAX,PI,PI4,PI8,PLM,Q,QBG,Q1,R(140),TIMA,TIMB,TMTGOF,
     4    ISTC,XMIN,XMEW
          COMMON FX(220),PHIB(220),L(220),XB(220),YB(220)
          REAL KLOAD
          COMMON /PHCOM/ ABC(1),AREA(400),AGSUM(2,400),COSW(400),
     2    COIT(800),CLX(400),CLY(400),CGSW(400),DEPX(400),DEPY(400),
     3    DEPXY(400),DEPYN(400),DELG(400),ETAB(221),EPX(400),EPY(400),
     4    EPXY(400),GBAS(400),GOLD(400),M(220),TYPE(400),
     5    RS(140),RH(140),RSAV(140),SIGE(400),WDR(140),XIB(221)
C INITIALIZE RIGHT HAND SIDES
          IF (ITER.LE.0) GO TO 22
          REWIND 8
          READ (8) (ABC(K),K=1,NMAX)
 22       SWW=1.
          DO 1 J=1,NMW
 1        R(J)=RSAV(J)
          J=99
          GW=1.
          GAP=1.
          NCRHS=0
          SWG=1.
          WRITE (6,16) J,GW,GAP,SWW,SWG,(R(K),K=1,NMW)
C ADD G DEPENDENT TERMS TO R.H.S.
          DO 2 J=1,NCELL
          SWW=7.
          SWG=7.
          GW=GOLD(J)
C SKIP CALCULATIONS WHEN G IS ZERO
          IF (GW.EQ.0.) GO TO 21
          SWW=COSW(J)
          ARW=AREA(J)
          GAP=GW*ARW
          JQ=1
```

```
          KQ=NMWP
C ARE COEFFICIENTS ON TAPE FOR THIS CELL
C COSW(J) NON ZERO
          IF (SWW.NE.0.) GO TO 11
C COMPUTE AND STORE COEFFICIENTS FOR THIS CELL,EQ.BY EQ. IN CRH
          XIW=CLX(J)
          DO 3 JY=1,N2
C IS THIS AN EQUATION TO TREAT
          IF (FX(JY).NE.0.) GO TO 12
C YES IT IS
          JQN=JQ+1
          KQN=KQ+1
          RJQ=0.
          RKQ=0.
          ETW=CLY(J)
          XW=XB(JY)
          YW=YB(JY)
          DX=XW-XIW
          DY=YW-ETW
 14       RSQ=DX**2+DY**2
          AL=.5*ALOG(RSQ)
          RAL=AL*RSQ
          RJQ=RJQ-AL
          RKQ=RKQ-RAL
          IF (ETW.LE.0.) GO TO 13
          DY=YW+ETW
          ETW=0.
          GO TO 14
C CRH (14C) CONTAINS THE CURRENT RIGHT HAND COEFFICIENTS
 13       CRH(JQ)=RJQ
          CRH(KQ)=RKQ
          GO TO 15
 12       JQN=JQ
          KQN=KQ
 15       JQ=JQN
          KQ=KQN
 3        CONTINUE
          SWG=1
          CALL TABLE (1,J,SWG,CRH)
          COSW(J)=SWG
          GO TO 411
 11     SWW=-1.
          CALL TABLE (1,J,SWW,CRH)
 411      DO 4 JY=2,NMWP
          JQ=JY-1
          R(JQ)=R(JQ)+GAP*CRH(JQ)
          KQ=JQ+NMWH
          R(KQ)=R(KQ)+GAP*CRH(KQ)
 4        CONTINUE
          NCRHS=NCRHS+1
C         WRITE (6,16) J,GW,GAP
          JL=J
 16       FORMAT (9H CUR RHS I5,4F12.1/(3X,1P10E12.5))
          GO TO 2
 21       SW=0.
          CALL TABLE (1,J,SW,CRH)
 2        CONTINUE
          REWIND 8
          WRITE (8) (ABC(K),K=1,NMAX)
          END FILE 8
```

```
      IF (NCRHS.LE.0) RETURN
      J=JL
      WRITE (6,16) J,GW,GAP,SWW,SWG,(R(K),K=1,NMW)
      RETURN
      END
$IBFTC TABLER  DECK
      SUBROUTINE TABLE (NTB,JCL,SWY,TBW)
      DIMENSION TBW(1)
      COMMON AA,CONTST,C2,CSM,C1M,CGM,CGB,CGC,CREP,DAY,DNMM,EMM,
     2 ITER,KL,KM,KLOAD,N,N2,NP,N2P,N7,N8,NMW,NMWP,NXCL,NYCL,NCELL,
     3 NMWH,NMAX,PI,PI4,PI8,PLM,Q,QBG,Q1,R(140),TIMA,TIMB,TMTGOF,
     4 TSTC,XMIN,XMEW
      COMMON FX(220),PHIB(220),L(220),XB(220),YB(220)
      REAL KLOAD
      COMMON /PHCOM/ ABC(1),AREA(400),AGSUM(2,400),COSW(400),
     2 COIT(800),CLX(400),CLY(400),CGSW(400),DEPX(400),DEPY(400),
     3 DEPXY(400),DEPYN(400),DELG(400),ETAB(221),EPX(400),EPY(400),
     4 EPXY(400),GBAS(400),GOLD(400),M(220),TYPE(400),
     5 RS(140),RH(140),RSAV(140),SIGE(400),WDR(140),XIB(221)
      REAL L,M
      DIMENSION TAB(70,140),TUB(8,1200)
      EQUIVALENCE (TAB(1,1),TUB(1,1))
      JG=JCL
      SW=SWY
      IF (K8.EQ.8) GO TO 31
      K7=70
      K8=8
      K6=NCELL/K7 +1
      K5=NCELL/K8 +1
31    NR=ABC(1)
      IF (NR.EQ.5) GO TO 11
      XIB(221)=1.
      WRITE (6,13) K5,K6,K7,K8,ABC(1)
13    FORMAT (33H INITIALIZE TAB AND TUB IN TABLE 4I6,F6.1)
      ABC(1)=5.
      REWIND 3
      REWIND 1
      DO 1 JQ=1,K6
1     WRITE (1) ((TAB(J,K),J=1,K7),K=1,140)
      DO 2 JQ=1,K5
2     WRITE (1) ((TUB(J,K),J=1,K8),K=1,1200)
      END FILE 1
      REWIND 1
11    NTW=NTB
C RHS SECTION TAB(K7,140) LOGR,RHO
      IF (JG.NE.1) GO TO 15
      READ (1) ((TAB(J,K),J=1,K7),K=1,140)
      WRITE (6,41) JG,XIB(221)
41    FORMAT (32H READ TAB FROM 1 IN CORE LOAD 6 I5,F8.1)
      XIB(221)=XIB(221)+1.
      KROW=1
15    IF (KROW.LE.K7) GO TO 16
      KROW=1
      WRITE (3) ((TAB(J,K),J=1,K7),K=1,140)
      READ (1) ((TAB(J,K),J=1,K7),K=1,140)
      WRITE (6,41) JG,XIB(221)
      XIB(221)=XIB(221)+1.
16    IF (SW) 22,17,23
23    DO 3 K=1,140
3     TAB(KROW,K)=TBW(K)
```

```
      GO TO 17
 22   CO 7 K=1,140
 7    TBW(K)=TAB(KROW,K)
 17   IF (JG.NE.NCELL) GO TO 18
      WRITE (3) ((TAB(J,K),J=1,K7),K=1,140)
 18   KROW=KROW+1
      RETURN
      END
$ORIGIN        WALT
$IBFTC SOLVER  DECK
      SUBROUTINE SOLVE
      COMMON AA,CONTST,C2,CSM,C1M,CGM,CGB,CGC,CREP,DAY,DNMM,EMM,
     2 ITER,KL,KM,KLOAD,N,N2,NP,N2P,N7,N8,NMW,NMWP,NXCL,NYCL,NCELL,
     3 NMWH,NMAX,PI,PI4,PI8,PLM,Q,QBG,Q1,R(140),TIMA,TIMB,TMTGOF,
     4 ISTC,XMIN,XMEW
      COMMON FX(220),PHIB(220),L(220),XB(220),YB(220)
      REAL KLOAD
C READ V MATRIX FROM TAPE 2
      DIMENSION V(140,140)
      DIMENSION NRW(150)
      N8=140
      REWIND 2
      READ (2) ((V(J,K),J=1,N8),K=1,N8)
      WRITE (6,601) (R(J),J=1,NMW)
 601  FORMAT (5H RHS ,1P10E12.4)
      CALL FACTOR (V,NRW,N7,N8)
      CALL SIMEQ (V,NRW,N7,N8,R)
      WRITE (6,601) (R(J),J=1,NMW)
      RETURN
      END
$ORIGIN        WALT
$IBFTC GCALPR  DECK
      SUBROUTINE GCALP
C CAP PHI DEPENDENT PART OF STRESS CALC
      COMMON AA,CONTST,C2,CSM,C1M,CGM,CGB,CGC,CREP,DAY,DNMM,EMM,
     2 ITER,KL,KM,KLOAD,N,N2,NP,N2P,N7,N8,NMW,NMWP,NXCL,NYCL,NCELL,
     3 NMWH,NMAX,PI,PI4,PI8,PLM,Q,QBG,Q1,R(140),TIMA,TIMB,TMTGOF,
     4 ISTC,XMIN,XMEW
      COMMON FX(220),PHIB(220),L(220),XB(220),YB(220)
      REAL KLOAD
      COMMON /STREP/ SX(400),SY(400),SXY(400),SZZ(400),SIGEQ(400),
     2 TEX(400),TEY(400),TEXY(400)
      COMMON /GPCOM/ ABC(1),AREA(400),AGSUM(2,400),COSW(400),
     2 COIT(800),CLX(400),CLY(400),CGSW(400),DEPX(400),DEPY(400),
     3 DEPXY(400),DEPYN(400),DELG(400),ETAB(221),EPX(400),EPY(400),
     4 EPXY(400),GBAS(400),GOLD(400),M(220),TYPE(400),
     5 RS(140),RH(140),RSAV(140),SIGE(400),WOR(140),XIB(221)
      REAL L,M
      DIMENSION TAS(20,510)
      IF (K2.EQ.20) GO TO 11
      K2=20
 11   KROW=1
      REWIND 8
      READ (8) (ABC(K),K=1,NMAX)
      CO 1 JQ=1,NCELL
      IF (JQ.NE.1) GO TO 12
      READ (4) ((TAS(J,K),J=1,K2),K=1,510)
      WRITE (6,41) JQ,XIB(221)
      XIB(221)=XIB(221)+1.
 41   FORMAT (32H READ TAS FROM 4 IN CORE LOAD 8 I5,F8.1)
```

```
 12       IF (KROW.LE.K2) GO TO 13
          KROW=1
          READ (4) ((TAS(J,K),J=1,K2),K=1,510)
          WRITE (6,41) JQ,XIB(221)
          XIB(221)=XIB(221)+1.
 13       KB=1
          IF (AREA (JQ).LE.0.) GO TO 15
          SX(JQ)=AGSUM(1,JQ)
          SY(JQ)=-AGSUM(1,JQ)
          SXY(JQ)=AGSUM(2,JQ)
          J=KROW
          JG=1
          DO 2 JJ=1,N2
          IF (FX(JJ).EQ.0.) GO TO 57
          RJB=FX(JJ)
          JW=JJ+N2
          RJW=FX(JW)
          GO TO 58
 57       RJB=R(JG)
          JW=JG+NMWH
          RJW=R(JW)
          JG=JG+1
 58       SX(JQ)=SX(JQ)+TAS(J,KB)*RJB+TAS(J,KB+1)*RJW
          SY(JQ)=SY(JQ)+TAS(J,KB+2)*RJB+TAS(J,KB+3)*RJW
          SXY(JQ)=SXY(JQ)+TAS(J,KB+4)*RJB+TAS(J,KB+5)*RJW
 2        KB=KB+6
          GO TO 16
 15       SX(JQ)=0.
          SY(JQ)=0.
          SXY(JQ)=0.
 16       KROW=KROW+1
 1        CONTINUE
          J=99
          GW=1.
          GAP=1.
          SWW=1.
          SWG=1.
          WRITE (6,20) J,GW,GAP,SWW,SWG
 20       FORMAT (39H CUMULATIVE STRESS AFTER NONZERO G USE I5,4F12.4)
C         WRITE (6,17) (SX(K),K=1,NCELL)
 17       FORMAT (5H SX  1P10E12.4)
C         WRITE (6,18) (SY(K),K=1,NCELL)
 18       FORMAT (5H SY  1P10E12.4)
C         WRITE (6,19) (SXY(K) ,K=1,NCELL)
 19       FORMAT (5H SXY 1P10E12.4)
          REWIND 8
          WRITE (8) (ABC(K),K=1,NMAX)
          WRITE (8) (SX(K),K=1,1200)
          END FILE 8
          RETURN
          END
$ORIGIN        WALT
$IBFTC TABLEC  DECK
          SUBROUTINE TABLE2(NTB,JCL,SWY,TBW)
          DIMENSION TBW(1)
          COMMON AA,CONTST,C2,CSM,C1M,CGM,CGB,CGC,CRFP,DAY,DNMM,EMM,
      2   ITER,KL,KM,KLOAD,N,N2,NP,N2P,N7,N8,NMW,NMWP,NXCL,NYCL,NCELL,
      3   NMWH,NMAX,PI,PI4,PI8,PLM,Q,QBG,Q1,R(140),TIMA,TIMB,TMTGOF,
      4   TSTC,XMIN,XMEW
          COMMON FX(220),PHIB(220),L(220),XB(220),YB(220)
```

```
      REAL KLOAD
      COMMON /GCCOM/ ABC(1),AREA(400),AGSUM(2,400),COSW(400),
     2  COIT(800),CLX(400),CLY(400),CGSW(400),DEPX(400),DEPY(400),
     3  DEPXY(400),DEPYN(400),DELG(400),ETAB(221),EPX(400),EPY(400),
     4  EPXY(400),GBAS(400),GOLD(400),M(220),TYPE(400),
     5  RS(140),RH(140),RSAV(140),SIGE(400),WDR(140),XIB(221)
      REAL L,M
      DIMENSION TAB(70,140),TUB(8,1200)
      EQUIVALENCE (TAB(1,1),TUB(1,1))
      JG=JCL
      SW=SWY
      IF (K8.EQ.8) GO TO 31
      K7=70
      K8=8
      K6=NCELL/K7 +1
      K5=NCELL/K8 +1
      N5=NCELL-(K5-1)*K8
      IF (N5.LE.0) K5=K5-1
 31   NR=ABC(1)
 11   NTW=NTB
C DERIVATIVES OF RHO SECTION NEEDED IN G PART OF STRESS CALCULATIONS
 12   IF (JG.NE.1) GO TO 19
      READ (1) ((TUB(J,K),J=1,K8),K=1,1200)
      WRITE (6,41) JG,XIB(221)
 41   FORMAT (32H READ TUB FROM 1 IN CORE LOAD 1015,F8.1)
      XIB(221)=XIB(221)+1.
      KROW=1
 19   IF (KROW.LE.K8) GO TO 20
      KROW=1
      WRITE (3) ((TUB(J,K),J=1,K8),K=1,1200)
      READ (1) ((TUB(J,K),J=1,K8),K=1,1200)
      WRITE (6,41) JG,XIB(221)
      XIB(221)=XIB(221)+1.
 20   IF (SW) 24,21,25
 25   DO 4 K=1,1200
 4    TUB(KROW,K)=TBW(K)
      GO TO 21
 24   DO 8 K=1,1200
 8    TBW(K)=TUB(KROW,K)
 21   IF(JG.NE.NCELL) GO TO 18
      WRITE (3) ((TUB(J,K),J=1,K8),K=1,1200)
      END FILE 3
      REWIND 3
      REWIND 1
      DO 5 JQ=1,K6
      READ (3) ((TAB(J,K),J=1,K7),K=1,140)
      WRITE (1) ((TAB(J,K),J=1,K7),K=1,140)
 5    CONTINUE
      DO 6 JQ=1,K5
      READ (3) ((TUB(J,K),J=1,K8),K=1,1200)
      WRITE (1) ((TUB(J,K),J=1,K8),K=1,1200)
 6    CONTINUE
      ENDFILE 1
      REWIND 1
      REWIND 3
 18   KROW=KROW+1
      RETURN
      END
$IBFTC GCALR   DECK
      SUBROUTINE GCAL
```

```
      COMMON AA,CONTST,C2,CSM,C1M,CGM,CGB,CGC,CRFP,DAY,DNMM,EMM,
     2 ITER,KL,KM,KLOAD,N,N2,NP,N2P,N7,N8,NMW,NMWP,NXCL,NYCL,NCELL,
     3 NMWH,NMAX,PI,PI4,PI8,PLM,Q,QBG,Q1,R(140),TIMA,TIMB,TMTGOF,
     4 TSTC,XMIN,XMEW
      REAL KLOAD
      COMMON /GCCOM/ ABC(1),AREA(400),AGSUM(2,400),COSW(400),
     2 COIT(800),CLX(400),CLY(400),CGSW(400),DEPX(400),DEPY(400),
     3 DEPXY(400),DEPYN(400),DELG(400),ETAB(221),EPX(400),EPY(400),
     4 EPXY(400),GBAS(400),GOLD(400),M(220),TYPE(400),
     5 RS(140),RH(140),RSAV(140),SIGE(400),WDR(140),XIB(221)
      REAL L,M
      DIMENSION SX(400),SY(400),SXY(400)
      DIMENSION CCV(1200)
C G-DEPENDENT PART OF STRESS CALCULATIONS
      JNUM=3*NCELL
 11   KROW=1
      REWIND 8
      READ (8) (ABC(K),K=1,NMAX)
      READ (8) (SX(K),K=1,1200)
      J8=NYCL
      JCK=0
      DO 3 J=1,NCELL
      SWW=7.
      SWG=7.
      GW=GOLD(J)
C SKIP CALCULATIONS WHEN G IS ZERO
      IF (GW.EQ.0.) GO TO 21
      XIW=CLX(J)
      SWW=CGSW(J)
      ARW=AREA(J)
      GAP=GW*ARW
C HAVE COEFFICIENTS BEEN COMPUTED
C YES IF CGSW NON ZERO
      IF (SWW.NE.0.) GO TO 31
      JC=1
C COMPUTE COEFFICIENTS
      DO 4 JQ=1,JNUM,3
      IF (AREA(JC).LE.0.) GO TO 41
      RX=0.
      RY=0.
      RXY=0.
      ETW=CLY(J)
      XW=CLX(JC)
      YW=CLY(JC)
      DX=XW-XIW
      DXS=DX**2
      DY=YW-ETW
 34   DYS=DY**2
      RSQ=DXS+DYS
      IF (RSQ.GT.0.) GO TO 42
C CELL ON ITSELF SECTION
      RX=COIT(J)
      RY=COIT(J+400)
      RXY=0.
      GO TO 331
 42   AL=ALOG(RSQ)
      RX=RX+AL+2.*DYS/RSQ+1.
      RY=RY+AL+2.*DXS/RSQ+1.
      RXY=RXY+2.*DX*DY/RSQ
 331  IF (ETW.LE.0.) GO TO 33
```

```
          CY=YW+ETW
          ETW=0.
          GO TO 34
 33       CCV(JQ)=RX
          CCV(JQ+1)=RY
          CCV(JQ+2)=RXY
 41       JC=JC+1
 4        CONTINUE
          SWG=1.
          CALL TABLE2(2,J,SWG,CCV)
          CGSW(J)=SWG
          IF (J.NE.75) GO TO 43
          DO 22 JX=1,1200,10
          JE=JX+9
          WRITE (6,23) JX,(CCV(K),K=JX,JE)
 22       CONTINUE
 23       FORMAT (4H 75 I5,1P10E12.4)
          GO TO 43
 31       SWW=-1.
          CALL TABLE2(2,J,SWW,CCV)
 43       JQ=1
          DO 5 JC=1,NCELL
          IF (AREA(JC).LE.0.) GO TO 44
          SX(JC)=SX(JC)+GAP*CCV(JQ)
          SY(JC)=SY(JC)+GAP*CCV(JQ+1)
          SXY(JC)=SXY(JC)+GAP*CCV(JQ+2)
 44       JQ=JQ+3
 5        CONTINUE
C         WRITE (6,20) J,GW,GAP,SWW,SWG
 20       FORMAT (39H CUMULATIVE STRESS AFTER NONZERO G USE I5,4F12.4)
          JCK=JCK+1
 17       FORMAT (5H SX  1P10E12.4)
 18       FORMAT (5H SY  1P10E12.4)
 19       FORMAT (5H SXY 1P10E12.4)
          GO TO 3
 21       SW=0.
          CALL TABLE2(2,J,SW,CCV)
 3        CONTINUE
          REWIND 8
          WRITE (8) (ABC(K),K=1,NMAX)
          WRITE (8) (SX(K),K=1,1200)
          END FILE 8
          IF (JCK.LE.0) RETURN
C         WRITE (6,17) (SX(K),K=1,NCELL)
C         WRITE (6,18) (SY(K),K=1,NCELL)
C         WRITE (6,19) (SXY(K) ,K=1,NCELL)
          RETURN
          END
$ORIGIN        WALT
$IBFTC GDRVR   DECK
          SUBROUTINE GDERIV
C         COMPUTES DELG BY TAKING DERIVATIVES OF PLASTIC
C STRAIN INCREMENTS,DEPX,ETC.
          DIMENSION C(20)
          COMMON AA,CONTST,C2,CSM,C1M,CGM,CGB,CGC,CREP,DAY,DNMM,EMM,
     2    ITER,KL,KM,KLOAD,N,N2,NP,N2P,N7,N8,NMW,NMWP,NXCL,NYCL,NCELL,
     3    NMWH,NMAX,PI,PI4,PI8,PLM,Q,QBG,Q1,R(140),TIMA,TIMB,TMTGOF,
     4    TSTC,XMIN,XMEW
          COMMON FX(220),PHIB(220),L(220),XB(220),YB(220)
          REAL KLOAD
```

```
      COMMON /GDCOM/ ABC(1),AREA(400),AGSUM(2,400),COSW(400),
     2 COIT(800),CLX(400),CLY(400),CGSW(400),DEPX(400),DEPY(400),
     3 CEPXY(400),DEPYN(400),DELG(400),ETAB(221),EPX(400),EPY(400),
     4 EPXY(400),GBAS(400),GOLD(400),M(220),TYPE(400),
     5 RS(140),RH(140),RSAV(140),SIGE(400),WDR(140),XIB(221)
      REAL L,M
      DIMENSION DRV(20,400)
      READ (4) ((DRV(J,K),J=1,20),K=1,400)
      XIB(221)=XIB(221)+1.
C COMPUTE DELG FOR INTERIOR POINTS AND MOST CENTER LINE POINTS
C       SECTION FOR INTERIOR PLASTIC POINTS
      NLB=264
      DGAV=0.
      DGNM=0.
      NDC=GBAS(NCELL+2)-GBAS(NCELL+1)
      IF (NDC.LT.0) GO TO 94
      DO 95 J=1,NCELL
      IF (DELG(J).EQ.0.) GO TO 95
      DW=DEPY(J)+EPY(J)
      IF (DW.NE.0.) GO TO 95
      DELG(J)=0.
      DEPYN(J)=0.
      DEPX(J)=0.
      DEPXY(J)=0.
95    CONTINUE
94    WRITE (6,96) NDC
96    FORMAT (5H NDC I5)
      NYCS=NYCL
      DO 1 JC=1,NCELL
      TYPW=TYPE(JC)
      JR=JC+1
      JT=JC-NYCL
      JB=JC+NYCL
      IF (TYPW-2.) 11,12,1
12    JL=JR
      JUL=JT+1
      JLL=JB+1
      GO TO 13
11    JL=JC-1
      JUL=JT-1
      JLL=JB-1
13    DO 2 K=1,19
2     C(K)=DRV(K,JC)
      IF (DELG(JC).EQ.0.) GO TO 1
      JCD=(JC-253)*(JC-276)
      IF (JCD.LE.0)  GO TO 1
      PRD=DELG(JC)*DELG(JC+1)*DELG(JL)*DELG(JUL)*DELG(JLL)*DELG(JT+1)
     2 *DELG(JB+1)*DELG(JT)*DELG(JB)
      IF (PRD.EQ.0.) GO TO 1
      IF (JC-264) 81,81,82
81    IF (TYPE(JC).EQ.2.) GO TO 1
82    DELG(JC)=C(1)*DEPX(JT)+C(2)*DEPX(JL)+C(3)*DEPX(JC)+C(4)*DEPX(JR
     2 )+C(5)*DEPX(JB)+C(6)*DEPYN(JT)+C(7)*DEPYN(JL)+C(8)*DEPYN(JC)+
     3 C(9)*DEPYN(JR)+C(10)*DEPYN(JB)+C(11)*DEPXY(JUL)+C(12)*DEPXY(JT)
     4 +C(13)*DEPXY(JT+1)+C(14)*DEPXY(JL)+C(15)*DEPXY(JC)+C(16)*
     5 DEPXY(JR)+C(17)*DEPXY(JLL)+C(18)*DEPXY(JB)+C(19)*DEPXY(JB+1)
      IF (JC.LE.NLB) GO TO 1
      IF (DEPY(JC).EQ.0.) GO TO 1
      DGAV=DGAV+DELG(JC)
      DGNM=DGNM+1.
```

```
      XJC=JC
      WRITE (6,92) DELG(JC),XJC,DGNM
    1 CONTINUE
      NYCL=NYCS
      DGS=1.1
      IF (DGNM.LE.C.)  GO TO 91
      DGS=DGAV/DGNM
   91 WRITE (6,92) DGS,DGAV,DGNM
   92 FORMAT (9H GBOTTOM 1P3E16.6)
      GMX=GBAS (NCELL+4)
      GMN=-GMX
      DO 93 J=NLB,NCELL
      IF (DEPYN(J).EQ.0.) GO TO 93
      IF (DELG(J).GT.GMX) DELG(J)=GMX
      IF (DELG(J).LT.GMN) DELG(J)=GMN
   93 CONTINUE
C     SECTION FOR BORDER PLASTIC POINTS
      DO 5 JW=1,NCELL
      J=NCELL+1-JW
      WDG=DELG(J)
      IF (WDG.NE.2.) GO TO 5
   97 WTP=TYPE(J)
      JT=J-NYCL
      JB=J+NYCL
      SD=0.
      KND=0
      IF (WTP.NE.1.) GO TO 21
      JUL=JT-1
      JL=J-1
      JLL=JB-1
      GO TO 22
   21 IF (WTP.NE.2.) GO TO 23
      JUL=JT+1
      JL=J+1
      JLL=JB+1
   22 WD=DELG(JUL)
      PD=WD*(2.-WD)
      IF (PD.EQ.0.) GO TO 24
      KND=KND+1
      SD=SD+WD
   24 WD=DELG(JT)
      PD=WD*(2.-WD)
      IF (PD.EQ.0.) GO TO 25
      KND=KND+1
      SD=SD+WD
   25 WD=DELG(JT+1)
      PD=WD*(2.-WD)
      IF (PD.EQ.0.) GO TO 26
      KND=KND+1
      SD=SD+WD
   26 WD=DELG(JL)
      PD=WD*(2.-WD)
      IF (PD.EQ.0.) GO TO 27
      KND=KND+1
      SD=SD+WD
   27 WD=DELG(J+1)
      PD=WD*(2.-WD)
      IF (PD.EQ.0.) GO TO 28
      KND=KND+1
      SD=SD+WD
```

```
 28       WD=DELG(JLL)
          PD=WD*(2.-WD)
          IF (PD.EQ.0.) GO TO 29
          KND=KND+1
          SD=SD+WD
 29       WD=DELG(JB)
          PD=WD*(2.-WD)
          IF (PD.EQ.0.) GO TO 30
          KND=KND+1
          SD=SD+WD
 30       WD=DELG(JB+1)
          PD=WD*(2.-WD)
          IF (PD.EQ.0.) GO TO 31
          KND=KND+1
          SD=SD+WD
 31       XKND=KND
          DELG(J)=SD
          IF (KND.LE.1) GO TO 5
 37       DELG(J)=SD/XKND
          GO TO 5
 23       IF (WTP-4.) 32,33,34
C         TYPE 3 POINT
 32       WD=DELG(JT)
          PD=WD*(2.-WD)
          IF (PD.EQ.0.) GO TO 35
          KND=KND+1
          SD=SD+WD
 35       WD=DELG(JT+1)
          PD=WD*(2.-WD)
          IF (PD.EQ.0.) GO TO 36
          KND=KND+2
          SD=SD+2.*WD
 36       DELG(J)=SD
          IF (KND.LE.1) GO TO 5
          XKND=KND
          GO TO 37
C         TYPE 4 POINT
 33       WD=DELG(JT)
          PD=WD*(2.-WD)
          IF (PD.EQ.0.) GO TO 38
          KND=KND+1
          SD=SD+WD
 38       WD=DELG(JT+1)
          PD=WD*(2.-WD)
          IF (PD.EQ.0.) GO TO 39
          KND=KND+1
          SD=SD+WD
 39       WD=DELG(J+1)
          PD=WD*(2.-WD)
          IF (PD.EQ.0.) GO TO 29
          KND=KND+1
          SD=SD+WD
          GO TO 29
 34       IF (WTP-6.) 51,52,53
C         TYPE 5 POINTS
 51       WD=DELG(J-1)
          PD=WD*(2.-WD)
          IF (PD.EQ.0.) GO TO 54
          KND=KND+1
          SD=SD+WD
```

```
 54       WD=DELG(JT-1)
          PD=WD*(2.-WD)
          IF (PD.EQ.0.) GO TO 55
          KND=KND+1
          SD=SD+WD
 55       WD=DELG(JT)
          PD=WD*(2.-WD)
          IF (PD.EQ.0.) GO TO 56
          KND=KND+1
          SD=SD+WD
 56       WD=DELG(JT+1)
          PD=WD*(2.-WD)
          IF (PD.EQ.0.) GO TO 36
          KND=KND+1
          SD=SD+WD
          GO TO 36
C         TYPE 6 POINTS
 52       WD=DELG(JB+1)
          PD=WD*(2.-WD)
          IF (PD.EQ.0.) GO TO 72
          KND=KND+1
          SD=SD+WD
 72       WD=DELG(JT+1)
          PD=WD*(2.-WD)
          IF (PD.EQ.0.) GO TO 29
          KND=KND+2
          SD=SD+2.*WD
          GO TO 29
 53       WRITE (6,40) J,WTP
 40       FORMAT (22H PLASTIC BORDER POINT I5,F5.0)
          IF (WTP-8.) 61,62,63
C         TYPE 7 POINTS
 61       WD=DELG(JT-1)
          PD=WD*(2.-WD)
          IF (PD.EQ.0.) GO TO 64
          SD=SD+WD
          KND=KND+1
 64       WD=DELG(JT)
          PD=WD*(2.-WD)
          IF (PD.EQ.0.) GO TO 62
          SD=SD+WD
          KND=KND+1
 62       WD=DELG(J-1)
          PD=WD*(2.-WD)
          IF (PD.EQ.0.) GO TO 66
          SD=SD+WD
          KND=KND+1
 66       WD=DELG(JB-1)
          PD=WD*(2.-WD)
          IF (PD.EQ.0.) GO TO 36
          SD=SD+WD
          KND=KND+1
          GO TO 36
 63       IF (WTP-10.) 5,65,67
C         TYPE 10 POINTS
 65       WD=DELG(J-1)
          PD=WD*(2.-WD)
          IF (PD.EQ.0.) GO TO 68
          SD=SD+WD
          KND=KND+1
```

```
 68       WD=DELG(JB-1)
          PD=WD*(2.-WD)
          IF (PD.EQ.0.) GO TO 29
          SD=SD+WD
          KND=KND+1
          GO TO 29
C         TYPE 11 POINTS
 67       WD=DELG(JT-1)
          PD=WD*(2.-WD)
          IF (PD.EQ.0.) GO TO 69
          SD=SD+WD
          KND=KND+1
 69       WD=DELG(JT)
          PD=WD*(2.-WD)
          IF (PD.EQ.0.) GO TO 71
          SD=SD+WD
          KND=KND+1
 71       WD=DELG(J-1)
          PD=WD*(2.-WD)
          IF (PD.EQ.0.) GO TO 36
          SD=SD+WD
          KND=KND+1
          GO TO 36
 5        CONTINUE
          RETURN
          END
$IBFTC GCALGR  DECK
          SUBROUTINE GCALG
          COMMON AA,CONTST,C2,CSM,C1M,CGM,CGB,CGC,CREP,DAY,DNMM,FMM,
     2    ITER,KL,KM,KLOAD,N,N2,NP,N2P,N7,N8,NMW,NMWP,NXCL,NYCL,NCELL,
     3    NMWH,NMAX,PI,PI4,PI8,PLM,Q,QBG,Q1,R(140),TIMA,TIMB,TMTGOF,
     4    TSTC,XMIN,XMEW
          COMMON FX(220),PHIB(220),L(220),XB(220),YB(220)
          REAL KLOAD
          COMMON /STRES/ SX(400),SY(400),SXY(400),SZZ(400),SIGEQ(400),
     2    TEX(400),TEY(400),TEXY(400)
          COMMON /GDCOM/ ABC(1),AREA(400),AGSUM(2,400),COSW(400),
     2    COIT(800),CLX(400),CLY(400),CGSW(400),DEPX(400),DEPY(400),
     3    DEPXY(400),DEPYN(400),DELG(400),ETAB(221),EPX(400),EPY(400),
     4    EPXY(400),GBAS(400),GOLD(400),M(220),TYPE(400),
     5    RS(140),RH(140),RSAV(140),SIGE(400),WDR(140),XIB(221)
          REAL L,M
C COMPUTE DELG AND GBAS+DELG=GNEW
C DELG IS THE PART OF G THAT DEPENDS ON CURRENT PLASTIC STRAIN INCREMENTS
C (DEPX,.....
C GNEW=GBAS+DELG
          IF (NR.EQ.5) GO TO 21
          CGA=SQRT(2.)/3.
          NR=5
          REWIND 8
          READ (8) (ABC(K),K=1,NMAX)
          READ (8) (SX(K),K=1,1200)
          DO 6 J=1,NCELL
          IF (AREA(J).LE.0.) GO TO 61
C COMPUTE EQUIVALENT MODIFIED TOTAL STRAIN  EPET
          SX(J)=SX(J)/PI8
          SY(J)=SY(J)/PI8
          SXY(J)=-SXY(J)/PI8
          SZ=0.
          EXE=SX(J)-XMEW*(SY(J)+SZ)
```

```
      EYE=SY(J)-XMEW*(SX(J)+SZ)
      EZE=SZ-XMEW*(SX(J)+SY(J))
      EXYE=(1.+XMEW)*SXY(J)
      TEX(J)=EXE+EPX(J)+DEPX(J)
      TEY(J)=EYE+EPY(J)+DEPY(J)
      TEZ=EZE-EPX(J)-EPY(J)-DEPX(J)-DEPY(J)
      TEXY(J)=EXYE+EPXY(J)+DEPXY(J)
      IF (J.NE.185) GO TO 51
      XH=CLY(172)-CLY(171)
      XK=CLX(184)-CLX(172)
      CXSX=(SX(184)-SX(160))/(2.*XK)
      CXSXY=(SXY(184)-SXY(160))/(2.*XK)
      CYSY=(SY(173)-SY(171))/(2.*XH)
      CYSXY=(SXY(173)-SXY(171))/(2.*XH)
      EQS1=DXSX+DYSXY
      RAT1=-DXSX/DYSXY
      EQS2=DXSXY+DYSY
      RAT2=-DYSY/DXSXY
      WRITE (6,52) DXSX,DYSXY,EQS1,RAT1
      WRITE (6,52) DYSY,DXSXY,EQS2,RAT2
52    FORMAT (12H EQUILIBRIUM 1P4E16.6)
      CYTX=(TEX(173)-2.*TEX(172)+TEX(171))/XH**2
      CXTY=(TEY(184)-2.*TEY(172)+TEY(160))/XK**2
      CXYTXY=-.5*(TEXY(159)+TEXY(185)-TEXY(161)-TEXY(183))/(XH*XK)
      COMP=DYTX+DXTY+DXYTXY
      WRITE (6,53) DYTX,DXTY,DXYTXY,COMP,TEX(172),TEY(172),TEXY(172)
53    FORMAT (15H COMPATIBILITY 1P7E12.4)
      IMAX=GBAS(NCELL+1)
      NC4=NCELL+4
      IF (ITER.NE.0) GO TO 611
      READ (5,62) IMAX,IGMX
62    FORMAT (4I5)
      GBAS(NCELL+1)=IMAX
      GBAS(NCELL+4)=IGMX
      GBAS(NCELL+2)=1.
      DLAST=0.
      GBAS(NCELL+3)=DLAST
611   WRITE (6,63) (GBAS(K), K=NCELL,NC4)
63    FORMAT (5H IMAX 6F9.1)
51    SZZ(J)=TEZ
      SES=.5*((SX(J)-SY(J))**2+(SY(J)-SZ)**2+(SZ-SX(J))**2+
     2  6.*SXY(J)**2)
      SIGEQ(J)=SQRT(SES)
      EXPR=EXE+DEPX(J)
      EYPR=EYE+DEPY(J)
      EZPR=EZE-DEPX(J)-DEPY(J)
      EXYPR=EXYE+DEPXY(J)
      EPET=SQRT(6.*EXYPR**2+(EXPR-EYPR)**2+(EXPR-EZPR)**2+(EYPR-
     2  EZPR)**2)*CGA
C COMPUTE EFFECTIVE PLASTIC STRAIN INCREMENT DEPEFF
      DEPEFF=(EPET-CGM*SIGE(J))/DNMM
C COMPUTE NEW PLASTIC STRAIN INCREMENTS DEPX,.....
42    DELG(J)=DEPEFF
      IF (DEPEFF.LE.0.) GO TO 61
      DW=DEPEFF/(3.*EPET)
      DEPX(J)=DW*(2.*EXPR-EYPR-EZPR)
      DEPYN(J)=DW*(2.*EYPR-EXPR-EZPR)
      DEPXY(J)=3.*DW*EXYPR
      GO TO 6
61    DEPYN(J)=0.
```

```
      DEPX(J)=0.
      DEPXY(J)=0.
6     CONTINUE
      NLB=NCELL
      DO 11 J=1,NLB,NYCL
      JE=J+NYCL-1
11    WRITE (6,12) (DELG(K),K=J,JE)
12    FORMAT (3X,1P10E12.4)
      DO 41 J=1,NCELL
      IF (DELG(J).LT.0.) DELG(J)=0.
      IF (DELG(J).GT.0.) DELG(J)=2.
41    CONTINUE
      RETURN
21    TSUM=0.
      DO 4 J=1,NCELL
      IF (DELG(J).EQ.0.) GO TO 4
      DAR=DELG(J)*AREA(J)
      WRITE (6,14) J,DAR,SIGEQ(J),SX(J),SY(J),SXY(J),DEPX(J),
     2 DEPYN(J),DEPXY(J)
14    FORMAT (14H NONZERO DELG I5,1P8E12.4)
4     CONTINUE
      NINROW=GBAS(NCELL+2)
      DLAST=GBAS(NCELL+3)
      AL=GBAS(NCELL+5)
      IF (NINROW.LT.IMAX) GO TO 64
      DO 65 J=1,NCELL
      DW=DEPY(J)+EPY(J)
      IF (DW.NE.0.) GO TO 65
      DN=DEPYN(J)
      IF (DN.EQ.0.) GO TO 65
      WRITE (6,66) J,DEPX(J),DN,DEPXY(J),DELG(J)
66    FORMAT (6H DROP ,I5,1P4E16.6)
      DEPYN(J)=0.
      DEPX(J)=0.
      DEPXY(J)=0.
      DELG(J)=0.
65    CONTINUE
64    DSUM=0.
      DO 7 J=1,NCELL
      IF (AREA(J).LE.0.) GO TO 7
      GOLD(J)=DELG(J)+GBAS(J)
      IF (TYPE(J).EQ.4.) GO TO 22
      DELY=ABS(DEPY(J)-DEPYN(J))
      TSUM=TSUM+DELY
      IF (DEPYN(J).EQ.0.) GO TO 22
      DSUM=DSUM+1.
22    DEPY(J)=DEPYN(J)
7     CONTINUE
      ITER=ITER+1
      DEN=DSUM
      IF (DEN.LE.0.) DEN=TSTC
      IF (NINROW.GE.IMAX) GO TO 71
      IF (DSUM.NE.DLAST) GO TO 72
      GBAS(NCELL+2)=NINROW+1
      GO TO 71
72    GBAS(NCELL+2)=1.
      DLAST=DSUM
      GBAS(NCELL+3)=DLAST
71    PCT=TSUM/DEN
      IF (PCT.LT.TSTC) CONTST=1.+CONTST
```

```
      CALL TIME1(TIMB)
      IF (TIMB.LT.TIMA) TIMB=TIMB+DAY
      TIME=(TIMB-TIMA)/XMIN
      IF (TIMB.GT.TMTGOF) CONTST=CONTST+.1
      TIML=TMTGOF-TIMB
      WRITE (6,36) ITER,TSUM,DSUM,PCT,TIME,TIML
36    FORMAT (18H CONVERGENCE TEST I5,1P5E12.4)
      REWIND 8
      WRITE (8) (ABC(K),K=1,NMAX)
      WRITE (8) (SX(K),K=1,3200)
      END FILE 8
      ISW=3*(ITER/3)-ITER
      IF (ISW.LT.0) RETURN
      K=NCELL
      CALL BCDUMP (GOLD(1),GOLD(K))
      CALL BCDUMP (DEPX(1),DEPX(K))
      CALL BCDUMP (DEPY(1),DEPY(K))
      CALL BCDUMP (DEPXY(1),DEPXY(K))
      WRITE (6,36) ISW
      RETURN
      END
$IBFTC TRMNLR  DECK
      SUBROUTINE TRMNL
      COMMON AA,CONTST,C2,CSM,C1M,CGM,CGB,CGC,CREP,DAY,DNMM,EMM,
     2  ITER,KL,KM,KLOAD,N,N2,NP,N2P,N7,N8,NMW,NMWP,NXCL,NYCL,NCELL,
     3  NMWH,NMAX,PI,PI4,PI8,PLM,Q,QBG,Q1,R(140),TIMA,TIMB,TMTGOF,
     4  TSTC,XMIN,XMEW
      COMMON FX(220),PHIB(220),L(220),XB(220),YB(220)
      REAL KLOAD
      COMMON /STRES/ SX(400),SY(400),SXY(400),SZZ(400),SIGEQ(400),
     2  TEX(400),TEY(400),TEXY(40)
      COMMON /GDCOM/ ABC(1),AREA(400),AGSUM(2,400),COSW(400),
     2  COIT(800),CLX(400),CLY(400),CGSW(400),DEPX(400),DEPY(400),
     3  DEPXY(400),DEPYN(400),DELG(400),ETAB(221),EPX(400),EPY(400),
     4  EPXY(400),GBAS(400),GOLD(400),M(220),TYPE(400),
     5  RS(140),RH(140),RSAV(140),SIGE(400),WDR(140),XIB(221)
      REAL L,M
      WRITE (6,17) AA,KLOAD,CONTST
17    FORMAT (30H TERMINAL CALCULATIONS FOR A K  3F12.5)
      WRITE (6,13)
13    FORMAT (1H1,6X,1HJ,6X,1HX,7X,1HY,9X,1HG,12X,3HEPX,11X,4HDEPX,
     2  10X,3HEPY,11X,4HDEPY,10X,4HEPXY,9X,5HDEPXY)
      DO 1 J=1,NCELL
      GBAS(J)=GOLD(J)
      GOLD(J)=GOLD(J)+DELG(J)
      EPX(J)=EPX(J)+DEPX(J)
      EPY(J)=EPY(J)+DEPY(J)
      EPXY(J)=EPXY(J)+DEPXY(J)
      SIGE(J)=SIGEQ(J)
      IF (SIGE(J).LT.1.) SIGE(J)=1.
      WRITE (6,12) J,CLX(J),CLY(J),GBAS(J)
     2  ,EPX(J),DEPX(J),EPY(J),DEPY(J),EPXY(J),DEPXY(J)
12    FORMAT (5X,I5,2F8.5,1P7E14.5)
1     CONTINUE
      WRITE (6,14)
14    FORMAT (1H1,6X,1HJ,7X,4HSIGE,12X,2HSX,12X,2HSY,12X,2HSZ,12X,
     2  3HSXY,11X,3HTEX,11X,3HTEY,11X,4HTEXY)
      DO 2 J=1,NCELL
      WRITE (6,15) J,SIGEQ(J),SX(J),SY(J),SZZ(J),SXY(J),TEX(J),
     2  TEY(J),TEXY(J)
```

```
 15       FORMAT (5XI5,1PE16.5,7E14.5)
 2        CONTINUE
          K=NCELL
C HAS PROCESS CONVERGED
          IF (CONTST.LT.1.) GO TO 11
C YES-COMPUTE AND DUMP GBAS,EPX,EPY,EPXY,SIGE
          CALL BCDUMP (GBAS(1),GBAS(K))
          CALL BCDUMP (EPX (1),EPX (K))
          CALL BCDUMP (EPY (1),EPY (K))
          CALL BCDUMP (EPXY(1),EPXY(K))
          CALL BCDUMP (SIGEQ(1),SIGEQ(K))
          CALL BCDUMP (GOLD(1),GOLD(K))
          CALL BCDUMP (DEPX(1),DEPX(K))
          CALL BCDUMP (DEPY(1),DEPY(K))
          CALL BCDUMP (DEPXY(1),DEPXY(K))
          CALL BCDUMP (TEX (1),TEX (K))
          CALL BCDUMP (TEY (1),TEY (K))
          CALL BCDUMP (TEXY(1),TEXY(K))
          CALL BCDUMO (SX(1),SX(K))
          CALL BCDUMP (SY(1),SY(K))
          CALL BCDUMP (SXY(1),SXY(K))
          K=133
          DO 23 J=341,394,2
          SY(J)=SY(K)
          SY(J+1)=CLX(K)
 23       K=K+12
          CALL BCDUMP (SY(341),SY(394))
          CALL BCDUMP (R(1),R(NMW))
          IF (CONTST.GT.1.) GO TO 22
          REWIND 8
          WRITE (8) (ABC(K),K=1,NMAX)
          END FILE 8
 16       RETURN
 11       K=NCELL
          CALL BCDUMP (GBAS(1),GBAS(K))
          CALL BCDUMP (DEPX (1),DEPX (K))
          CALL BCDUMP (DEPY (1),DEPY (K))
          CALL BCDUMP (DEPXY(1),DEPXY(K))
 22       STOP
          END
```

List of References

1. Griffith, A. A., The Phenomena of Rapture and Flow in Solids. Phil. Trans. Roy. Soc. Series A221, 1921, pp. 163-198.

2. Griffith, A. A., The Theory of Rupture. Proc. 1st Int. Congr. Appl. Mech. Delft, 1924.

3. Inglis, C. E., Stresses in a Plate Due to the Presence of Cracks and Sharp Corners. Proc. Inst. Naval Arch., Vol. 60, 1913, pp. 219-242.

4. Irwin, G. R., Fracture Dynamics. Fracturing of Metals, ASM Cleveland, 1948, pp. 147-166.

5. Orowan, E., Fracture and Strength of Solids. Physical Soc. London, Vol. 12, 1949, p. 185.

6. Orowan, E., Energy Criteria of Fracture. Weld. J. Res. Suppl., Vol. 20, 1955, p. 157s.

7. Irwin, G. R., Analysis of Stresses and Strains Near the End of a Crack Traversing a Plate. J. Appl. Mech., Vol. 24, 1957, p. 361.

8. Irwin, G. R., Relation of Stresses Near a Crack to the Crack Extension Force. IXth Intern. Congress of Applied Mechanics, Vol. VIII, Paper No. 101(II). Univ. of Brussels, 1957, pp. 245-251.

9. Irwin, G. R., Fracture. Encyclopedia of Physics, Vol. VI, Editor S. Flügge, Springer Verlag, 1958, p. 551.

10. Westergaard, H. M., Bearing Pressures and Cracks. J. Appl. Mech., Vol. 61, 1939, pp. A49-A53.

11. Sneddon, I. N., The Distribution of Stress in the Neighborhood of a Crack in an Elastic Solid. Proc. Roy. Soc. London, Vol. A-187, 1946, pp. 229-260.

12. Williams, M. L., On the Stress Distribution at the Base of a Stationary Crack. J. Appl. Mech., Vol. 24, 1957, pp. 109-114.

13. Williams, M. L., The Bending Stress Distribution at the Base of a Stationary Crack. J. Appl. Mech., Vol. 28, 1961, pp. 78-82.

14. Wigglesworth, L. A., Stress Distribution in a Notched Plate. Mathematika, Vol. 4, 1957, pp. 76-96.

15. Erdogan, F. E., On the Stress Distribution in Plates with Colinear Cuts Under Arbitrary Loads. Proc. 4th U.S. Natl. Congress on Applied Mechanics, Univ. of Calif., Berkley, 1962.

16. Irwin, G. R., Crack Extension Force for a Part Through Crack in Plate. J. Appl. Mech., Vol. 29, 1962, p. 651.

17. Paris, P. C. and Sih, G. C., Stress Analysis of Cracks. Fracture Toughness Testing and its Applications. ASTM, STP. 381, 1965, p. 30.

18. Gross, B., Srawley, J. E., and Brown, Jr., W. F., Stress Intensity Factors for a Single-Edge-Notch Tension Specimen by Boundary Collocation of a Stress Function. NASA TN D-2395, 1964.

19. Gross, B. and Srawley, J. E., Stress Intensity Factors for Single-Edge-Notch Specimens in Bending or Combined Bending and Tension by Boundary Collocation of a Stress Function. NASA TN D-2603, 1965.

20. Gross, B. and Srawley, J. E., Stress Intensity Factors for Three-Point Bend Specimens by Boundary Collocation. NASA TN D-3092, 1965.

21. Gross, B., Some Plane Problem Elastostatic Solutions for Plates Having a V-Notch. Ph.D. Dissertation. Case Western Reserve University, 1970.

22. Gross, B. and Mendelson, A., Plane Elastostatic Analysis of V-Notched Plates. NASA TN D-6040, 1970.

23. Bueckner, H. F., Some Stress Singularities and Their Computation by Means of Integral Equation. Boundary Value Problems in Differential Equations. Editor R. E. Langer, Univ. of Wisconsin Press, 1960, pp. 215-230.

24. Walker, Jr., G. E., A Study of the Applicability of the Method of Potential to Inclusions of Various Shapes in Two- and Three-Dimensional Elastic and Thermo-Elastic Stress Fields. Ph.D. Dissertation. University of Washington, 1969.

25. Hays, D. J., Some Applications of Elastic-Plastic Analysis to Fracture Mechanics. Ph.D. Dissertation. Imperial College of Science & Technology, University of London, 1970.

26. Rice, J. R., Mathematical Analysis in the Mechanics of Fracture. Fracture, Vol. II. Ed. H. Liebowitz, Academic Press, New York, 1968.

27. Hult, J. A. H. and McClintock, F. A., Elastic-Plastic Stress and Strain Distributions Around Sharp Notches Under Repeated Shear. IXth Intern. Congress Appl. Mech., Vol. 8, Univ. of Brussels, 1957, pp. 51-58.

28. Koskinen, M. F., Elastic-Plastic Deformation of a Single Grooved Flat Plate Under Longitudinal Shear. Trans., Am. Soc. Mech. Eng., Vol. 85, D, 1963, pp. 585-594.

29. McClintock, F. A. and Irwin, G. R., Plasticity Aspects of Fracture Mechanics. Fracture Toughness Testing and its Applications. ASTM, STP. 381, 1965, p. 84.

30. Irwin, G. R., Plastic Zone Near a Crack and Fracture Toughness. Proc. VIIth Sagamore Ordnance Materials Research Conference, Aug. 1960, p. IV-63.

31. Rice, J. R., Stresses Due to a Sharp Notch in a Work-Hardening Elastic-Plastic Material Loaded by Longitudinal Shear. J. Appl. Mech., Vol. 34, 1967, p. 287.

32. Rice, J. R., Mechanics of Crack Tip Deformation and Extension by Fatigue. Fatigue Crack Propagation. ASTM, STP. 415, 1967.

33. Swedlow, J. L., Williams, M. L., and Yang, W. H., Elasto-Plastic Stresses and Strains in Cracked Plates. Proc. 1st Int. Conference on Fracture. Sandai, Japan, 1965.

34. Swedlow, J. L., The Thickness Effect and Plastic Flow in Cracked Plates. ARL. 65-216, Wright-Patterson Air Force Base, Ohio, Oct. 1965.

35. Swedlow, J. L., Elasto-Plastic Cracked Plates in Plane Strain. J. Fract. Mechanics, Vol. 5, No. 1, March 1969, pp. 33-44.

36. Rice, J. R. and Rosengren, G. F., Plane Strain Deformation Near a Crack Tip in a Power-Law Hardening Material. J. Mech. Phys. Solids, Vol. 16, 1968, pp. 1-12.

37. Hutchison, J. W., Singular Behavior at the End of a Tensile Crack in a Hardening Material. J. Mech. Phys. Solids, Vol. 16, 1968, pp. 18-31.

38. Hutchison, J. W., Plastic Stress and Strain Fields at a Crack Tip. J. Mech. Phys. Solids, Vol. 16, 1968, pp. 337-347.

39. Rice, J. R., A Path Independent Integral and the Approximate Analysis of Strain Concentration by Notches and Cracks. ARPA SD-86, Report E39, Brown University, May 1967.

40. Jaswon, M. A., Integral Equation Methods in Potential Theory I. Proc. Roy. Soc., Ser. A, Vol. 275, 1963, pp. 23-32.

41. Symm, G. T., Integral Equation Method in Potential Theory II. Proc. Roy. Soc., Ser. A, Vol. 275, 1963, pp. 33-46.

42. Symm, G. T., Integral Equation Method in Elasticity and Potential Theory. National Physical Laboratory, Mathematic Division, London, Dec. 1964.

43. Rizzo, F. J., An Integral Equation Approach to Boundary Value Problems in Classical Elastostatics. Quart. of Appl. Math., Vol. 25, 1967, p. 83.

44. Jaswon, M. A. and Ponter, A. R., An Integral Equation Solution of the Torsion Problem. Proc. Roy. Soc., Ser. A, Vol. 273, 1963, pp. 237-246.

45. Rim, K. and Henry, A. S., An Integral Equation Method in Plane Elasticity. NASA CR-779, 1967.

46. Segedin, C. M. and Brickell, D. G. A., Integral Equation Method for a Corner Plate. Proc. ASCE, Vol. 94, No. ST. 1, Jan 1968.

47. Timoshenko, S. and Goodier, J. N., Theory of Elasticity. McGraw-Hill Book Co. Inc., New York, 1951.

48. Kellog, O. D., Foundation of Potential Theory. Frederick Ungar Publ. Co., New York, 1929.

49. Collatz, L., The Numerical Treatment of Differential Equations. Springer Verlag, Berlin, 1960.

50. Courant, R. and Hilbert, D., Methods of Mathematical Physics, Vol. I, Interscience Publ. Inc., New York, 1953.

51. Mendelson, A., Plasticity: Theory and Application. The MacMillan Co., New York, 1968.

52. Roberts Jr., E. and Mendelson, A., Analysis of Plastic Thermal Stresses and Strains in Finite Thin Plate of Strain-Hardening Material. NASA TN D-2206, 1964.

53. Mendelson, A. and Manson, S. S., Practical Solution of Plastic Deformation Problem in Elastic-Plastic Range. NASA TR R-28, 1959.

54. Bubsey, R. T. and Jones, M. H., Private Communications. NASA Lewis Research Center, Cleveland, Ohio, Nov. 1972.

55. Sokolnikoff, I. S., Mathematical Theory of Elasticity. McGraw-Hill Book Co., New York, 1956.

56. Dwight, H. B., Tables of Integrals and Other Mathematical Data. The MacMillan Co., New York, 1961.

57. Ilyushin, A. A., Some Problems in the Theory of Plastic Deformations. BMB-12, Trans. by Grad. Div. Appl. Math., Brown University, for David W. Taylor Model Basin, 1946 (contract NObs-34166.)

Table 1. - Dimensionless Elastic x-Directional Stresses $\frac{\sigma_x}{\sigma_0}$ and y-Directional Stresses $\frac{\sigma_y}{\sigma_0}$ Along x Axis ($\tilde{y} = 0$) in the Vicinity of the Notch for a Specimen With a Single Edge Notch Subjected to Pure Bending; $\tilde{q} = 1.0$, $\tilde{a} = 0.2$

	x/a \ α	10°	30°	60°
$\tilde{\sigma}_x$	0.01	7.13	7.04	6.28
	.02	5.01	4.93	4.47
	.04	3.47	3.43	3.15
	.06	2.77	2.75	2.56
	.10	2.07	2.06	1.94
	.20	1.35	1.35	1.29
$\tilde{\sigma}_y$	0.01	7.40	7.44	7.36
	.02	5.27	5.27	5.24
	.04	3.73	3.72	3.71
	.06	3.04	3.03	3.03
	.10	2.33	2.27	2.33
	.20	1.61	1.60	1.61

Table 2. - Dimensionless Elastic x-Directional Stresses $\frac{\sigma_x}{\sigma_0}$ and y-Directional Stresses $\frac{\sigma_y}{\sigma_0}$ Along x Axis ($\tilde{y} = 0$) in the Vicinity of the Notch for a Specimen With a Single Edge Notch Subjected to Pure Bending; $\tilde{q} = 1.0$, $\tilde{a} = 0.3$

	x/a \ α	3°	10°	30°	60°
$\tilde{\sigma}_x$	0.01	7.72	7.88	7.66	6.72
	.02	5.45	5.54	5.33	4.80
	.04	3.80	3.85	3.72	3.40
	.06	3.06	3.09	3.00	2.77
	.10		2.30	2.26	2.11
	.20		1.51	1.50	1.42
$\tilde{\sigma}_y$	.01	7.81	7.99	7.84	7.81
	.02	5.54	5.65	5.52	5.54
	.04	3.88	3.95	3.86	3.89
	.06	3.13	3.18	3.10	3.14
	.10		2.39	2.33	2.37
	.20		1.54	1.51	1.54

Table 3. - Dimensionless Elastic x-Directional Stresses $\frac{\sigma_x}{\sigma_0}$ and y-Directional Stresses $\frac{\sigma_y}{\sigma_0}$ Along x Axis ($\tilde{y} = 0$) in the Vicinity of the Notch for a Specimen With a Single Edge Notch Subjected to Pure Bending; $\tilde{q} = 1.0$, $\tilde{a} = 0.4$

	x/a \ α	10^o	30^o	60^o
$\tilde{\sigma}_x$	0.01	8.82	8.55	7.53
	.02	6.24	6.07	5.40
	.04	4.36	4.26	3.84
	.06	3.51	3.44	3.13
	.10	2.63	2.59	2.39
	.20	1.70	1.68	1.58
$\tilde{\sigma}_y$	0.01	8.74	8.73	8.66
	.02	6.13	6.13	6.11
	.04	4.23	4.23	4.25
	.06	3.36	3.36	3.39
	.10	2.45	2.45	2.48
	.20	1.44	1.44	1.47

Table 4. - Dimensionless Elastic x-Directional Stresses $\frac{\sigma_x}{\sigma_0}$ and y-Directional Stresses $\frac{\sigma_y}{\sigma_0}$ Along x Axis ($\tilde{y} = 0$) in the Vicinity of the Notch for a Specimen With a Single Edge Notch Subjected to Pure Bending; $\tilde{q} = 1.0$, $\tilde{a} = 0.5$

	α / x/a	10^o	30^o	60^o
$\tilde{\sigma}_x$	0.01	10.63	10.46	8.98
	.02	7.54	7.42	6.44
	.04	5.28	5.20	4.58
	.06	4.24	4.19	3.72
	.10	3.15	3.13	2.80
	.20	1.96	1.94	1.79
$\tilde{\sigma}_y$	0.01	10.29	10.49	10.21
	.02	7.17	7.29	7.15
	.04	4.86	4.94	4.88
	.06	3.79	3.85	3.82
	.10	2.63	2.67	2.68
	.20	1.30	1.32	1.35

Table 5. - Dimensionless Elastic x-Directional Stresses $\frac{\sigma_x}{\sigma_0}$ and y-Directional Stresses $\frac{\sigma_y}{\sigma_0}$ Along x Axis ($\tilde{y} = 0$) in the Vicinity of the Notch for a Specimen With a Single Edge Notch Subjected to Pure Bending; $\tilde{q} = 1.0$, $\tilde{a} = 0.6$

	x/a \ α	10°	30°	60°
$\tilde{\sigma}_x$	0.01	13.80	13.46	11.59
	.02	9.78	9.56	8.30
	.04	6.80	6.68	5.87
	.06	5.42	5.33	4.73
	.10	3.94	3.88	3.50
	.20	2.27	2.24	2.04
$\tilde{\sigma}_y$	0.01	13.06	13.26	12.98
	.02	8.96	9.11	8.99
	.04	5.91	6.01	5.98
	.06	4.46	4.53	4.54
	.10	2.85	2.91	2.93
	.20	.83	.88	.90

Table 6. - The Order of Stress Singularity n at the Tip of the Notch for Specimens With a Single Edge Notch Subjected to Pure Bending and Behaving Elastically; $\tilde{q} = 1.0$

$\tilde{a}$ \ α	3°		10°		30°		60°	
	Obtained herein	Ref. [22]	Obtained herein	Ref. [22]	Obtained herein	Ref. [22]	Obtained herein	Ref. [22]
0.2			0.4990		0.4986		0.4875	
0.3	0.4999		0.4999		0.4978		0.4896	
0.4		0.5000*	0.5007	0.4999	0.4989	0.4985	0.4929	0.4878
0.5			0.4999		0.4989		0.4886	
0.6			0.4999		0.5010		0.4863	
0.7			0.5010		0.5000			

*Value obtained for $\alpha = 0^\circ$

Table 7. - Dimensionless Stress Intensity Factors $\frac{K_I}{\sigma_0 w^n}$ for a Specimen With a Single Edge Notch Subjected to Pure Bending and Behaving Elastically; $\tilde{q} = 1.0$

$\tilde{a}$ \ α	3°		10°		30°		60°	
	Obtained herein	Ref. [22]	Obtained herein	Ref. [22]	Obtained herein	Ref. [22]	Obtained herein	Ref. [22]
0.2			0.840	0.836	0.843	0.844	0.893	0.895
0.3	1.084	1.093*	1.101	1.093	1.096	1.100	1.147	1.155
0.4			1.400	1.414	1.410	1.422	1.442	1.484
0.5			1.846	1.876	1.890	1.885	1.946	1.965
0.6			2.590	2.627	2.610	2.640	2.750	2.752
0.7			3.920	4.044				

*Value obtained for $\alpha = 0^\circ$

Table 8. - Dimensionless Elastic Plane-Stress y-Directional Notch Opening Displacements $\frac{2E}{\sigma_0}\frac{u_y}{w}$ for a Specimen With a Single Edge Notch Subjected to Pure Bending;

$\mu = 0.33$, $\tilde{q} = 1.0$

$\tilde{a}$ \ α	3°		10°		30°		60°	
	Obtained herein	Ref. [21]	Obtained herein	Ref.* [21]	Obtained herein	Ref. [21]	Obtained herein	Ref. [21]
0.2			1.24	1.23	1.23		1.27	
0.3	2.16	2.17*	2.24	2.17	2.22		2.24	2.26
0.4			3.74	3.74	3.75		3.80	
0.5			6.38	6.36	6.45		6.52	6.56
0.6			11.38	11.35	11.60			
0.7			22.64	22.59	23.29			

*Values obtained for $\alpha = 0^\circ$

Table 9. - Dimensionless Elastic Plane-Stress Rice's Integral $\frac{JE}{\sigma_0^2 w}$ for a Specimen With a 10^o Edge Notch Subjected to Pure Bending; $\mu = 0.33$, $\tilde{q} = 1.0$

$\tilde{a}$	Obtained	
	By integration of equation (61)	From stress intensity factor K_I equation (60)
0.3	1.193	1.212
0.5	3.546	3.408

Table 10. - Dimensionless x-Directional Stress $\frac{\sigma_x}{\sigma_0}$ at Location $(\tilde{x},\tilde{y})$ for a Specimen With a 10^{o} Edge Notch Subjected to Pure Bending; Plane Strain, $\tilde{q} = 0.40$, $\tilde{a} = 0.5$, $\alpha = 10^{o}$, $m = 0.05$, $\mu = 0.33$

$\tilde{x}$ \ $\tilde{y}$	0	0.008	0.016	0.032	0.060	0.132	0.356	0.510
-0.128			.130	.190	.248	.194	-.050	-.074
-.056		.232	.361	.503	.468	.168	-.086	-.094
-.028		.531	.731	.728	.464	.118	-.099	-.100
-.012		1.282	1.060	.672	.392	.088	-.105	-.103
.002	6.845	1.189	.730	.475	.325	.067	-.110	-.105
.006	4.041	1.562	.761	.454	.314	.063	-.111	-.106
.012	2.838	1.886	1.016	.486	.302	.057	-.113	-.106
.028	1.793	1.627	1.266	.686	.329	.052	-.116	-.107
.056	1.172	1.141	1.055	.808	.442	.069	-.119	-.109
.080	.920	.907	.870	.746	.488	.098	-.119	-.108

$\tilde{x}$ \ $\tilde{y}$	0	0.050	0.150	0.300	0.450	0.600	0.750	0.950
0.325	.151	.137	.061	-.021	-.045	-.035	-.022	-.009
.375	.090	.081	.030	-.007	-.029	-.020	-.014	-.005
.425	.046	.040	.003	.009	-.020	-.009	-.006	-.003
.475	.019	.015	-.011	.016	-.017	-.002	.001	-.001

Table 11. - Dimensionless y-Directional Stress $\frac{\sigma_y}{\sigma_0}$ at Location $(\tilde{x},\tilde{y})$ for a Specimen With a 10° Edge Notch Subjected to Pure Bending; Plane Strain, $\tilde{q} = 0.40$, $\tilde{a} = 0.5$, $\alpha = 10^{\circ}$, $m = 0.05$, $\mu = 0.33$

$\tilde{x}$ \ $\tilde{y}$	0	0.008	0.016	0.032	0.060	0.132	0.356	0.510
-0.128			-.006	.007	.039	.165	.239	.192
-.056		.012	.018	.094	.277	.440	.270	.173
-.028		.036	.164	.467	.680	.595	.274	.160
-.012		.328	.808	1.106	1.101	.675	.273	.151
.002	6.602	4.110	2.723	1.783	1.235	.727	.269	.143
.006	3.804	3.824	2.873	1.888	1.274	.739	.268	.140
.012	2.620	2.804	2.632	1.928	1.309	.752	.266	.136
.028	1.558	1.608	1.686	1.638	1.292	.767	.257	.124
.056	.949	.960	.987	1.043	1.022	.721	.234	.099
.080	.679	.683	.695	.730	.765	.631	.207	.074

$\tilde{x}$ \ $\tilde{y}$	0	0.050	0.150	0.300	0.450	0.600	0.750	0.950
0.325	-.506	-.498	-.446	-.378	-.335	-.309	-.291	-.276
.375	-.707	-.699	-.642	-.537	-.443	-.384	-.347	-.320
.425	-.924	.916	-.851	-.690	-.548	-.454	-.399	-.363
.475	-1.161	-1.154	-1.096	-.815	-.660	-.512	-.443	-.403

Table 12. - Dimensionless z-Directional Stress $\frac{\sigma_z}{\sigma_0}$ at Location $(\tilde{x},\tilde{y})$ for a Specimen With a 10° Edge Notch Subjected to Pure Bending; Plane Strain, $\tilde{q} = 0.40$, $\tilde{a} = 0.5$, $\alpha = 10^{\circ}$, $m = 0.05$, $\mu = 0.33$

$\tilde{x}$ \ $\tilde{y}$	0	0.008	0.016	0.032	0.060	0.132	0.356	0.510
-0.128			.041	.065	.094	.119	.062	.037
-.056		.080	.125	.197	.246	.201	.061	.026
-.028		.187	.295	.394	.377	.235	.058	.020
-.012		.775	.909	.849	.463	.252	.055	.016
.002	5.678	2.606	1.696	1.094	.527	.262	.053	.012
.006	2.926	2.642	1.783	1.133	.524	.265	.052	.011
.012	1.801	2.195	1.773	1.155	.532	.267	.051	.010
.028	1.106	1.068	.974	.767	.535	.270	.046	.005
.056	.700	.693	.674	.611	.483	.261	.040	-.003
.080	.528	.525	.517	.487	.413	.241	.029	-.011

$\tilde{x}$ \ $\tilde{y}$	0	0.050	0.150	0.300	0.450	0.600	0.750	0.950
0.325	-.117	-.119	-.127	-.132	-.125	-.114	-.103	-.094
.375	-.204	-.204	-.202	-.179	-.156	-.133	-.119	-.107
.425	-.290	-.289	-.280	-.225	-.187	-.152	-.134	-.121
.475	-.449	-.444	-.402	-.264	-.224	-.170	-.146	-.134

Table 13. - Dimensionless Shear Stress $\frac{\sigma_{xy}}{\sigma_0}$ at Location $(\tilde{x},\tilde{y})$ for a Specimen With a 10^{o} Edge Notch Subjected to Pure Bending; Plane Strain, $\tilde{q} = 0.40$, $\tilde{a} = 0.5$, $\alpha = 10^{o}$, $m = 0.05$, $\mu = 0.33$

$\tilde{x}$ \ $\tilde{y}$	0	0.008	0.016	0.032	0.060	0.132	0.356	0.510
-0.128			-.018	-.046	-.113	-.223	-.135	-.072
-.056		-.019	-.075	-.206	-.352	-.310	-.102	-.047
-.028		-.130	-.313	-.505	-.491	-.284	-.079	-.034
-.012		-.599	-.866	-.711	-.459	-.241	-.064	-.026
.002	.000	-.571	-.639	-.503	-.326	-.189	-.050	-.018
.006	.000	.296	-.220	-.360	-.276	-.172	-.046	-.016
.012	.000	.497	.214	-.138	-.195	-.145	-.039	-.013
.028	.000	.259	.356	.220	.011	-.071	-.022	-.004
.056	.000	.105	.189	.263	.206	.051	.010	.012
.080	.000	.065	.123	.206	.236	.129	.037	.026

$\tilde{x}$ \ $\tilde{y}$	0	0.050	0.150	0.300	0.450	0.600	0.750	0.950
0.325	.000	.066	.160	.172	.114	.056	.011	-.042
.375	.000	.050	.128	.146	.097	.043	.004	-.046
.425	.000	.033	.086	.101	.066	.023	-.005	-.044
.475	.000	.017	.036	.034	.016	.001	-.018	-.035

Table 14. - Dimensionless x-Directional Stress $\frac{\sigma_x}{\sigma_0}$ at Location $(\tilde{x},\tilde{y})$ for a Specimen With a 10° Edge Notch Subjected to Pure Bending; Plane Strain, $\tilde{q} = 0.50$, $\tilde{a} = 0.5$, $\alpha = 10^{\circ}$, $m = 0.05$, $\mu = 0.33$

$\tilde{x}$ \ $\tilde{y}$	0	0.008	0.016	0.032	0.060	0.132	0.356	0.510
-0.128			.147	.232	.314	.247	-.063	-.093
-.056		.279	.451	.636	.599	.206	-.109	-.117
-.028		.715	.985	.915	.578	.136	-.124	-.125
-.012		1.759	1.475	.792	.455	.099	-.131	-.128
.002	9.662	1.689	.956	.470	.344	.077	-.137	-.130
.006	5.755	2.187	.986	.435	.322	.073	-.138	-.131
.012	4.084	2.630	1.351	.469	.304	.069	-.140	-.132
.028	2.547	2.270	1.678	.757	.353	.069	-.144	-.133
.056	1.526	1.474	1.335	.955	.504	.096	-.147	-.134
.080	1.146	1.127	1.073	.898	.574	.130	-.145	-.132

$\tilde{x}$ \ $\tilde{y}$	0	0.050	0.150	0.300	0.450	0.600	0.750	0.950
0.325	.179	.164	.075	-.023	-.055	-.043	-.027	-.011
.375	.107	.097	.037	-.007	-.036	-.025	-.017	-.007
.425	.054	.048	.004	.012	-.024	-.011	-.007	-.004
.475	.022	.018	-.013	.020	-.021	-.003	.001	-.002

Table 15. - Dimensionless y-Directional Stress $\frac{\sigma_y}{\sigma_0}$ at Location $(\tilde{x},\tilde{y})$ for a Specimen With a 10^{o} Edge Notch Subjected to Pure Bending; Plane Strain, $\tilde{q} = 0.50$, $\tilde{a} = 0.5$, $\alpha = 10^{o}$, $m = 0.05$, $\mu = 0.33$

$\tilde{x}$ \ $\tilde{y}$	0	0.008	0.016	0.032	0.060	0.132	0.356	0.510
-0.128			-.009	.008	.049	.215	.302	.241
-.056		.017	.029	.140	.387	.587	.340	.216
-.028		.042	.216	.659	.965	.788	.343	.200
-.012		.439	1.189	1.615	1.417	.882	.341	.189
.002	9.479	5.863	3.898	2.516	1.667	.934	.336	.177
.006	5.485	5.396	4.072	2.612	1.688	.944	.334	.174
.012	3.684	3.821	3.617	2.562	1.678	.953	.331	.168
.028	1.779	1.860	1.975	1.904	1.522	.950	.319	.153
.056	1.017	1.037	1.088	1.196	1.192	.868	.288	.121
.080	.742	.750	.771	.832	.891	.747	.252	.090

$\tilde{x}$ \ $\tilde{y}$	0	0.050	0.150	0.300	0.450	0.600	0.750	0.950
0.325	-.631	-.621	-.559	-.474	-.419	-.388	-.364	-.346
.375	-.875	-.865	-.797	-.668	-.553	-.480	-.434	-.401
.425	-1.139	-1.129	-1.051	-.856	-.683	-.567	-.500	-.455
.475	-1.425	-1.415	-1.346	-1.009	-.821	-.641	-.555	-.505

Table 16. - Dimensionless z-Directional Stress $\frac{\sigma_z}{\sigma_0}$ at Location $(\tilde{x},\tilde{y})$ for a Specimen With a 10^{o} Edge Notch Subjected to Pure Bending; Plane Strain, $\tilde{q} = 0.50$, $\tilde{a} = 0.5$, $\alpha = 10^{o}$, $m = 0.05$, $\mu = 0.33$

$\tilde{x}$ \ $\tilde{y}$	0	0.008	0.016	0.032	0.060	0.132	0.356	0.510
-0.128			.045	.079	.120	.152	.079	.049
-.056		.098	.158	.256	.326	.261	.076	.037
-.028		.250	.462	.753	.715	.305	.072	.025
-.012		1.079	1.307	1.185	.902	.324	.069	.020
.002	8.471	3.710	2.387	1.472	.971	.334	.066	.016
.006	4.601	3.721	2.488	1.503	.967	.335	.065	.014
.012	2.926	3.163	2.444	1.496	.942	.337	.063	.012
.028	1.428	1.454	1.533	1.252	.747	.336	.058	.007
.056	.839	.829	.799	.710	.560	.318	.047	-.004
.080	.623	.619	.609	.571	.484	.290	.035	-.014

$\tilde{x}$ \ $\tilde{y}$	0	0.050	0.150	0.300	0.450	0.600	0.750	0.950
0.325	-.149	-.151	-.159	-.164	-.156	-.142	-.129	-.118
.375	-.253	-.254	-.251	-.223	-.194	-.167	-.149	-.135
.425	-.434	-.419	-.345	-.279	-.233	-.191	-.167	-.151
.475	-.677	-.674	-.641	-.326	-.278	-.213	-.183	-.167

Table 17. - Dimensionless Shear Stress $\frac{\sigma_{xy}}{\sigma_0}$ at Location $(\tilde{x},\tilde{y})$ for a Specimen With a 10° Edge Notch Subjected to Pure Bending; Plane Strain, $\tilde{q} = 0.50$, $\tilde{a} = 0.5$, $\alpha = 10^{\circ}$, $m - 0.05$, $\mu = 0.33$

$\tilde{x}$ \ $\tilde{y}$	0	0.008	0.016	0.032	0.060	0.132	0.356	0.510
-0.128			-.020	-.055	-.142	-.285	-.168	-.089
-.056		-.025	-.104	-.278	-.457	-.391	-.123	-.057
-.028		-.173	-.444	-.711	-.638	-.344	-.094	-.041
-.012		-.836	-1.245	-1.008	-.578	-.278	-.075	-.030
.002	.000	-.887	-.932	-.655	-.369	-.203	-.057	-.021
.006	.000	.362	-.318	-.442	-.292	-.180	-.052	-.018
.012	.000	.703	.332	-.117	-.175	-.145	-.044	-.014
.028	.000	.415	.568	.364	.071	-.053	-.022	-.003
.056	.000	.166	.294	.385	.267	.086	.018	.017
.080	.000	.092	.173	.278	.299	.172	.051	.034

$\tilde{x}$ \ $\tilde{y}$	0	0.050	0.150	0.300	0.450	0.600	0.750	0.950
0.325	.000	.079	.193	.209	.139	.068	.013	-.053
.375	.000	.060	.154	.176	.118	.053	.005	-.059
.425	.000	.040	.103	.121	.080	.028	-.006	-.055
.475	.000	.021	.043	.041	.019	.001	-.022	-.044

Table 18. - Dimensionless x-Directional Stress $\frac{\sigma_x}{\sigma_0}$ at Location $(\tilde{x},\tilde{y})$ for a Specimen With a 10^o Edge Notch Subjected to Pure Bending; Plane strain, $\tilde{q} = 0.70$, $\tilde{a} = 0.5$, $\alpha = 10^o$, $m = 0.05$, $\mu = 0.33$

$\tilde{x}$ \ $\tilde{y}$	0	0.008	0.016	0.032	0.060	0.132	0.356	0.510
-0.128			.200	.319	.432	.351	-.089	-.131
-.056		.476	.683	.888	.797	.308	-.152	-.164
-.028		1.099	1.470	1.291	.735	.225	-.173	-.174
-.012		2.580	2.213	1.146	.540	.177	-.183	-.178
.002	13.564	2.523	1.497	.694	.368	.154	-.190	-.181
.006	8.178	3.265	1.531	.647	.335	.146	-.192	-.182
.012	5.888	3.720	2.063	.698	.308	.130	-.194	-.183
.028	3.783	3.335	2.481	1.103	.373	.119	-.199	-.185
.056	2.286	2.199	1.970	1.367	.625	.140	-.201	-.186
.080	1.678	1.646	1.557	1.270	.747	.176	-.198	-.183

$\tilde{x}$ \ $\tilde{y}$	0	0.050	0.150	0.300	0.450	0.600	0.750	0.950
0.325	.252	.227	.099	-.031	-.072	-.059	-.038	-.015
.375	.161	.137	.046	-.010	-.046	-.035	-.024	-.009
.425	.095	.068	.000	.014	-.029	-.016	-.010	-.004
.475	.046	.032	-.023	.025	-.025	-.005	.000	-.002

Table 19. - Dimensionless y-Directional Stress $\frac{\sigma_y}{\sigma_0}$ at Location $(\tilde{x},\tilde{y})$ for a Specimen With a 10^{o} Edge Notch Subjected to Pure Bending; Plane Strain, $\tilde{q} = 0.70$, $\tilde{a} = 0.5$, $\alpha = 10^{o}$, $m = 0.05$, $\mu = 0.33$

$\tilde{x}$ \ $\tilde{y}$	0	0.008	0.016	0.032	0.060	0.132	0.356	0.510
-0.128			-.013	.015	.078	.310	.428	.338
-.056		.025	.043	.197	.557	.853	.481	.304
-.028		.054	.292	.939	1.400	1.152	.485	.281
-.012		.611	1.684	2.318	2.045	1.288	.481	.265
.002	13.486	8.384	5.637	3.672	2.427	1.358	.473	.249
.006	8.029	7.834	5.943	3.831	2.464	1.363	.469	.244
.012	5.568	5.573	5.369	3.784	2.454	1.360	.465	.236
.028	2.601	2.712	2.899	2.787	2.178	1.315	.447	.214
.056	1.335	1.364	1.435	1.575	1.574	1.160	.401	.169
.080	.932	.945	.979	1.078	1.182	.993	.349	.125

$\tilde{x}$ \ $\tilde{y}$	0	0.050	0.150	0.300	0.450	0.600	0.750	0.950
0.325	-.882	-.868	-.780	-.664	-.587	-.540	-.507	-.482
.375	-1.215	-1.198	-1.106	-.931	-.771	-.669	-.605	-.558
.425	-1.540	-1.518	-1.454	-1.190	-.949	-.789	-.697	-.632
.475	-1.969	-1.952	-1.862	-1.397	-1.137	-.894	-.774	-.702

Table 20. - Dimensionless z-Directional Stress $\frac{\sigma_z}{\sigma_0}$ at Location $(\tilde{x},\tilde{y})$ for a Specimen With a 10° Edge Notch Subjected to Pure Bending; Plane Strain, $\tilde{q} = 0.70$, $\tilde{a} = 0.5$, $\alpha = 10^{\circ}$, $m = 0.05$, $\mu = 0.33$

$\tilde{x}$ \ $\tilde{y}$	0	0.008	0.016	0.032	0.060	0.132	0.356	0.510
-0.128			.062	.110	.167	.218	.112	.068
-.056		.165	.240	.358	.619	.462	.109	.046
-.028		.380	.861	1.096	1.050	.631	.103	.035
-.012		1.567	1.913	1.702	1.273	.679	.098	.029
.002	12.354	5.351	3.502	2.145	1.376	.689	.093	.022
.006	7.026	5.437	3.668	2.200	1.378	.682	.092	.020
.012	4.717	4.548	3.645	2.201	1.360	.661	.089	.018
.028	2.831	2.823	2.610	1.908	1.253	.562	.082	.010
.056	1.195	1.176	1.229	1.259	.988	.429	.066	-.005
.080	.861	.855	.837	.775	.637	.386	.050	-.019

$\tilde{x}$ \ $\tilde{y}$	0	0.050	0.150	0.300	0.450	0.600	0.750	0.950
0.325	-.208	-.211	-.225	-.230	-.218	-.198	-.180	-.164
.375	-.499	-.496	-.439	-.311	-.270	-.232	-.208	-.187
.425	-.707	-.725	-.705	-.510	-.323	-.266	-.234	-.210
.475	-.945	-.944	-.927	-.659	-.383	-.297	-.255	-.233

Table 21. - Dimensionless Shear Stress $\frac{\sigma_{xy}}{\sigma_0}$ at Location $(\tilde{x},\tilde{y})$ for a Specimen With a 10^{o} Edge Notch Subjected to Pure Bending; Plane Strain, $\tilde{q} = 0.70$, $\tilde{a} = 0.5$, $\alpha = 10^{o}$, $m = 0.05$, $\mu = 0.33$

$\tilde{x}$ \ $\tilde{y}$	0	0.008	0.016	0.032	0.060	0.132	0.356	0.510
-0.128			-.030	-.081	-.202	-.396	-.233	-.124
-.056		-.050	-.171	-.418	-.657	-.541	-.168	-.078
-.028		-.239	-.630	-1.057	-.936	-.468	-.126	-.055
-.012		-1.165	-1.781	-1.484	-.865	-.369	-.098	-.040
.002	.000	-1.329	-1.380	-.969	-.569	-.259	-.073	-.027
.006	.000	.423	-.506	-.657	-.457	-.226	-.065	-.023
.012	.000	.949	.451	-.172	-.282	-.175	-.054	-.017
.028	.000	.583	.801	.545	.116	-.048	-.023	-.001
.056	.000	.260	.458	.599	.427	.128	.032	.026
.080	.000	.147	.276	.442	.462	.235	.076	.050

$\tilde{x}$ \ $\tilde{y}$	0	0.050	0.150	0.300	0.450	0.600	0.750	0.950
0.325	.000	.104	.260	.287	.192	.094	.018	-.074
.375	.000	.075	.207	.242	.161	.072	.007	-.081
.425	.000	.053	.139	.166	.109	.038	-.008	-.077
.475	.000	.034	.060	.054	.026	.002	-.031	-.062

Table 22. - Dimensionless x-Directional Stress $\frac{\sigma_x}{\sigma_0}$ at Location $(\tilde{x},\tilde{y})$ for a Specimen With a 10° Edge Notch Subjected to Pure Bending; Plane Strain, $\tilde{q} = 0.40$, $\tilde{a} = 0.5$, $\alpha = 10^{\circ}$, $m = 0.10$, $\mu = 0.33$

$\tilde{x}$ \ $\tilde{y}$	0	0.008	0.016	0.032	0.060	0.132	0.356	0.510
-0.128			.131	.190	.247	.194	-.049	-.074
-.056		.238	.364	.501	.465	.169	-.086	-.094
-.028		.533	.731	.723	.463	.119	-.099	-.100
-.012		1.266	1.062	.674	.392	.089	-.105	-.103
.002	6.700	1.179	.742	.486	.325	.068	-.110	-.105
.006	3.960	1.544	.776	.468	.313	.063	-.111	-.106
.012	2.787	1.861	1.017	.498	.301	.058	-.112	-.106
.028	1.773	1.613	1.265	.696	.330	.052	-.116	-.107
.056	1.170	1.139	1.055	.811	.444	.069	-.120	-.109
.080	.921	.908	.871	.748	.489	.098	-.119	-.108

$\tilde{x}$ \ $\tilde{y}$	0	0.050	0.150	0.300	0.450	0.600	0.750	0.950
0.325	.151	.138	.062	-.021	-.045	-.035	-.022	-.009
.375	.091	.082	.030	-.007	-.030	-.020	-.014	-.005
.425	.046	.040	.002	.009	-.020	-.009	-.006	-.003
.475	.019	.016	-.011	.016	-.017	-.002	.001	-.001

Table 23. - Dimensionless y-Directional Stress $\frac{\sigma_y}{\sigma_0}$ at Location $(\tilde{x},\tilde{y})$ for a Specimen With a 10^o Edge Notch Subjected to Pure Bending; Plane Strain, $\tilde{q} = 0.40$, $\tilde{a} = 0.5$, $\alpha = 10^o$, $m = 0.10$, $\mu = 0.33$

$\tilde{x}$ \ $\tilde{y}$	0	0.008	0.016	0.032	0.060	0.132	0.356	0.510
-0.128			-.006	.007	.039	.165	.238	.192
-.056		.012	.018	.094	.274	.438	.270	.173
-.028		.034	.157	.455	.669	.593	.274	.160
-.012		.317	.793	1.087	.999	.673	.273	.152
.002	6.499	4.051	2.692	1.774	1.232	.726	.269	.143
.006	3.767	3.781	2.850	1.885	1.273	.738	.268	.140
.012	2.615	2.794	2.624	1.934	1.313	.752	.266	.136
.028	1.574	1.622	1.697	1.647	1.299	.768	.257	.124
.056	.958	.969	.995	1.049	1.026	.724	.235	.099
.080	.684	.689	.700	.735	.768	.633	.207	.074

$\tilde{x}$ \ $\tilde{y}$	0	0.050	0.150	0.300	0.450	0.600	0.750	0.950
0.325	-.506	-.498	-.446	-.378	-.334	-.309	-.291	-.276
.375	-.708	-.699	-.642	-.537	-.443	-.384	-.347	-.320
.425	-.925	-.917	-.852	-.691	-.548	-.453	-.399	-.363
.475	-1.162	-1.155	-1.097	-.816	-.660	-.512	-.443	-.403

Table 24. - Dimensionless z-Directional Stress $\frac{\sigma_z}{\sigma_0}$ at Location $(\tilde{x},\tilde{y})$ for a Specimen With a 10^{o} Edge Notch Subjected to Pure Bending; Plane Strain, $\tilde{q} = 0.40$, $\tilde{a} = 0.5$, $\alpha = 10^{o}$, $m = 0.10$, $\mu = 0.33$

$\tilde{x}$ \ $\tilde{y}$	0	0.008	0.016	0.032	0.060	0.132	0.356	0.510
-0.128			.041	.065	.094	.118	.062	.039
-.056		.082	.126	.196	.244	.200	.061	.026
-.028		.187	.293	.389	.374	.235	.058	.020
-.012		.716	.865	.792	.459	.251	.055	.016
.002	5.488	2.516	1.643	1.049	.526	.262	.053	.012
.006	2.845	2.544	1.728	1.088	.524	.264	.052	.011
.012	1.783	2.053	1.698	1.101	.533	.267	.051	.010
.028	1.105	1.068	.977	.773	.538	.270	.047	.005
.056	.702	.696	.676	.613	.485	.261	.038	-.003
.080	.530	.527	.519	.489	.415	.241	.029	-.011

$\tilde{x}$ \ $\tilde{y}$	0	0.050	0.150	0.300	0.450	0.600	0.750	0.950
0.325	-.117	-.119	-.127	-.132	-.125	-.114	-.103	-.094
.375	-.204	-.204	-.202	-.179	-.156	-.133	-.119	-.107
.425	-.290	-.289	-.280	-.225	-.187	-.152	-.134	-.121
.475	-.424	-.421	-.389	-.264	-.224	-.170	-.146	-.133

Table 25. - Dimensionless Shear Stress $\frac{\sigma_{xy}}{\sigma_0}$ at Location $(\tilde{x},\tilde{y})$ for a Specimen With a 10^o Edge Notch Subjected to Pure Bending; Plane Strain, $\tilde{q} = 0.40$, $\tilde{a} = 0.5$, $\alpha = 10^o$, $m = 0.10$, $\mu = 0.33$

$\tilde{x}$ \ $\tilde{y}$	0	0.008	0.016	0.032	0.060	0.132	0.356	0.510
-0.128			-.018	-.046	-.113	-.222	-.135	-.072
-.056		-.020	-.076	-.206	-.349	-.309	-.102	-.047
-.028		-.127	-.308	-.502	-.489	-.285	-.079	-.034
-.012		-.581	-.848	-.705	-.462	-.243	-.064	-.026
.002	.000	-.568	-.628	-.501	-.333	-.191	-.050	-.018
.006	.000	.283	-.218	-.360	-.282	-.174	-.046	-.016
.012	.000	.483	.206	-.140	-.200	-.147	-.040	-.013
.028	.000	.250	.345	.216	.009	-.073	-.022	-.004
.056	.000	.103	.186	.261	.206	.050	.010	.012
.080	.000	.064	.122	.205	.236	.128	.037	.026

$\tilde{x}$ \ $\tilde{y}$	0	0.050	0.150	0.300	0.450	0.600	0.750	0.950
0.325	.000	.066	.161	.173	.114	.056	.011	-.042
.375	.000	.050	.128	.146	.097	.043	.004	-.047
.425	.000	.033	.086	.101	.066	.023	-.004	-.044
.475	.000	.018	.037	.034	.016	.001	-.018	-.035

Table 26. - Dimensionless x-Directional Stress $\frac{\sigma_x}{\sigma_0}$ at Location $(\tilde{x},\tilde{y})$ for a Specimen With a 10^o Edge Notch Subjected to Pure Bending; Plane Strain, $\tilde{q} = 0.50$, $\tilde{a} = 0.5$, $\alpha = 10^o$, $m = 0.10$, $\mu = 0.33$

$\tilde{x}$ \ $\tilde{y}$	0	0.008	0.016	0.032	0.060	0.132	0.356	0.510
-0.128			.157	.238	.314	.244	-.063	-.093
-.056		.281	.455	.644	.599	.204	-.108	-.117
-.028		.682	.966	.928	.579	.136	-.124	-.125
-.012		1.677	1.426	.840	.465	.099	-.131	-.128
.002	9.086	1.584	.966	.567	.363	.076	-.137	-.130
.006	5.380	2.056	1.005	.541	.348	.072	-.139	-.131
.012	3.798	2.520	1.338	.579	.329	.066	-.140	-.132
.028	2.385	2.049	1.652	.846	.368	.063	-.145	-.133
.056	1.511	1.467	1.346	1.005	.525	.085	-.148	-.135
.080	1.164	1.146	1.096	.928	.593	.120	-.147	-.133

$\tilde{x}$ \ $\tilde{y}$	0	0.050	0.150	0.300	0.450	0.600	0.750	0.950
0.325	.184	.168	.076	-.025	-.056	-.043	-.027	-.011
.375	.110	.099	.037	-.008	-.036	-.025	-.017	-.007
.425	.056	.049	.004	.011	-.024	-.011	-.007	-.004
.475	.023	.019	-.013	.020	-.021	-.003	.001	-.002

Table 27. - Dimensionless y-Directional Stress $\frac{\sigma_y}{\sigma_0}$ at Location $(\tilde{x},\tilde{y})$ for a Specimen With a 10° Edge Notch Subjected to Pure Bending; Plane Strain, $\tilde{q} = 0.50$, $\tilde{a} = 0.5$, $\alpha = 10^{\circ}$, $m = 0.10$, $\mu = 0.33$

$\tilde{x}$ \ $\tilde{y}$	0	0.008	0.016	0.032	0.060	0.132	0.356	0.510
-0.128			-.008	.009	.049	.213	.300	.240
-.056		.016	.025	.129	.374	.573	.338	.216
-.028		.043	.209	.629	.917	.768	.342	.199
-.012		.420	1.093	1.488	1.335	.860	.340	.188
.002	8.892	5.511	3.653	2.370	1.593	.915	.335	.177
.006	5.127	5.091	3.834	2.489	1.629	.925	.333	.174
.012	3.458	3.678	3.447	2.496	1.650	.937	.330	.168
.028	1.880	1.948	2.056	1.995	1.569	.944	.318	.153
.056	1.108	1.123	1.163	1.247	1.2352	.879	.289	.121
.080	.792	.799	.817	.869	.923	.765	.254	.090

$\tilde{x}$ \ $\tilde{y}$	0	0.050	0.150	0.300	0.450	0.600	0.750	0.950
0.325	-.632	-.622	-.558	-.473	-.419	-.387	-.364	-.346
.375	-.880	-.869	-.799	-.669	-.553	-.480	-.434	-.401
.425	-1.147	-1.136	-1.057	-.858	-.683	-.567	-.500	-.455
.475	-1.436	-1.426	-1.356	-1.012	-.822	-.641	-.555	-.505

Table 28. - Dimensionless z-Directional Stress $\frac{\sigma_z}{\sigma_0}$ at Location $(\tilde{x},\tilde{y})$ for a Specimen With a 10^o Edge Notch Subjected to Pure Bending; Plane Strain, $\tilde{q} = 0.50$, $\tilde{a} = 0.5$, $\alpha = 10^o$, $m = 0.10$, $\mu = 0.33$

$\tilde{x}$ \ $\tilde{y}$	0	0.008	0.016	0.032	0.060	0.132	0.356	0.510
-0.128			.049	.081	.120	.151	.078	.048
-.056		.098	.158	.255	.321	.256	.076	.032
-.028		.239	.388	.678	.627	.298	.072	.025
-.012		.999	1.207	1.110	.795	.316	.069	.020
.002	7.795	3.421	2.228	1.410	.867	.327	.065	.015
.006	4.195	3.439	2.331	1.452	.869	.329	.064	.014
.012	2.643	2.912	2.291	1.466	.858	.331	.063	.012
.028	1.408	1.352	1.383	1.204	.757	.332	.057	.006
.056	.864	.855	.828	.743	.581	.318	.047	-.004
.080	.645	.642	.631	.593	.500	.292	.035	-.014

$\tilde{x}$ \ $\tilde{y}$	0	0.050	0.150	0.300	0.450	0.600	0.750	0.950
0.325	-.148	-.150	-.159	-.164	-.157	-.142	-.129	-.118
.375	-.254	-.254	-.251	-.223	-.194	-.167	-.149	-.135
.425	-.415	-.404	-.347	-.279	-.233	-.191	-.167	-.151
.475	-.632	-.629	-.589	-.327	-.278	-.212	-.183	-.167

Table 29. - Dimensionless Shear Stress $\frac{\sigma_{xy}}{\sigma_0}$ at Location $(\tilde{x},\tilde{y})$ for a Specimen With a 10^o Edge Notch Subjected to Pure Bending; Plane Strain, $\tilde{q} = 0.50$, $\tilde{a} = 0.5$, $\alpha = 10^o$, $m = 0.10$, $\mu = 0.33$

$\tilde{x}$ \ $\tilde{y}$	0	0.008	0.016	0.032	0.060	0.132	0.356	0.510
-0.128			-.021	-.056	-.143	-.284	-.168	-.089
-.056		-.023	-.097	-.271	-.455	-.389	-.124	-.058
-.028		-.164	-.420	-.690	-.633	-.346	-.096	-.042
-.012		-.791	-1.168	-.956	-.592	-.285	-.077	-.031
.002	.000	-.800	-.856	-.645	-.408	-.215	-.059	-.022
.006	.000	.370	-.285	-.447	-.336	-.193	-.054	-.019
.012	.000	.663	.305	-.142	-.223	-.160	-.046	-.015
.028	.000	.359	.493	.321	.047	-.071	-.024	-.004
.056	.000	.147	.264	.361	.275	.073	.015	.016
.080	.000	.087	.166	.274	.307	.165	.049	.033

$\tilde{x}$ \ $\tilde{y}$	0	0.050	0.150	0.300	0.450	0.600	0.750	0.950
0.325	.000	.081	.197	.212	.141	.069	.013	-.053
.375	.000	.061	.157	.179	.119	.053	.005	-.059
.425	.000	.040	.105	.124	.081	.029	-.006	-.056
.475	.000	.022	.044	.042	.020	.002	-.022	-.044

Table 30. - Dimensionless x-Directional Stress $\frac{\sigma_x}{\sigma_0}$ at Location $(\tilde{x},\tilde{y})$ for a Specimen With a 10^o Edge Notch Subjected to Pure Bending; Plane Strain, $\tilde{q} = 0.70$, $\tilde{a} = 0.5$, $\alpha = 10^o$, $m = 0.10$, $\mu = 0.33$

$\tilde{x}$ \ $\tilde{y}$	0	0.008	0.016	0.032	0.060	0.132	0.356	0.510
-0.128			.202	.321	.435	.348	-.089	-.131
-.056		.433	.667	.907	.811	.293	-.152	-.164
-.028		1.034	1.446	1.333	.752	.206	-.173	-.174
-.012		2.472	2.168	1.210	.562	.160	-.183	-.178
.002	13.103	2.428	1.502	.792	.394	.144	-.191	-.181
.006	7.882	3.148	1.539	.746	.366	.142	-.192	-.182
.012	5.680	3.680	2.026	.788	.337	.133	-.195	-.183
.028	3.709	3.288	2.458	1.154	.391	.129	-.199	-.184
.056	2.300	2.213	1.987	1.393	.639	.137	-.202	-.185
.080	1.695	1.664	1.575	1.291	.762	.169	-.199	-.183

$\tilde{x}$ \ $\tilde{y}$	0	0.050	0.150	0.300	0.450	0.600	0.750	0.950
0.325	.150	.206	.124	-.022	-.072	-.058	-.038	-.016
.375	.094	.092	.070	-.004	-.047	-.034	-.023	-.009
.425	.079	.039	.027	.016	-.031	-.015	-.010	-.005
.475	.037	.014	-.008	.025	-.028	-.005	.001	-.003

Table 31. - Dimensionless y-Directional Stress $\frac{\sigma_y}{\sigma_0}$ at Location $(\tilde{x},\tilde{y})$ for a Specimen With a 10° Edge Notch Subjected to Pure Bending; Plane Strain, $\tilde{q} = 0.70$, $\tilde{a} = 0.5$, $\alpha = 10^{\circ}$, $m = 0.10$, $\mu = 0.33$

$\tilde{x}$ \ $\tilde{y}$	0	0.008	0.016	0.032	0.060	0.132	0.356	0.510
-0.128			-.012	.014	.076	.310	.428	.339
-.056		.024	.039	.196	.562	.843	.482	.305
-.028		.054	.288	.909	1.351	1.120	.486	.281
-.012		.591	1.620	2.223	1.978	1.254	.482	.265
.002	12.951	8.062	5.418	3.561	2.374	1.338	.474	.249
.006	7.657	7.534	5.716	3.730	2.424	1.354	.472	.244
.012	5.338	5.453	5.196	3.722	2.439	1.367	.466	.237
.028	2.781	2.849	3.018	2.875	2.232	1.353	.449	.214
.056	1.475	1.502	1.569	1.698	1.682	1.211	.404	.170
.080	1.028	1.041	1.074	1.167	1.265	1.042	.351	.125

$\tilde{x}$ \ $\tilde{y}$	0	0.050	0.150	0.300	0.450	0.600	0.750	0.950
0.325	-1.142	-.995	-.827	-.673	-.589	-.542	-.510	-.484
.375	-1.204	-1.208	-1.121	-.933	-.773	-.672	-.608	-.561
.425	-1.450	-1.503	-1.412	-1.185	-.951	-.792	-.700	-.636
.475	-1.909	-1.892	-1.822	-1.394	-1.142	-.896	-.777	-.707

Table 32. - Dimensionless z-Directional Stress $\frac{\sigma_z}{\sigma_0}$ at Location $(\tilde{x},\tilde{y})$ for a Specimen With a 10° Edge Notch Subjected to Pure Bending; Plane Strain, $\tilde{q} = 0.70$, $\tilde{a} = 0.5$, $\alpha = 10^{\circ}$, $m = 0.10$, $\mu = 0.33$

$\tilde{x}$ \ $\tilde{y}$	0	0.008	0.016	0.032	0.060	0.132	0.356	0.510
-0.128			.063	.111	.168	.217	.112	.069
-.056		.151	.233	.364	.591	.434	.109	.047
-.028		.359	.802	1.072	1.002	.550	.103	.036
-.012		1.475	1.825	1.657	1.218	.596	.099	.029
.002	11.691	5.068	3.346	2.106	1.331	.617	.094	.023
.006	6.619	5.148	3.509	2.166	1.341	.620	.092	.021
.012	4.455	4.390	3.488	2.184	1.333	.617	.090	.018
.028	2.541	2.555	2.528	1.929	1.247	.583	.082	.010
.056	1.246	1.226	1.240	1.245	1.006	.445	.067	-.005
.080	.899	.892	.874	.811	.669	.400	.050	-.019

$\tilde{x}$ \ $\tilde{y}$	0	0.050	0.150	0.300	0.450	0.600	0.750	0.950
0.325	-.410	-.305	-.232	-.229	-.218	-.198	-.181	-.165
.375	-.469	-.469	-.421	-.309	-.270	-.233	-.208	-.188
.425	-.632	-.675	-.628	-.466	-.324	-.266	-.234	-.212
.475	-.892	-.894	-.872	-.611	-.386	-.297	-.256	-.234

Table 33. - Dimensionless Shear Stress $\frac{\sigma_{xy}}{\sigma_0}$ at Location $(\tilde{x},\tilde{y})$ for a Specimen With a 10^{o} Edge Notch Subjected to Pure Bending; Plane Strain, $\tilde{q} = 0.70$, $\tilde{a} = 0.5$, $\alpha = 10^{o}$, $m = 0.10$, $\mu = 0.33$

$\tilde{x}$ \ $\tilde{y}$	0	0.008	0.016	0.032	0.060	0.132	0.356	0.510
-0.128			-.029	-.080	-.203	-.398	-.234	-.124
-.056		-.041	-.157	-.414	-.665	-.539	-.169	-.078
-.028		-.230	-.616	-1.041	-.936	-.469	-.127	-.055
-.012		-1.138	-1.721	-1.440	-.876	-.377	-.099	-.040
.002	.000	-1.270	-1.338	-.965	-.590	-.273	-.073	-.027
.006	.000	.416	-.513	-.671	-.479	-.241	-.066	-.023
.012	.000	.890	.380	-.215	-.304	-.193	-.054	-.018
.028	.000	.533	.728	.493	.102	-.067	-.023	-.001
.056	.000	.256	.451	.591	.434	.121	.033	.026
.080	.000	.147	.277	.445	.474	.242	.079	.050

$\tilde{x}$ \ $\tilde{y}$	0	0.050	0.150	0.300	0.450	0.600	0.750	0.950
0.325	.000	.097	.252	.280	.191	.094	.018	-.074
.375	.000	.039	.183	.232	.160	.072	.007	-.082
.425	.000	.034	.118	.158	.109	.039	-.008	-.078
.475	.000	.027	.048	.053	.025	.002	-.031	-.062

Table 34. - Dimensionless x-Directional Stress $\frac{\sigma_x}{\sigma_0}$ at Location $(\tilde{x},\tilde{y})$ for a Specimen With a 3^o Edge Notch Subjected to Pure Bending; Plane Strain, $\tilde{q} = 0.50$, $\tilde{a} = 0.3$, $\alpha = 3^o$, $m = 0.10$, $\mu = 0.33$

$\tilde{x}$ \ $\tilde{y}$	0	0.008	0.016	0.032	0.060	0.132	0.356	0.510
-0.128		-.045	-.011	.042	.097	.086	-.023	-.035
-.056		.108	.189	.266	.239	.078	-.050	-.051
-.028		.391	.478	.405	.228	.047	-.060	-.057
-.012		.987	.736	.361	.174	.028	-.064	-.060
.002	5.264	.901	.492	.220	.127	.014	-.068	-.062
.006	3.096	1.179	.521	.211	.119	.011	-.069	-.063
.012	2.150	1.409	.716	.247	.114	.008	-.070	-.063
.028	1.317	1.187	.904	.427	.147	.004	-.073	-.066
.056	.831	.816	.738	.542	.259	.195	-.077	-.068
.080	.642	.632	.603	.506	.310	.045	-.077	-.069

$\tilde{x}$ \ $\tilde{y}$	0	0.050	0.100	0.150	0.200	0.300	0.400	0.500
0.525	.037	.035	.030	.024	.017	.007	-.006	-.016
.575	.021	.019	.015	.011	.009	.009	-.001	-.011
.625	.008	.007	.005	.001	.000	.012	.002	-.006
.675	.001	.001	-.001	-.004	-.006	.013	.004	-.002

Table 35. - Dimensionless y-Directional Stress $\frac{\sigma_y}{\sigma_0}$ at Location $(\tilde{x},\tilde{y})$ for a Specimen With a 3^o Edge Notch Subjected to Pure Bending; Plane Strain, $\tilde{q} = 0.50$, $\tilde{a} = 0.3$, $\alpha = 3^o$, $m = 0.10$, $\mu = 0.33$

$\tilde{x}$ \ $\tilde{y}$	0	0.008	0.016	0.032	0.060	0.132	0.356	0.510
-0.128		-.003	.001	.010	.040	.154	.284	.306
-.056		.003	.021	.087	.223	.355	.308	.281
-.028		.030	.122	.339	.493	.471	.313	.270
-.012		.237	.571	.768	.718	.534	.314	.262
.002	4.951	3.085	2.029	1.303	.900	.580	.314	.255
.006	2.842	2.869	2.154	1.401	.941	.591	.314	.253
.012	1.964	2.111	1.991	1.461	.990	.605	.313	.250
.028	1.202	1.243	1.308	1.286	1.018	.629	.309	.240
.056	.779	.788	.810	.858	.847	.619	.299	.222
.080	.602	.606	.616	.645	.674	.571	.284	.204

$\tilde{x}$ \ $\tilde{y}$	0	0.050	0.100	0.150	0.200	0.300	0.400	0.500
0.525	-.465	-.463	-.457	-.448	-.438	-.417	-.396	-.378
.575	-.567	-.565	-.558	-.547	-.534	-.507	-.478	-.454
.625	-.676	-.673	-.665	-.652	-.634	-.595	-.557	-.528
.675	-.791	-.789	-.783	-.771	-.748	-.670	-.634	-.599

Table 36. - Dimensionless z-Directional Stress $\frac{\sigma_z}{\sigma_0}$ at Location $(\tilde{x},\tilde{y})$ for a Specimen With a 3^o Edge Notch Subjected to Pure Bending; Plane Strain, $\tilde{q} = 0.50$, $\tilde{a} = 0.3$, $\alpha = 3^o$, $m = 0.10$, $\mu = 0.33$

$\tilde{x}$ \ $\tilde{y}$	0	0.008	0.016	0.032	0.060	0.132	0.356	0.510
-0.128		-.016	-.004	.017	.045	.079	.086	.089
-.056		.037	.069	.116	.152	.143	.085	.076
-.028		.139	.198	.245	.239	.171	.084	.070
-.012		.461	.553	.411	.294	.185	.082	.067
.002	4.064	1.871	1.158	.648	.339	.196	.081	.064
.006	1.991	1.860	1.217	.679	.350	.199	.081	.063
.012	1.358	1.312	1.160	.685	.364	.202	.080	.061
.028	.831	.802	.730	.565	.384	.209	.078	.058
.056	.532	.526	.511	.462	.365	.211	.073	.041
.080	.411	.409	.402	.380	.325	.203	.068	.044

$\tilde{x}$ \ $\tilde{y}$	0	0.050	0.100	0.150	0.200	0.300	0.400	0.500
0.525	-.141	-.141	-.141	-.140	-.139	-.135	-.133	-.130
.575	-.180	-.180	-.179	-.177	-.173	-.164	-.158	-.153
.625	-.220	-.220	-.218	-.215	-.209	-.192	-.183	-.176
.675	-.261	-.260	-.259	-.256	-.250	-.217	-.208	-.198

Table 37. - Dimensionless Shear Stress $\frac{\sigma_{xy}}{\sigma_0}$ at at Location $(\tilde{x},\tilde{y})$ for a Specimen With a 3^o Edge Notch Subjected to Pure Bending; Plane Strain, $\tilde{q} = 0.50$, $\tilde{a} = 0.3$, $\alpha = 3^o$, $m = 0.10$, $\mu = 0.33$

$\tilde{x}$ \ $\tilde{y}$	0	0.008	0.016	0.032	0.060	0.132	0.356	0.510
-0.128		.001	-.007	-.029	-.076	-.156	-.122	-.085
-.056		-.028	-.077	-.176	-.265	-.242	-.124	-.091
-.028		-.124	-.267	-.398	-.365	-.236	-.117	-.089
-.012		-.451	-.653	-.541	-.357	-.213	-.110	-.087
.002	.000	-.390	-.448	-.379	-.278	-.182	-.104	-.085
.006	.000	.263	-.128	-.268	-.244	-.172	-.101	-.084
.012	.000	.406	.198	-.096	-.186	-.155	-.098	-.083
.028	.000	.205	.285	.175	-.025	-.106	-.089	-.079
.056	.000	.080	.143	.193	.128	-.020	-.072	-.072
.080	.000	.047	.088	.144	.150	.036	-.056	-.066

$\tilde{x}$ \ $\tilde{y}$	0	0.050	0.100	0.150	0.200	0.300	0.400	0.500
0.525	.000	.015	.029	.041	.048	.046	.028	.006
.575	.000	.011	.021	.030	.037	.035	.019	.000
.625	.000	.006	.012	.017	.023	.019	.006	-.007
.675	.000	.002	.003	.002	-.002	-.003	-.006	-.017

Table 38. - Dimensionless x-Directional Stress $\frac{\sigma_x}{\sigma_0}$ at Location $(\tilde{x},\tilde{y})$ for a Specimen With a 3^o Edge Notch Subjected to Pure Bending; Plane Strain, $\tilde{q} = 0.70$, $\tilde{a} = 0.3$, $\alpha = 3^o$, $m = 0.10$, $\mu = 0.33$

$\tilde{x}$ \ $\tilde{y}$	0	0.008	0.016	0.032	0.060	0.132	0.356	0.510
-0.128		-.066	-.018	.060	.141	.121	-.032	-.050
-.056		.134	.266	.398	.349	.102	-.070	-.072
-.028		.514	.716	.640	.321	.055	-.084	-.080
-.012		1.380	1.108	.558	.220	.027	-.090	-.083
.002	7.898	1.293	.700	.318	.148	.010	-.095	-.087
.006	4.633	1.694	.735	.295	.140	.007	-.097	-.087
.012	3.231	2.100	1.028	.337	.136	.003	-.098	-.088
.028	1.958	1.743	1.298	.587	.191	.002	-.102	-.091
.056	1.183	1.144	1.040	.748	.350	.266	-.107	-.095
.080	.898	.883	.841	.700	.424	.063	-.107	-.097

$\tilde{x}$ \ $\tilde{y}$	0	0.050	0.100	0.150	0.200	0.300	0.400	0.500
0.525	.051	.048	.041	.033	.024	.010	-.008	-.023
.575	.028	.026	.020	.015	.012	.014	-.001	-.015
.625	.011	.009	.006	.001	.001	.018	.004	-.010
.675	.001	.000	-.002	-.006	-.009	.019	.006	-.004

Table 39. - Dimensionless y-Directional Stress $\frac{\sigma_y}{\sigma_0}$ at Location $(\tilde{x},\tilde{y})$ for a Specimen With a 3^o Edge Notch Subjected to Pure Bending; Plane Strain, $\tilde{q} = 0.70$, $\tilde{a} = 0.3$, $\alpha = 3^o$, $m = 0.10$, $\mu = 0.33$

$\tilde{x}$ \ $\tilde{y}$	0	0.008	0.016	0.032	0.060	0.132	0.356	0.510
-0.128		-.004	.001	.013	.057	.222	.400	.430
-.056		.003	.024	.118	.328	.516	.433	.395
-.028		.037	.175	.513	.749	.681	.439	.378
-.012		.356	.931	1.261	1.118	.766	.440	.367
.002	7.672	4.753	3.136	2.012	1.353	.825	.439	.357
.006	4.388	4.364	3.281	2.106	1.389	.838	.439	.354
.012	2.929	3.126	2.928	2.108	1.416	.854	.437	.349
.028	1.584	1.646	1.751	1.715	1.380	.877	.432	.336
.056	1.018	1.033	1.070	1.149	1.147	.853	.416	.310
.080	.796	.802	.818	.863	.912	.783	.394	.285

$\tilde{x}$ \ $\tilde{y}$	0	0.050	0.100	0.150	0.200	0.300	0.400	0.500
0.525	-.649	-.646	-.638	-.626	-.612	-.583	-.554	-.530
.575	-.790	-.787	-.777	-.762	-.745	-.707	-.668	-.635
.625	-.940	-.936	-.925	-.908	-.883	-.828	-.777	-.739
.675	-1.100	-1.098	-1.088	-1.072	-1.040	-.932	-.883	-.839

Table 40. - Dimensionless z-Directional Stress $\frac{\sigma_z}{\sigma_0}$ at Location $(\tilde{x},\tilde{y})$ for a Specimen With a 3° Edge Notch Subjected to Pure Bending; Plane Strain, $\tilde{q} = 0.70$, $\tilde{a} = 0.3$, $\alpha = 3^\circ$, $m = 0.10$, $\mu = 0.33$

$\tilde{x}$ \ $\tilde{y}$	0	0.008	0.016	0.032	0.060	0.132	0.356	0.510
-0.128		-.023	-.006	.024	.065	.113	.122	.125
-.056		.045	.096	.170	.223	.204	.120	.107
-.028		.182	.294	.444	.392	.243	.117	.099
-.012		.815	.971	.857	.577	.262	.115	.094
.002	6.628	2.914	1.845	1.114	.656	.275	.113	.089
.006	3.473	2.913	1.930	1.148	.665	.279	.113	.088
.012	2.106	2.422	1.886	1.161	.665	.283	.112	.086
.028	1.169	1.118	1.021	.945	.598	.290	.109	.081
.056	.726	.719	.696	.626	.494	.290	.102	.071
.080	.559	.556	.547	.516	.441	.279	.095	.062

$\tilde{x}$ \ $\tilde{y}$	0	0.050	0.100	0.150	0.200	0.300	0.400	0.500
0.525	-.198	-.197	-.197	-.196	-.194	-.189	-.185	-.182
.575	-.251	-.251	-.250	-.247	-.242	-.229	-.221	-.215
.625	-.307	-.306	-.303	-.299	-.291	-.267	-.255	-.247
.675	-.363	-.362	-.360	-.356	-.346	-.301	-.289	-.278

Table 41. - Dimensionless Shear Stress $\frac{\sigma_{xy}}{\sigma_0}$ at Location $(\tilde{x},\tilde{y})$ for a Specimen With a 3^o Edge Notch Subjected to Pure Bending; Plane Strain, $\tilde{q} = 0.70$, $\tilde{a} = 0.3$, $\alpha = 3^o$, $m = 0.10$, $\mu = 0.33$

$\tilde{x}$ \ $\tilde{y}$	0	0.008	0.016	0.032	0.060	0.132	0.356	0.510
-0.128		.002	-.010	-.041	-.110	-.223	-.170	-.117
-.056		-.032	-.099	-.252	-.393	-.343	-.172	-.125
-.028		-.148	-.369	-.596	-.545	-.326	-.160	-.122
-.012		-.678	-1.000	-.805	-.513	-.288	-.151	-.119
.002	.000	-.665	-.715	-.535	-.354	-.240	-.142	-.116
.006	.000	-.350	-.216	-.362	-.297	-.224	-.139	-.115
.012	.000	.600	.296	-.101	-.206	-.200	-.134	-.113
.028	.000	.325	.446	.279	.006	-.131	-.122	-.109
.056	.000	.123	.219	.291	.193	-.017	-.097	-.100
.080	.000	.069	.130	.210	.217	.058	-.075	-.090

$\tilde{x}$ \ $\tilde{y}$	0	0.050	0.100	0.150	0.200	0.300	0.400	0.500
0.525	.000	.021	.040	.055	.065	.062	.037	.006
.575	.000	.015	.029	.042	.051	.047	.024	-.001
.625	.000	.009	.016	.023	.031	.025	.008	-.011
.675	.000	.002	.003	.002	-.003	-.005	-.009	-.024

C3

Table 42. - Dimensionless x-Directional Stress $\frac{\sigma_x}{\sigma_0}$ at Location $(\tilde{x},\tilde{y})$ for a Specimen With a 3^o Edge Notch Subjected to Pure Bending; Plane Strain, $\tilde{q} = 0.90$, $\tilde{a} = 0.3$, $\alpha = 3^o$, $m = 0.10$, $\mu = 0.33$

$\tilde{x}$ \ $\tilde{y}$	0	0.008	0.016	0.032	0.060	0.132	0.356	0.510
-0.128		-.065	.002	.102	.199	.151	-.044	-.065
-.056		.304	.460	.588	.455	.106	-.094	-.091
-.028		.910	1.148	.936	.381	.035	-.110	-.100
-.012		2.181	1.766	.820	.203	-.003	-.118	-.105
.002	11.560	2.117	1.192	.464	.062	-.020	-.123	-.108
.006	6.937	2.719	1.231	.429	.041	-.024	-.125	-.109
.012	4.959	3.188	1.658	.480	.026	-.030	-.127	-.111
.028	3.133	2.762	2.029	.830	.093	-.028	-.131	-.114
.056	1.860	1.789	1.595	1.054	.341	.000	-.134	-.118
.080	1.338	1.310	1.230	.968	.478	.040	-.134	-.119

$\tilde{x}$ \ $\tilde{y}$	0	0.050	0.100	0.150	0.200	0.300	0.400	0.500
0.525	.060	.056	.049	.039	.029	.014	-.008	-.028
.575	.032	.029	.023	.018	.015	.019	.000	-.019
.625	.011	.010	.006	.000	.001	.024	.008	-.013
.675	.000	.000	-.003	-.007	-.010	.025	.010	-.007

Table 43. - Dimensionless y-Directional Stress $\frac{\sigma_y}{\sigma_0}$ at Location $(\tilde{x},\tilde{y})$ for a Specimen With a 3^o Edge Notch Subjected to Pure Bending; Plane Strain, $\tilde{q} = 0.90$, $\tilde{a} = 0.3$, $\alpha = 3^o$, $m = 0.10$, $\mu = 0.33$

$\tilde{x}$ \ $\tilde{y}$	0	0.008	0.016	0.032	0.060	0.132	0.356	0.510
-0.128		-.006	.002	.023	.089	.318	.526	.558
-.056		.006	.041	.184	.495	.735	.559	.507
-.028		.045	.239	.735	1.102	.951	.563	.484
-.012		.504	1.368	1.852	1.630	1.043	.562	.468
.002	11.148	6.927	4.619	2.975	1.942	1.093	.558	.454
.006	6.517	6.422	4.854	3.109	1.977	1.100	.556	.450
.012	4.478	4.592	4.366	3.087	1.980	1.101	.554	.444
.028	2.203	2.272	2.423	2.323	1.767	1.079	.544	.425
.056	1.119	1.142	1.201	1.320	1.326	1.005	.518	.390
.080	.828	.839	.869	.959	1.070	.923	.488	.356

$\tilde{x}$ \ $\tilde{y}$	0	0.050	0.100	0.150	0.200	0.300	0.400	0.500
0.525	-.820	-.816	-.806	-.791	-.774	-.740	-.705	-.676
.575	-.992	-.988	-.976	-.958	-.938	-.893	-.846	-.807
.625	-1.177	-1.172	-1.159	-1.137	-1.106	-1.041	-.980	-.937
.675	-1.372	-1.368	-1.357	-1.337	-1.299	-1.166	-1.108	-1.063

Table 44. - Dimensionless z-Directional Stress $\frac{\sigma_z}{\sigma_0}$ at Location $(\tilde{x},\tilde{y})$ for a Specimen With a 3^o Edge Notch Subjected to Pure Bending; Plane Strain, $\tilde{q} = 0.90$, $\tilde{a} = 0.3$, $\alpha = 3^o$, $m = 0.10$, $\mu = 0.33$

$\tilde{x}$ \ $\tilde{y}$	0	0.008	0.016	0.032	0.060	0.132	0.356	0.510
-0.128		-.023	.001	.041	.095	.155	.159	.162
-.056		.102	.165	.255	.328	.278	.154	.137
-.028		.315	.622	.790	.697	.378	.150	.126
-.012		1.292	1.512	1.291	.878	.409	.146	.120
.002	10.103	4.361	2.806	1.663	.962	.417	.143	.114
.006	5.645	4.394	2.938	1.711	.969	.414	.142	.112
.012	3.728	3.723	2.901	1.724	.961	.402	.141	.110
.028	2.004	2.019	1.995	1.491	.875	.347	.136	.103
.056	.983	.967	.923	.816	.658	.332	.127	.090
.080	.715	.709	.692	.636	.511	.318	.117	.078

$\tilde{x}$ \ $\tilde{y}$	0	0.050	0.100	0.150	0.200	0.300	0.400	0.500
0.525	-.251	-.251	-.250	-.248	-.246	-.239	-.235	-.232
.575	-.317	-.316	-.315	-.310	-.304	-.288	-.279	-.273
.625	-.438	-.432	-.415	-.385	-.365	-.335	-.321	-.313
.675	-.605	-.602	-.594	-.579	-.545	-.429	-.362	-.353

Table 45. - Dimensionless Shear Stress $\frac{\sigma_{xy}}{\sigma_0}$ at Location $(\tilde{x},\tilde{y})$ for a Specimen With a 3^o Edge Notch Subjected to Pure Bending; Plane Strain, $\tilde{q} = 0.90$, $\tilde{a} = 0.3$, $\alpha = 3^o$, $m = 0.10$, $\mu = 0.33$

$\tilde{x}$ \ $\tilde{y}$	0	0.008	0.016	0.032	0.060	0.132	0.356	0.510
-0.128		.000	-.020	-.069	-.165	-.306	-.212	-.142
-.056		-.066	-.175	-.401	-.578	-.444	-.208	-.152
-.028		-.228	-.564	-.908	-.810	-.397	-.192	-.149
-.012		-.974	-1.477	-1.234	-.765	-.328	-.180	-.145
.002	.000	-1.032	-1.102	-.811	-.518	-.252	-.168	-.141
.006	.000	.431	-.378	-.550	-.424	-.229	-.164	-.140
.012	.000	.831	.399	-.152	-.276	-.194	-.158	-.138
.028	.000	.499	.686	.457	.079	-.110	-.142	-.132
.056	.000	.222	.396	.526	.365	.004	-.112	-.121
.080	.000	.127	.239	.382	.377	.084	-.086	-.110

$\tilde{x}$ \ $\tilde{y}$	0	0.050	0.100	0.150	0.200	0.300	0.400	0.500
0.525	.000	.025	.048	.066	.077	.071	.039	.000
.575	.000	.018	.035	.049	.060	.053	.024	-.009
.625	.000	.010	.019	.027	.036	.028	.005	-.019
.675	.000	.002	.003	.000	-.006	-.009	-.013	-.031

Table 46. - Dimensionless x-Directional Stress $\frac{\sigma_x}{\sigma_0}$ at Location $(\tilde{x},\tilde{y})$ for a Specimen With a 10^o Edge Notch Subjected to Pure Bending; Plane Strain, $\tilde{q} = 0.50$, $\tilde{a} = 0.3$, $\alpha = 10^o$, $m = 0.10$, $\mu = 0.33$

$\tilde{x}$ \ $\tilde{y}$	0	0.008	0.016	0.032	0.060	0.132	0.356	0.510
-0.128			-.042	.019	.084	.088	-.028	-.030
-.056		.113	.192	.265	.233	.074	-.053	-.046
-.028		.418	.496	.408	.221	.042	-.062	-.052
-.012		1.024	.758	.363	.164	.022	-.067	-.055
.002	5.409	.922	.507	.220	.115	.009	-.070	-.058
.006	3.163	1.200	.535	.211	.108	.005	-.071	-.058
.012	2.195	1.437	.731	.246	.103	.002	-.073	-.059
.028	1.345	1.212	.921	.427	.136	-.002	-.075	-.062
.056	.844	.818	.748	.545	.254	.014	-.079	-.065
.080	.649	.638	.609	.508	.307	.039	-.079	-.066

$\tilde{x}$ \ $\tilde{y}$	0	0.050	0.100	0.150	0.200	0.300	0.400	0.500
0.525	.037	.035	.030	.022	.014	.001	-.010	-.010
.575	.021	-.028	.016	.010	.005	.003	-.006	-.005
.625	.010	.009	.006	.000	-.002	.004	-.004	.001
.675	.003	.002	-.001	-.003	-.007	.005	-.003	.007

Table 47. - Dimensionless y-Directional Stress $\frac{\sigma_y}{\sigma_0}$ at Location $(\tilde{x},\tilde{y})$ for a Specimen With a 10^o Edge Notch Subjected to Pure Bending; Plane Strain, $\tilde{q} = 0.50$, $\tilde{a} = 0.3$, $\alpha = 10^o$, $m = 0.10$, $\mu = 0.33$

$\tilde{x}$ \ $\tilde{y}$	0	0.008	0.016	0.032	0.060	0.132	0.356	0.510
-0.128			-.005	.007	.038	.155	.301	.324
-.056		-.002	.022	.092	.231	.362	.321	.295
-.028		.033	.130	.351	.507	.480	.325	.281
-.012		.248	.586	.787	.734	.544	.325	.273
.002	5.131	3.144	2.068	1.327	.914	.590	.324	.265
.006	2.922	2.936	2.197	1.424	.953	.601	.324	.263
.012	2.012	2.159	2.032	1.483	1.000	.615	.323	.259
.028	1.223	1.264	1.330	1.306	1.033	.639	.318	.249
.056	.790	.798	.822	.872	.862	.629	.306	.229
.080	.609	.613	.624	.654	.685	.580	.290	.209

$\tilde{x}$ \ $\tilde{y}$	0	0.050	0.100	0.150	0.200	0.300	0.400	0.500
0.525	-.491	-.489	-.482	-.474	-.463	-.440	-.418	-.400
.575	-.597	-.547	-.587	-.577	-.565	-.536	-.504	-.477
.625	-.708	-.706	-.698	-.687	-.669	-.631	-.590	-.553
.675	-.827	-.825	-.819	-.808	-.788	-.719	-.680	-.622

Table 48. - Dimensionless z-Directional Stress $\frac{\sigma_z}{\sigma_0}$ at Location $(\tilde{x},\tilde{y})$ for a Specimen With a 10° Edge Notch Subjected to Pure Bending; Plane Strain, $\tilde{q} = 0.50$, $\tilde{a} = 0.3$, $\alpha = 10^{\circ}$, $m = 0.10$, $\mu = 0.33$

$\tilde{x}$ \ $\tilde{y}$	0	0.008	0.016	0.032	0.060	0.132	0.356	0.510
-0.128			-.016	.009	.041	.080	.090	.097
-.056		.037	.071	.118	.153	.144	.088	.082
-.028		.149	.206	.251	.240	.172	.087	.076
-.012		.485	.570	.426	.296	.187	.085	.072
.002	4.213	1.908	1.183	.660	.340	.198	.084	.068
.006	2.059	1.901	1.243	.692	.350	.200	.083	.067
.012	1.389	1.360	1.187	.699	.364	.204	.083	.066
.028	.847	.817	.743	.572	.386	.210	.080	.062
.056	.539	.534	.518	.467	.368	.212	.075	.054
.080	.415	.413	.407	.384	.327	.204	.070	.047

$\tilde{x}$ \ $\tilde{y}$	0	0.050	0.100	0.150	0.200	0.300	0.400	0.500
.525	-.150	-.150	-.149	-.149	-.148	-.145	-.141	-.135
.575	-.190	-.190	-.189	-.187	-.185	-.176	-.168	-.159
.625	-.230	-.230	-.229	-.227	-.221	-.207	-.196	-.182
.675	-.272	-.272	-.270	-.268	-.262	-.236	-.225	-.203

Table 49. - Dimensionless Shear Stress $\frac{\sigma_{xy}}{\sigma_0}$ at Location $(\tilde{x},\tilde{y})$ for a Specimen With a 10° Edge Notch Subjected to Pure Bending; Plane Strain, $\tilde{q} = 0.50$, $\tilde{a} = 0.3$, $\alpha = 10^{\circ}$, $m = 0.10$, $\mu = 0.33$

$\tilde{x}$ \ $\tilde{y}$	0	0.008	0.016	0.032	0.060	0.132	0.356	0.510
-0.128			-.003	-.029	-.081	-.159	-.121	-.088
-.056		-.021	-.075	-.180	-.273	-.247	-.125	-.093
-.028		-.127	-.275	-.409	-.373	-.241	-.118	-.091
-.012		-.463	-.668	-.555	-.363	-.217	-.111	-.089
.002	.000	-.417	-.463	-.391	-.280	-.186	-.105	-.087
.006	.000	.258	-.136	-.277	-.245	-.175	-.103	-.086
.012	.000	.412	.200	-.098	-.188	-.158	-.100	-.085
.028	.000	.210	.293	.184	-.027	-.108	-.091	-.081
.056	.000	.083	.148	.200	.131	-.022	-.073	-.074
.080	.000	.048	.091	.148	.153	.036	-.057	-.067

$\tilde{x}$ \ $\tilde{y}$	0	0.050	0.100	0.150	0.200	0.300	0.400	0.500
0.525	.000	.015	.028	.038	.045	.044	.030	.009
.575	.000	.010	.020	.028	.034	.032	.020	.003
.625	.000	.006	.011	.015	.020	.016	.005	-.007
.675	.000	.002	.002	.001	-.002	-.006	-.013	-.025

Table 50. - Dimensionless x-Directional Stress $\frac{\sigma_x}{\sigma_0}$ at Location $(\tilde{x},\tilde{y})$ for a Specimen With a 10° Edge Notch Subjected to Pure Bending; Plane Strain, $\tilde{q} = 0.70$, $\tilde{a} = 0.3$, $\alpha = 10^{\circ}$, $m = 0.10$, $\mu = 0.33$

$\tilde{x}$ \ $\tilde{y}$	0	0.008	0.016	0.032	0.060	0.132	0.356	0.510
-0.128			-.031	.054	.135	.114	-.043	-.040
-.056		.242	.359	.456	.350	.065	-.077	-.063
-.028		.686	.872	.717	.310	.008	-.089	-.071
-.012		1.625	1.307	.625	.200	-.020	-.095	-.074
.002	8.738	1.532	.870	.363	.114	-.036	-.099	-.078
.006	5.161	1.947	.902	.339	.096	-.039	-.100	-.079
.012	3.643	2.393	1.213	.383	.085	-.041	-.102	-.080
.028	2.248	2.010	1.505	.652	.124	-.038	-.105	-.083
.056	1.353	1.306	1.180	.812	.305	-.012	-.109	-.087
.080	.997	.978	.925	.748	.405	.269	-.109	-.089

$\tilde{x}$ \ $\tilde{y}$	0	0.050	0.100	0.150	0.200	0.300	0.400	0.500
0.525	.049	.046	.040	.028	.018	.001	-.013	-.013
.575	.027	-.053	.020	.013	.007	.003	-.009	-.006
.625	.012	.011	.007	.000	-.002	.005	-.005	.002
.675	.003	.002	-.001	-.004	-.009	.006	-.004	-.010

Table 51. - Dimensionless y-Directional Stress $\frac{\sigma_y}{\sigma_0}$ at Location $(\tilde{x},\tilde{y})$ for a Specimen With a 10^o Edge Notch Subjected to Pure Bending; Plane Strain, $\tilde{q} = 0.70$, $\tilde{a} = 0.3$, $\alpha = 10^o$, $m = 0.10$, $\mu = 0.33$

$\tilde{x}$ \ $\tilde{y}$	0	0.008	0.016	0.032	0.060	0.132	0.356	0.510
-0.128			-.008	.013	.064	.240	.430	.461
-.056		-.003	.030	.136	.364	.545	.451	.415
-.028		.042	.190	.558	.808	.704	.453	.394
-.012		.386	1.008	1.368	1.202	.779	.451	.381
.002	8.472	5.164	3.415	2.188	1.446	.825	.448	.369
.006	4.845	4.770	3.583	2.290	1.472	.835	.447	.365
.012	3.252	3.429	3.200	2.284	1.478	.846	.445	.360
.028	1.667	1.732	1.840	1.777	1.366	.859	.437	.344
.056	.968	.984	1.026	1.121	1.133	.837	.417	.315
.080	.739	.747	.767	.828	.900	.772	.393	.287

$\tilde{x}$ \ $\tilde{y}$	0	0.050	0.100	0.150	0.200	0.300	0.400	0.500
0.525	-.684	-.682	-.672	-.661	-.646	-.615	-.585	-.561
.575	-.828	-.747	-.815	-.802	-.785	-.746	-.704	-.668
.625	-.980	-.976	-.966	-.951	-.928	-.876	-.822	-.772
.675	-1.142	-1.139	-1.131	-1.115	-1.089	-.998	-.946	-.867

Table 52. - Dimensionless z-Directional Stress $\frac{\sigma_z}{\sigma_0}$ at Location $(\tilde{x},\tilde{y})$ for a Specimen With a 10° Edge Notch Subjected to Pure Bending; Plane Strain, $\tilde{q}= 0.70$, $\tilde{a} = 0.3$, $\alpha = 10^{\circ}$, $m = 0.10$, $\mu = 0.33$

$\tilde{x}$ \ $\tilde{y}$	0	0.008	0.016	0.032	0.060	0.132	0.356	0.510
-0.128			-.013	.022	.066	.117	.128	.139
-.056		.079	.128	.195	.236	.201	.124	.116
-.028		.240	.350	.542	.467	.235	.120	.107
-.012		.951	1.104	.945	.623	.250	.118	.101
.002	7.429	3.214	2.052	1.219	.703	.260	.115	.096
.006	3.963	3.213	2.144	1.255	.702	.263	.114	.095
.012	2.481	2.704	2.093	1.267	.686	.265	.113	.092
.028	1.292	1.235	1.212	1.026	.599	.271	.110	.086
.056	.766	.756	.728	.638	.474	.272	.102	.075
.080	.573	.569	.558	.520	.431	.264	.094	.065

$\tilde{x}$ \ $\tilde{y}$	0	0.050	0.100	0.150	0.200	0.300	0.400	0.500
0.525	-.210	-.210	-.209	-.209	-.207	-.203	-.197	-.189
.575	-.265	-.264	-.262	-.260	-.257	-.245	-.235	-.223
.625	-.319	-.319	-.317	-.314	-.307	-.287	-.273	-.254
.675	-.389	-.384	-.373	-.369	-.362	-.327	-.313	-.283

Table 53. - Dimensionless Shear Stress $\frac{\sigma_{xy}}{\sigma_0}$ at Location $(\tilde{x},\tilde{y})$ for a Specimen With a 10° Edge Notch Subjected to Pure Bending; Plane Strain, $\tilde{q} = 0.70$, $\tilde{a} = 0.3$, $\alpha = 10^{\circ}$, $m = 0.10$, $\mu = 0.33$

$\tilde{x}$ \ $\tilde{y}$	0	0.008	0.016	0.032	0.060	0.132	0.356	0.510
-0.128			-.010	-.054	-.136	-.239	-.163	-.118
-.056		-.036	-.122	-.297	-.443	-.351	-.167	-.125
-.028		-.172	-.418	-.670	-.606	-.323	-.156	-.122
-.012		-.743	-1.100	-.894	-.567	-.277	-.148	-.119
.002	.000	-.762	-.800	-.595	-.383	-.225	-.139	-.117
.006	.000	.354	-.253	-.405	-.315	-.209	-.136	-.115
.012	.000	.648	.320	-.114	-.206	-.185	-.132	-.114
.028	.000	.363	.503	.329	.056	-.120	-.120	-.110
.056	.000	.151	.273	.372	.252	-.013	-.097	-.101
.080	.000	.087	.164	.265	.267	.062	-.076	-.091

$\tilde{x}$ \ $\tilde{y}$	0	0.050	0.100	0.150	0.200	0.300	0.400	0.500
0.525	.000	.019	.037	.050	.059	.057	.037	.007
.575	.000	.013	.026	.036	.044	.040	.023	.000
.625	.000	.008	.014	.020	.025	.019	.003	-.012
.675	.000	.002	.003	.001	-.004	-.010	-.020	-.036

Table 54. - Dimensionless x-Directional Stress $\frac{\sigma_x}{\sigma_0}$ at Location $(\tilde{x},\tilde{y})$ for a Specimen With a 10^o Edge Notch Subjected to Pure Bending; Plane Strain, $\tilde{q} = 0.90$, $\tilde{a} = 0.3$, $\alpha = 10^o$, $m = 0.10$, $\mu = 0.33$

$\tilde{x}$ \ $\tilde{y}$	0	0.008	0.016	0.032	0.060	0.132	0.356	0.510
-0.128			-.032	.073	.169	.143	-.055	-.052
-.056		.390	.519	.605	.416	.087	-.098	-.080
-.028		.973	1.217	.957	.337	.025	-.114	-.091
-.012		2.212	1.821	.832	.176	-.002	-.122	-.095
.002	11.758	2.108	1.213	.461	.044	-.008	-.127	-.099
.006	6.987	2.714	1.241	.422	.021	-.009	-.128	-.100
.012	4.971	3.187	1.656	.467	.010	-.015	-.130	-.102
.028	3.109	2.768	2.012	.895	.082	-.013	-.135	-.106
.056	1.812	1.741	1.551	1.019	.340	.005	-.139	-.110
.080	1.296	1.269	1.192	.942	.481	.044	-.138	-.113

$\tilde{x}$ \ $\tilde{y}$	0	0.050	0.100	0.150	0.200	0.300	0.400	0.500
0.525	.061	.057	.049	.034	.022	.001	-.016	-.015
.575	.033	-.073	.025	.015	.008	.004	-.010	-.007
.625	.015	.013	.009	-.000	-.003	.006	-.006	.003
.675	.003	.003	-.002	-.006	-.011	.007	-.004	.013

Table 55. - Dimensionless y-Directional Stress $\frac{\sigma_y}{\sigma_o}$ at Location $(\tilde{x},\tilde{y})$ for a Specimen With a 10^o Edge Notch Subjected to Pure Bending; Plane Strain, $\tilde{q} = 0.90$, $\tilde{a} = 0.3$, $\alpha = 10^o$, $m = 0.10$, $\mu = 0.33$

$\tilde{x}$ \ $\tilde{y}$	0	0.008	0.016	0.032	0.060	0.132	0.356	0.510
-0.128			-.010	.020	.091	.316	.559	.596
-.056		-.003	.040	.178	.478	.708	.586	.537
-.028		.049	.239	.737	1.081	.922	.588	.509
-.012		.509	1.382	1.878	1.624	1.029	.586	.492
.002	11.471	7.014	4.673	3.014	1.951	1.102	.581	.477
.006	6.642	6.528	4.910	3.144	1.984	1.116	.579	.472
.012	4.538	4.650	4.405	3.109	1.983	1.126	.576	.465
.028	2.141	2.241	2.376	2.292	1.773	1.126	.566	.445
.056	1.132	1.156	1.220	1.359	1.394	1.058	.539	.406
.080	.870	.881	.912	1.004	1.115	.967	.506	.369

$\tilde{x}$ \ $\tilde{y}$	0	0.050	0.100	0.150	0.200	0.300	0.400	0.500
0.525	-.879	-.876	-.863	-.850	-.832	-.792	-.754	-.723
.575	-1.063	-.955	-1.046	-1.029	-1.008	-.959	-.906	-.860
.625	-1.255	-1.251	-1.239	-1.219	-1.191	-1.126	-1.057	-.993
.675	-1.458	-1.454	-1.444	-1.425	-1.393	-1.280	-1.215	-1.116

Table 56. - Dimensionless z-Directional Stress $\frac{\sigma_z}{\sigma_0}$ at Location $(\tilde{x},\tilde{y})$ for a Specimen With a 10^{o} Edge Notch Subjected to Pure Bending; Plane Strain, $\tilde{q} = 0.90$, $\tilde{a} = 0.3$, $\alpha = 10^{o}$, $m = 0.10$, $\mu = 0.33$

$\tilde{x}$ \ $\tilde{y}$	0	0.008	0.016	0.032	0.060	0.132	0.356	0.510
-0.128			-.014	.031	.086	.152	.166	.180
-.056		.128	.184	.258	.312	.263	.161	.151
-.028		.338	.654	.804	.670	.353	.156	.138
-.012		1.312	1.547	1.311	.862	.400	.153	.131
.002	10.338	4.411	2.850	1.684	.959	.426	.150	.125
.006	5.716	4.456	2.979	1.729	.963	.429	.149	.123
.012	3.751	3.766	2.931	1.734	.956	.425	.147	.120
.028	1.779	2.032	1.996	1.476	.877	.393	.142	.112
.056	.972	.956	.914	.838	.716	.351	.132	.098
.080	.715	.710	.694	.642	.527	.334	.122	.085

$\tilde{x}$ \ $\tilde{y}$	0	0.050	0.100	0.150	0.200	0.300	0.400	0.500
.525	-.270	-.270	-.269	-.269	-.267	-.261	-.254	-.243
.575	-.340	-.339	-.337	-.335	-.330	-.315	-.302	-.286
.625	-.502	-.499	-.489	-.473	-.445	-.373	-.351	-.327
.675	-.661	-.658	-.652	-.640	-.619	-.520	-.468	-.367

Table 57. - Dimensionless Shear Stress $\frac{\sigma_{xy}}{\sigma_0}$ at Location $(\tilde{x},\tilde{y})$ for a Specimen With a 10^o Edge Notch Subjected to Pure Bending; Plane Strain, $\tilde{q} = 0.90$, $\tilde{a} = 0.3$, $\alpha = 10^o$, $m = 0.10$, $\mu = 0.33$

$\tilde{x}$ \ $\tilde{y}$	0	0.008	0.016	0.032	0.060	0.132	0.356	0.510
-0.128			-.016	-.077	-.183	-.304	-.209	-.151
-.056		-.058	-.175	-.410	-.590	-.441	-.212	-.160
-.028		-.219	-.551	-.903	-.803	-.405	-.198	-.156
-.012		-.985	-1.479	-1.214	-.738	-.345	-.187	-.152
.002	.000	-1.080	-1.108	-.779	-.475	-.274	-.175	-.149
.006	.000	.421	-.374	-.514	-.377	-.253	-.172	-.147
.012	.000	.844	.417	-.109	-.225	-.220	-.166	-.145
.028	.000	.513	.712	.497	.123	-.136	-.150	-.139
.056	.000	.222	.397	.526	.355	-.008	-.119	-.128
.080	.000	.123	.231	.368	.360	.080	-.093	-.115

$\tilde{x}$ \ $\tilde{y}$	0	0.050	0.100	0.150	0.200	0.300	0.400	0.500
0.525	.000	.024	.045	.062	.072	.070	.045	.008
.575	.000	.016	.032	.044	.054	.049	.027	-.001
.625	.000	.009	.017	.024	.030	.022	.002	-.017
.675	.000	.002	.003	.000	-.007	-.014	-.026	-.047

Table 58. - Dimensionless x-Directional Stress $\frac{\sigma_x}{\sigma_0}$ at Location $(\tilde{x},\tilde{y})$ for a Specimen With a 10° Edge Notch Subjected to Pure Bending; Plane Stress, $\tilde{q} = 0.50$, $\tilde{a} = 0.3$, $\alpha = 10^{\circ}$, $m = 0.10$, $\mu = 0.33$

$\tilde{x}$ \ $\tilde{y}$	0	0.013	0.024	0.036	0.060	0.132	0.186	0.500
-0.040		.115	.263	.321	.283	.087	.014	-.053
-.024		.293	.422	.407	.286	.067	.001	-.057
-.012		.532	.503	.420	.262	.051	-.009	-.059
-.004		.558	.482	.395	.239	.041	-.015	-.061
.002	2.665	.483	.463	.375	.223	.034	-.019	-.062
.006	1.604	.544	.465	.367	.215	.030	-.021	-.063
.014	1.168	.736	.513	.371	.205	.024	-.026	-.064
.031	.951	.814	.624	.439	.217	.018	-.031	-.067
.053	.798	.743	.637	.502	.278	.025	-.032	-.069
.088	.599	.580	.539	.476	.332	.060	-.018	-.072

$\tilde{x}$ \ $\tilde{y}$	0	0.050	0.100	0.150	0.200	0.300	0.400	0.500
0.630	.010	.009	.005	.001	-.002	.005	-.005	.001
.650	.007	.006	.003	-.002	-.005	.006	-.005	.003
.670	.004	.003	.001	-.003	-.007	.006	-.004	.005
.690	.002	.002	.000	-.003	-.006	.004	-.002	.006

Table 59. - Dimensionless y-Directional Stress $\frac{\sigma_y}{\sigma_0}$ at Location $(\tilde{x},\tilde{y})$ for a Specimen With a 10^o Edge Notch Subjected to Pure Bending; Plane Stress, $\tilde{q} = 0.50$, $\tilde{a} = 0.3$, $\alpha = 10^o$, $m = 0.10$, $\mu = 0.33$

$\tilde{x}$ \ $\tilde{y}$	0	0.013	0.024	0.036	0.060	0.132	0.186	0.500
-0.040		.008	.054	.133	.277	.401	.389	.283
-.024		.053	.195	.330	.464	.475	.428	.277
-.012		.304	.537	.626	.649	.530	.454	.272
-.004		.965	.946	.893	.778	.563	.470	.268
.002	3.030	1.570	1.233	1.067	.868	.586	.481	.265
.006	2.021	1.726	1.376	1.160	.921	.599	.488	.263
.014	1.680	1.741	1.518	1.292	1.011	.623	.499	.259
.031	1.584	1.560	1.477	1.335	1.060	.655	.516	.249
.053	1.009	1.017	1.022	1.013	.942	.657	.520	.235
.088	.654	.659	.668	.679	.689	.589	.489	.209

$\tilde{x}$ \ $\tilde{y}$	0	0.050	0.100	0.150	0.200	0.300	0.400	0.500
0.630	-.719	-.717	-.709	-.696	-.678	-.635	-.592	-.552
.650	-.767	-.765	-.757	-.744	-.724	-.672	-.628	-.581
.670	-.816	-.814	-.808	-.796	-.774	-.706	-.664	-.608
.690	-.866	-.864	-.859	-.849	-.831	-.737	-.702	-.625

Table 60. - Dimensionless Shear Stress $\frac{\sigma_{xy}}{\sigma_0}$ at Location $(\tilde{x},\tilde{y})$ for a Specimen With a 10^{o} Edge Notch Subjected to Pure Bending; Plane Stress, $\tilde{q} = 0.50$, $\tilde{a} = 0.3$, $\alpha = 10^{o}$, $m = 0.10$, $\mu = 0.33$

$\tilde{x}$ \ $\tilde{y}$	0	0.013	0.024	0.036	0.060	0.132	0.186	0.500
-0.040		-.032	-.124	-.215	-.300	-.258	-.209	-.098
-.024		-.118	-.271	-.349	-.364	-.253	-.199	-.096
-.012		-.363	-.443	-.437	-.378	-.238	-.187	-.095
-.004		-.583	-.485	-.436	-.359	-.223	-.177	-.093
.002	.000	-.421	-.414	-.388	-.328	-.210	-.168	-.092
.006	.000	-.209	-.331	-.337	-.300	-.200	-.162	-.091
.014	.000	.006	-.152	-.217	-.232	-.177	-.149	-.089
.031	.000	.070	.056	.006	-.071	-.122	-.117	-.085
.053	.000	.083	.121	.126	.073	-.050	-.073	-.078
.088	.000	.055	.093	.120	.131	.040	-.008	-.066

$\tilde{x}$ \ $\tilde{y}$	0	0.050	0.100	0.150	0.200	0.300	0.400	0.500
0.630	.000	.006	.012	.016	.021	.017	.007	-.004
.650	.000	.004	.008	.010	.013	.009	-.001	-.011
.670	.000	.003	.004	.004	.002	-.001	-.008	-.019
.690	.000	.001	.001	-.001	-.009	-.010	-.014	-.032

Table 61. - Dimensionless x-Directional Stress $\frac{\sigma_x}{\sigma_0}$ at Location $(\tilde{x},\tilde{y})$ for a Specimen With a 10° Edge Notch Subjected to Pure Bending; Plane Stress, $\tilde{q} = 0.70$, $\tilde{a} = 0.3$, $\alpha = 10^{\circ}$, $m = 0.10$, $\mu = 0.33$

$\tilde{x}$ \ $\tilde{y}$	0	0.013	0.024	0.036	0.060	0.132	0.186	0.500
-0.040		.263	.425	.457	.365	.112	.012	-.074
-.024		.572	.648	.541	.342	.084	-.006	-.079
-.012		.958	.729	.507	.287	.062	-.019	-.082
-.004		.945	.652	.440	.245	.049	-.027	-.084
.002	5.337	.768	.595	.395	.218	.040	-.032	-.086
.006	3.136	.872	.595	.384	.206	.035	-.035	-.086
.014	2.130	1.206	.675	.406	.194	.028	-.040	-.088
.031	1.546	1.266	.865	.553	.240	.023	-.047	-.092
.053	1.177	1.070	.881	.662	.356	.039	-.044	-.095
.088	.821	.792	.729	.638	.444	.088	-.022	-.098

$\tilde{x}$ \ $\tilde{y}$	0	0.050	0.100	0.150	0.200	0.300	0.400	0.500
0.630	.040	.039	.012	-.019	-.031	.006	.002	.005
.650	.040	.038	.009	-.026	-.039	.009	.003	.007
.670	.035	.035	.007	-.028	-.045	.010	.005	.009
.690	.033	.030	.005	-.027	-.042	.008	.008	.011

Table 62. - Dimensionless y-Directional Stress $\frac{\sigma_y}{\sigma_0}$ at Location $(\tilde{x},\tilde{y})$ for a Specimen With a 10^o Edge Notch Subjected to Pure Bending; Plane Stress, $\tilde{q} = 0.70$, $\tilde{a} = 0.3$, $\alpha = 10^o$, $m = 0.10$, $\mu = 0.33$

$\tilde{x}$ \ $\tilde{y}$	0	0.013	0.024	0.036	0.060	0.132	0.186	0.500
-0.040		.024	.111	.241	.448	.587	.560	.399
-.024		.104	.340	.548	.721	.693	.613	.390
-.012		.532	.890	.985	.976	.769	.649	.382
-.004		1.700	1.553	1.395	1.169	.814	.670	.377
.002	5.574	2.721	2.030	1.669	1.297	.845	.684	.372
.006	3.441	2.902	2.228	1.803	1.365	.862	.692	.369
.014	2.547	2.730	2.327	1.948	1.466	.891	.707	.363
.031	2.076	2.050	1.936	1.820	1.469	.922	.724	.349
.053	1.225	1.237	1.274	1.288	1.259	.906	.723	.329
.088	.829	.839	.858	.883	.909	.796	.669	.291

$\tilde{x}$ \ $\tilde{y}$	0	0.050	0.100	0.150	0.200	0.300	0.400	0.500
0.630	-.986	-.987	-.985	-.972	-.950	-.891	-.826	-.772
.650	-1.058	-1.052	-1.051	-1.046	-1.022	-.942	-.872	-.812
.670	-1.130	-1.130	-1.135	-1.137	-1.108	-.987	-.919	-.849
.690	-1.232	-1.235	-1.239	-1.238	-1.217	-1.022	-.965	-.875

Table 63. - Dimensionless Shear Stress $\frac{\sigma_{xy}}{\sigma_0}$ at Location $(\tilde{x},\tilde{y})$ for a Specimen With a 10^{o} Edge Notch Subjected to Pure Bending; Plane Stress, $\tilde{q} = 0.70$, $\tilde{a} = 0.3$, $\alpha = 10^{o}$, $m = 0.10$, $\mu = 0.33$

$\tilde{x}$ \ $\tilde{y}$	0	0.013	0.024	0.036	0.060	0.132	0.186	0.500
-0.040		-.090	-.238	-.361	-.440	-.358	-.286	-.135
-.024		-.251	-.484	-.563	-.518	-.346	-.270	-.132
-.012		-.668	-.745	-.677	-.523	-.321	-.252	-.130
-.004		-1.007	-.765	-.643	-.485	-.297	-.236	-.127
.002	.000	-.639	-.596	-.536	-.432	-.275	-.223	-.126
.006	.000	-.220	-.426	-.435	-.386	-.259	-.214	-.124
.014	.000	.170	-.094	-.214	-.276	-.225	-.194	-.122
.031	.000	.208	.212	.124	-.357	-.145	-.149	-.116
.053	.000	.165	.235	.238	.143	-.046	-.087	-.107
.088	.000	.085	.142	.180	.190	.067	.000	-.091

$\tilde{x}$ \ $\tilde{y}$	0	0.050	0.100	0.150	0.200	0.300	0.400	0.500
0.630	.000	.003	.005	.014	.029	.028	.007	-.010
.650	.000	.002	.004	.008	.018	.014	-.003	-.018
.670	.000	.002	.005	.004	.002	-.003	-.013	-.028
.690	.000	.004	.007	.001	-.017	.020	-.021	-.043

Table 64. - Dimensionless x-Directional Stress $\frac{\sigma_x}{\sigma_0}$ at Location $(\tilde{x},\tilde{y})$ for a Specimen With a 10° Edge Notch Subjected to Pure Bending; Plane Stress, $\tilde{q} = 0.90$, $\tilde{a} = 0.3$, $\alpha = 10^{\circ}$, $m = 0.10$, $\mu = 0.33$

$\tilde{x}$ \ $\tilde{y}$	0	0.013	0.024	0.036	0.060	0.132	0.186	0.500
-0.040		.408	.642	.674	.467	.094	.029	-.093
-.024		.827	.960	.805	.429	.053	.004	-.099
-.012		1.359	1.064	.758	.356	.018	-.004	-.102
-.004		1.325	.947	.659	.303	.001	-.016	-.105
.002	7.527	1.062	.861	.594	.270	-.012	-.021	-.107
.006	4.390	1.204	.854	.577	.256	-.020	-.028	-.108
.014	2.948	1.666	.954	.608	.245	-.034	-.042	-.111
.031	2.112	1.730	1.202	.810	.314	-.045	-.057	-.114
.053	1.584	1.450	1.213	.937	.471	-.022	-.060	-.118
.088	1.107	1.072	.991	.868	.576	.059	-.038	-.122

$\tilde{x}$ \ $\tilde{y}$	0	0.050	0.100	0.150	0.200	0.300	0.400	0.500
0.630	-.037	-.025	-.009	.025	.053	.041	-.045	-.016
.650	-.040	-.030	-.012	.019	.048	.046	-.045	-.011
.670	-.045	-.032	-.016	.017	.043	.046	-.046	-.002
.690	-.043	-.033	-.016	.011	.036	.040	-.037	.004

Table 65. - Dimensionless y-Directional Stress $\frac{\sigma_y}{\sigma_0}$ at Location $(\tilde{x},\tilde{y})$ for a Specimen With a 10° Edge Notch Subjected to Pure Bending; Plane Stress, $\tilde{q} = 0.90$, $\tilde{a} = 0.3$, $\alpha = 10^{\circ}$, $m = 0.10$, $\mu = 0.33$

$\tilde{x}$ \ $\tilde{y}$	0	0.013	0.024	0.036	0.060	0.132	0.186	0.500
-0.040		.028	.140	.315	.584	.776	.741	.521
-.024		.149	.501	.781	.955	.907	.821	.508
-.012		.762	1.262	1.390	1.333	1.013	.865	.497
-.004		2.387	2.163	1.925	1.586	1.074	.888	.489
.002	7.831	3.791	2.805	2.282	1.749	1.113	.900	.483
.006	4.773	4.009	3.062	2.455	1.833	1.133	.906	.479
.014	3.433	3.709	3.147	2.629	1.951	1.161	.913	.471
.031	2.647	2.598	2.479	2.399	1.930	1.170	.916	.451
.053	1.551	1.579	1.639	1.676	1.614	1.117	.899	.424
.088	1.007	1.019	1.042	1.073	1.111	.983	.826	.373

$\tilde{x}$ \ $\tilde{y}$	0	0.050	0.100	0.150	0.200	0.300	0.400	0.500
0.630	-1.304	-1.293	-1.259	-1.208	-1.160	-1.108	-1.074	-1.014
.650	-1.421	-1.406	-1.372	-1.318	-1.257	-1.192	-1.156	-1.074
.670	-1.542	-1.533	-1.511	-1.477	-1.420	-1.296	-1.247	-1.130
.690	-1.692	-1.688	-1.673	-1.648	-1.610	-1.419	-1.381	-1.157

Table 66. - Dimensionless Shear Stress $\frac{\sigma_{xy}}{\sigma_0}$ at Location $(\tilde{x},\tilde{y})$ for a Specimen With a 10^{o} Edge Notch Subjected to Pure Bending; Plane Stress, $\tilde{q} = 0.90$, $\tilde{a} = 0.3$, $\alpha = 10^{o}$, $m = 0.10$, $\mu = 0.33$

$\tilde{x}$ \ $\tilde{y}$	0	0.013	0.024	0.036	0.060	0.132	0.186	0.500
-0.040		-.114	-.321	-.504	-.626	-.456	-.358	-.170
-.024		-.338	-.659	-.773	-.717	-.444	-.337	-.166
-.012		-.932	-1.023	-.916	-.705	-.414	-.312	-.163
-.004		-1.404	-1.043	-.860	-.641	-.384	-.292	-.161
.002	.000	-.876	-.798	-.704	-.561	-.356	-.275	-.158
.006	.000	-.282	-.555	-.560	-.495	-.335	-.262	-.157
.014	.000	.265	-.088	-.247	-.341	-.288	-.237	-.153
.031	.000	.300	.315	.201	-.017	-.181	-.179	-.146
.053	.000	.225	.321	.335	.223	-.050	-.105	-.135
.088	.000	.117	.198	.259	.292	.090	-.002	-.115

$\tilde{x}$ \ $\tilde{y}$	0	0.050	0.100	0.150	0.200	0.300	0.400	0.500
0.630	.000	.013	.025	.035	.039	.024	.003	.006
.650	.000	.004	.008	.013	.022	.017	-.005	-.007
.670	.000	-.004	-.007	-.007	-.001	.005	-.012	-.029
.690	.000	-.009	-.016	-.022	-.025	-.008	-.019	-.071

Table 67. - Dimensionless x-Directional Total Plastic Strain $\frac{E\varepsilon^p_x}{\sigma_0}$ at Location $(\tilde{x},\tilde{y})$ for a Specimen With a 10^o Edge Notch Subjected to Pure Bending; Plane Strain, $\tilde{q} = 0.40$, $\tilde{a} = 0.5$, $\alpha = 10^o$, $m = 0.05$, $\mu = 0.33$

$\tilde{x}$ \ $\tilde{y}$	0	0.008	0.016	0.024	0.032	0.044	0.060	0.084
-0.020		.000	.319	.387	.064	-.055	.000	.000
-.012		3.451	1.641	-.487	-1.107	-.677	.000	.000
.002	.834	-24.700	-13.582	-8.458	-5.174	-2.010	-.026	.000
.006	.224	-15.174	-13.110	-8.718	-5.322	-2.011	.000	.000
.012	.000	-1.617	-6.563	-6.139	-4.069	-1.490	.000	.000
.020	.000	.000	-.360	-1.384	-1.319	-.387	.000	.000
.028	.000	.000	.000	.000	.000	.000	.000	.000

$\tilde{x}$ \ $\tilde{y}$	0	0.050	0.100	0.150	0.200
0.425	.000	.000	.000	.000	.000
.475	.484	.445	.333	.153	.000

Table 68. - Dimensionless y-Directional Total Plastic Strain $\frac{E\varepsilon_y^p}{\sigma_0}$ at Location $(\tilde{x},\tilde{y})$ for a Specimen With a 10^o Edge Notch Subjected to Pure Bending; Plane Strain, $\tilde{q} = 0.40$, $\tilde{a} = 0.5$, $\alpha = 10^o$, $m = 0.05$, $\mu = 0.33$

$\tilde{x}$ \ $\tilde{y}$	0	0.008	0.016	0.024	0.032	0.044	0.060	0.084
-0.020		.000	-.234	-.235	.087	.140	.000	.000
-.012		-3.208	-1.349	.772	1.370	.856	.000	.000
.002	.406	25.557	14.139	8.884	5.523	2.263	.037	.000
.006	.112	16.038	13.693	9.166	5.682	2.264	.000	.000
.012	.000	2.265	7.132	6.587	4.427	1.717	.000	.000
.020	.000	.000	.602	1.709	1.583	.502	.000	.000
.028	.000	.000	.000	.000	.000	.000	.000	.000

$\tilde{x}$ \ $\tilde{y}$	0	0.050	0.100	0.150	0.200
0.425	.000	.000	.000	.000	.000
.475	-.555	-.513	-.390	-.184	.000

Table 69. - Dimensionless Total Plastic Shear Strain $\frac{E\epsilon^{p}_{xy}}{\sigma_0}$ at Location $(\tilde{x},\tilde{y})$ for a Specimen With a 10^{o} Edge Notch Subjected to Pure Bending; Plane Strain, $\tilde{q} = 0.40$, $\tilde{a} = 0.5$, $\alpha = 10^{o}$, $m = 0.05$, $\mu = 0.33$

$\tilde{x}$ \ $\tilde{y}$	0	0.008	0.016	0.024	0.032	0.044	0.060	0.084
-0.020		.000	-.522	-1.596	-1.422	-.464	.000	.000
-.012		-3.801	-7.918	-6.512	-4.357	-1.579	.000	.000
.002	.000	-2.807	-3.139	-2.664	-2.040	-1.217	-.023	.000
.006	.000	4.168	-2.738	-3.617	-2.753	-1.207	.000	.000
.012	.000	2.101	1.873	-.116	-.779	-.508	.000	.000
.020	.000	.000	.426	.615	.224	-.020	.000	.000
.028	.000	.000	.000	.000	.000	.000	.000	.000

$\tilde{x}$ \ $\tilde{y}$	0	0.050	0.100	0.150	0.200
0.425	.000	.000	.000	.000	.000
.475	.000	.014	.020	.011	.000

Table 70. - Dimensionless x-Directional Total Plastic Strain $\frac{E\epsilon_x^p}{\sigma_0}$ at Location $(\tilde{x},\tilde{y})$ for a Specimen With a 10^o Edge Notch Subjected to Pure Bending; Plane Strain, $\tilde{q} = 0.50$, $\tilde{a} = 0.5$, $\alpha = 10^o$, $m = 0.05$, $\mu = 0.33$

$\tilde{x}$ \ $\tilde{y}$	0	0.008	0.016	0.024	0.032	0.060	0.084	0.132
-0.056		.000	.000	.000	.000	.000	.000	.000
-.028		.000	.307	1.333	.884	-.622	-.157	.000
-.012		8.259	2.912	-2.168	-4.259	-2.691	-.682	.000
.002	1.414	-42.038	-26.057	-18.546	-13.623	-3.895	-.614	.000
.006	.610	-27.678	-26.095	-19.444	-14.315	-3.802	-.457	.000
.012	.288	-5.615	-15.435	-15.467	-12.428	-3.295	-.179	.000
.028	.000	.092	-.072	-1.406	-2.225	-.527	.000	.000
.036	.000	.000	.000	-.059	-.302	.000	.000	.000
.044	.000	.000	.000	.000	.000	.000	.000	.000

$\tilde{x}$ \ $\tilde{y}$	0	0.050	0.100	0.150	0.200	0.250	0.300
0.375	.000	.000	.000	.000	.000	.000	.000
.425	.587	.416	.011	.000	.000	.000	.000
.475	4.006	3.911	3.604	2.700	1.178	.124	.000

Table 7a. - Dimensionless y-Directional Total Plastic Strain $\frac{E\epsilon_y^p}{\sigma_0}$ at Location $(\tilde{x},\tilde{y})$ for a Specimen With a 10^o Edge Notch Subjected to Pure Bending; Plane Strain, $\tilde{q} = 0.50$, $\tilde{a} = 0.5$, $\alpha = 10^o$, $m = 0.05$, $\mu = 0.33$

$\tilde{x}$ \ $\tilde{y}$	0	0.008	0.016	0.024	0.032	0.060	0.084	0.132
-0.056		.000	.000	.000	.000	.000	.000	.000
-.028		.000	-.241	-1.131	-.650	.828	.227	.000
-.012		-7.905	-2.483	2.585	4.650	2.975	.817	.000
.002	.740	43.255	26.843	19.140	14.110	4.203	.737	.000
.006	.282	28.890	26.914	20.060	14.813	4.105	.560	.000
.012	.074	6.649	16.239	16.075	12.924	3.583	.233	.000
.028	.000	.000	.399	1.821	2.599	.656	.000	.000
.036	.000	.000	.000	.185	.470	.000	.000	.000
.044	.000	.000	.000	.000	.000	.000	.000	.000

$\tilde{x}$ \ $\tilde{y}$	0	0.050	0.100	0.150	0.200	0.250	0.300
0.375	.000	.000	.000	.000	.000	.000	.000
.425	-.663	-.478	-.013	.000	.000	.000	.000
.475	-4.220	-4.124	-3.813	-2.893	-1.304	-.150	.000

Table 72. - Dimensionless Total Plastic Shear Strain $\frac{E\epsilon^p_{xy}}{\sigma_0}$ at Location $(\tilde{x},\tilde{y})$ for a Specimen With a 10° Edge Notch Subjected to Pure Bending; Plane Strain, $\tilde{q} = 0.50$, $\tilde{a} = 0.5$, $\alpha = 10^\circ$, $m = 0.05$, $\mu = 0.33$

$\tilde{x}$ \ $\tilde{y}$	0	0.008	0.016	0.024	0.032	0.060	0.084	0.132
-0.056		.000	.000	.000	.000	.000	.000	.000
-.028		.000	-.316	-2.804	-4.018	-2.470	-.345	.000
-.012		-9.863	-17.708	-16.122	-12.747	-3.539	-.710	.000
.002	.000	-17.199	-16.991	-13.426	-9.867	-2.357	-.352	.000
.006	.000	7.209	-5.397	-7.518	-6.653	-1.766	-.217	.000
.012	.000	7.068	4.519	-.004	-1.883	-.919	-.061	.000
.028	.000	.093	.881	1.815	1.488	.072	.000	.000
.036	.000	.000	.000	.266	.420	.000	.000	.000
.044	.000	.000	.000	.000	.000	.000	.000	.000

$\tilde{x}$ \ $\tilde{y}$	0	0.050	0.100	0.150	0.200	0.250	0.300
0.375	.000	.000	.000	.000	.000	.000	.000
.425	.000	.030	.002	.000	.000	.000	.000
.475	.000	.119	.199	.183	.078	.011	.000

Table 73. - Dimensionless x-Directional Total Plastic Strain $\frac{E\varepsilon_x^p}{\sigma_0}$ at Location $(\tilde{x},\tilde{y})$ for a Specimen With a 10^o Edge Notch Subjected to Pure Bending; Plane Strain, $\tilde{q} = 0.70$, $\tilde{a} = 0.5$, $\alpha = 10^o$, $m = 0.05$, $\mu = 0.33$

$\tilde{x}$ \ $\tilde{y}$	0	0.008	0.016	0.024	0.032	0.060	0.084	0.132
-0.056		.000	.000	.000	.000	.457	-.144	-.234
-.028		.000	5.391	4.977	2.602	-3.441	-3.845	-1.384
-.012		16.475	5.153	-4.622	-9.315	-9.734	-6.897	-1.838
.002	2.128	-65.211	-42.914	-32.963	-26.551	-14.030	-8.394	-1.707
.006	1.096	-45.114	-44.188	-35.018	-28.207	-14.380	-8.430	-1.573
.012	.716	-12.594	-29.027	-29.741	-26.039	-14.048	-8.117	-1.332
.028	1.626	1.597	-1.078	-6.310	-9.505	-8.996	-5.678	-.472
.036	.498	1.171	.658	-1.722	-4.209	-6.038	-4.227	-.154
.044	.165	.560	.649	-.084	-1.483	-3.546	-2.735	.000
.056	.000	.000	.144	.189	-.017	-1.083	-.781	.000

$\tilde{x}$ \ $\tilde{y}$	0	0.050	0.100	0.150	0.200	0.250	0.300	0.350
0.375	2.934	2.507	1.682	.798	.246	.000	.000	.000
.425	6.746	6.539	5.706	4.386	3.144	2.420	1.133	.027
.475	12.228	11.913	11.360	10.120	7.951	6.181	3.764	2.182

Table 74. - Dimensionless y-Directional Total Plastic Strain $\frac{E\varepsilon_y^p}{\sigma_0}$ at Location $(\tilde{x},\tilde{y})$ for a Specimen With a 10^o Edge Notch Subjected to Pure Bending; Plane Strain, $\tilde{q} = 0.70$, $\tilde{a} = 0.5$, $\alpha = 10^o$, $m = 0.05$, $\mu = 0.33$

$\tilde{x}$ \ $\tilde{y}$	0	0.008	0.016	0.024	0.032	0.060	0.084	0.132
-0.056		.000	.000	.000	.000	-.284	.318	.314
-.028		.000	-5.110	-4.641	-2.241	3.787	4.143	1.560
-.012		-15.960	-4.526	5.227	9.874	10.154	7.233	2.034
.002	1.300	66.963	44.062	33.836	27.255	14.484	8.746	1.897
.006	.582	46.890	45.390	35.920	28.929	14.834	8.781	1.757
.012	.221	14.076	30.220	30.629	26.762	14.497	8.462	1.503
.028	-.901	-.769	1.913	7.040	10.130	9.408	5.994	.562
.036	-.222	-.601	.009	2.356	4.775	6.425	4.520	.193
.044	-.068	-.260	-.191	.606	1.982	3.902	2.998	.000
.056	.000	.000	-.037	.033	.306	1.346	.948	.000

$\tilde{x}$ \ $\tilde{y}$	0	0.050	0.100	0.150	0.200	0.250	0.300	0.350
0.375	-3.086	-2.653	-1.813	-.887	-.290	.000	.000	.000
.425	-6.977	-6.775	-5.940	-4.611	-3.348	-2.597	-1.256	-.033
.475	-12.539	-12.223	-11.670	-10.425	-8.241	-6.427	-3.971	-2.352

Table 75. - Dimensionless Total Plastic Shear Strain $\frac{E\epsilon^{p}_{xy}}{\sigma_0}$ at Location $(\tilde{x},\tilde{y})$ for a Specimen With a 10^{o} Edge Notch Subjected to Pure Bending; Plane Strain, $\tilde{q} = 0.70$, $\tilde{a} = 0.5$, $\alpha = 10^{o}$, $m = 0.05$, $\mu = 0.33$

$\tilde{x}$ \ $\tilde{y}$	0	0.008	0.016	0.024	0.032	0.060	0.084	0.132
-0.056		.000	.000	.000	.000	-2.063	-2.063	-.546
-.028		.000	-5.681	-10.765	-13.456	-10.975	-6.635	-1.474
-.012		-19.571	-32.549	-30.593	-25.708	-11.809	-6.336	-1.277
.002	.000	-27.702	-28.244	-23.145	-18.287	-7.955	-4.203	-.768
.006	.000	10.644	-9.485	-12.994	-12.359	-6.261	-3.420	-.611
.012	.000	14.751	8.408	.350	-3.331	-3.633	-2.246	-.401
.028	.000	2.164	6.467	7.934	6.456	1.340	.093	-.042
.036	.000	.951	3.198	5.240	5.442	2.084	.642	.003
.044	.000	.330	1.272	2.783	3.592	2.001	.800	.000
.056	.000	.000	.156	.523	.994	1.106	.422	.000

$\tilde{x}$ \ $\tilde{y}$	0	0.050	0.100	0.150	0.200	0.250	0.300	0.350
0.375	.000	.290	.414	.302	.125	.000	.000	.000
.425	.000	.442	.759	.867	.837	.736	.329	.008
.475	.000	.387	.628	.668	.502	.500	.293	.195

Table 76. - Dimensionless x-Directional Total Plastic Strain $\frac{E\varepsilon^p_x}{\sigma_0}$ at Location $(\tilde{x},\tilde{y})$ for a Specimen With a 10^o Edge Notch Subjected to Pure Bending; Plane Strain, $\tilde{q} = 0.40$, $\tilde{a} = 0.5$, $\alpha = 10^o$, $m = 0.10$, $\mu = 0.33$

$\tilde{x}$ \ $\tilde{y}$	0	0.008	0.016	0.024	0.032	0.044	0.060	0.084
-0.020		.000	.105	.189	.051	-.015	.000	.000
-.012		1.492	.810	-.139	-.425	-.277	.000	.000
.002	.724	-11.228	-6.075	-3.757	-2.310	-.919	-.026	.000
.006	.187	-6.866	-5.885	-3.897	-2.402	-.930	.000	.000
.012	.000	-.741	-2.962	-2.776	-1.878	-.722	.000	.000
.020	.000	.000	-.214	-.675	-.663	-.233	.000	.000
.028	.000	.000	.000	.000	.000	.000	.000	.000

$\tilde{x}$ \ $\tilde{y}$	0	0.050	0.100	0.150	0.200
0.425	.000	.000	.000	.000	.000
.475	.258	.236	.174	.074	.000

Table 77. - Dimensionless y-Directional Total Plastic Strain $\frac{E\varepsilon_y^p}{\sigma_0}$ at Location $(\tilde{x},\tilde{y})$ for a Specimen With a 10^o Edge Notch Subjected to Pure Bending; Plane Strain, $\tilde{q} = 0.40$, $\tilde{a} = 0.5$, $\alpha = 10^o$, $m = 0.10$, $\mu = 0.33$

$\tilde{x}$ \ $\tilde{y}$	0	0.008	0.016	0.024	0.032	0.044	0.060	0.084
-0.020		.000	-.069	-.089	.045	.057	.000	.000
-.012		-1.298	-.557	.381	.637	.401	.000	.000
.002	.406	12.018	6.585	4.141	2.613	1.114	.038	.000
.006	.107	7.652	6.417	4.298	2.713	1.123	.000	.000
.012	.000	1.257	3.460	3.165	2.177	.889	.000	.000
.020	.000	.000	.395	.918	.858	.315	.000	.000
.028	.000	.000	.000	.000	.000	.000	.000	.000

$\tilde{x}$ \ $\tilde{y}$	0	0.050	0.100	0.150	0.200
0.425	.000	.000	.000	.000	.000
.475	-.304	-.280	-.209	-.090	.000

Table 78. - Dimensionless Total Plastic Shear Strain $\frac{E\epsilon^p_{xy}}{\sigma_0}$ at Location $(\tilde{x},\tilde{y})$ for a Specimen With a 10^o Edge Notch Subjected to Pure Bending; Plane Strain, $\tilde{q} = 0.40$, $\tilde{a} = 0.5$, $\alpha = 10^o$, $m = 0.10$, $\mu = 0.33$

$\tilde{x}$ \ $\tilde{y}$	0	0.008	0.016	0.024	0.032	0.044	0.060	0.084
-0.020		.000	-.157	-.660	-.592	-.182	.000	.000
-.012		-1.574	-3.488	-2.883	-1.924	-.719	.000	.000
.002	.000	-4.638	-4.119	-2.980	-1.924	-.792	-.024	.000
.006	.000	1.881	-1.270	-1.663	-1.292	-.589	.000	.000
.012	.000	1.040	.851	-.068	-.379	-.261	.000	.000
.020	.000	.000	.258	.307	.113	-.014	.000	.000
.028	.000	.000	.000	.000	.000	.000	.000	.000

$\tilde{x}$ \ $\tilde{y}$	0	0.050	0.100	0.150	0.200
0.425	.000	.000	.000	.000	.000
.475	.000	.008	.010	.005	.000

Table 79. - Dimensionless x-Directional Total Plastic Strain $\frac{E\varepsilon_x^p}{\sigma_0}$ at Location $(\tilde{x},\tilde{y})$ for a Specimen With a 10^o Edge Notch Subjected to Pure Bending; Plane Strain, $\tilde{q} = 0.50$, $\tilde{a} = 0.5$, $\alpha = 10^o$, $m = 0.10$, $\mu = 0.33$

$\tilde{x}$ \ $\tilde{y}$	0	0.008	0.016	0.024	0.032	0.060	0.084	0.132
-0.056		.000	.000	.000	.000	.000	.000	.000
-.028		.000	.000	.595	.443	-.213	-.054	.000
-.012		3.615	1.456	-.643	-1.505	-1.141	-.308	.000
.002	1.178	-17.730	-10.655	-7.386	-5.337	-1.668	-.355	.000
.006	.482	-11.578	-10.595	-7.747	-5.611	-1.624	-.310	.000
.012	.188	-2.166	-6.157	-6.105	-4.859	-1.448	-.195	.000
.028	.000	.000	-.023	-.521	-.928	-.440	.000	.000
.036	.000	.000	.000	-.005	-.009	-.050	.000	.000
.044	.000	.000	.000	.000	.000	.000	.000	.000

$\tilde{x}$ \ $\tilde{y}$	0	0.050	0.100	0.150	0.200	0.250	0.300
0.375	.000	.000	.000	.000	.000	.000	.000
.425	.352	.267	.045	.000	.000	.000	.000
.475	1.953	1.911	1.789	1.289	.622	.101	.000

Table 80. - Dimensionless y-Directional Total Plastic Strain $\frac{E\varepsilon_y^p}{\sigma_0}$ at Location $(\tilde{x},\tilde{y})$ for a Specimen With a 10^o Edge Notch Subjected to Pure Bending; Plane Strain, $\tilde{q} = 0.50$, $\tilde{a} = 0.5$, $\alpha = 10^o$, $m = 0.10$, $\mu = 0.33$

$\tilde{x}$ \ $\tilde{y}$	0	0.008	0.016	0.024	0.032	0.060	0.084	0.132
-0.056		.000	.000	.000	.000	.000	.000	.000
-.028		.000	.000	-.460	-.280	.347	.086	.000
-.012		-3.309	-1.080	1.012	1.847	1.342	.395	.000
.002	.683	18.810	11.358	7.922	5.777	1.890	.442	.000
.006	.246	12.658	11.330	8.307	6.064	1.841	.388	.000
.012	.060	3.033	6.869	6.661	5.310	1.653	.249	.000
.028	.000	.000	.181	.794	1.195	.557	.000	.000
.036	.000	.000	.000	.022	.170	.073	.000	.000
.044	.000	.000	.000	.000	.000	.000	.000	.000

$\tilde{x}$ \ $\tilde{y}$	0	0.050	0.100	0.150	0.200	0.250	0.300
0.375	.000	.000	.000	.000	.000	.000	.000
.425	-.407	-.312	-.055	.000	.000	.000	.000
.475	-2.119	-2.075	-1.948	-1.426	-.714	-.122	.000

Table 81. - Dimensionless Total Plastic Shear Strain $\frac{E\epsilon^p_{xy}}{\sigma_0}$ at Location $(\tilde{x},\tilde{y})$ for a Specimen With a 10^o Edge Notch Subjected to Pure Bending; Plane Strain, $\tilde{q} = 0.50$, $\tilde{a} = 0.5$, $\alpha = 10^o$, $m = 0.10$, $\mu = 0.33$

$\tilde{x}$ \ $\tilde{y}$	0	0.008	0.016	0.024	0.032	0.060	0.084	0.132
-0.056		.000	.000	.000	.000	.000	.000	.000
-.028		.000	.000	-1.120	-1.665	-1.045	-.134	.000
-.012		-4.180	-7.576	-6.783	-5.309	-1.688	-.362	.000
.002	.000	-7.351	-7.107	-5.594	-4.139	-1.181	-.236	.000
.006	.000	3.060	-2.246	-3.141	-2.797	-.908	-.172	.000
.012	.000	2.868	1.799	-.059	-.833	-.522	-.080	.000
.028	.000	.000	.249	.647	.594	.039	.000	.000
.036	.000	.000	.000	.023	.126	.016	.000	.000
.044	.000	.000	.000	.000	.000	.000	.000	.000

$\tilde{x}$ \ $\tilde{y}$	0	0.050	0.100	0.150	0.200	0.250	0.300
0.375	.000	.000	.000	.000	.000	.000	.000
.425	.000	.020	.007	.000	.000	.000	.000
.475	.000	.060	.101	.090	.043	.009	.000

Table 82. - Dimensionless x-Directional Total Plastic Strain $\frac{E\varepsilon_x^p}{\sigma_0}$ at Location $(\tilde{x},\tilde{y})$ for a Specimen With a 10^o Edge Notch Subjected to Pure Bending; Plane Strain, $\tilde{q} = 0.70$, $\tilde{a} = 0.5$, $\alpha = 10^o$, $m = 0.10$, $\mu = 0.33$

$\tilde{x}$ \ $\tilde{y}$	0	0.008	0.016	0.024	0.032	0.060	0.084	0.132
-0.056		.000	.000	.000	.000	.295	-.067	-.151
-.028		.000	2.411	2.520	1.485	-1.355	-1.639	-.631
-.012		7.525	2.795	-1.467	-3.552	-4.177	-3.032	-.844
.002	1.919	-28.978	-18.845	-14.253	-11.387	-6.146	-3.831	-.860
.006	.988	-19.855	-19.374	-15.258	-12.204	-6.322	-3.910	-.835
.012	.622	-5.234	-12.673	-13.024	-11.382	-6.261	-3.866	-.790
.028	.585	.606	-.471	-2.842	-4.358	-4.350	-3.070	-.498
.036	.179	.175	.264	-.746	-1.916	-3.056	-2.411	-.303
.044	.156	.203	.169	-.052	-.706	-2.021	-1.729	-.121
.056	.000	.000	.073	.096	-.058	-.931	-.965	.000

$\tilde{x}$ \ $\tilde{y}$	0	0.050	0.100	0.150	0.200	0.250	0.300	0.350
0.325	.877	.424	.037	.000	.000	.000	.000	.000
.375	.980	.986	.872	.590	.191	.000	.000	.000
.425	2.490	2.557	2.344	1.929	1.405	1.080	.575	.000
.475	5.206	5.008	4.885	4.386	3.494	2.718	1.724	1.020

Table 83. - Dimensionless y-Directional Total Plastic Strain $\frac{E\varepsilon_y^p}{\sigma_0}$ at Location $(\tilde{x},\tilde{y})$ for a Specimen With a 10^o Edge Notch Subjected to Pure Bending; Plane Strain, $\tilde{q} = 0.70$, $\tilde{a} = 0.5$, $\alpha = 10^o$, $m = 0.10$, $\mu = 0.33$

$\tilde{x}$ \ $\tilde{y}$	0	0.008	0.016	0.024	0.032	0.060	0.084	0.132
-0.056		.000	.000	.000	.000	-1.184	-1.224	-.355
-.028		.000	-2.181	-2.214	-1.152	1.663	1.887	.744
-.012		-7.060	-2.220	2.031	4.077	4.557	3.321	.974
.002	1.173	30.584	19.908	15.069	12.056	6.563	4.133	.988
.006	.504	21.478	20.489	16.110	12.894	6.742	4.210	.962
.012	.198	6.611	13.778	13.873	12.078	6.679	4.162	.913
.028	-.185	-.076	1.192	3.525	4.957	4.732	3.340	.592
.036	-.046	-.021	.227	1.290	2.432	3.404	2.662	.371
.044	-.048	-.051	.041	.454	1.122	2.332	1.955	.154
.056	.000	.000	-.006	.067	.283	1.171	1.134	.000

$\tilde{x}$ \ $\tilde{y}$	0	0.050	0.100	0.150	0.200	0.250	0.300	0.350
0.325	-.960	-.469	-.043	.000	.000	.000	.000	.000
.375	-1.083	-1.086	-.963	-.664	-.227	.000	.000	.000
.425	-2.669	-2.749	-2.530	-2.100	-1.554	-1.199	-.655	.000
.475	-5.481	-5.282	-5.159	-4.654	-3.743	-2.921	-1.884	-1.135

Table 84. - Dimensionless Total Plastic Shear Strain $\frac{E\epsilon^p_{xy}}{\sigma_0}$ at Location $(\tilde{x},\tilde{y})$ for a Specimen With a 10^o Edge Notch Subjected to Pure Bending; Plane Strain, $\tilde{q} = 0.70$, $\tilde{a} = 0.5$, $\alpha = 10^o$, $m = 0.10$, $\mu = 0.33$

$\tilde{x}$ \ $\tilde{y}$	0	0.008	0.016	0.024	0.032	0.060	0.084	0.132
-0.056		.000	.000	.000	.000	-1.184	-1.224	-.355
-.028		.000	-2.376	-4.865	-6.090	-5.014	-2.997	-.706
-.012		-8.688	-14.733	-13.867	-11.662	-5.653	-2.964	-.625
.002	.000	-12.502	-12.826	-10.642	-8.510	-3.990	-2.087	-.422
.006	.000	4.782	-4.376	-6.097	-5.840	-3.210	-1.744	-.357
.012	.000	6.386	3.550	-.086	-1.772	-1.987	-1.206	-.266
.028	.000	.735	2.561	3.389	2.812	.531	-.017	-.059
.036	.000	.133	1.212	2.246	2.451	1.044	.315	-.005
.044	.000	.127	.358	1.269	1.713	1.147	.462	.011
.056	.000	.000	.085	.337	.660	.890	.464	.000

$\tilde{x}$ \ $\tilde{y}$	0	0.050	0.100	0.150	0.200	0.250	0.300	0.350
0.325	.000	.072	.014	.000	.000	.000	.000	.000
.375	.000	.065	.173	.192	.086	.000	.000	.000
.425	.000	.156	.290	.358	.356	.314	.162	.000
.475	.000	.170	.260	.282	.224	.224	.137	.092

Table 85. - Dimensionless x-Directional Total Plastic Strain $\frac{E\varepsilon_x^p}{\sigma_0}$ at Location $(\tilde{x},\tilde{y})$ for a Specimen With a 3^o Edge Notch Subjected to Pure Bending; Plane Strain, $\tilde{q} = 0.50$, $\tilde{a} = 0.3$, $\alpha = 3^o$, $m = 0.10$, $\mu = 0.33$

$\tilde{x}$ \ $\tilde{y}$	0	0.008	0.016	0.024	0.032	0.044	0.060
-0.012		.237	.213	-.086	-.055	.000	.000
-.006		1.090	-.867	-.834	-.470	.000	.000
-.002		-3.159	-2.445	-1.501	-.770	-.001	.000
.002	.503	-7.137	-3.512	-1.961	-.961	-.056	.000
.006	.021	-3.797	-3.212	-1.938	-.963	-.060	.000
.012	.000	-.101	-1.186	-1.122	-.591	.000	.000
.020	.000	.000	.000	-.010	.000	.000	.000

Table 86. - Dimensionless y-Directional Total Plastic Strain $\frac{E\varepsilon_y^p}{\sigma_0}$ at Location $(\tilde{x},\tilde{y})$ for a Specimen With a 3^o Edge Notch Subjected to Pure Bending; Plane Strain, $\tilde{q} = 0.50$, $\tilde{a} = 0.3$, $\alpha = 3^o$, $m = 0.10$, $\mu = 0.33$

$\tilde{x}$ \ $\tilde{y}$	0	0.008	0.016	0.024	0.032	0.044	0.060
-0.012		-.181	-.091	.179	.091	.000	.000
-.006		-.810	1.092	.998	.579	.000	.000
-.002		3.601	2.730	1.698	.902	.002	.000
.002	.190	7.692	3.838	2.180	1.105	.736	.000
.006	.009	4.320	3.546	2.165	1.110	.784	.000
.012	.000	.249	1.452	1.319	.712	.000	.000
.020	.000	.000	.000	.017	.000	.000	.000

Table 87. - Dimensionless Total Plastic Shear Strain $\frac{E\epsilon^p_{xy}}{\sigma_0}$ at Location $(\tilde{x},\tilde{y})$ for a Specimen With a 3^o Edge Notch Subjected to Pure Bending; Plane Strain, $\tilde{q} = 0.50$, $\tilde{a} = 0.3$, $\alpha = 3^o$, $m = 0.10$, $\mu = 0.33$

$\tilde{x}$ \ $\tilde{y}$	0	0.008	0.016	0.024	0.032	0.044	0.060
-0.012		-.251	-1.200	-.753	-.195	.000	.000
-.006		-4.630	-3.210	-1.726	-.769	.000	.000
-.002		-7.377	-3.386	-1.810	-.856	-.001	.000
.002	.000	-2.690	-2.151	-1.400	-.724	-.046	.000
.006	.000	1.255	-.533	-.726	-.468	-.037	.000
.012	.000	.203	.411	.016	-.103	.000	.000
.020	.000	.000	.000	.005	.000	.000	.000

Table 88. - Dimensionless x-Directional Total Plastic Strain $\frac{E\varepsilon_x^p}{\quad}$ at Location $(\tilde{x},\tilde{y})$ for a Specimen With a 3^o Edge Notch Subjected to Pure Bending; Plane Strain, $\tilde{q} = 0.70$, $\tilde{a} = 0.3$, $\alpha = 3^o$, $m = 0.10$, $\mu = 0.33$

$\tilde{x}$ \ $\tilde{y}$	0	0.008	0.016	0.024	0.032	0.044	0.060	0.084
-0.028		.000	.000	.000	.076	-.048	-.068	.000
-.020		.000	.610	.281	-.191	-.509	-.438	.000
-.012		2.414	.664	-.952	-1.486	-1.410	-.927	-.070
-.006		2.222	-2.818	-3.425	-3.044	-2.115	-1.224	-.138
.002	1.019	-15.749	-9.434	-6.572	-4.700	-2.833	-1.421	-.167
.006	.330	-9.975	-9.190	-6.770	-4.875	-2.911	-1.408	-.142
.012	.054	-1.613	-5.125	-5.186	-4.135	-2.607	-1.241	-.056
.020	.000	.025	-.923	-2.094	-2.263	-1.719	-.829	.000
.028	.000	.000	-.002	-.322	-.671	-.721	-.341	.000
.036	.000	.000	.000	.000	.000	-.088	.000	.000

Table 89. - Dimensionless y-Directional Total Plastic Strain $\frac{E\varepsilon_y^p}{\sigma_0}$ at Location $(\tilde{x},\tilde{y})$ for a Specimen With a 3^o Edge Notch Subjected to Pure Bending; Plane Strain, $\tilde{q} = 0.70$, $\tilde{a} = 0.3$, $\alpha = 3^o$, $m = 0.10$, $\mu = 0.33$

$\tilde{x}$ \ $\tilde{y}$	0	0.008	0.016	0.024	0.032	0.044	0.060	0.084
-0.028		.000	.000	.000	-.014	.122	.106	.000
-.020		.000	-.484	-.117	.356	.654	.540	.000
-.012		-2.172	-.365	1.237	1.743	1.614	1.063	.914
-.006		-1.741	3.242	3.780	3.349	2.350	1.374	.174
.002	.471	16.669	10.014	7.002	5.046	3.092	1.582	.207
.006	.166	10.889	9.794	7.218	5.230	3.175	1.568	.177
.012	.020	2.310	5.706	5.631	4.489	2.863	1.393	.071
.020	.000	.049	1.307	2.461	2.570	1.947	.958	.000
.028	.000	.000	.017	.491	.856	.873	.421	.000
.036	.000	.000	.000	.000	.000	.127	.000	.000

Table 90. - Dimensionless Total Plastic Shear Strain $\frac{E\varepsilon^p_{xy}}{\sigma_0}$ at Location $(\tilde{x},\tilde{y})$ for a Specimen With a 3^o Edge Notch Subjected to Pure Bending; Plane Strain, $\tilde{q} = 0.70$, $\tilde{a} = 0.3$, $\alpha = 3^o$, $m = 0.10$, $\mu = 0.33$

$\tilde{x}$ \ $\tilde{y}$	0	0.008	0.016	0.024	0.032	0.044	0.060	0.084
-0.028		.000	.000	.000	-.421	-.557	-.221	.000
-.020		-1.224	-2.163	-2.124	-1.609	-.820	.000	.000
-.012		-3.059	-5.783	-5.036	-3.805	-2.310	-1.138	-.077
-.006		-11.557	-9.164	-6.331	-4.362	-2.383	-1.124	-.122
.002	.000	-5.990	-5.690	-4.467	-3.256	-1.904	-.885	-.111
.006	.000	2.941	-1.607	-2.443	-2.174	-1.450	-.709	-.082
.012	.000	2.185	1.595	.055	-.620	-.720	-.425	-.025
.020	.000	.079	1.046	.938	.411	-.035	-.129	.000
.028	.000	.000	.019	.356	.377	.166	.004	.000
.036	.000	.000	.000	.000	.000	.043	.000	.000

Table 91. - Dimensionless x-Directional Total Plastic Strain $\frac{E\varepsilon_x^p}{\sigma_0}$ at Location $(\tilde{x},\tilde{y})$ for a Specimen With a 3^o Edge Notch Subjected to Pure Bending; Plane Strain, $\tilde{q} = 0.90$, $\tilde{a} = 0.3$, $\alpha = 3^o$, $m = 0.10$, $\mu = 0.33$

$\tilde{x}$ \ $\tilde{y}$	0	0.008	0.016	0.024	0.032	0.060	0.084	0.132
-0.056		.000	.000	.000	.000	.004	-.054	.000
-.028		.000	1.305	1.443	.707	-1.500	-1.490	-.285
-.012		6.289	1.717	-1.973	-3.646	-4.056	-2.757	-.436
.002	1.844	-24.618	-16.095	-12.367	-9.973	-5.593	-3.377	-.408
.006	.884	-16.319	-16.136	-12.939	-10.468	-5.669	-3.411	-.367
.012	.521	-3.786	-10.102	-10.667	-9.471	-5.424	-3.298	-.288
.028	.383	.452	-.160	-1.863	-3.083	-3.310	-2.413	.000
.036	.112	.126	.208	-.342	-1.115	-2.064	-1.757	.000
.044	.000	.000	.099	.022	-.285	-1.156	-1.119	.000
.056	.000	.000	.000	.000	-.001	-.401	-.485	.000

$\tilde{x}$ \ $\tilde{y}$	0	0.050	0.100	0.150	0.200	0.250	0.300	0.350
0.575	.000	.000	.000	.000	.000	.000	.000	.000
.625	.296	.262	.171	.037	.000	.000	.000	.000
.675	1.418	1.386	1.299	1.146	.891	.634	.304	.094

Table 92. - Dimensionless y-Directional Total Plastic Strain $\frac{E\epsilon_y^p}{\sigma_0}$ at Location $(\tilde{x},\tilde{y})$ for a Specimen With a 3^o Edge Notch Subjected to Pure Bending; Plane Strain, $\tilde{q} = 0.90$, $\tilde{a} = 0.3$, $\alpha = 3^o$, $m = 0.10$, $\mu = 0.33$

$\tilde{x}$ \ $\tilde{y}$	0	0.008	0.016	0.024	0.032	0.060	0.084	0.132
-0.056		.000	.000	.000	.000	.010	.088	.000
-.028		.000	-1.141	-1.227	-.469	1.708	1.652	.337
-.012		-5.882	-1.239	2.424	4.055	4.329	2.951	.503
.002	.764	25.995	16.984	13.030	10.502	5.893	3.582	.471
.006	.322	17.697	17.066	13.629	11.011	5.972	3.613	.426
.012	.093	4.941	11.015	11.354	10.018	5.723	3.494	.337
.028	-.139	-.094	.686	2.381	3.534	3.571	2.581	.000
.036	-.038	-.029	.093	.708	1.468	2.288	1.907	.000
.044	.000	.000	.005	.175	.525	1.342	1.246	.000
.056	.000	.000	.000	.000	.034	.510	.566	.000

$\tilde{x}$ \ $\tilde{y}$	0	0.050	0.100	0.150	0.200	0.250	0.300	0.350
0.575	.000	.000	.000	.000	.000	.000	.000	.000
.625	-.349	-.310	-.205	-.046	.000	.000	.000	.000
.675	-1.569	-1.536	-1.444	-1.281	-1.004	-.720	-.356	-.115

Table 93. - Dimensionless Total Plastic Shear Strain $\frac{E\varepsilon^p_{xy}}{\sigma_0}$ at Location $(\tilde{x},\tilde{y})$ for a Specimen With a 3^o Edge Notch Subjected to Pure Bending; Plane Strain, $\tilde{q} = 0.90$, $\tilde{a} = 0.3$, $\alpha = 3^o$, $m = 0.10$, $\mu = 0.33$

$\tilde{x}$ \ $\tilde{y}$	0	0.008	0.016	0.024	0.032	0.060	0.084	0.132
-0.056		.000	.000	.000	.000	-.086	-.224	.000
-.028		.000	-1.427	-3.325	-4.412	-3.743	-2.092	-.270
-.012		-7.265	-12.017	-11.188	-9.334	-4.587	-2.285	-.295
.002	.000	-9.886	-10.078	-8.399	-6.724	-3.204	-1.650	-.199
.006	.000	4.526	-3.028	-4.598	-4.474	-2.577	-1.383	-.161
.012	.000	5.159	3.231	.285	-1.168	-1.583	-.957	-.107
.028	.000	.169	.644	.814	.683	.125	-.047	.000
.036	.000	.091	.677	1.335	1.560	.670	.136	.000
.044	.000	.000	.172	.504	.810	.617	.201	.000
.056	.000	.000	.000	.000	.070	.337	.158	.000

$\tilde{x}$ \ $\tilde{y}$	0	0.050	0.100	0.150	0.200	0.250	0.300	0.350
0.575	.000	.000	.000	.000	.000	.000	.000	.000
.625	.000	.005	.006	.002	.000	.000	.000	.000
.675	.000	.003	.004	.000	-.008	-.004	-.005	-.002

Table 94. - Dimensionless x-Directional Total Plastic Strain $\frac{E\varepsilon_x^p}{\sigma_0}$ at Location $(\tilde{x},\tilde{y})$ for a Specimen With a 10^o Edge Notch Subjected to Pure Bending; Plane Strain, $\tilde{q} = 0.50$, $\tilde{a} = 0.3$, $\alpha = 10^o$, $m = 0.10$, $\mu = 0.33$

$\tilde{x}$ \ $\tilde{y}$	0	0.008	0.016	0.024	0.032	0.044	0.060
-0.012		.286	.223	-.094	-.076	.000	.000
-.006		1.120	-.852	-.849	-.508	.000	.000
-.002		-3.075	-2.426	-1.519	-.815	-.058	.000
.002	.512	-7.100	-3.508	-1.987	-1.011	-.124	.000
.006	.035	-3.849	-3.236	-1.977	-1.017	-.136	.000
.012	.000	-.127	-1.243	-1.179	-.651	-.025	.000
.020	.000	.000	.000	-.050	-.045	.000	.000

Table 95. - Dimensionless y-Directional Total Plastic Strain $\frac{E\epsilon_y^p}{\sigma_0}$ at Location $(\tilde{x},\tilde{y})$ for a Specimen With a 10^o Edge Notch Subjected to Pure Bending; Plane Strain, $\tilde{q} = 0.50$, $\tilde{a} = 0.3$, $\alpha = 10^o$, $m = 0.10$, $\mu = 0.33$

$\tilde{x}$ \ $\tilde{y}$	0	0.008	0.016	0.024	0.032	0.044	0.060
-0.012		-.220	-.096	.192	.123	.000	.000
-.006		-.834	1.083	1.018	.622	.000	.000
-.002		3.525	2.717	1.721	.952	.077	.000
.002	.223	7.666	3.841	2.211	1.161	.159	.000
.006	.016	4.385	3.577	2.209	1.169	.173	.000
.012	.000	.301	1.519	1.384	.779	.032	.000
.020	.000	.000	.000	.077	.063	.000	.000

Table 96. - Dimensionless Total Plastic Shear Strain $\frac{E\epsilon^{p}_{xy}}{\sigma_0}$ at Location $(\tilde{x},\tilde{y})$ for a Specimen With a 10^{o} Edge Notch Subjected to Pure Bending; Plane Strain, $\tilde{q} = 0.50$, $\tilde{a} = 0.3$, $\alpha = 10^{o}$, $m = 0.10$, $\mu = 0.33$

$\tilde{x}$ \ $\tilde{y}$	0	0.008	0.016	0.024	0.032	0.044	0.060
-0.012		-.302	-1.237	-.806	-.261	.000	.000
-.006		-4.617	-3.222	-1.764	-.825	.000	.000
-.002		-7.375	-3.403	-1.843	-.905	-.060	.000
.002	.000	-2.769	-2.181	-1.429	-.766	-.098	.000
.006	.000	1.221	-.559	-.748	-.499	-.081	.000
.012	.000	.244	.423	.015	-.113	-.009	.000
.020	.000	.000	.000	.025	.008	.000	.000

Table 97. - Dimensionless x-Directional Total Plastic Strain $\frac{E\varepsilon_x^p}{\sigma_0}$ at Location $(\tilde{x},\tilde{y})$ for a Specimen With a 10^o Edge Notch Subjected to Pure Bending; Plane Strain, $\tilde{q} = 0.70$, $\tilde{a} = 0.3$, $\alpha = 10^o$, $m = 0.10$, $\mu = 0.33$

$\tilde{x}$ \ $\tilde{y}$	0	0.008	0.016	0.024	0.032	0.044	0.060	0.084
-0.036		.000	.000	.000	.000	.019	-.048	.000
-.028		.000	.000	.331	.213	-.157	-.352	-.117
-.012		3.370	.965	-1.066	-1.860	-1.953	-1.473	-.622
-.006		2.770	-2.993	-3.848	-3.625	-2.840	-1.843	-.771
.002	1.178	-16.666	-10.188	-7.302	-5.463	-3.644	-2.079	-.846
.006	.463	-10.734	-9.938	-7.514	-5.649	-3.708	-2.038	-.809
.012	.165	-1.846	-5.619	-5.781	-4.817	-3.324	-1.779	-.666
.020	.000	.095	-1.065	-2.406	-2.720	-2.307	-1.288	-.380
.028	.000	.000	-.005	-.393	-.827	-1.022	-.633	-.060
.036	.000	.000	.000	.000	-.067	-.231	-.128	.000

$\tilde{x}$ \ $\tilde{y}$	0	0.050	0.100
0.625	.000	.000	.000
.675	.055	.038	.000

Table 98. - Dimensionless y-Directional Total Plastic Strain $\frac{E\varepsilon_y^p}{}$ at Location $(\tilde{x},\tilde{y})$ for a Specimen With a 10^o Edge Notch Subjected to Pure Bending; Plane Strain, $\tilde{q} = 0.70$, $\tilde{a} = 0.3$, $\alpha = 10^o$, $m = 0.10$, $\mu = 0.33$

$\tilde{x}$ \ $\tilde{y}$	0	0.008	0.016	0.024	0.032	0.044	0.060	0.084
-0.036		.000	.000	.000	.000	.021	.087	.000
-.028		.000	.000	-.236	-.092	.279	.450	.150
-.012		-3.082	-.624	1.387	2.147	2.186	1.634	.708
-.006		-2.233	3.471	4.241	3.960	3.103	2.021	.865
.002	.572	17.670	10.826	7.775	5.841	3.929	2.268	.942
.006	.198	11.731	10.601	8.007	6.036	3.998	2.224	.902
.012	.040	2.628	6.256	6.268	5.204	3.607	1.950	.749
.020	.000	.109	1.512	2.816	3.061	2.561	1.437	.439
.028	.000	.000	.114	.609	1.051	1.200	.741	.073
.036	.000	.000	.000	.000	.121	.313	.166	.000

$\tilde{x}$ \ $\tilde{y}$	0	0.050	0.100
0.625	.000	.000	.000
.675	-.068	-.047	.000

Table 99. - Dimensionless Total Plastic Shear Strain $\frac{E\epsilon^{p}_{xy}}{\sigma_0}$ at Location $(\tilde{x},\tilde{y})$ for a Specimen With a 10^{o} Edge Notch Subjected to Pure Bending; Plane Strain, $\tilde{q} = 0.70$, $\tilde{a} = 0.3$, $\alpha = 10^{o}$, $m = 0.10$, $\mu = 0.33$

$\tilde{x}$ \ $\tilde{y}$	0	0.008	0.016	0.024	0.032	0.044	0.060	0.084
-0.036		.000	.000	.000	.000	-.257	-.255	.000
-.028		.000	.000	-.741	-1.285	-1.377	-.975	-.188
-.012		-3.985	-7.003	-6.157	-4.796	-3.157	-1.759	-.566
-.006		-12.985	-10.406	-7.322	-5.207	-3.160	-1.662	-.564
.002	.000	-6.688	-6.363	-5.065	-3.821	-2.437	-1.261	-.452
.006	.000	3.025	-1.852	-2.778	-2.570	-1.852	-.984	-.365
.012	.000	2.558	1.745	.041	-.751	-.926	-.552	-.226
.020	.000	.263	1.306	1.113	.513	-.018	-.129	-.079
.028	.000	.000	.178	.536	.532	.307	.061	-.053
.036	.000	.000	.000	.000	.097	.146	.037	.000

$\tilde{x}$ \ $\tilde{y}$	0	0.050	0.100
0.625	.000	.000	.000
.675	.000	.000	.000

Table 100. - Dimensionless x-Directional Total Plastic Strain $\frac{E\varepsilon^p_x}{\sigma_0}$ at Location $(\tilde{x},\tilde{y})$ for a Specimen With a 10^o Edge Notch Subjected to Pure Bending; Plane Strain, $\tilde{q} = 0.90$, $\tilde{a} = 0.3$, $\alpha = 10^o$, $m = 0.10$, $\mu = 0.33$

$\tilde{x}$ \ $\tilde{y}$	0	0.008	0.016	0.024	0.032	0.060	0.084	0.132
-0.056		.000	.000	.000	.000	.003	-.050	.000
-.028		.000	1.530	1.592	.751	-1.520	-1.653	-.208
-.012		6.442	1.946	-1.779	-3.555	-3.992	-2.987	-.390
.002	1.787	-24.803	-16.059	-12.286	-9.935	-5.600	-3.733	-.415
.006	.867	-16.684	-16.239	-12.948	-10.480	-5.690	-3.775	-.395
.012	.500	-3.894	-10.255	-10.771	-9.558	-5.455	-3.664	-.357
.028	.063	.527	-.144	-1.885	-3.205	-3.522	-2.653	-.127
.036	.000	.053	.258	-.354	-1.230	-2.347	-2.081	-.111
.044	.000	.000	.054	.032	-.390	-1.538	-1.408	.000
.056	.000	.000	.000	.000	-.012	-.575	-.473	.000

$\tilde{x}$ \ $\tilde{y}$	0	0.050	0.100	0.150	0.200	0.300	0.400	0.500
0.575	.000	.000	.000	.000	.000	.000	.000	.000
.625	.699	.666	.576	.431	.274	.012	.000	.000
.675	1.985	1.952	1.853	1.689	1.422	.776	.391	.010

Table 101. - Dimensionless y-Directional Total Plastic Strain $\frac{E\varepsilon_y^p}{\sigma_0}$ at Location $(\tilde{x},\tilde{y})$ for a Specimen With a 10^o Edge Notch Subjected to Pure Bending; Plane Strain, $\tilde{q} = 0.90$, $\tilde{a} = 0.3$, $\alpha = 10^o$, $m = 0.10$, $\mu = 0.33$

$\tilde{x}$ \ $\tilde{y}$	0	0.008	0.016	0.024	0.032	0.060	0.084	0.132
-0.056		.000	.000	.000	.000	.016	.077	.000
-.028		.000	-1.357	-1.358	-.507	1.722	1.805	.249
-.012		-6.028	-1.456	2.243	3.971	4.260	3.175	.452
.002	.885	26.204	16.967	12.963	10.472	5.901	3.933	.481
.006	.351	18.091	17.188	13.653	11.032	5.992	3.974	.459
.012	.112	5.075	11.186	11.470	10.112	5.753	3.861	.416
.028	-.017	-.144	.694	2.411	3.660	3.787	2.830	.154
.036	.000	-.011	.058	.733	1.597	2.584	2.245	.014
.044	.000	.000	.006	.197	.661	1.747	1.558	.000
.056	.000	.000	.000	.000	.066	.719	.558	.000

$\tilde{x}$ \ $\tilde{y}$	0	0.050	0.100	0.150	0.200	0.300	0.400	0.500
0.575	.000	.000	.000	.000	.000	.000	.000	.000
.625	-.792	-.757	-.660	-.501	-.325	-.015	.000	.000
.675	-2.165	-2.131	-2.027	-1.857	-1.577	-.877	-.458	-.012

Table 102. - Dimensionless Total Plastic Shear Strain $\frac{E\varepsilon^{p}_{xy}}{\sigma_0}$ at Location $(\tilde{x},\tilde{y})$ for a Specimen With a 10^{o} Edge Notch Subjected to Pure Bending; Plane Strain, $\tilde{q} = 0.90$, $\tilde{a} = 0.3$, $\alpha = 10^{o}$, $m = 0.10$, $\mu = 0.33$

$\tilde{x}$ \ $\tilde{y}$	0	0.008	0.016	0.024	0.032	0.060	0.084	0.132
-0.056		.000	.000	.000	.000	-.123	-.180	.000
-.028		.000	-1.476	-3.346	-4.304	-3.738	-2.226	-.207
-.012		-7.261	-12.033	-11.066	-9.158	-4.460	-2.408	-.282
.002	.000	-10.429	-10.300	-8.423	-6.666	-3.075	-1.735	-.222
.006	.000	4.381	-3.187	-4.634	-4.456	-2.426	-1.450	-.192
.012	.000	5.230	3.244	.302	-1.132	-1.397	-1.001	-.149
.028	.000	.562	1.989	2.677	2.326	.569	-.049	-.034
.036	.000	.037	.283	.638	.727	.331	.057	-.022
.044	.000	.000	.094	.655	1.096	.829	.252	.000
.056	.000	.000	.000	.000	.121	.457	.143	.000

$\tilde{x}$ \ $\tilde{y}$	0	0.050	0.100	0.150	0.200	0.300	0.400	0.500
0.575	.000	.000	.000	.000	.000	.000	.000	.000
.625	.000	.010	.017	.018	.015	.001	.000	.000
.675	.000	.003	.004	-.003	-.010	-.018	-.019	-.001

Table 103. - Dimensionless x-Directional Total Plastic Strain $\frac{E\varepsilon_x^p}{\sigma_0}$ at Location $(\tilde{x},\tilde{y})$ for a Specimen With a 10^o Edge Notch Subjected to Pure Bending; Plane Stress, $\tilde{q} = 0.50$, $\tilde{a} = 0.3$, $\alpha = 10^o$, $m = 0.10$, $\mu = 0.33$

$\tilde{x}$ \ $\tilde{y}$	0	0.013	0.024	0.036	0.048	0.060
-0.004		.159	.011	-.034	.000	.000
.002	6.627	-.971	-.311	-.186	-.074	.000
.006	2.411	-1.027	-.501	-.290	-.134	.000
.014	.954	-.401	-.577	-.424	-.236	-.025
.031	.384	.080	-.226	-.304	-.170	.000
.053	.000	.000	.000	.000	.000	.000

Table 104. - Dimensionless y-Directional Total Plastic Strain $\frac{E\varepsilon_y^p}{\sigma_0}$ at Location $(\tilde{x},\tilde{y})$ for a Specimen With a 10^o Edge Notch Subjected to Pure Bending; Plane Stress, $\tilde{q} = 0.50$, $\tilde{a} = 0.3$, $\alpha = 10^o$, $m = 0.10$, $\mu = 0.33$

$\tilde{x}$ \ $\tilde{y}$	0	0.013	0.024	0.036	0.048	0.060
-0.004		1.453	.923	.466	.000	.000
.002	9.770	4.273	2.021	1.031	.320	.000
.006	4.949	4.672	2.567	1.328	.516	.000
.014	3.187	4.105	2.962	1.707	.808	.762
.031	2.687	2.660	2.290	1.484	.615	.000
.053	.000	.000	.000	.000	.000	.000

Table 105. - Dimensionless Total Plastic Shear Strain $\frac{E\epsilon^p_{xy}}{\sigma_0}$ at Location $(\tilde{x},\tilde{y})$ for a Specimen With a 10^o Edge Notch Subjected to Pure Bending; Plane Stress, $\tilde{q} = 0.50$, $\tilde{a} = 0.3$, $\alpha = 10^o$, $m = 0.10$, $\mu = 0.33$

$\tilde{x}$ \ $\tilde{y}$	0	0.013	0.024	0.036	0.048	0.060
-0.004		-1.850	-.952	-.438	.000	.000
.002	.000	-2.033	-1.253	-.681	-.211	.000
.006	.000	-1.007	-1.113	-.688	-.280	.000
.014	.000	.029	-.536	-.502	-.285	-.029
.031	.000	.242	.164	.013	-.035	.000
.053	.000	.000	.000	.000	.000	.000

Table 106. - Dimensionless x-Directional Total Plastic Strain $\frac{E\epsilon^p_x}{\sigma_0}$ at Location $(\tilde{x},\tilde{y})$ for a Specimen With a 10^o Edge Notch Subjected to Pure Bending; Plane Stress, $\tilde{q} = 0.70$, $\tilde{a} = 0.3$, $\alpha = 10^o$, $m = 0.10$, $\mu = 0.33$

$\tilde{x}$ \ $\tilde{y}$	0	0.013	0.024	0.036	0.048	0.060	0.078	0.102
-0.024		.000	.053	.238	.091	-.014	-.040	.000
-.012		1.812	.959	.125	-.256	-.338	-.265	-.073
-.004		.700	-.256	-.713	-.831	-.748	-.492	-.171
.002	17.352	-2.936	-1.564	-1.436	-1.303	-1.071	-.660	-.232
.006	7.912	-2.902	-2.062	-1.779	-1.539	-1.239	-.756	-.266
.014	3.736	-.815	-1.958	-2.027	-1.781	-1.456	-.869	-.313
.031	1.551	.636	-.430	-1.156	-1.298	-1.162	-.736	-.266
.053	.860	.680	.374	.030	-.201	-.302	-.238	.000
.088	.000	.000	.000	.000	.000	.000	.000	.000

$\tilde{x}$ \ $\tilde{y}$	0	0.050	0.100	0.150	0.200	0.250	0.300	0.350
0.630	.035	.033	.000	.000	.000	.000	.000	.000
.650	.345	.317	.240	.139	.020	.000	.000	.000
.670	.645	.642	.580	.492	.334	.184	.000	.000
.690	1.080	1.080	1.015	.898	.761	.407	.120	.000

Table 107. - Dimensionless y-Directional Total Plastic Strain $\frac{E\varepsilon_y^p}{\sigma_0}$ at Location $(\tilde{x},\tilde{y})$ for a Specimen With a 10^o Edge Notch Subjected to Pure Bending; Plane Stress, $\tilde{q} = 0.70$, $\tilde{a} = 0.3$, $\alpha = 10^o$, $m = 0.10$, $\mu = 0.33$

$\tilde{x}$ \ $\tilde{y}$	0	0.013	0.024	0.036	0.048	0.060	0.078	0.102
-0.024		.000	.002	.247	.419	.417	.207	.000
-.012		.082	1.504	1.922	1.817	1.442	.869	.203
-.004		5.920	4.913	4.000	3.089	2.362	1.381	.437
.002	22.007	12.674	7.709	5.501	4.092	3.006	1.724	.574
.006	12.239	13.274	8.825	6.202	4.584	3.327	1.906	.644
.014	8.067	10.976	9.004	6.819	5.102	3.748	2.103	.735
.031	5.752	5.928	5.664	5.279	4.207	3.172	1.813	.616
.053	.966	1.046	1.241	1.341	1.337	1.194	.702	.000
.088	.000	.000	.000	.000	.000	.000	.000	.000

$\tilde{x}$ \ $\tilde{y}$	0	0.050	0.100	0.150	0.200	0.250	0.300	0.350
0.630	-.065	-.063	.000	.000	.000	.000	.000	.000
.650	-.654	-.602	-.473	-.289	-.043	.000	.000	.000
.670	-1.233	-1.229	-1.150	-1.021	-.711	-.372	.000	.000
.690	-2.088	-2.095	-2.019	-1.855	-1.605	-.814	-.237	.000

Table 108. - Dimensionless Total Plastic Shear Strain $\frac{E\varepsilon^p_{xy}}{\sigma_0}$ at Location $(\tilde{x},\tilde{y})$ for a Specimen With a 10^o Edge Notch Subjected to Pure Bending; Plane Stress, $\tilde{q} = 0.70$, $\tilde{a} = 0.3$, $\alpha = 10^o$, $m = 0.10$, $\mu = 0.33$

$\tilde{x}$ \ $\tilde{y}$	0	0.013	0.024	0.036	0.048	0.060	0.078	0.102
-0.024		.000	-.080	-.752	-.777	-.589	-.233	.000
-.012		-2.520	-3.382	-2.784	-2.050	-1.387	-.706	-.147
-.004		-7.516	-4.838	-3.459	-2.427	-1.703	-.896	-.263
.002	.000	-5.585	-4.310	-3.228	-2.371	-1.705	-.928	-.297
.006	.000	-2.256	-3.292	-2.761	-2.147	-1.586	-.896	-.299
.014	.000	.758	-1.051	-1.523	-1.447	-1.179	-.726	-.269
.031	.000	.910	.829	.438	.067	-.133	-.224	-.116
.053	.000	.365	.524	.503	.384	.236	.065	.000
.088	.000	.000	.000	.000	.000	.000	.000	.000

$\tilde{x}$ \ $\tilde{y}$	0	0.050	0.100	0.150	0.200	0.250	0.300	0.350
0.630	.000	.000	.000	.000	.000	.000	.000	.000
.650	.000	.002	.003	.003	.001	.000	.000	.000
.670	.000	.004	.008	.005	.002	.004	.000	.000
.690	.000	.009	.015	.001	-.035	-.037	.007	.000

Table 109. - Dimensionless x-Directional Total Plastic Strain $\frac{E\epsilon^p_x}{\sigma_0}$ at Location $(\tilde{x},\tilde{y})$ for a Specimen With a 10^o Edge Notch Subjected to Pure Bending; Plane Stress, $\tilde{q} = 0.90$, $\tilde{a} = 0.3$, $\alpha = 10^o$, $m = 0.10$, $\mu = 0.33$

$\tilde{x}$ \ $\tilde{y}$	0	0.013	0.024	0.036	0.060	0.102	0.132	0.186
-0.040		.000	.000	.000	.296	-.226	.000	.000
-.024		.000	1.947	1.374	-.067	-.688	-.516	-.034
-.012		4.399	2.150	.371	-1.024	-1.147	-.817	-.092
-.004		1.121	-.494	-1.352	-1.838	-1.447	-.985	-.121
.002	26.683	-4.952	-2.787	-2.629	-2.405	-1.616	-1.086	-.124
.006	12.948	-4.813	-3.598	-3.201	-2.691	-1.707	-1.134	-.122
.014	6.650	-1.224	-3.326	-3.559	-3.034	-1.826	-1.183	-.106
.031	3.173	1.500	-.484	-1.964	-2.527	-1.729	-1.051	.000
.053	2.616	2.137	1.260	.281	-.958	-1.070	-.590	.000
.088	.373	.368	.327	.248	.015	-.100	.000	.000

$\tilde{x}$ \ $\tilde{y}$	0	0.050	0.100	0.150	0.200	0.300	0.400	0.500
0.630	1.163	1.160	1.074	.954	.830	.561	.000	.000
.650	1.698	1.677	1.590	1.467	1.309	.959	.000	.000
.670	2.236	2.251	2.210	2.169	2.016	1.439	.856	.000
.690	2.938	2.957	2.944	2.915	2.811	1.980	1.456	.622

Table 110. - Dimensionless y-Directional Total Plastic Strain $\frac{E\epsilon_y^p}{\sigma_0}$ at Location $(\tilde{x},\tilde{y})$ for a Specimen With a 10^o Edge Notch Subjected to Pure Bending; Plane Stress, $\tilde{q} = 0.90$, $\tilde{a} = 0.3$, $\alpha = 10^o$, $m = 0.10$, $\mu = 0.33$

$\tilde{x}$ \ $\tilde{y}$	0	0.013	0.024	0.036	0.060	0.102	0.132	0.186
-0.040		.000	.000	.000	.227	.779	.000	.000
-.024		.000	.002	1.149	2.149	1.784	1.131	.069
-.012		.249	3.286	4.352	4.167	2.672	1.665	.183
-.004		10.289	9.036	7.747	5.668	3.225	1.951	.236
.002	32.583	20.852	13.422	10.076	6.673	3.534	2.116	.240
.006	18.787	21.679	15.100	11.147	7.167	3.688	2.190	.234
.014	12.782	17.848	15.172	12.035	7.782	3.874	2.250	.199
.031	9.090	9.428	9.474	9.588	6.975	3.656	1.985	.001
.053	2.589	2.878	3.462	3.960	3.998	2.370	1.147	.000
.088	.280	.316	.381	.478	.609	.280	.000	.000

$\tilde{x}$ \ $\tilde{y}$	0	0.050	0.100	0.150	0.200	0.300	0.400	0.500
0.630	-2.441	-2.396	-2.175	-1.847	-1.547	-1.063	.000	.000
.650	-3.500	-3.424	-3.217	-2.881	-2.466	-1.809	.000	.000
.670	-4.581	-4.567	-4.470	-4.312	-3.910	-2.727	-1.822	.000
.690	-5.970	-5.979	-5.940	-5.841	-5.554	-3.798	-3.048	-1.238

Table III. - Dimensionless Total Plastic Shear Strain $\frac{E\varepsilon^p_{xy}}{\sigma_0}$ at Location $(\tilde{x},\tilde{y})$ for a Specimen With a 10^o Edge Notch Subjected to Pure Bending; Plane Stress, $\tilde{q} = 0.90$, $\tilde{a} = 0.3$, $\alpha = 10^o$, $m = 0.10$, $\mu = 0.33$

$\tilde{x}$ \ $\tilde{y}$	0	0.013	0.024	0.036	0.060	0.102	0.132	0.186
-0.040		.000	.000	.000	-1.468	-.962	.000	.000
-.024		.000	-2.570	-3.666	-3.180	-1.667	-.864	-.043
-.012		-6.082	-7.238	-6.157	-3.907	-1.916	-1.053	-.099
-.004		-12.898	-8.697	-6.520	-3.936	-1.891	-1.066	-.115
.002	.000	-8.921	-7.219	-5.683	-3.624	-1.773	-1.025	-.109
.006	.000	-3.340	-5.306	-4.694	-3.259	-1.657	-.974	-.100
.014	.000	1.663	-1.389	-2.369	-2.305	-1.361	-.831	-.076
.031	.000	1.789	1.763	1.085	-.177	-.625	-.448	.000
.053	.000	1.090	1.569	1.606	.931	.074	-.075	.000
.088	.000	.114	.207	.290	.324	.078	.000	.000

$\tilde{x}$ \ $\tilde{y}$	0	0.050	0.100	0.150	0.200	0.300	0.400	0.500
0.630	.000	.037	.067	.081	.078	.033	.000	.000
.650	.000	.013	.026	.043	.064	.039	.000	.000
.670	.000	-.012	-.017	-.021	-.002	.021	-.026	.000
.690	.000	-.026	-.047	-.083	-.128	-.030	-.059	-.115

Table 112. - The Order of Stress Singularity n at the Tip of the Notch for a Specimen With a Single Edge Notch Subjected to Pure Bending; Plane Strain, $\mu = 0.33$

			$\tilde{q}$					
$\tilde{a}$	α	m	0.4	0.5	0.6	0.7	0.8	0.9
0.3	3^{o}	0.10		0.488	0.490	0.487	0.473	0.475
0.3	10^{o}	0.10		.496	.497	.492	.480	.487
0.5	10^{o}	0.05	0.499	.496	.480	.472		
0.5	10^{o}	0.10	.496	.498	.480	.478		

Table 113. - The Order of Stress Singularity n at the Tip of the Notch for a Specimen With a 10^{o} Edge Notch Subjected to Pure Bending; Plane Stress, $\tilde{a} = 0.3$, $\alpha = 10^{o}$, m = 0.10, $\mu = 0.33$

$\tilde{q}$	0.5	0.6	0.7	0.8	0.9
n	0.419	0.434	0.448	0.451	0.458

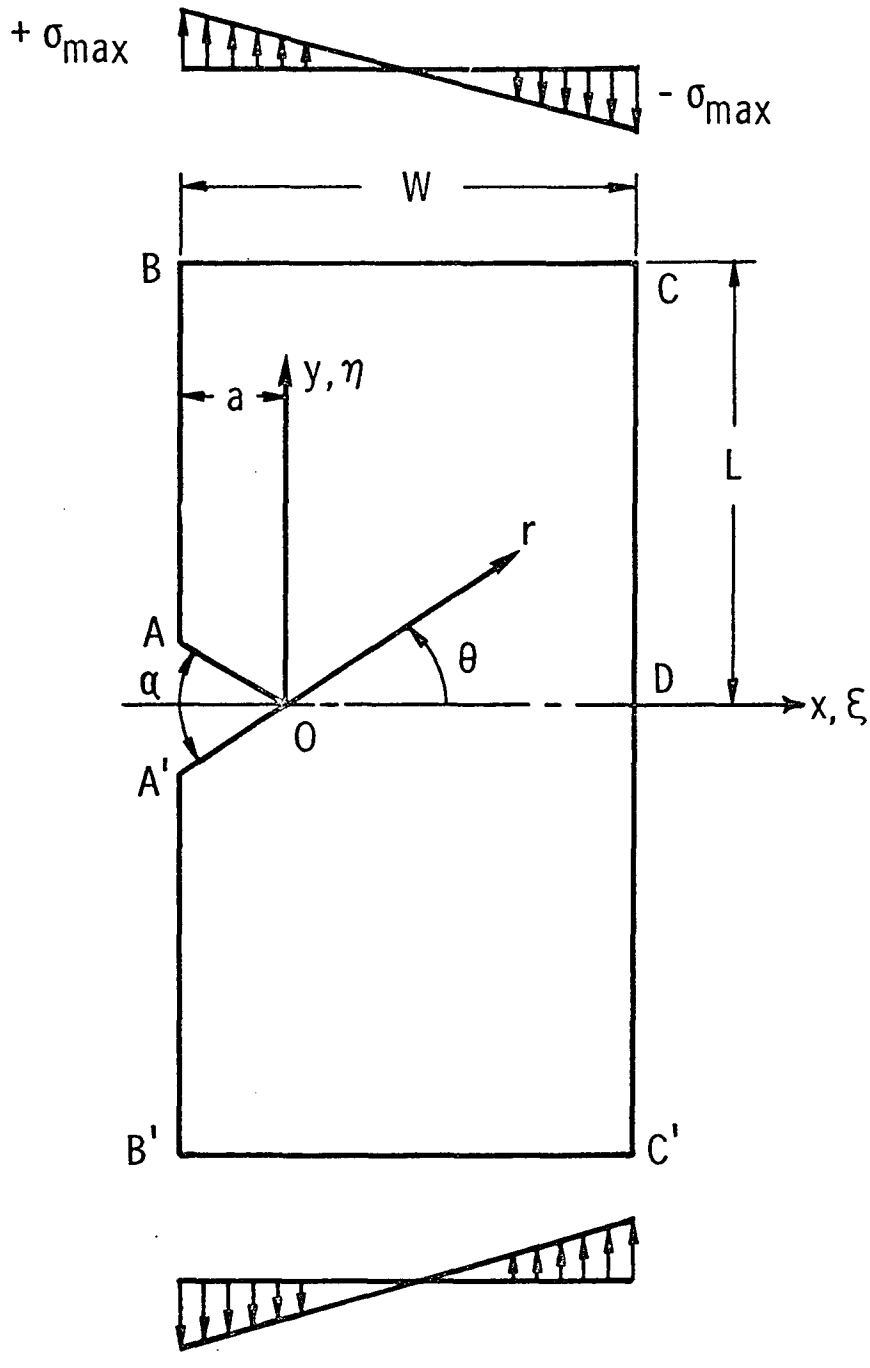

Fig. 1. Single edge V-notched plate subject to pure bending load.

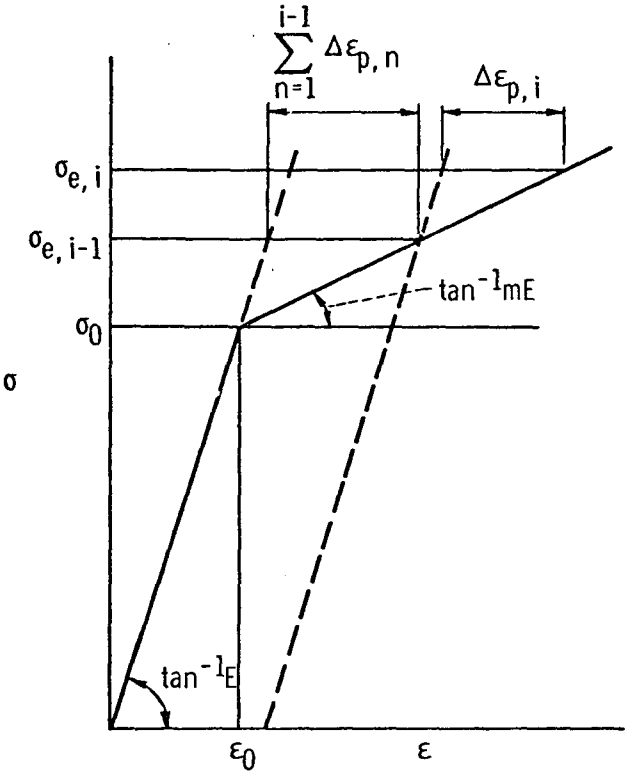

Fig. 2. Stress-strain curve for material with strain hardening parameter m.

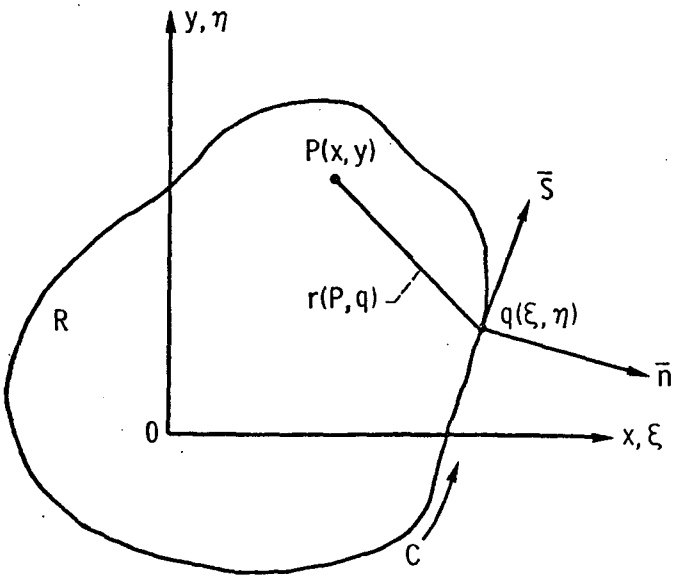

Fig. 3. Sign convention for a simply connected region R.

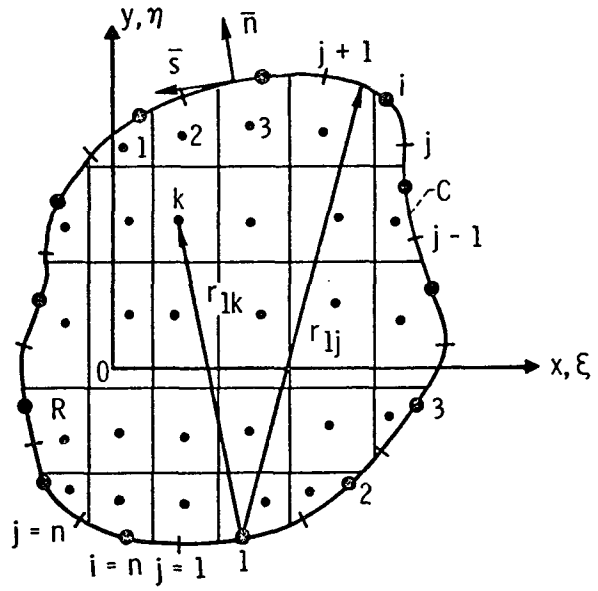

Fig. 4. Boundary and interior region subdivisions for $P(x,y) \subset C$.

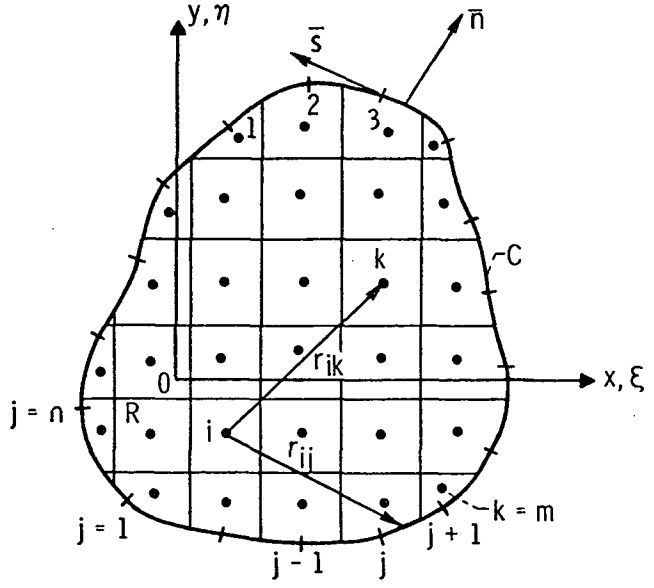

Fig. 5. Boundary and interior region subdivisions for $P(x,y) \subset R$.

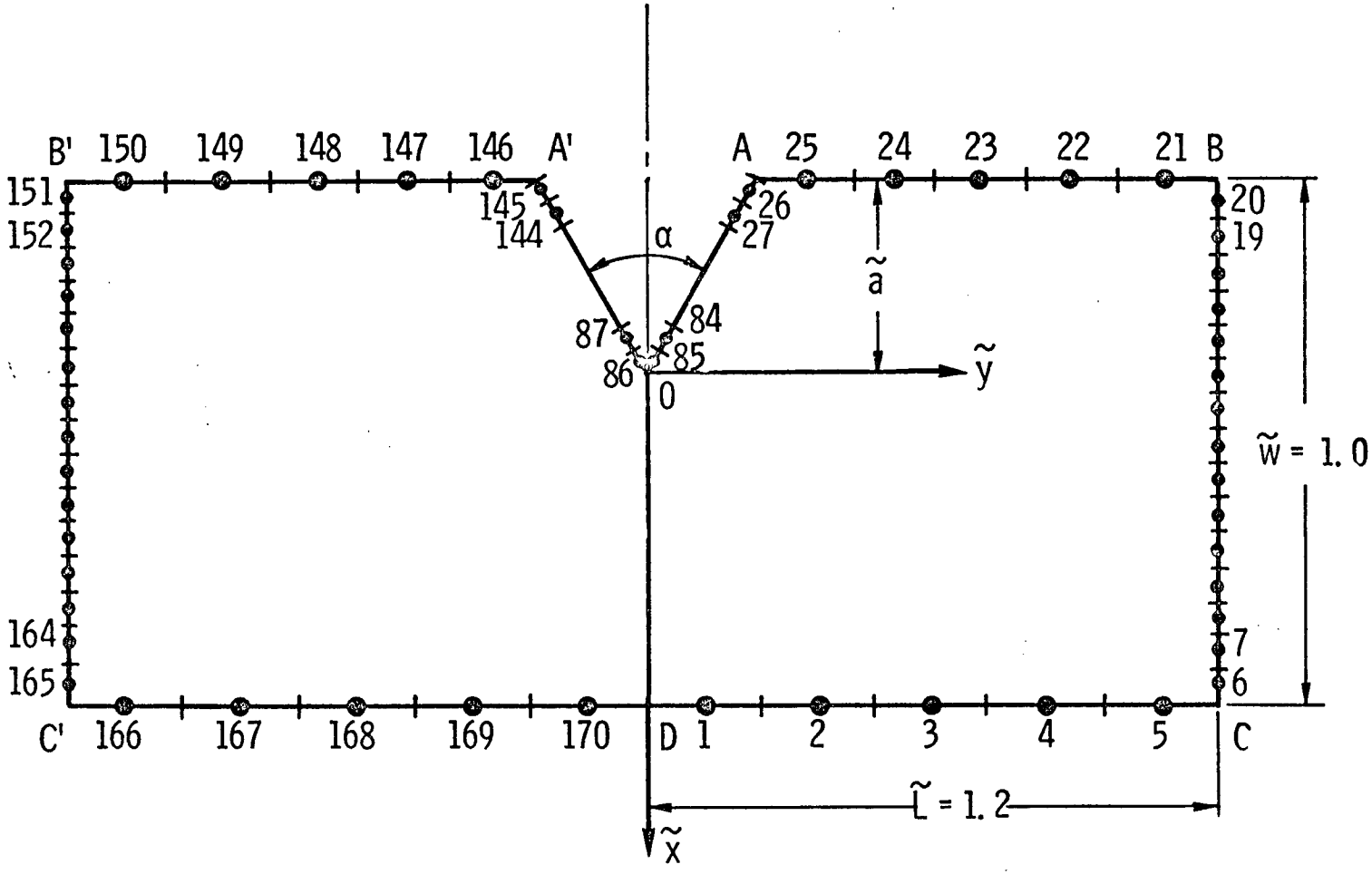

Fig. 6. Distribution of boundary subdivisions and nodal points.

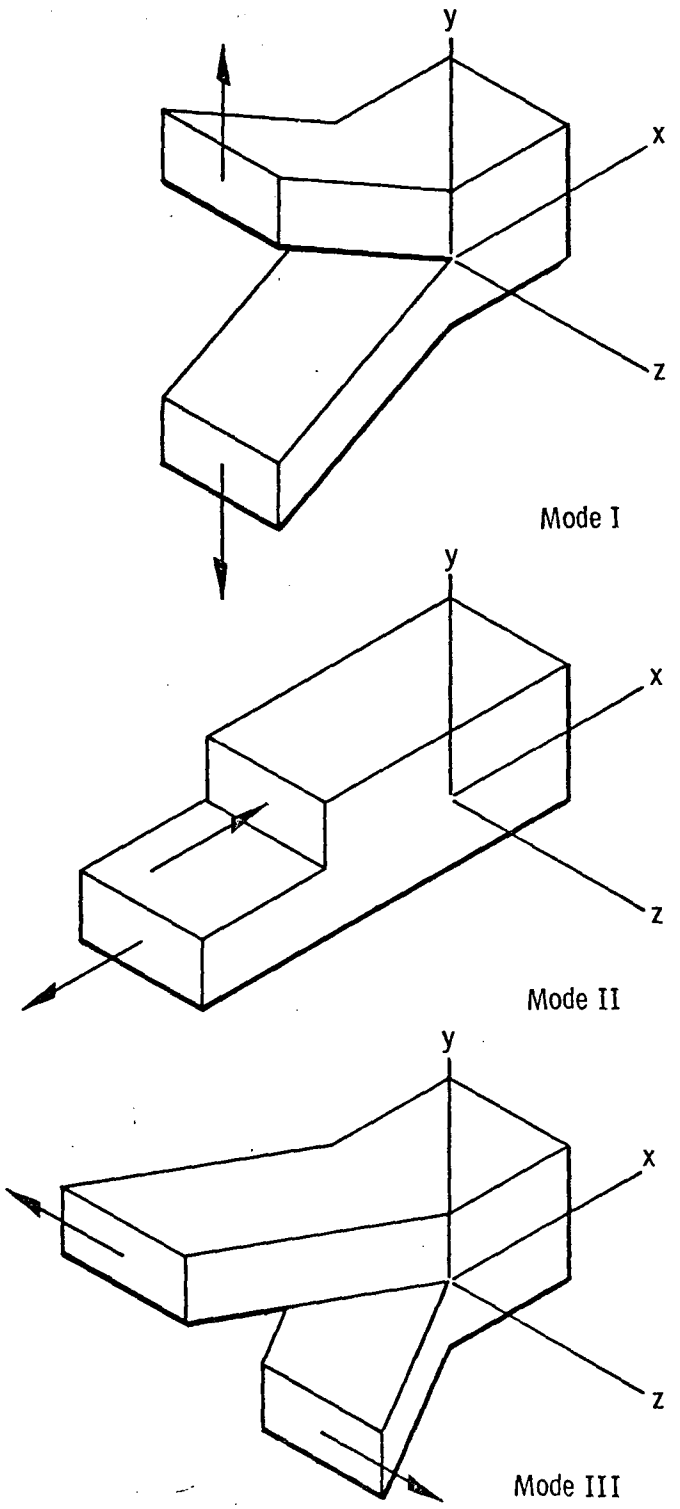

Figure 7. - Three displacements modes for crack surfaces.

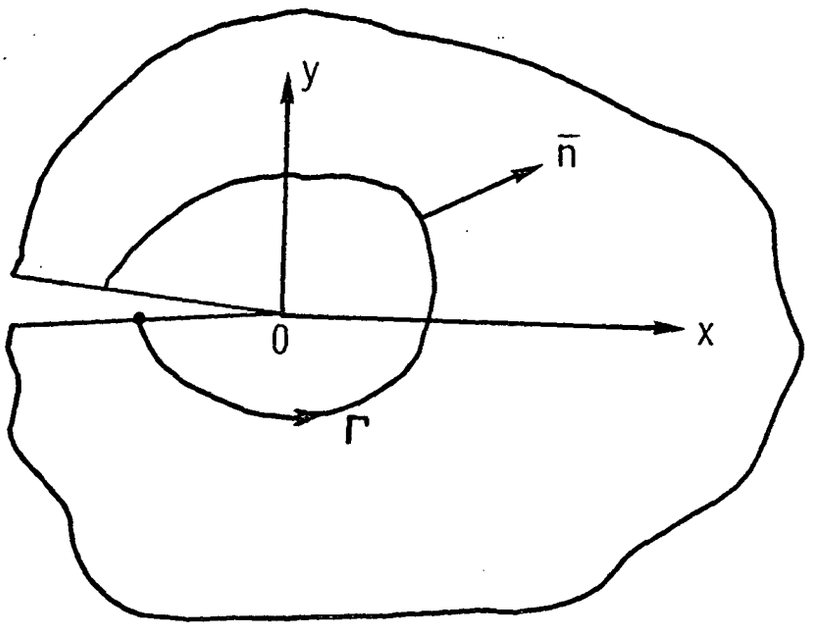

(a) Arbitrary path.

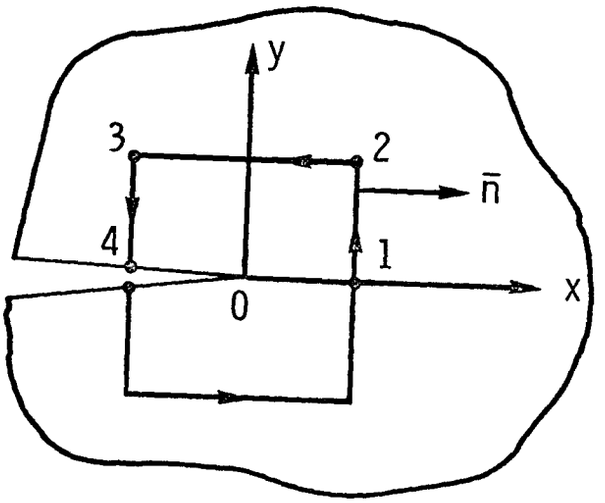

(b) Rectangular path.

Fig. 8. A continuous contour for Rice's integral.

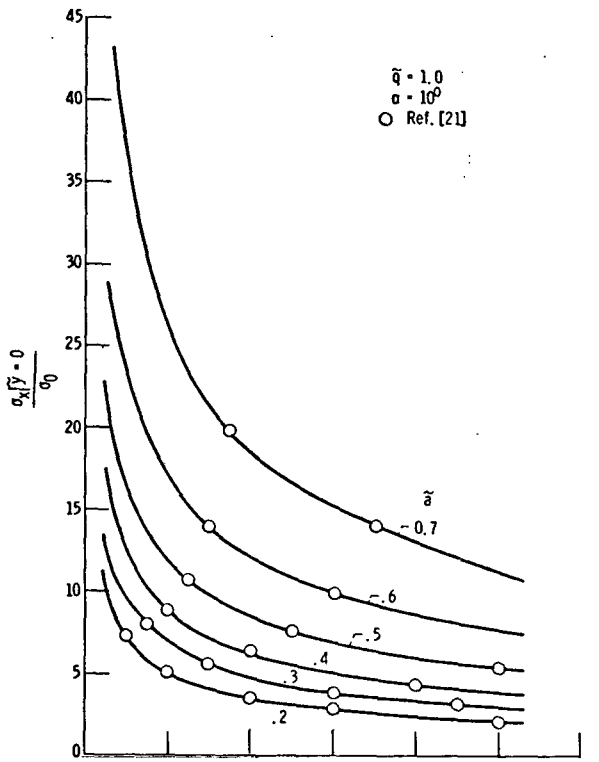

(a) Dimensionless x-directional stress as a function of $\tilde{x}$.

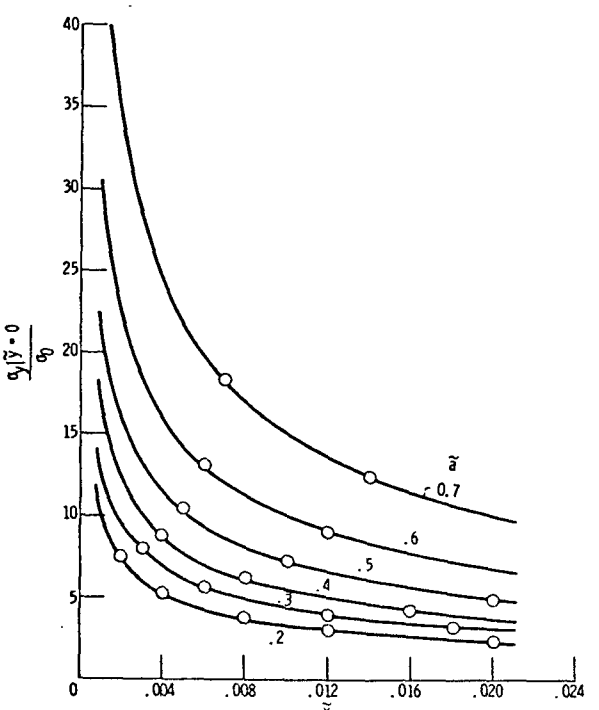

(b) Dimensionless y-directional stress as a function of $\tilde{x}$.

Fig. 9. Dimensionless elastic x-directional and y-directional stress distribution in the vicinity of the notch for a specimen with a 10^0 edge notch subjected to pure bending.

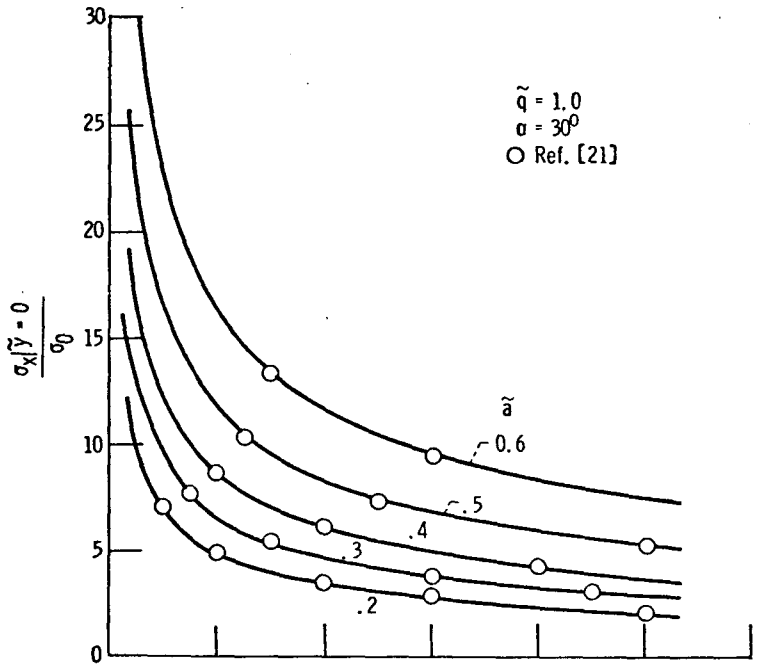

(a) Dimensionless x-directional stress as a function of $\tilde{x}$.

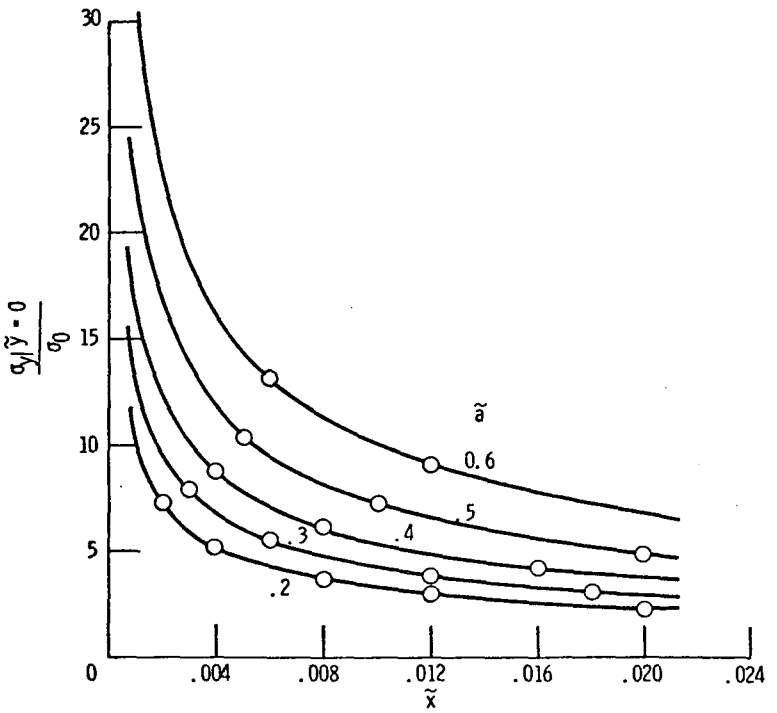

(b) Dimensionless y-directional stress as a function of $\tilde{x}$.

Fig. 10. Dimensionless elastic x-directional and y-directional stress distribution in the vicinity of the notch for a specimen with a 30° edge notch subjected to pure bending.

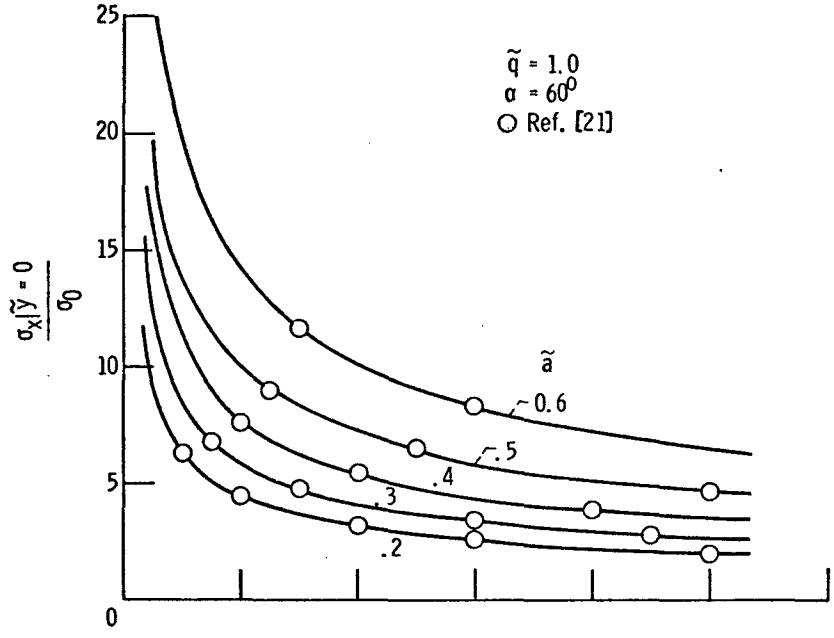

(a) Dimensionless x-directional stress as a function of $\tilde{x}$.

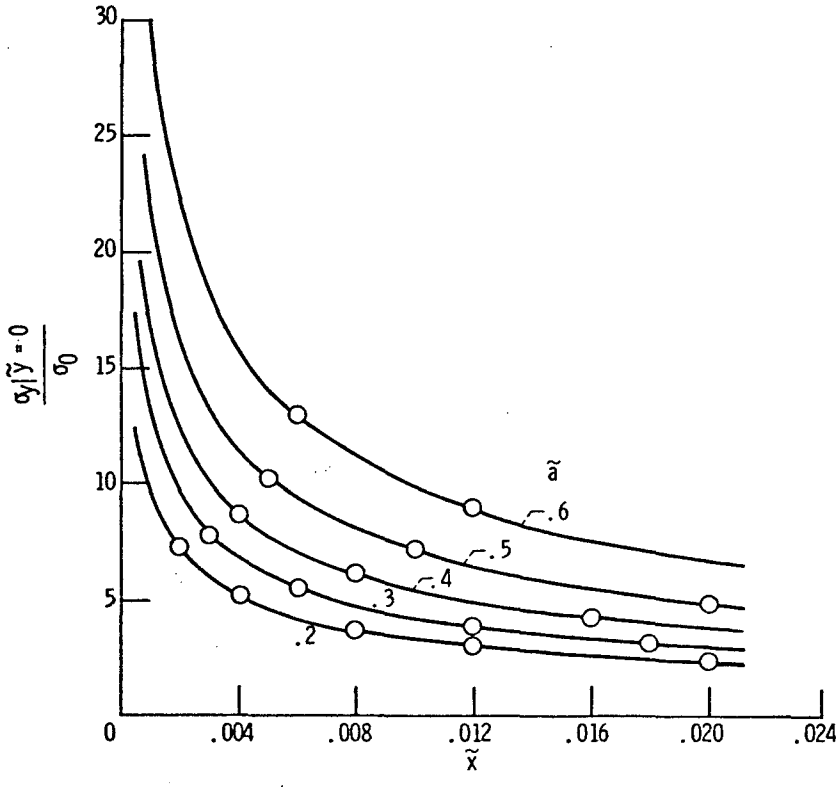

(b) Dimensionless y-directional stress as a function of $\tilde{x}$.

Fig. 11. Dimensionless elastic x-directional and y-directional stress distribution in the vicinity of the notch for a specimen with a 60° edge notch subjected to pure bending.

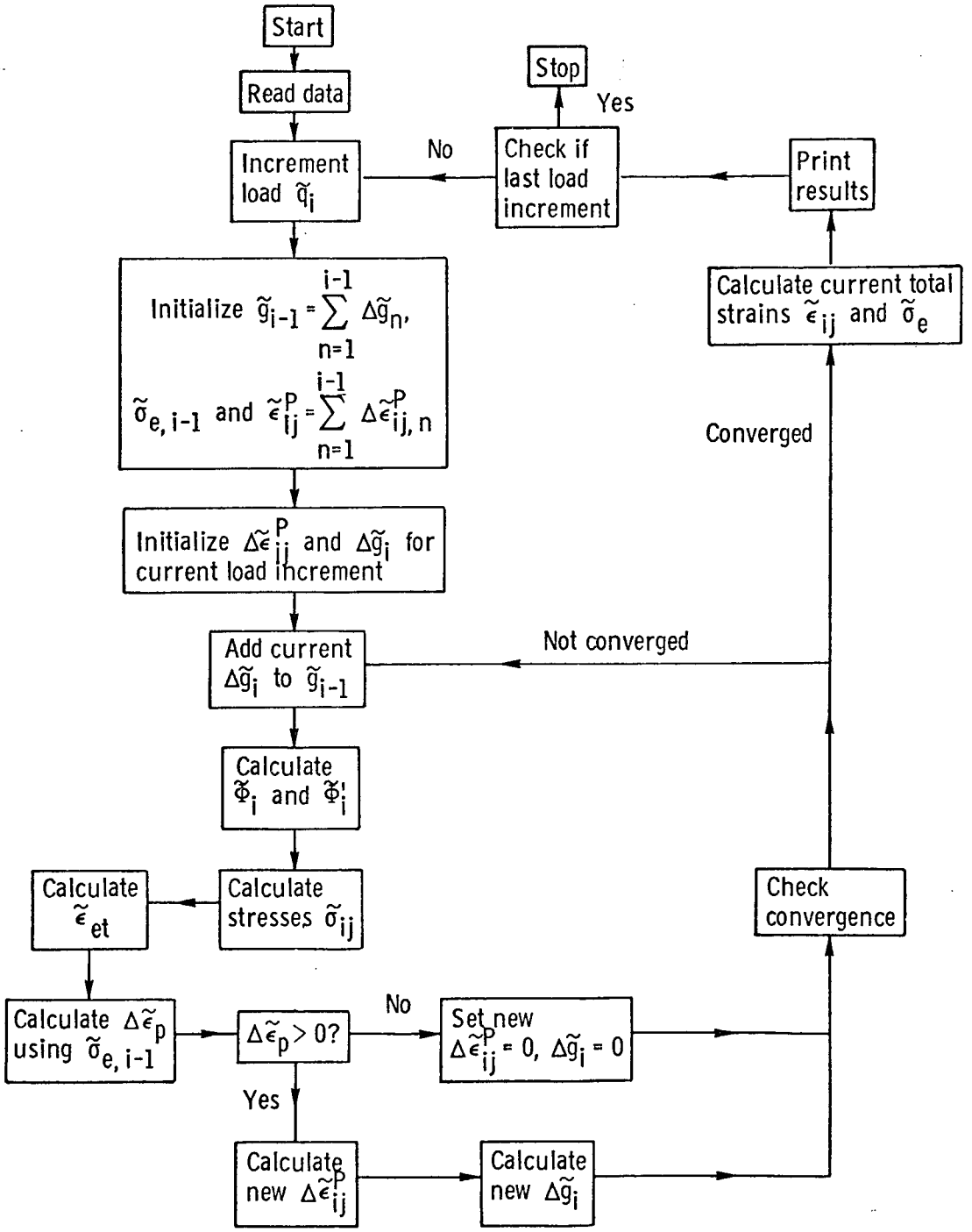

Fig. 12. Flow diagram for method of successive elastic solutions.

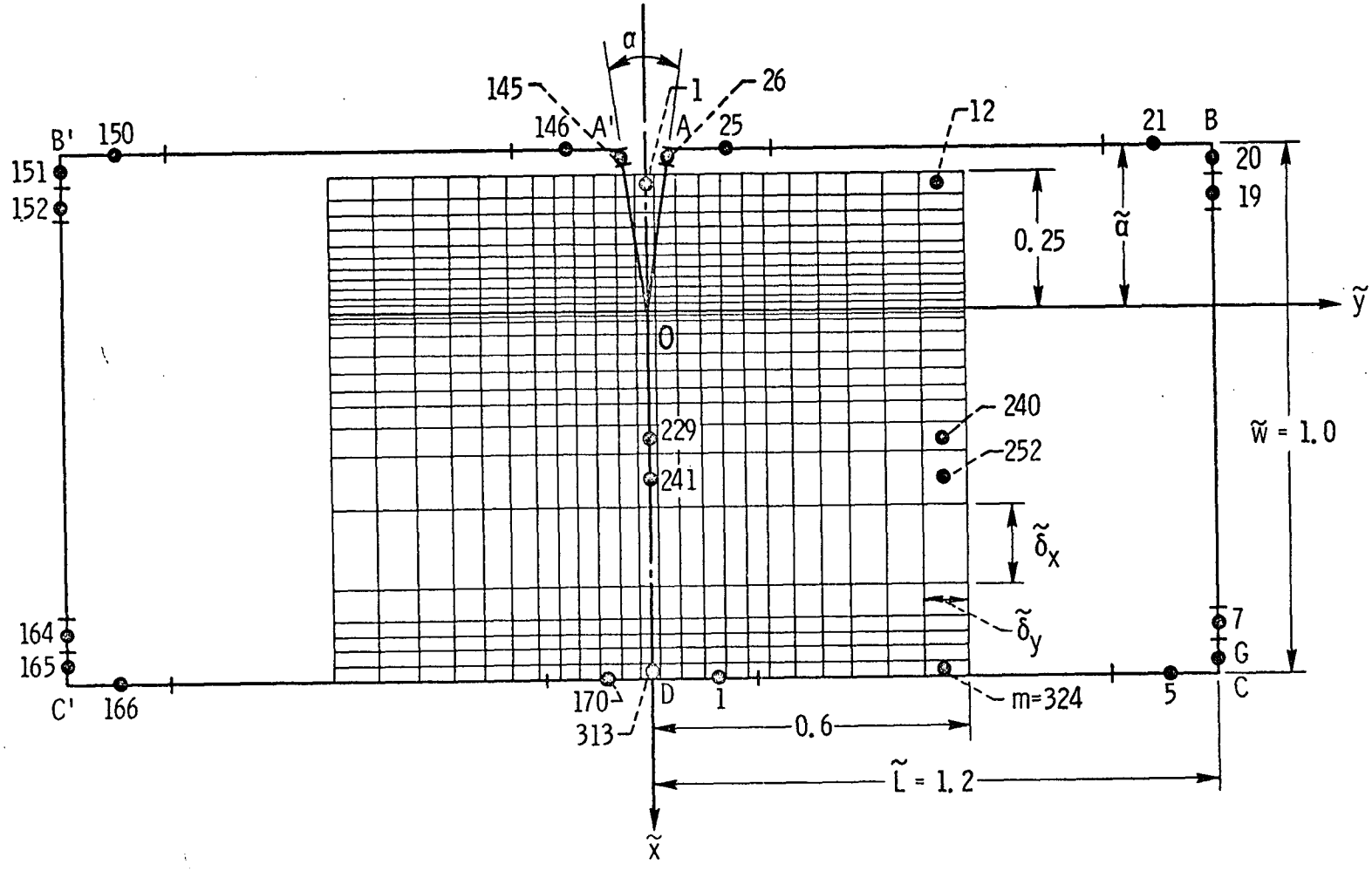

Fig. 13. Distribution of boundary subdivisions and typical interior grid for elasto-plastic problem.

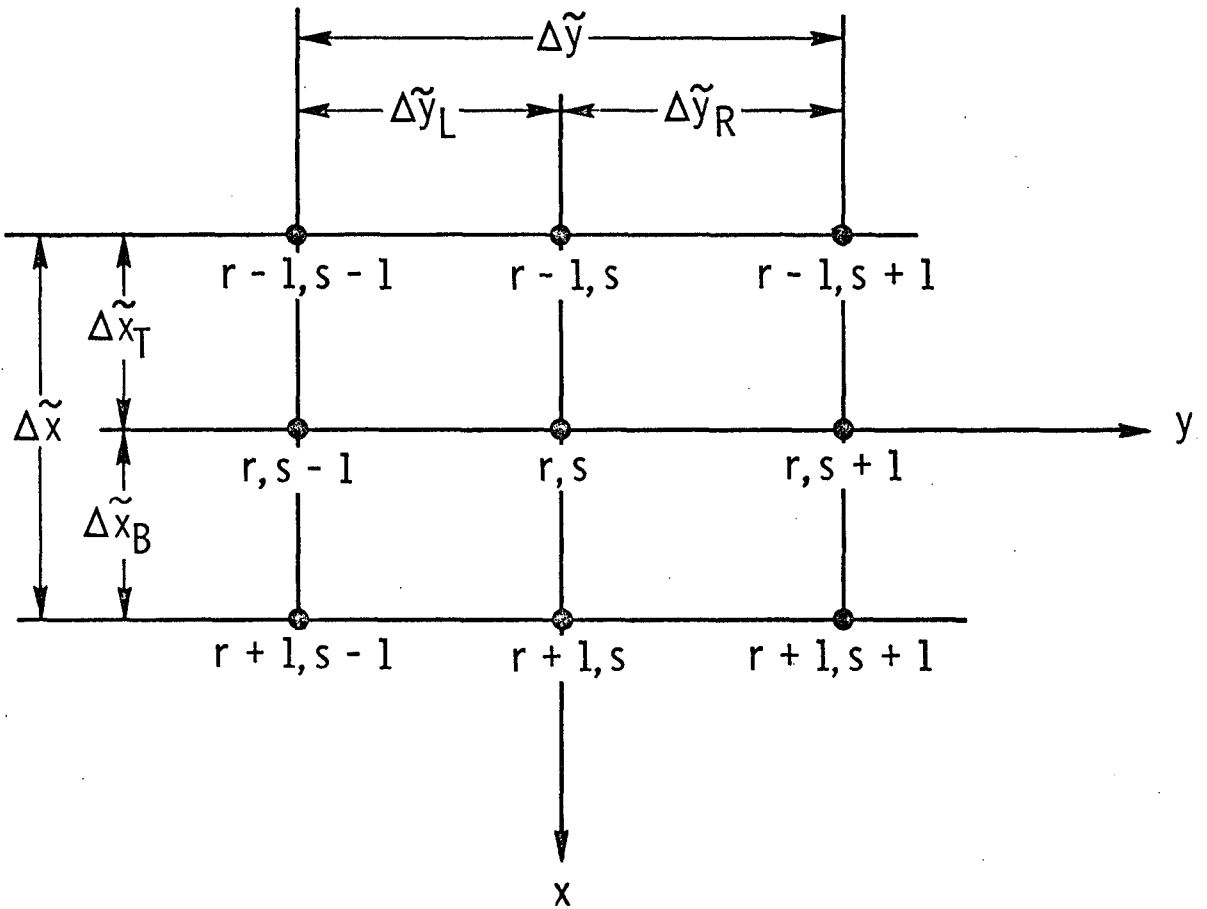

Fig. 14. Finite difference net for station (r, s).

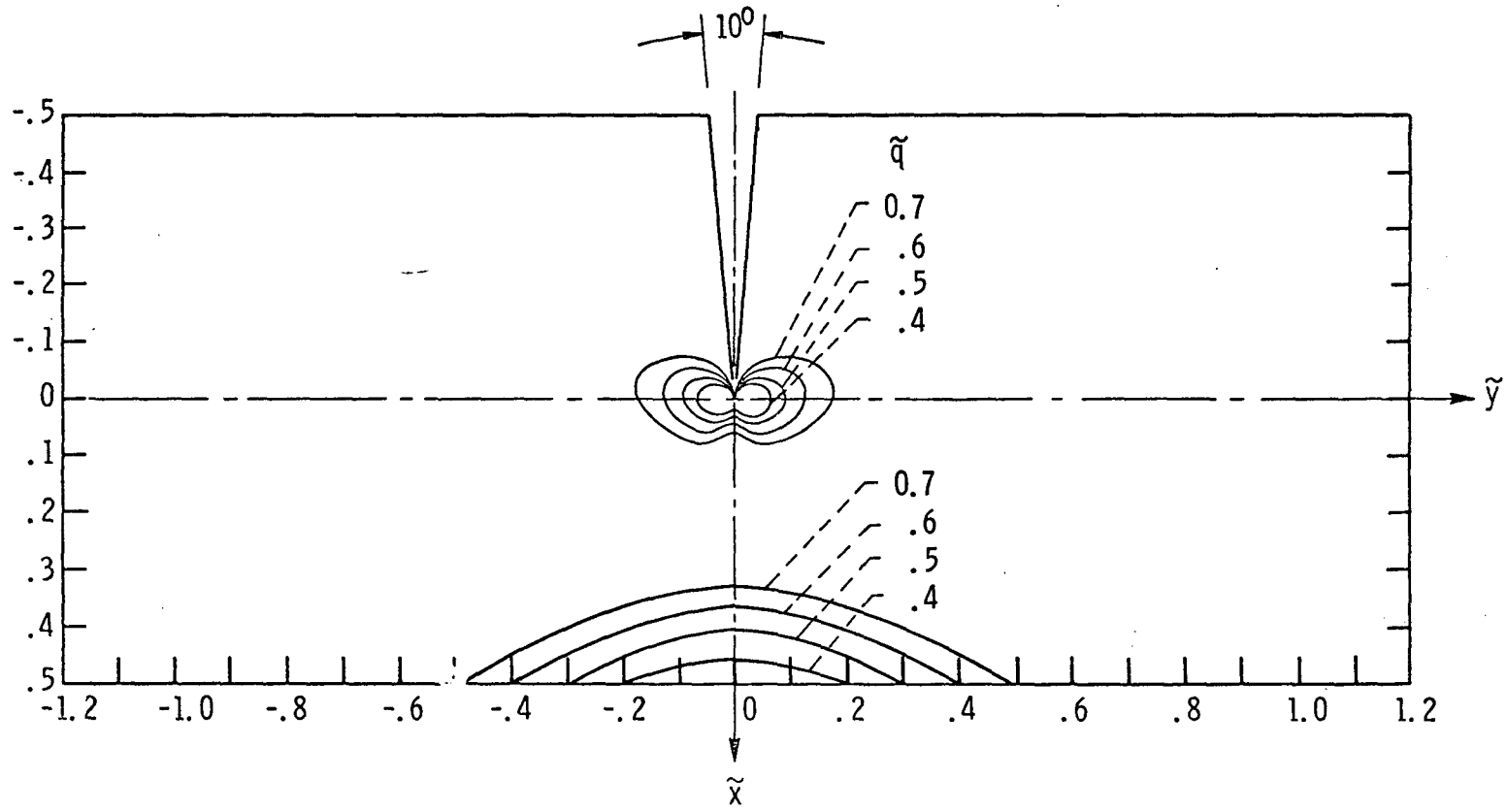

Fig. 15. Growth of the plastic zone size with load for a specimen with a 10^{0} edge notch subjected to pure bending; plane strain, $\tilde{a} = 0.5$, $\alpha = 10^{0}$, $m = 0.05$, $\mu = 0.33$.

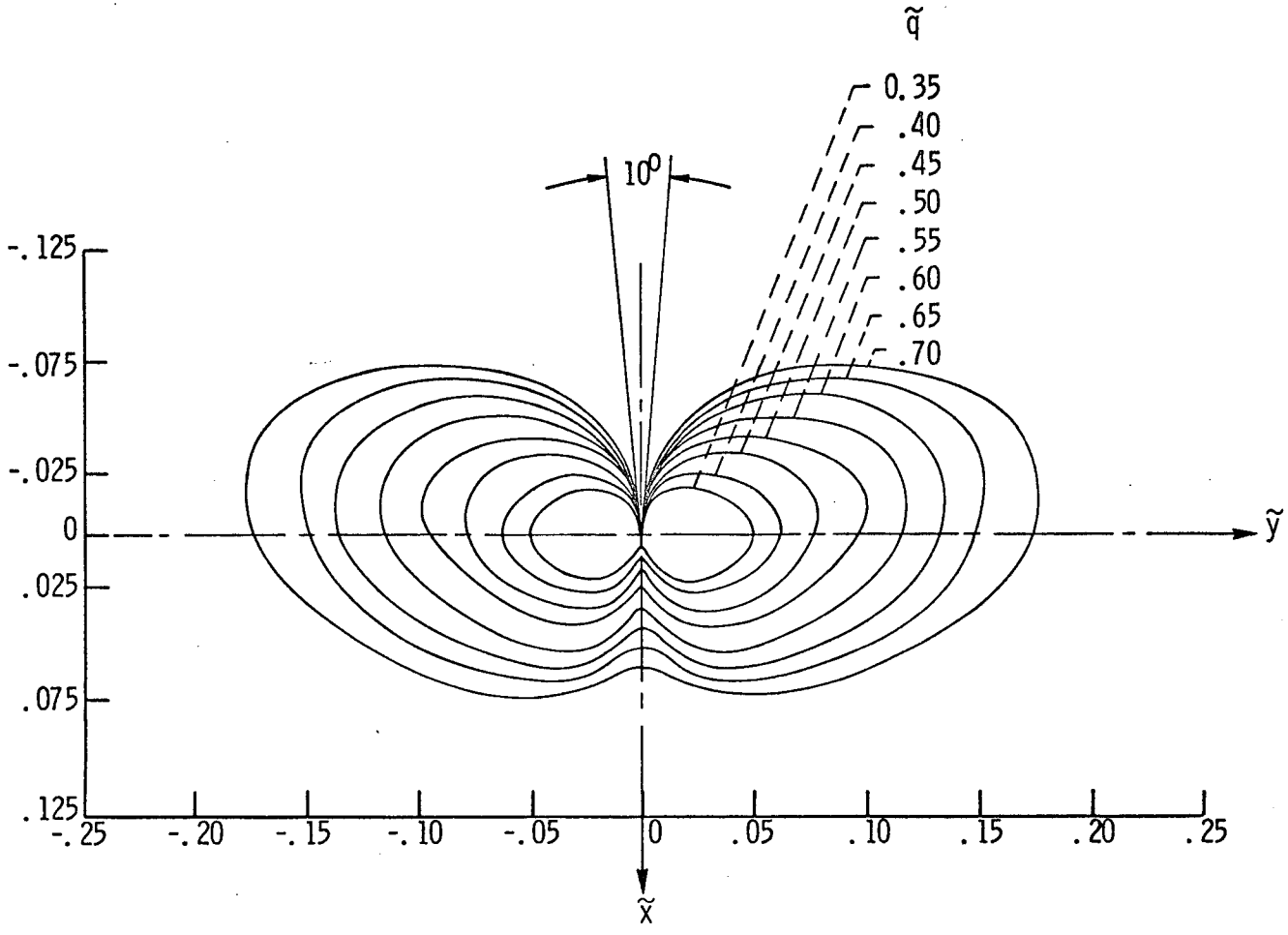

Fig. 16. Growth of the plastic zone size with load in the vicinity of the notch for a specimin with a 10^0 edge notch subjected to pure bending; plane strain, $\tilde{a} = 0.5$, $\alpha = 10^0$, $m = 0.05$, $\mu = 0.33$.

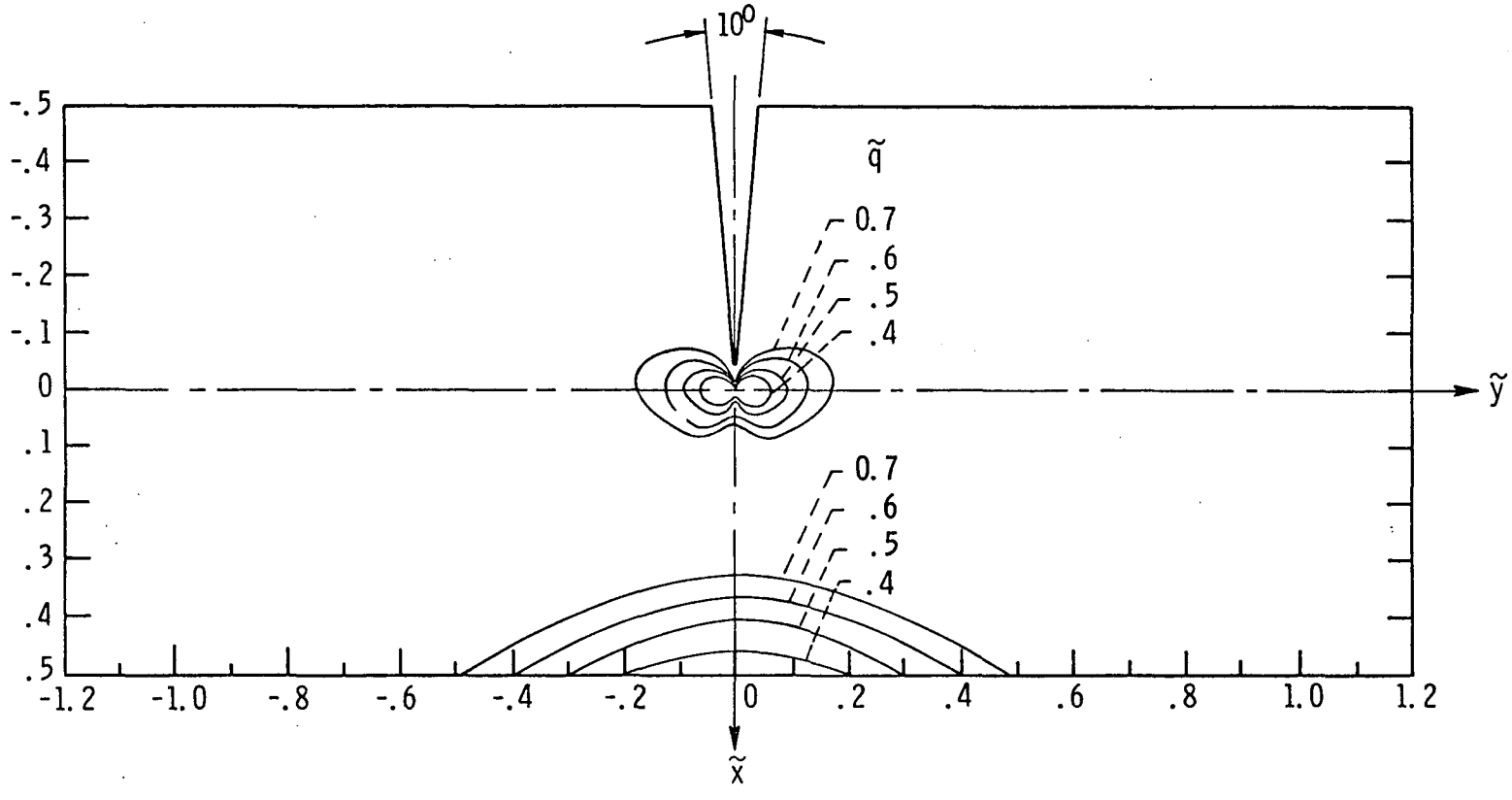

Fig. 17. Growth of the plastic zone size with load for a specimen with a 10^0 edge notch subjected to pure bending; plane strain, $\tilde{a} = 0.5$, $\alpha = 10^0$, $m = 0.10$, $\mu = 0.33$.

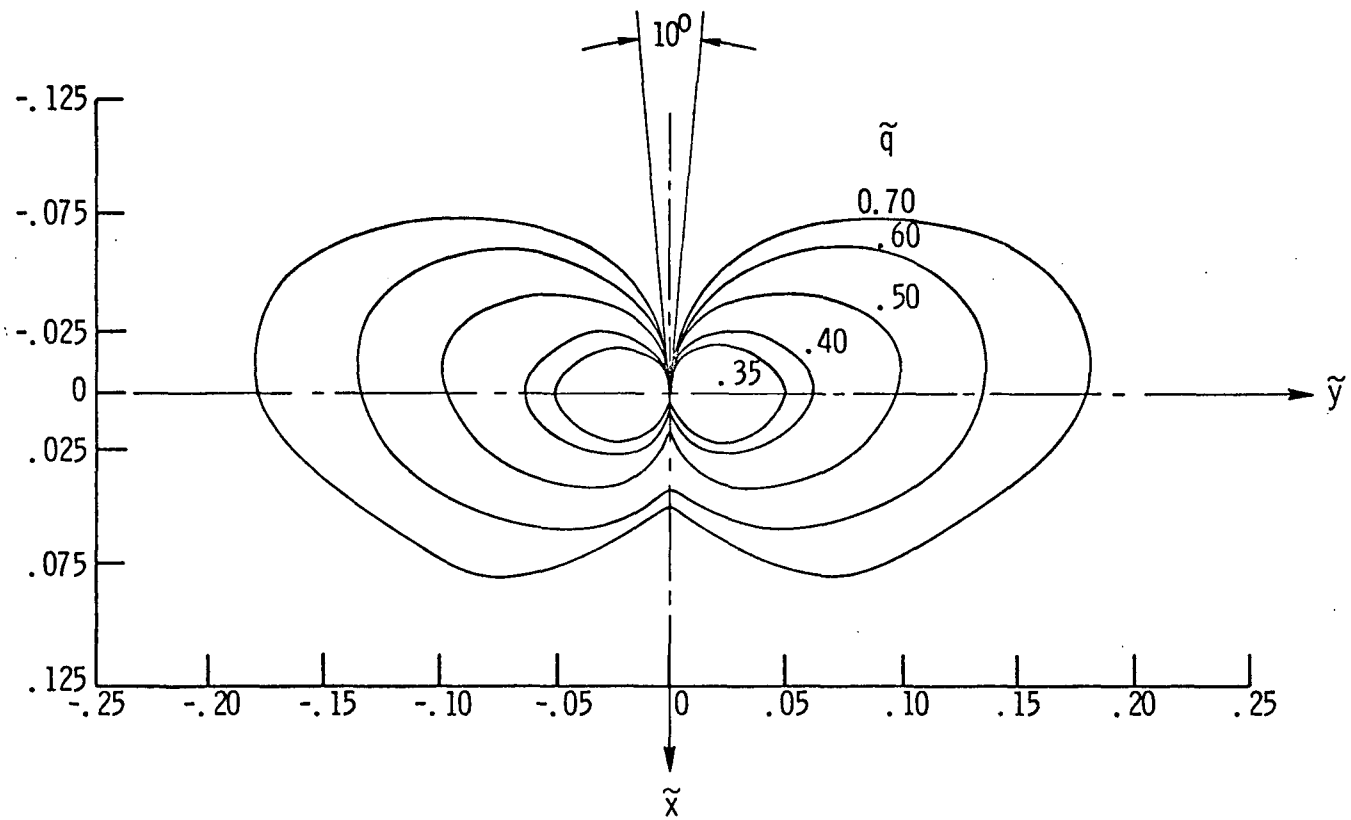

Fig. 18. Growth of the plastic zone size with load in the vicinity of the notch for a specimen with 10^0 edge notch subjected to pure bending; plane strain, $\tilde{a} = 0.5$, $\alpha = 10^0$, $m = 0.10$, $\mu = 0.33$.

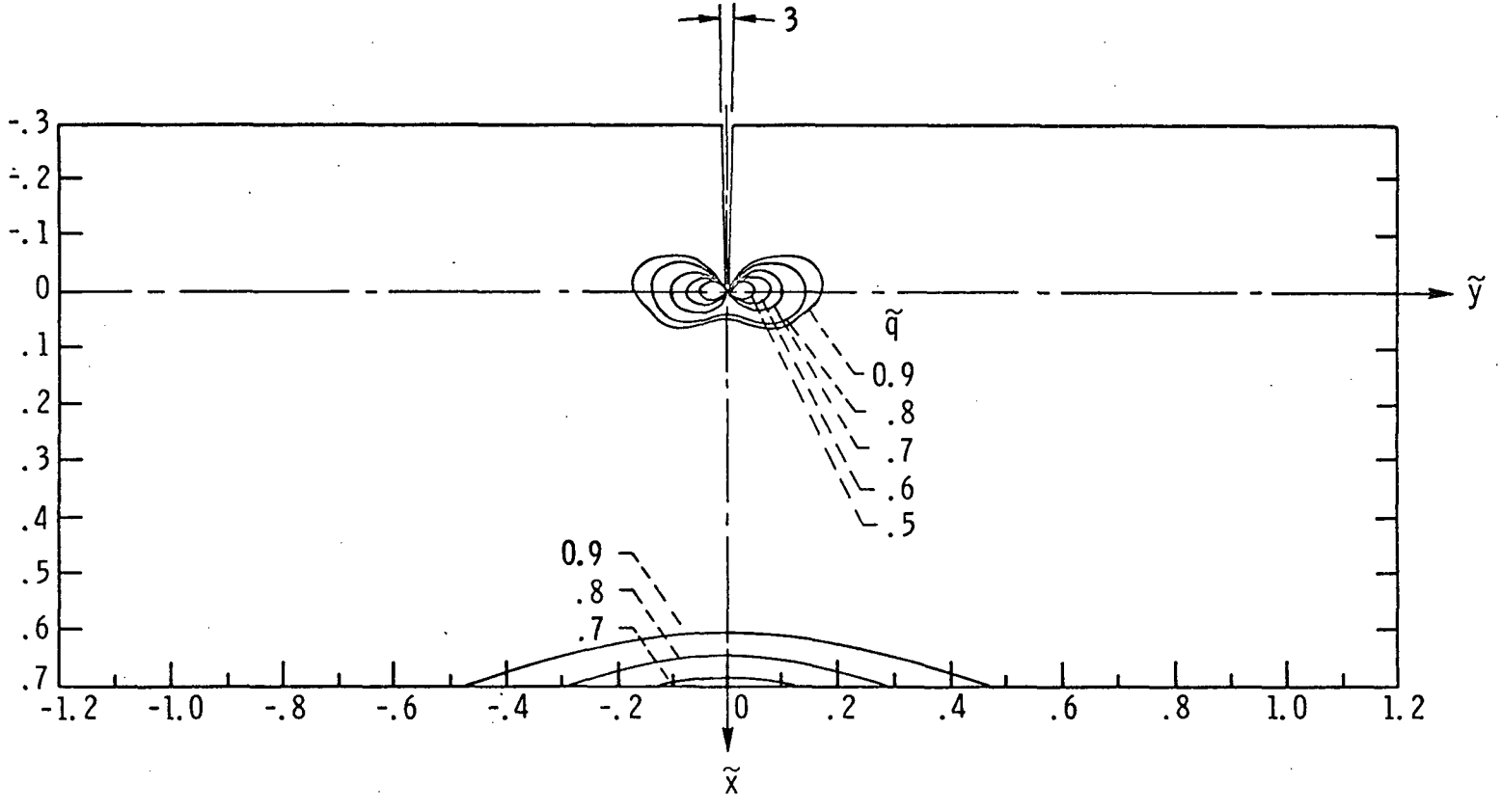

Fig. 19. Growth of the plastic zone size with load for a specimen with a 3^0 edge notch subjected to pure bending; plane strain, $\tilde{a} = 0.3$, $\alpha = 3^0$, $m = 0.10$, $\mu = 0.33$.

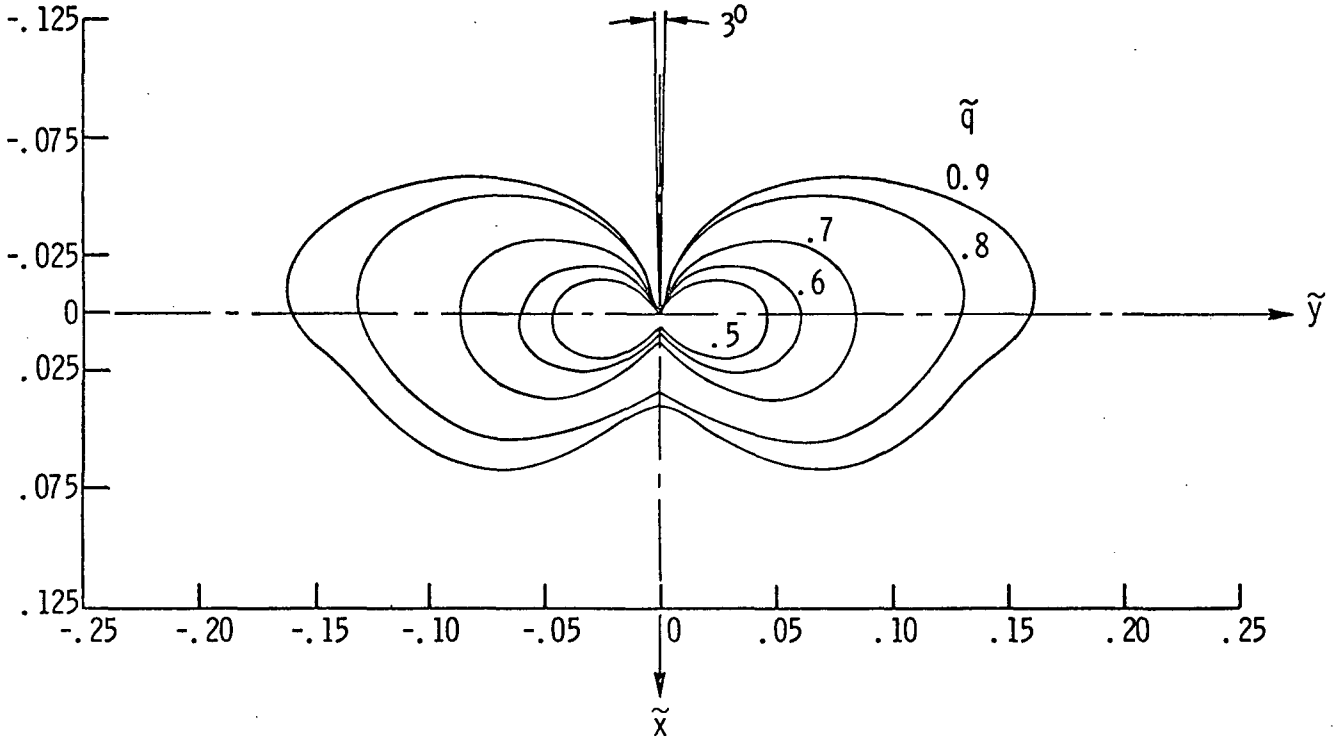

Fig. 20. Growth of the plastic zone size with load in the vicinity of the notch for a specimen with a 3^0 edge notch subjected to pure bending; plane strain, $\tilde{a} = 0.3$, $\alpha = 3^0$, $m = 0.10$, $\mu = 0.33$.

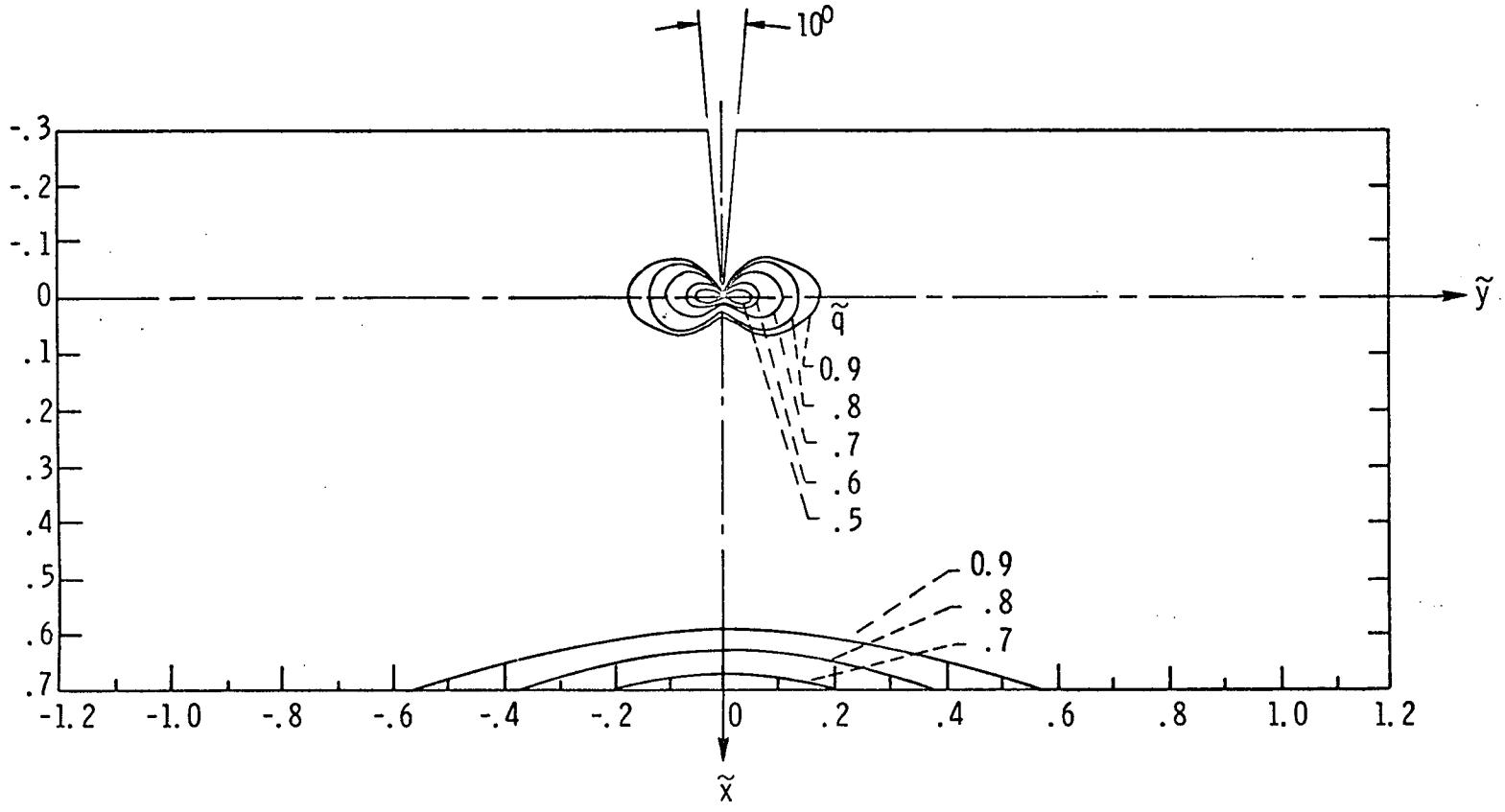

Fig. 21. Growth of the plastic zone size with load for a specimen with a 10^0 edge notch subjected to pure bending; plane strain, $\tilde{a} = 0.3$, $\alpha = 10^0$, $m = 0.10$, $\mu = 0.33$.

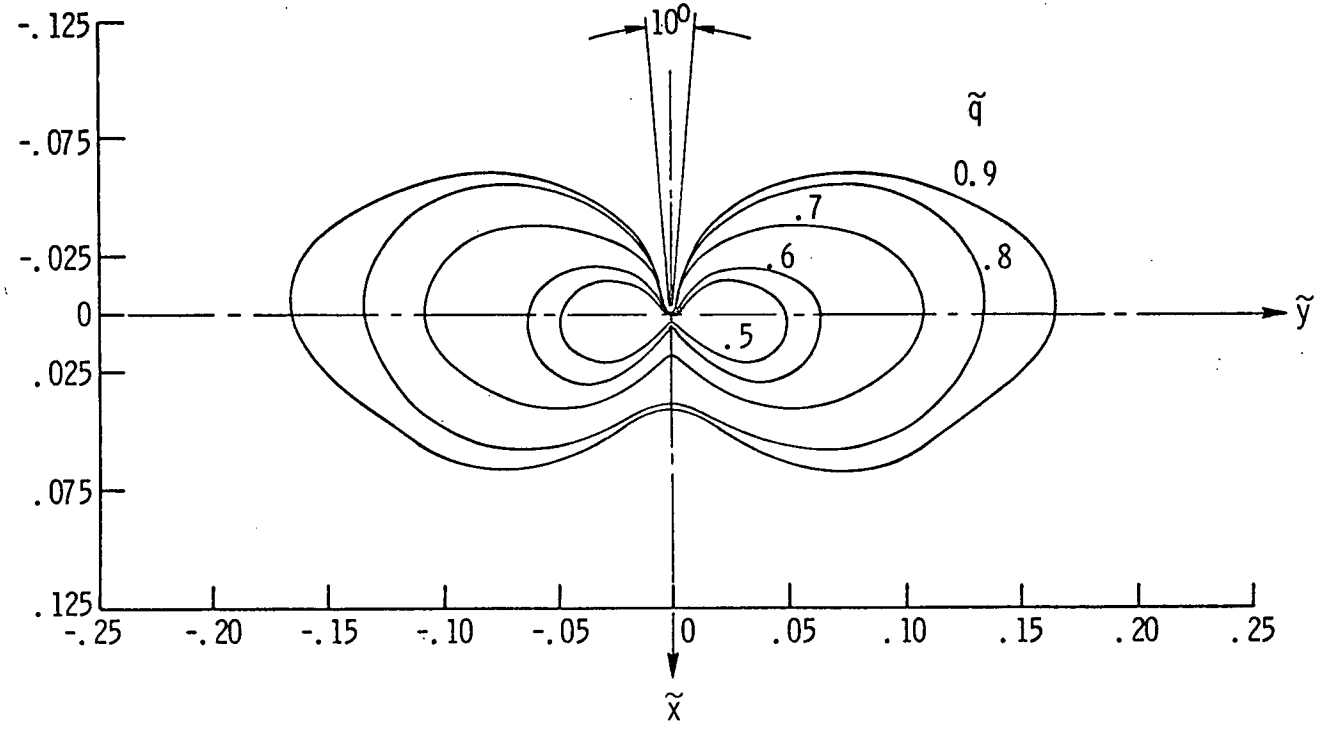

Fig. 22. Growth of plastic zone size with load in the vicinity of the notch for a specimen with a 10^0 edge notch subjected to pure bending; plane strain, $\tilde{a} = 0.3$, $\alpha = 10^0$, $m = 0.10$, $\mu = 0.33$.

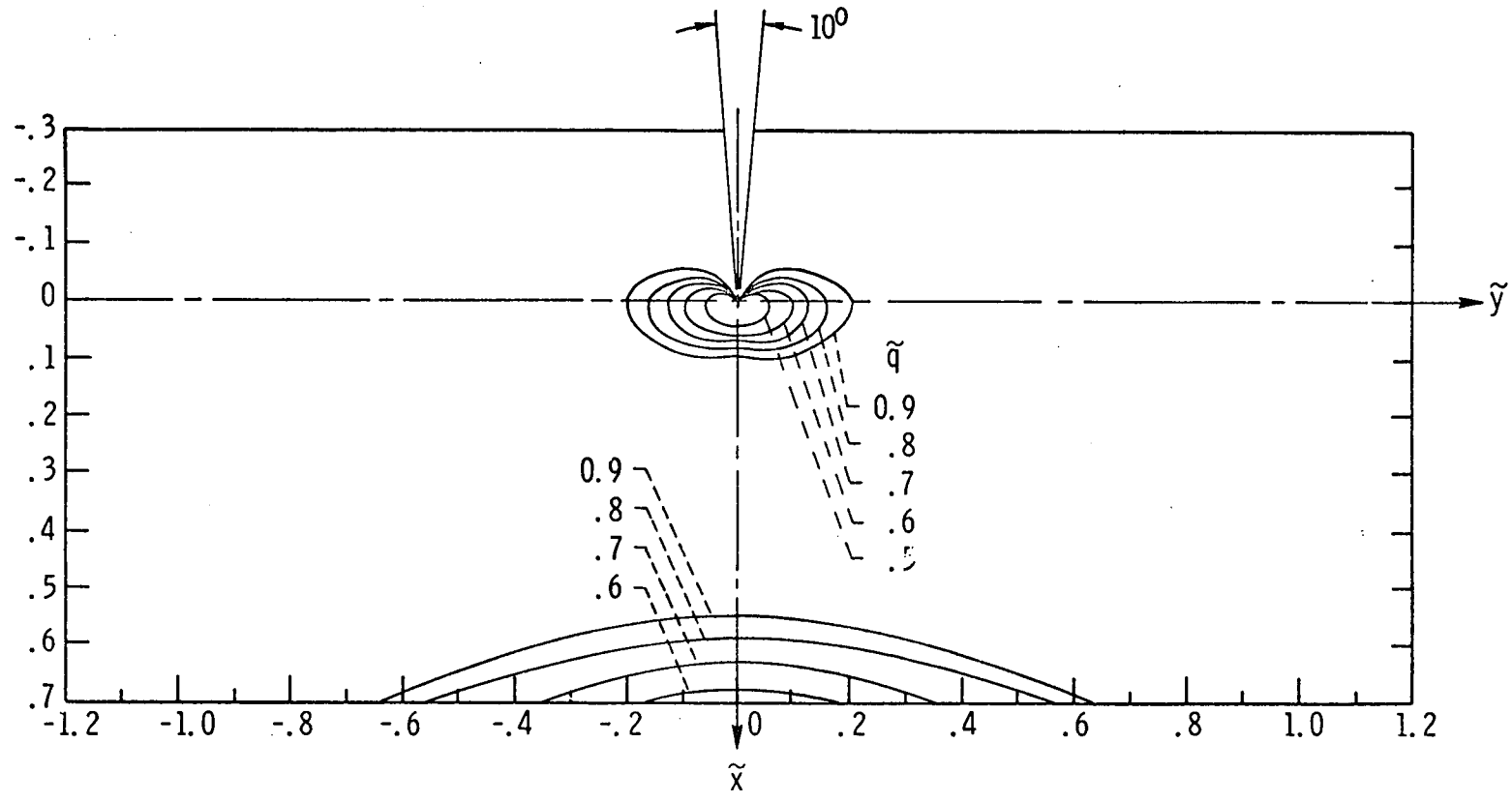

Fig. 23. Growth of the plastic zone size with load for a specimen with a 10^0 edge notch subjected to pure bending; plane stress, $\tilde{a} = 0.3$, $\alpha = 10^0$, $m = 0.10$, $\mu = 0.33$.

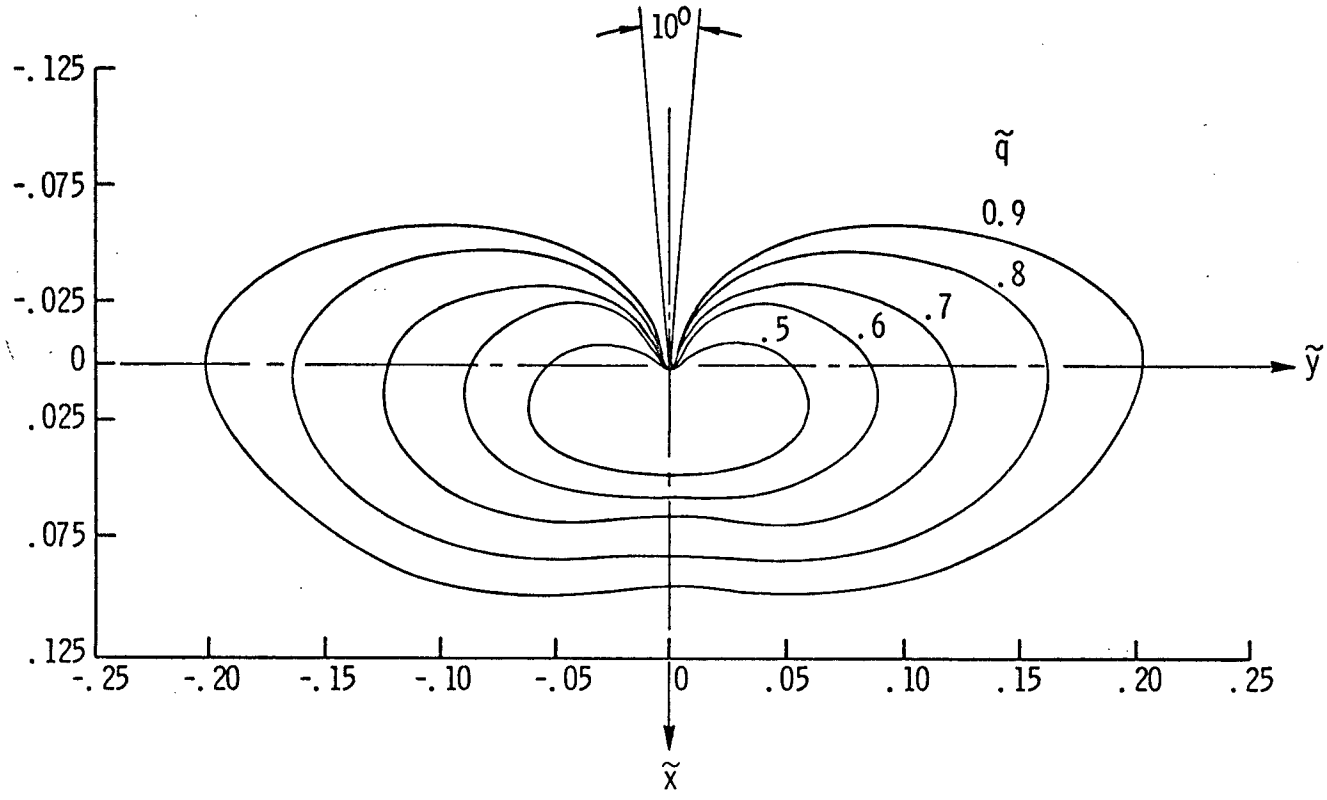

Fig. 24. Growth of the plastic zone size with load in the vicinity of the notch for a specimen with a 10^0 edge notch subjected to pure bending; plane stress, $\tilde{a} = 0.3$, $\alpha = 10^0$, $m = 0.10$, $\mu = 0.33$.

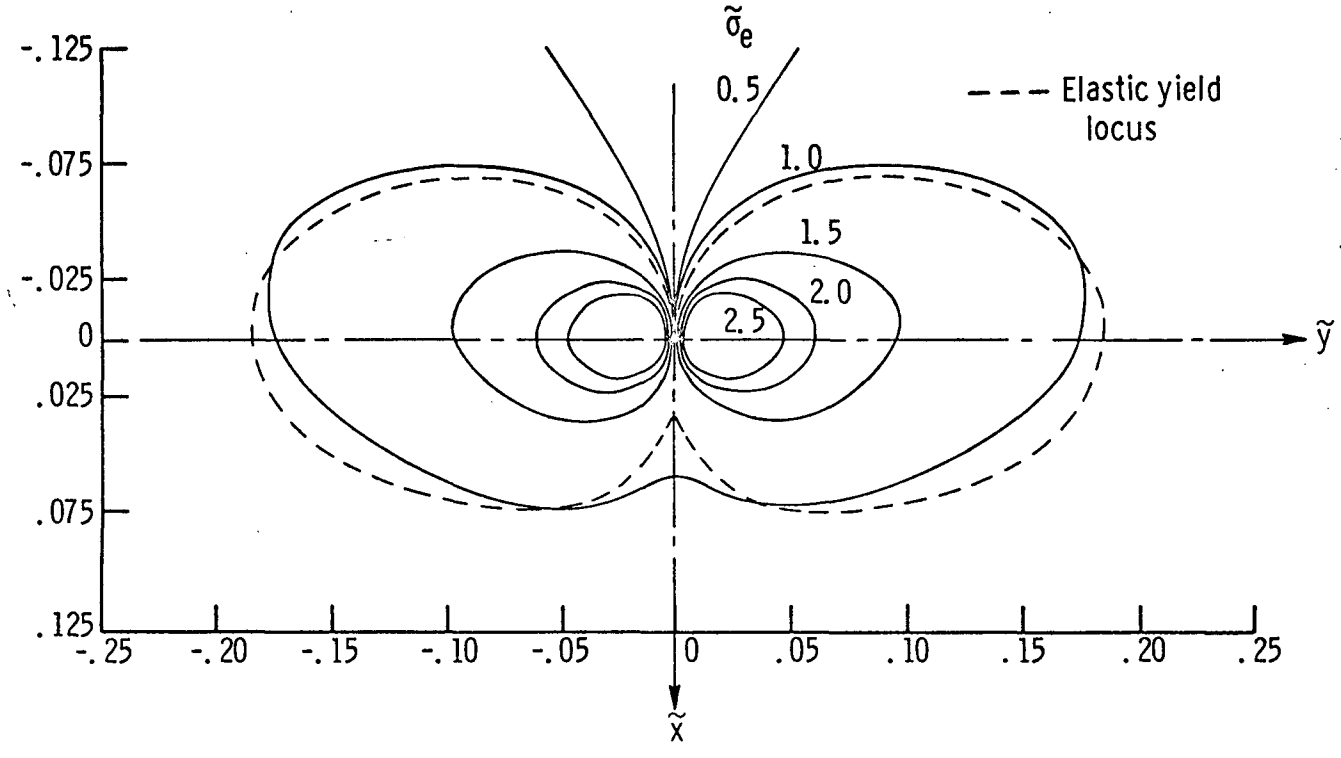

Fig. 25. Dimensionless equivalent stress contours in the vicinity of the notch for a specimen with a 10^0 edge notch subjected to pure bending; plane strain, $\tilde{q} = 0.7$, $\tilde{a} = 0.5$, $\alpha = 10^0$, $m = 0.05$, $\mu = 0.33$.

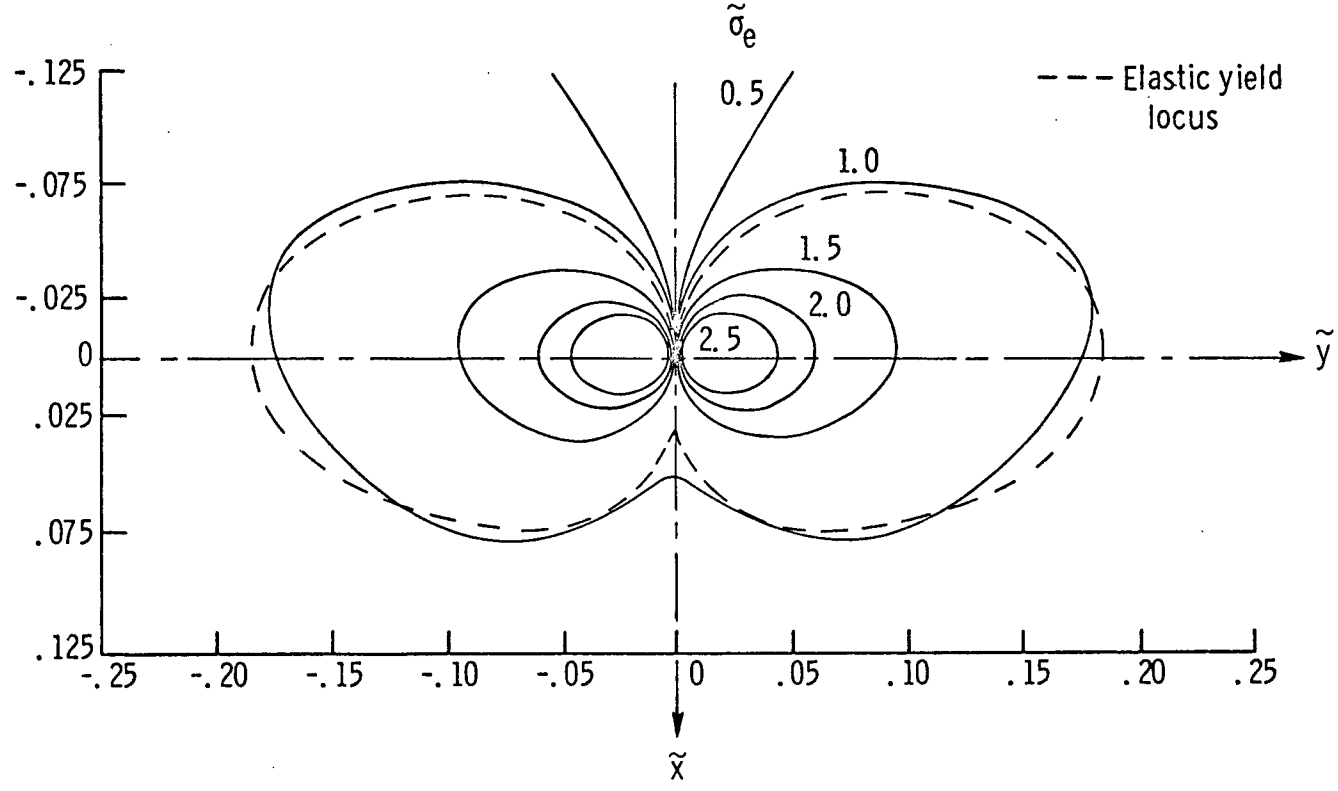

Fig. 26. Dimensionless equivalent stress contours in the vicinity of the notch for a specimen with a 10^0 edge notch subjected to pure bending; plane strain, $\tilde{q} = 0.7$, $\tilde{a} = 0.5$, $\alpha = 10^0$, $m = 0.10$, $\mu = 0.33$.

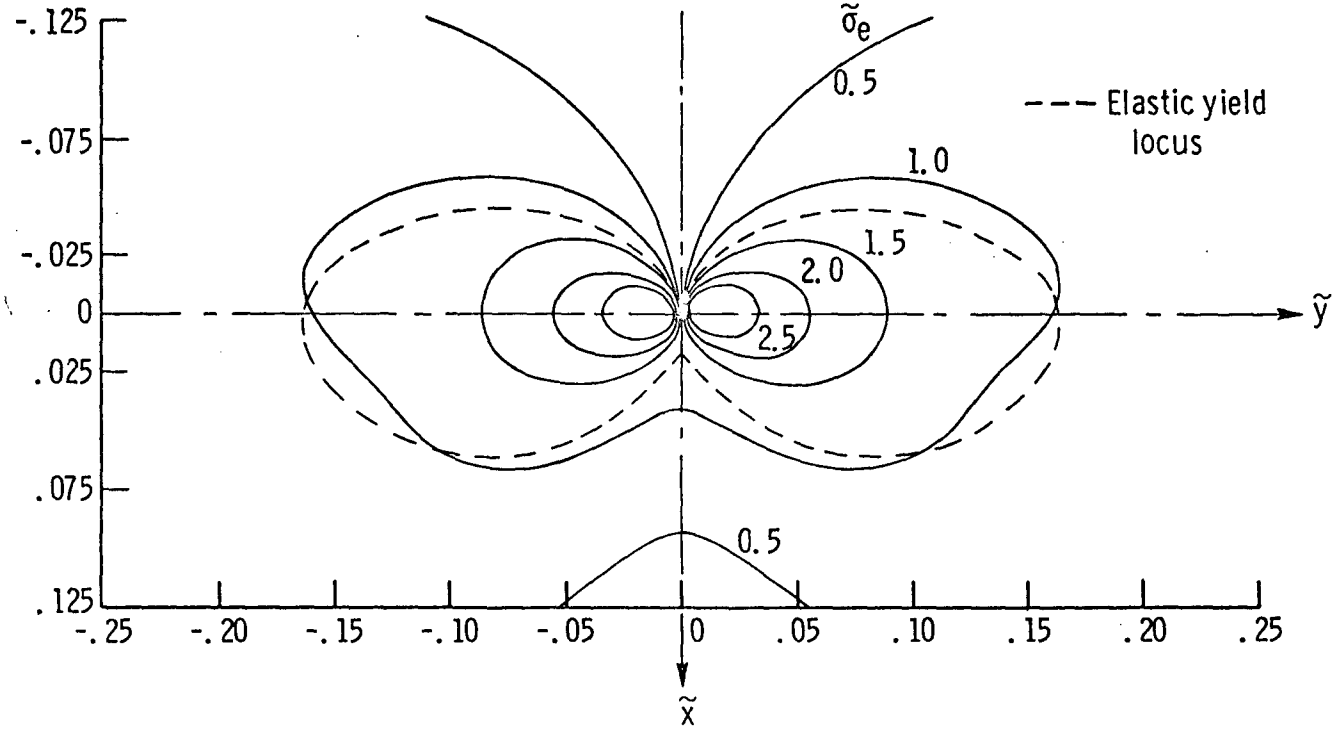

Fig. 27. Dimensionless equivalent stress contours in the vicinity of the notch for a specimen with a 3^0 edge notch subjected to pure bending; plane strain, $\tilde{q} = 0.9$, $\tilde{a} = 0.3$, $m = 0.10$, $\mu = 0.33$.

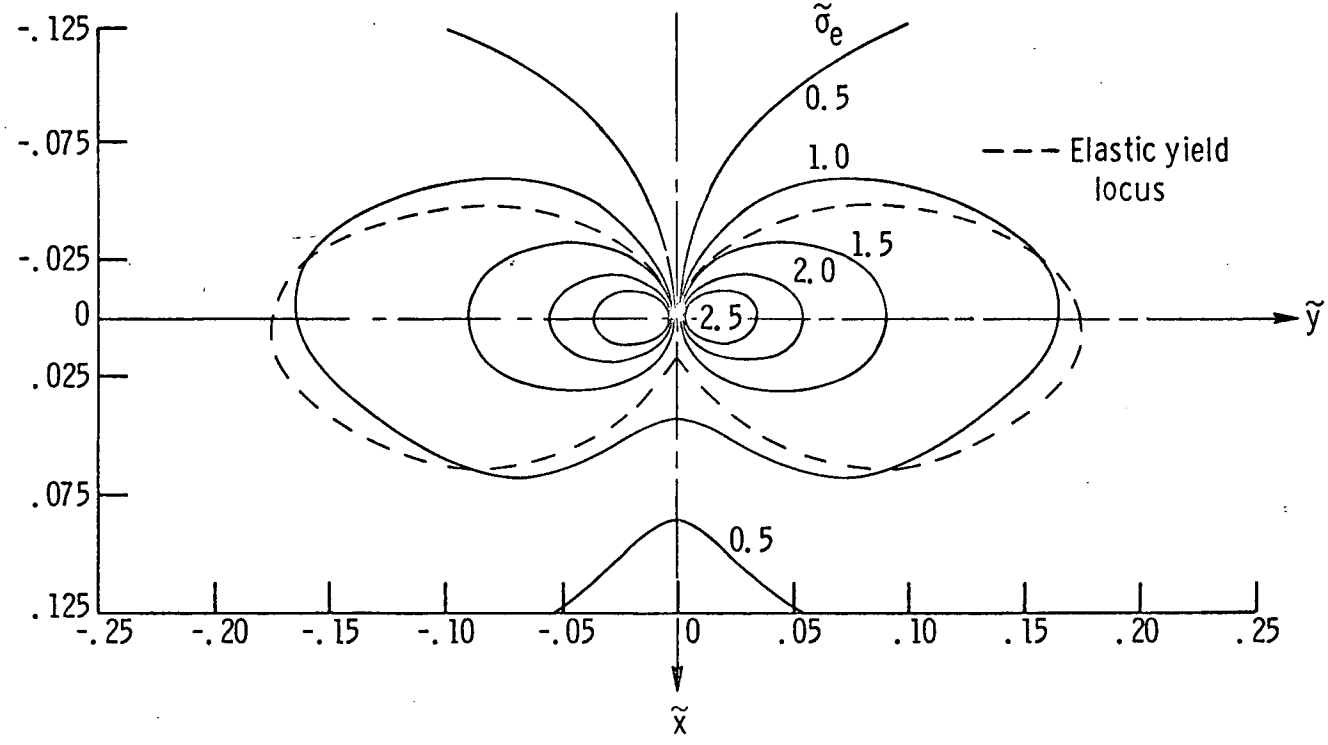

Fig. 28. Dimensionless equivalent stress contours in the vicinity of the notch for a specimen with a 10^0 edge notch subjected to pure bending; plane strain, $\tilde{q} = 0.9$, $\tilde{a} = 0.3$, $\alpha = 10^0$, $m = 0.10$, $\mu = 0.33$.

C-4

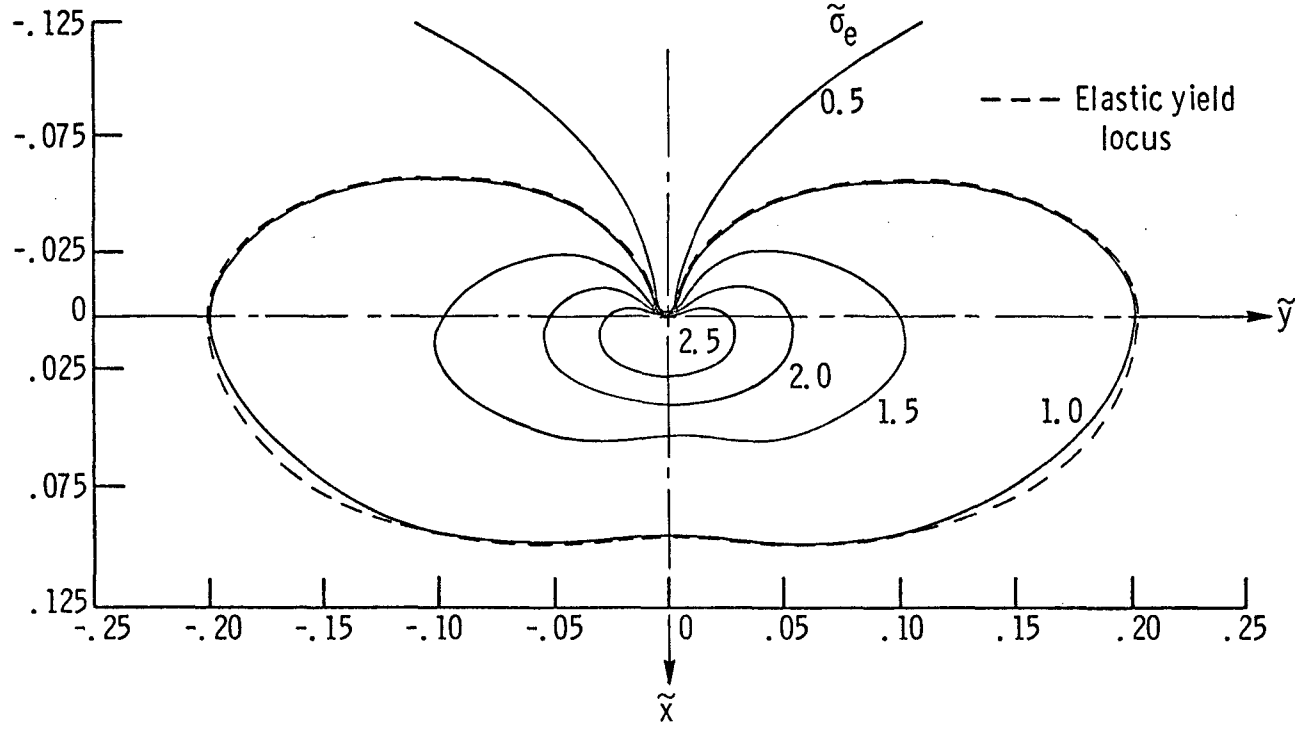

Fig. 29. Dimensionless equivalent stress contours in the vicinity of the notch for a specimen with a 10^0 edge notch subjected to pure bending; plane stress, $\tilde{q} = 0.9$, $\tilde{a} = 0.3$, $\alpha = 10^0$, $m = 0.10$, $\mu = 0.33$.

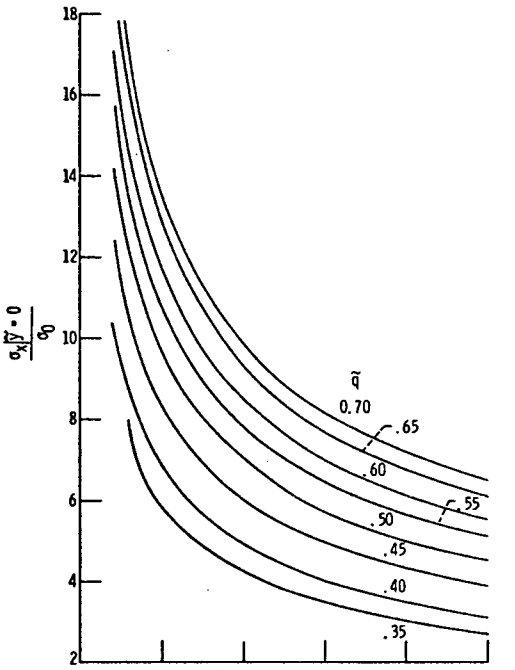

(a) Dimensionless x-directional stress as a function of $\tilde{x}$.

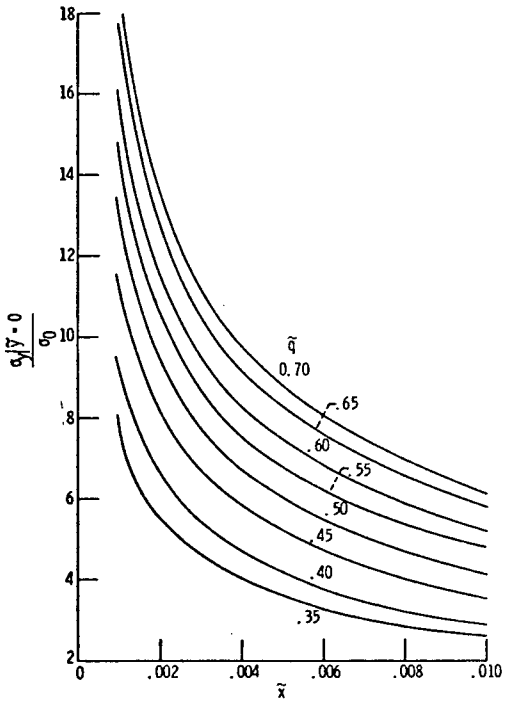

(b) Dimensionless y-directional stress as a function of $\tilde{x}$.

Fig. 30. Dimensionless x-directional and y-directional stress distribution in the vicinity of the notch for a specimen with a 10^0 edge notch subjected to pure bending; plane strain, $\tilde{a} = 0.5$, $\alpha = 10^0$, $m = 0.05$, $\mu = 0.33$.

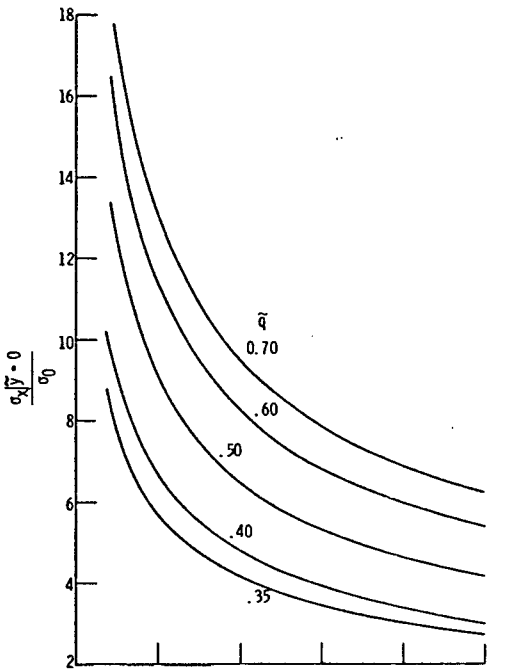

(a) Dimensionless x-directional stress as a function of $\tilde{x}$.

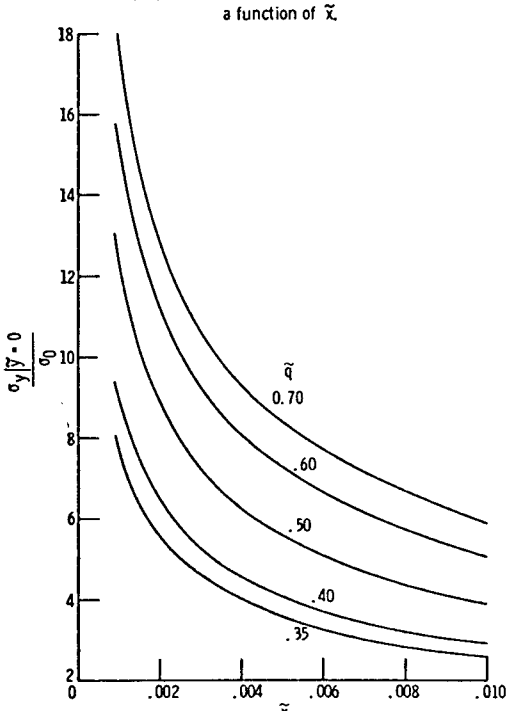

(b) Dimensionless y-directional stress as a function of $\tilde{x}$.

Fig. 31. Dimensionless x-directional and y-directional stress distribution in the vicinity of the notch for a specimen with a 10^0 edge notch subjected to pure bending; plane strain, $\tilde{a} = 0.5$, $\alpha = 10^0$, $m = 0.10$, $\mu = 0.33$.

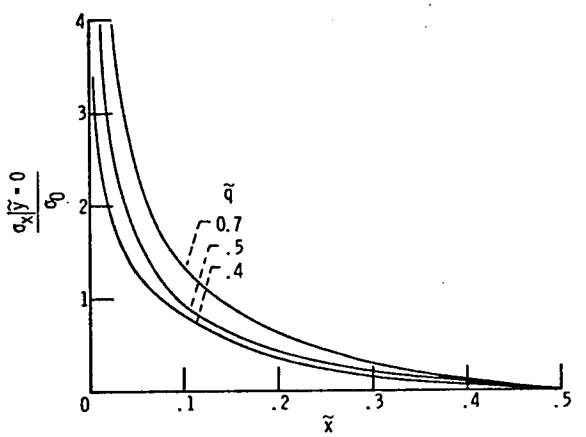

Fig. 32. Dimensionless x-directional stress distribution along x axis for a specimen with a 10^0 edge notch subjected to pure bending; plane strain, $\tilde{a} = 0.5$, $\alpha = 10^0$, $m = 0.05$, $\mu = 0.33$.

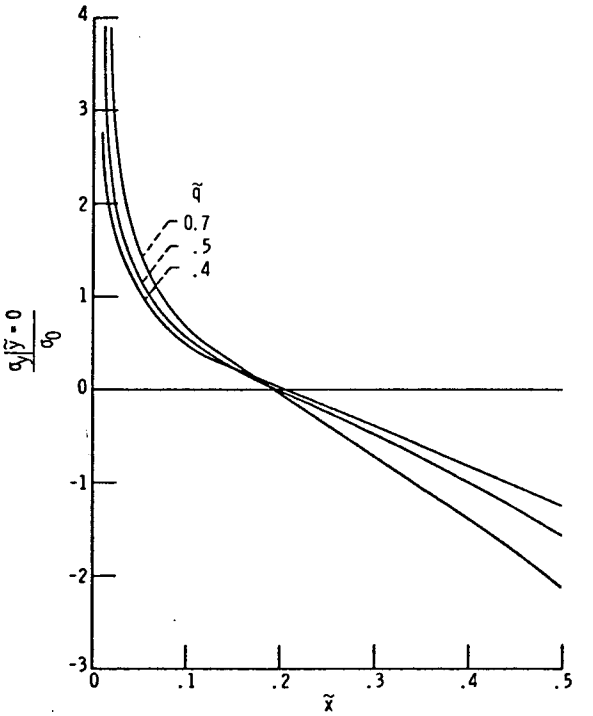

Fig. 33. Dimensionless y-directional stress distribution along x axis for a specimen with a 10^0 edge notch subjected to pure bending; plane strain, $\tilde{a} = 0.5$, $\alpha = 10^0$, $m = 0.05$, $\mu = 0.33$.

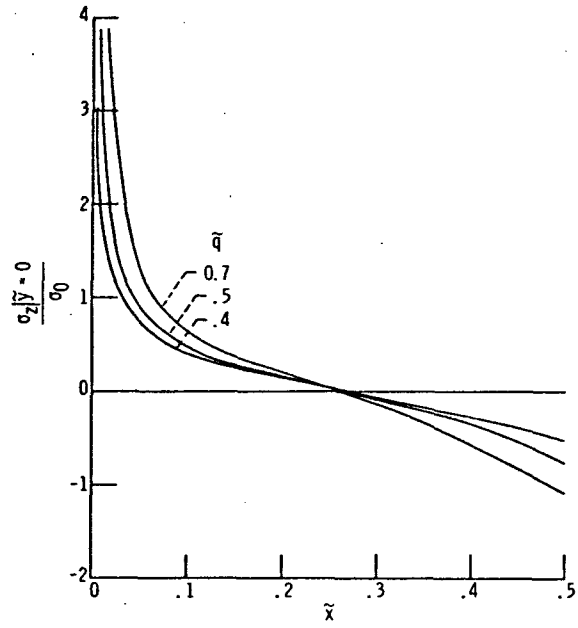

Fig. 34. Dimensionless z-directional stress distribution along x axis for a specimen with a 10^0 edge notch subjected to pure bending; plane strain, $\tilde{a} = 0.5$, $\alpha = 10^0$, $m = 0.05$, $\mu = 0.33$.

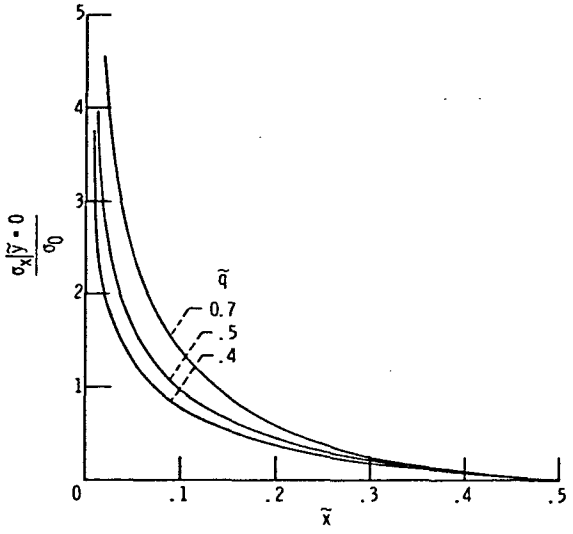

Fig. 35. Dimensionless x-directional stress distribution along x axis for a specimen with a 10^0 edge notch subjected to pure bending; plane strain, $\tilde{a} = 0.5$, $\alpha = 10^0$, $m = 0.10$, $\mu = 0.33$.

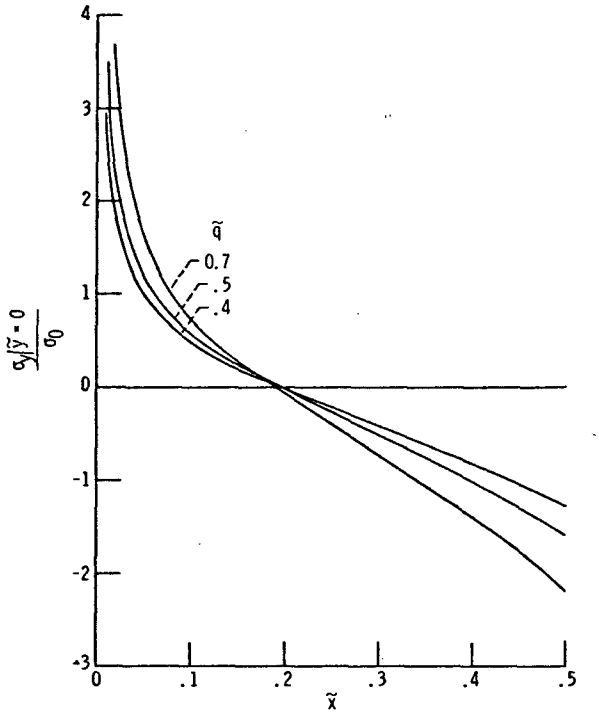

Fig. 36. Dimensionless y-directional stress distribution along x axis for a specimen with a 10^0 edge notch subjected to pure bending; plane strain, $\tilde{a} = 0.5$, $\alpha = 10^0$, $m = 0.10$, $\mu = 0.33$.

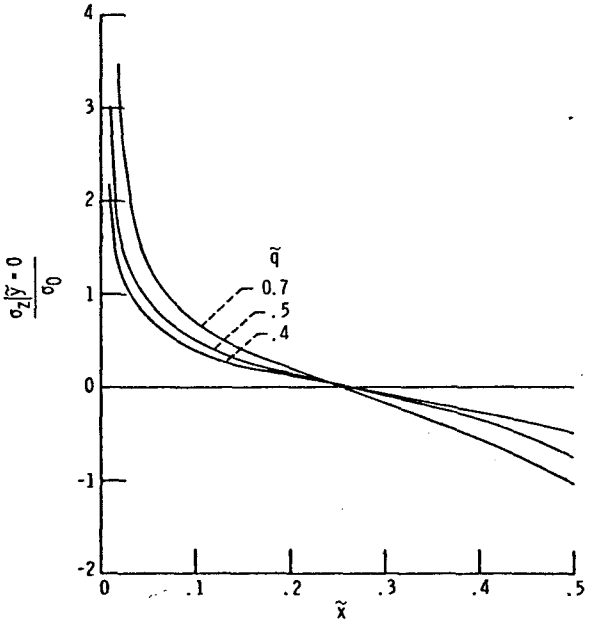

Fig. 37. Dimensionless z-directional stress distribution along x axis for a specimen with a 10^0 edge notch subjected to pure bending; plane strain, $\tilde{a} = 0.5$, $\alpha = 10^0$, $m = 0.10$, $\mu = 0.33$.

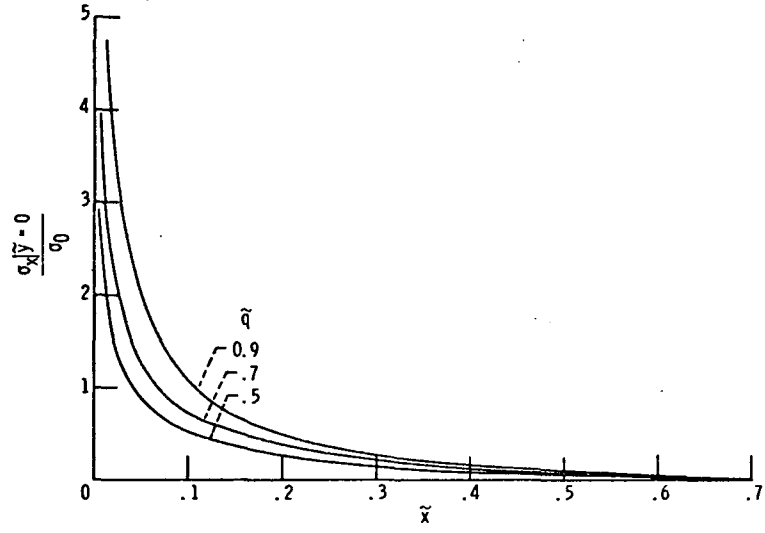

Fig. 38. Dimensionless x-directional stress distribution along x axis for a specimen with a 3^0 edge notch subjected to pure bending; plane strain, $\tilde{a} = 0.3$, $\alpha = 3^0$, $m = 0.10$, $\mu = 0.33$.

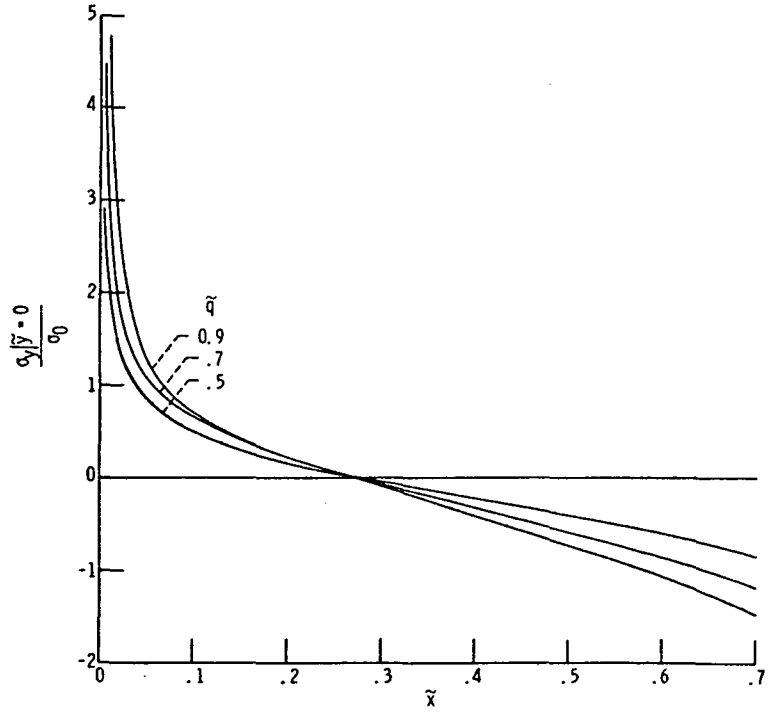

Fig. 39. Dimensionless y-directional stress distribution along x axis for a specimen with a 3^0 edge notch subjected to pure bending; plane strain, $\tilde{a} = 0.3$, $\alpha = 3^0$, $m = 0.10$, $\mu = 0.33$.

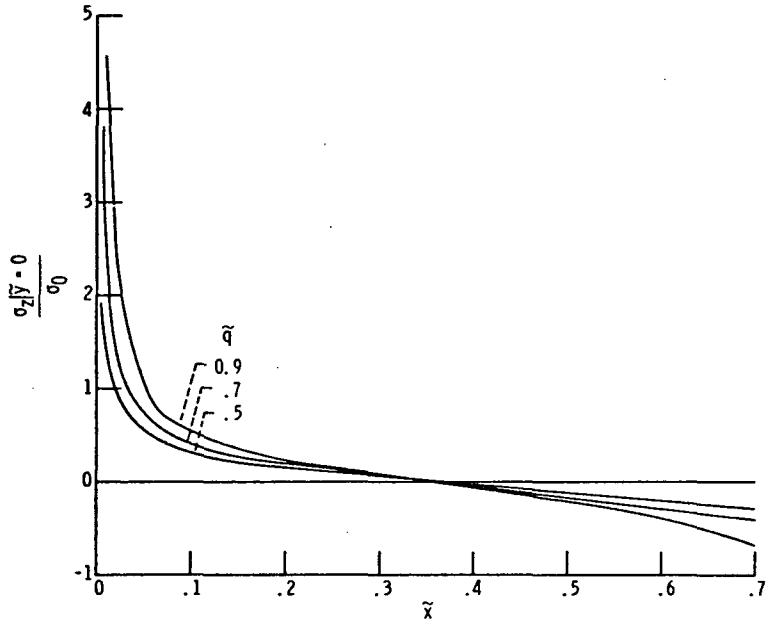

Fig. 40. Dimensionless z-directional stress distribution along x axis for a specimen with a 3^0 edge notch subjected to pure bending; plane strain, $\tilde{a} = 0.3$, $\alpha = 3^0$, $m = 0.10$, $\mu = 0.33$.

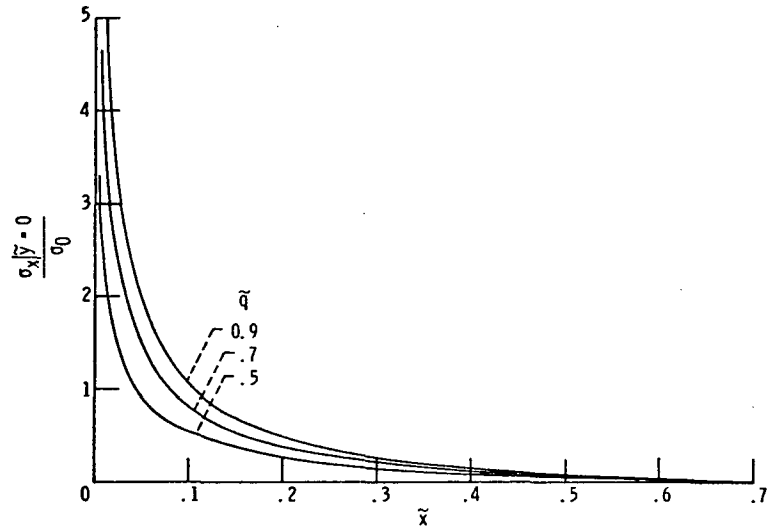

Fig. 41. Dimensionless x-directional stress distribution along x axis for a specimen with a 10^0 edge notch subjected to pure bending; plane strain, $\tilde{a} = 0.3$, $\alpha = 10^0$, $m = 0.10$, $\mu = 0.33$.

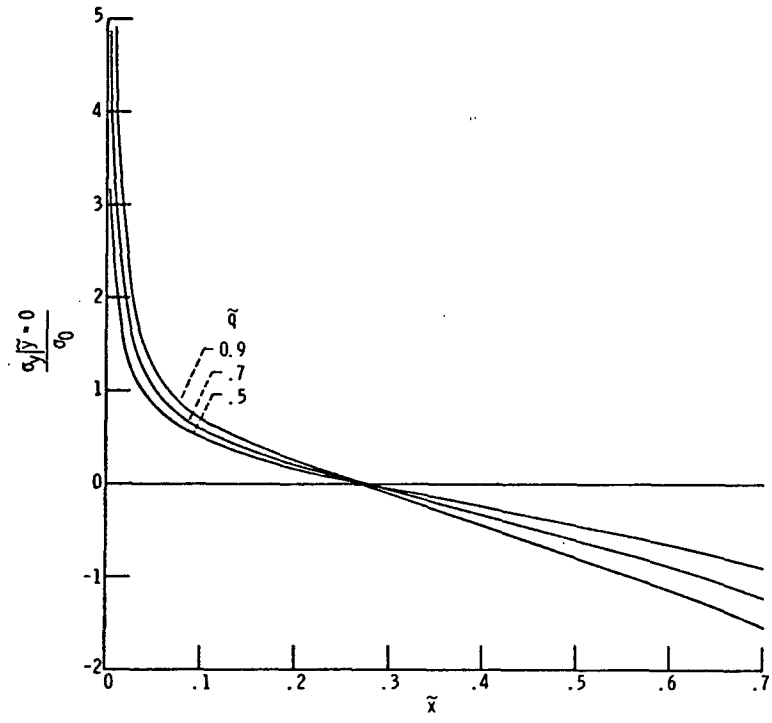

Fig. 42. Dimensionless y-directional stress distribution along x axis for a specimen with a 10^0 edge notch subjected to pure bending; plane strain, $\tilde{a} = 0.3$, $\alpha = 10^0$, $m = 0.10$, $\mu = 0.33$.

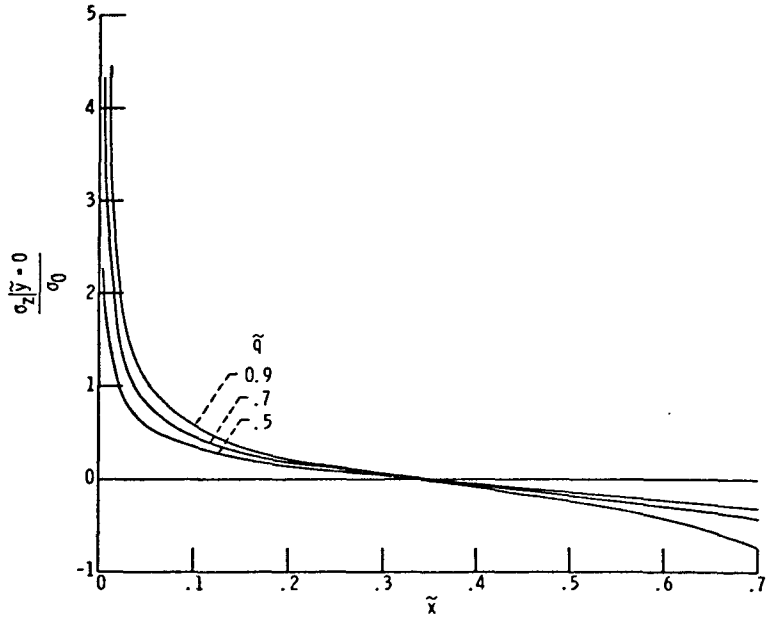

Fig. 43. Dimensionless z-directional stress distribution along x axis for a specimen with a 10^0 edge notch subjected to pure bending; plane strain, $\tilde{a} = 0.3$, $\alpha = 10^0$, $m = 0.10$, $\mu = 0.33$.

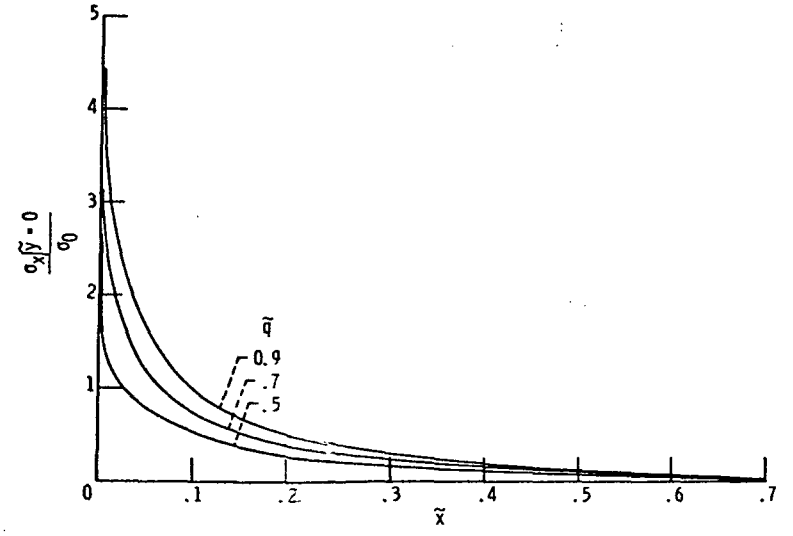

Fig. 44. Dimensionless x-directional stress distribution along x axis for a specimen with a 10^0 edge notch subjected to pure bending; plane stress, $\tilde{a} = 0.3$, $\alpha = 10^0$, $m = 0.10$, $\mu = 0.33$.

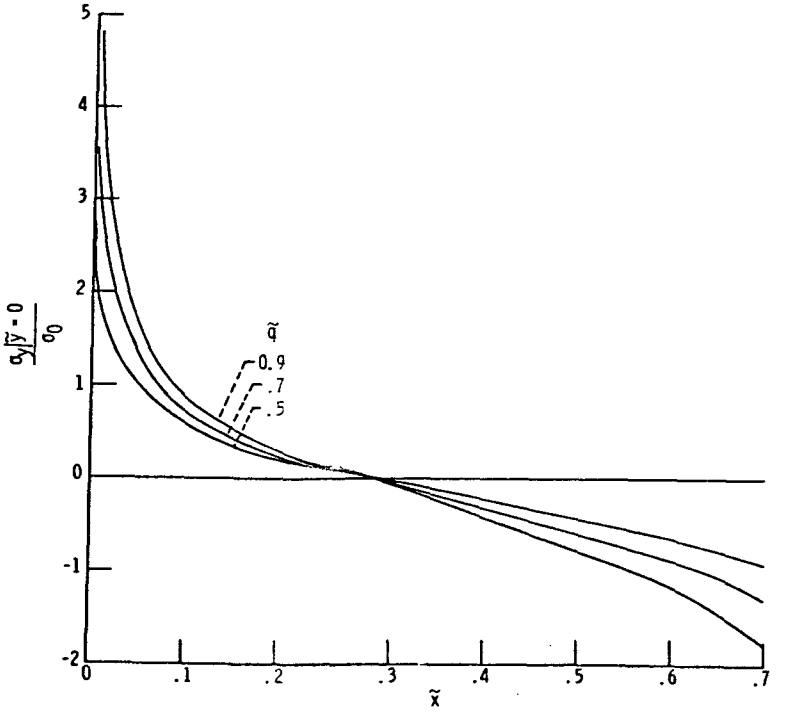

Fig. 45. Dimensionless y-directional stress distribution along x axis for a specimen with a 10^0 edge notch subjected to pure bending; plane stress, $\tilde{a} = 0.3$, $\alpha = 10^0$, $m = 0.10$, $\mu = 0.33$.

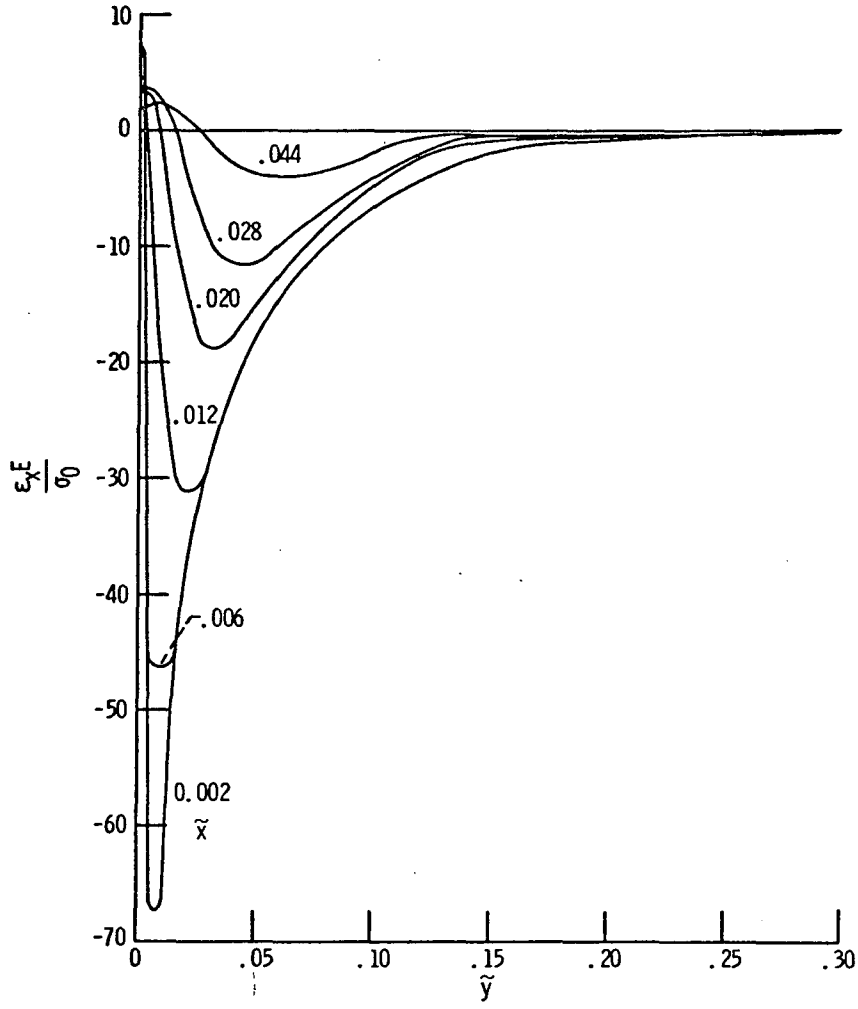

Fig. 46. Dimensionless x-directional total strain distribution along $\tilde{x}$ = const. lines in the vicinity of the notch for a specimen with a 10^0 edge notch subjected to pure bending; plane strain, $\tilde{q} = 0.7$, $\tilde{a} = 0.5$, $\alpha = 10^0$, $m = 0.05$, $\mu = 0.33$.

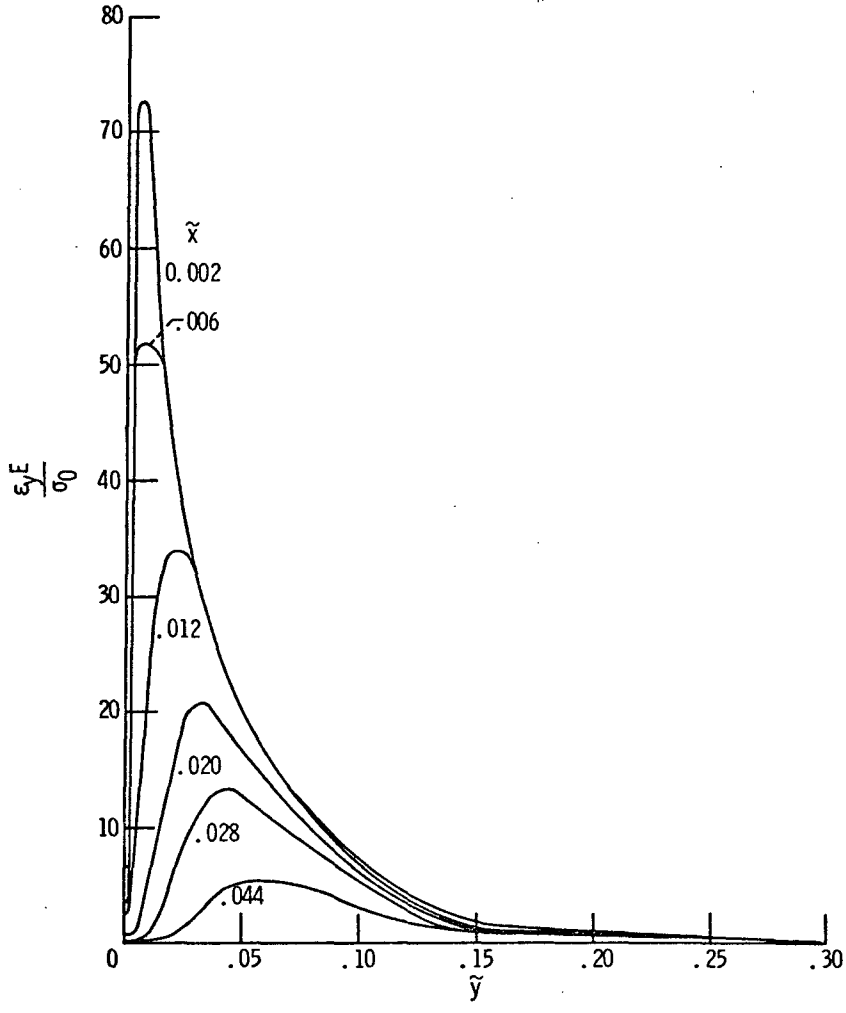

Fig. 47. Dimensionless y-directional total strain distribution along $\tilde{x}$ = const. lines in the vicinity of the notch for a specimen with a 10^0 edge notch subjected to pure bending; plane strain, $\tilde{q} = 0.7$, $\tilde{a} = 0.5$, $\alpha = 10^0$, $m = 0.05$, $\mu = 0.33$.

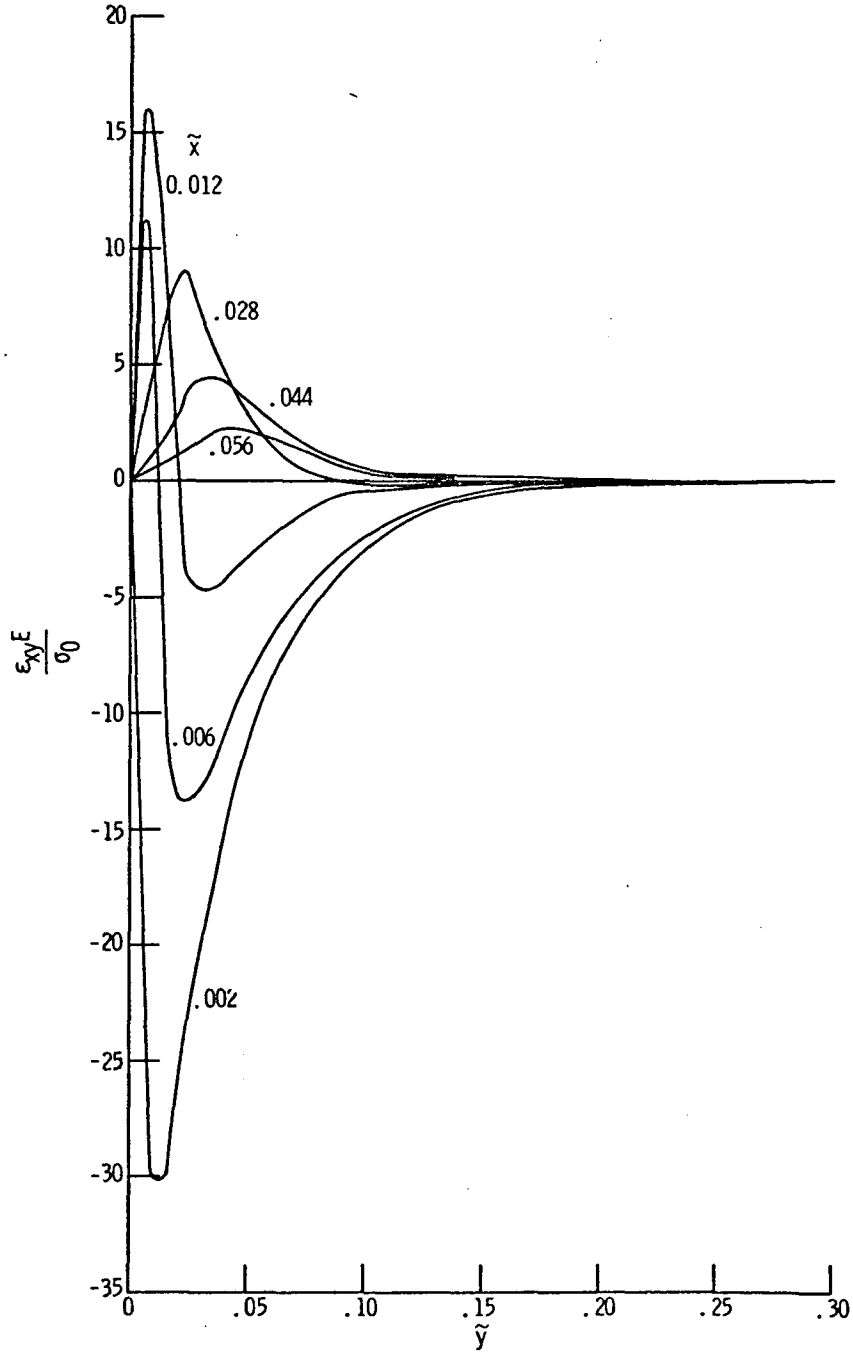

Fig. 48. Dimensionless total shear strain distribution along $\tilde{x}$ = const. lines in the vicinity of the notch for a specimen with a 10^0 edge notch subjected to pure bending; plane strain, $\tilde{q} = 0.7$, $\tilde{a} = 0.5$, $\alpha = 10^0$, $m = 0.05$, $\mu = 0.33$.

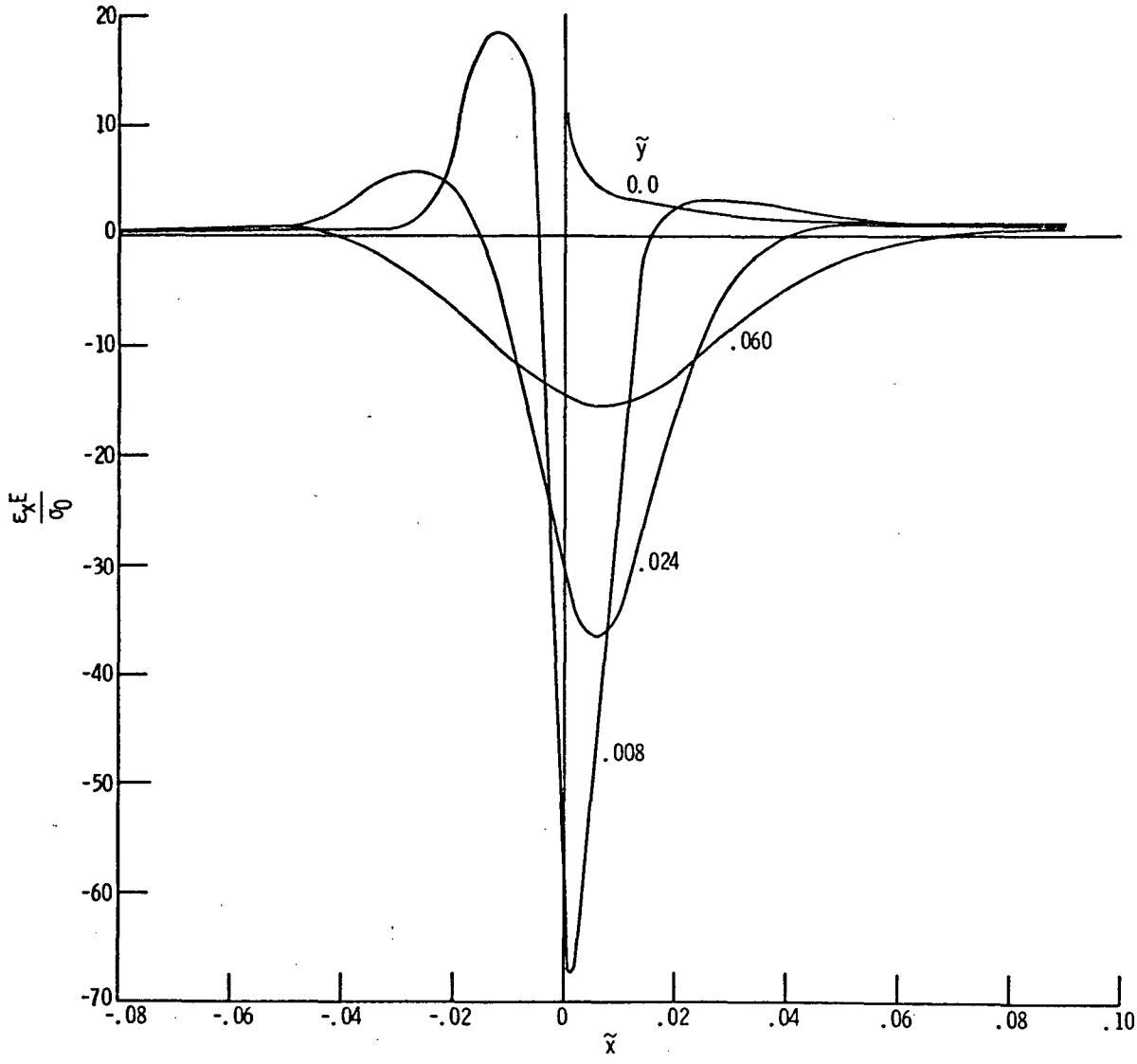

Fig. 49. Dimensionless x-directional total strain distribution along $\tilde{y}$ = const. lines in the vicinity of the notch for a specimen with a 10^0 edge notch subjected to pure bending; plane strain, $\tilde{q} = 0.7$, $\tilde{a} = 0.5$, $\alpha = 10^0$, $m = 0.05$, $\mu = 0.33$.

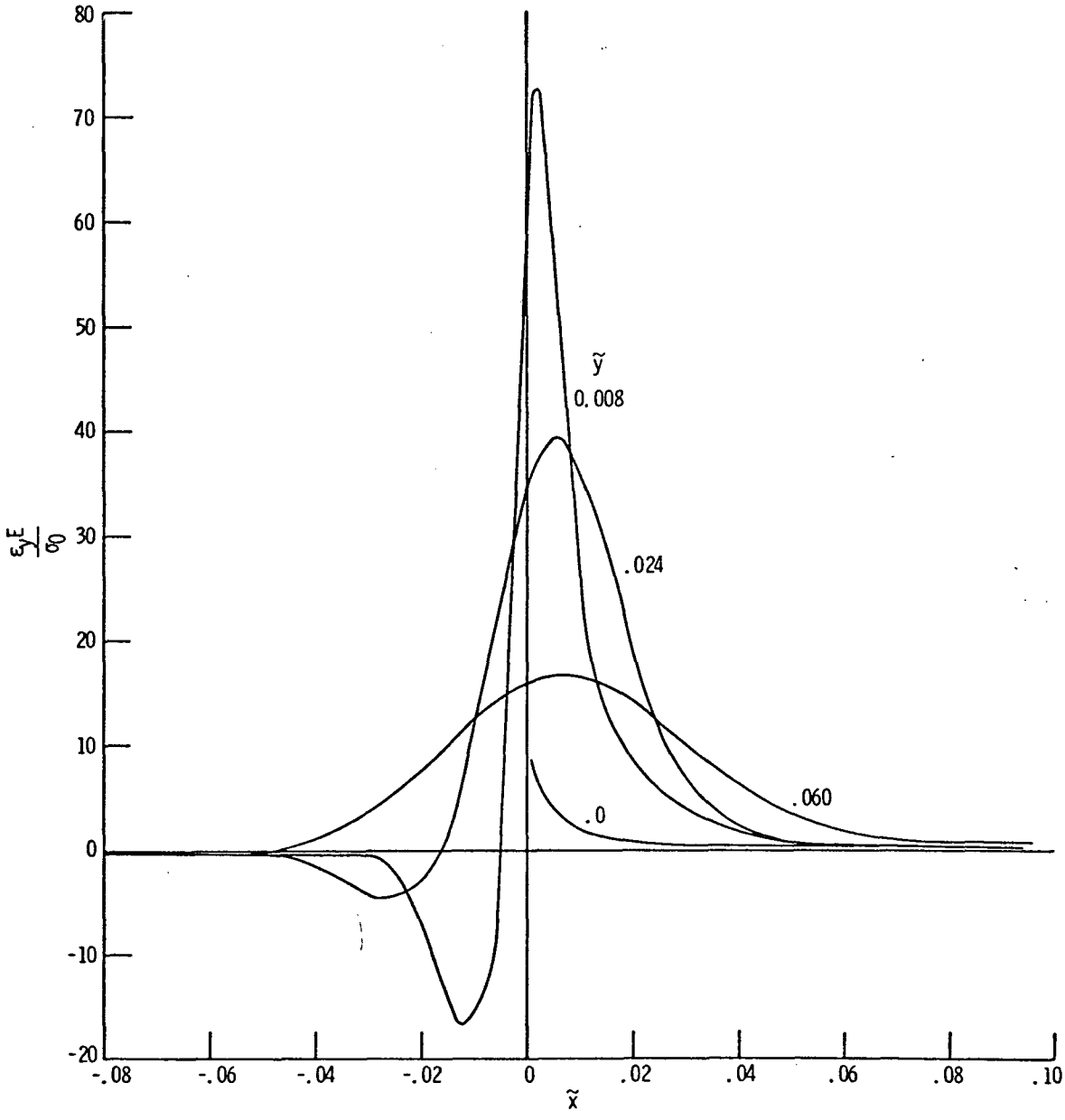

Fig. 50. Dimensionless y-directional total strain distribution along $\tilde{y}$ = const. lines in the vicinity of the notch for a specimen with a 10^0 edge notch subjected to pure bending; plane strain, $\tilde{q} = 0.7$, $\tilde{a} = 0.5$, $\alpha = 10^0$, $m = 0.05$, $\mu = 0.33$.

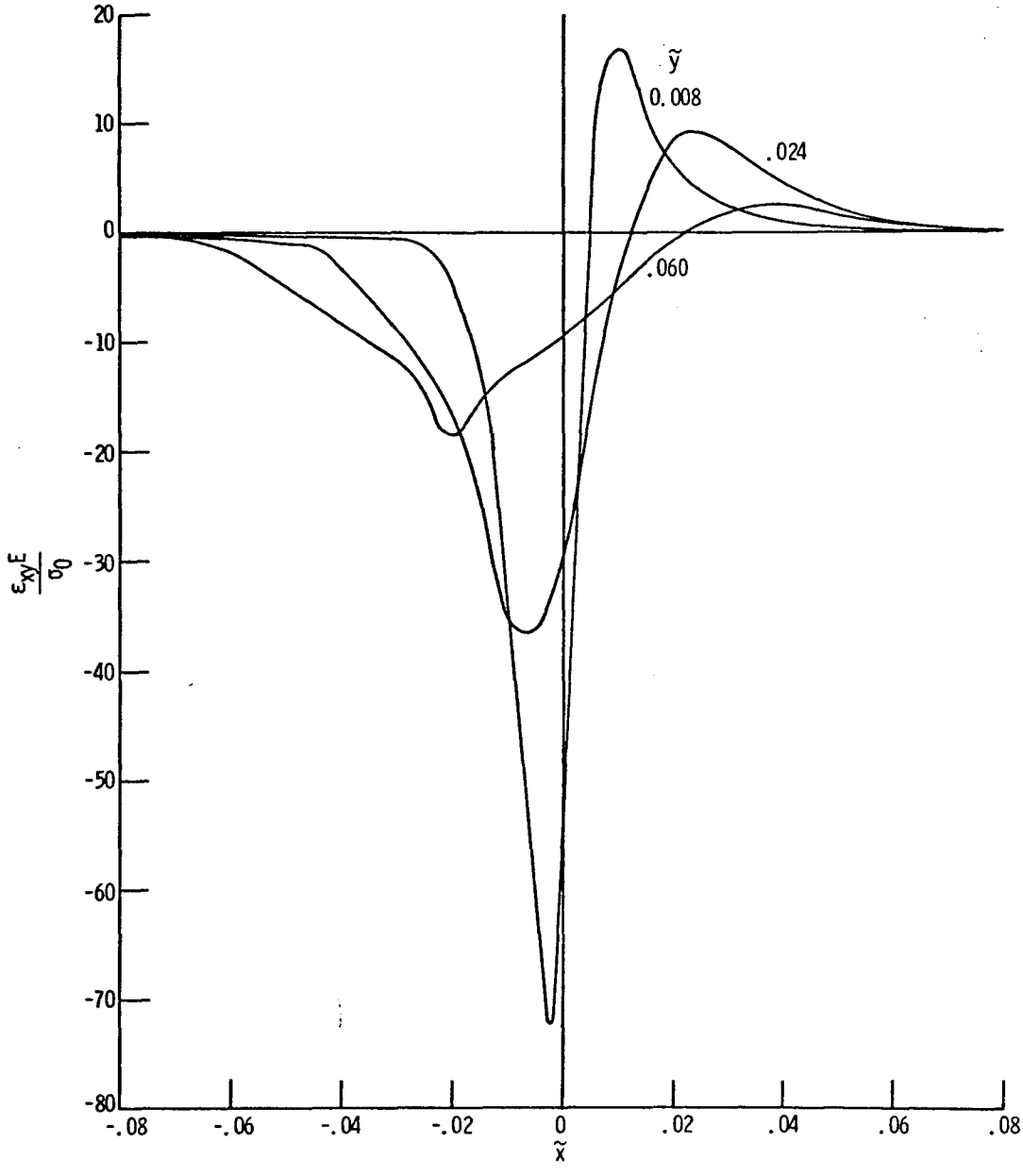

Fig. 51. Dimensionless total shear strain distribution along $\tilde{y}$ = const. lines in the vicinity of the notch for a specimen with a 10^0 edge notch subjected to pure bending; plane strain, $\tilde{q} = 0.7$, $\tilde{a} = 0.5$, $\alpha = 10^0$, $m = 0.05$, $\mu = 0.33$.

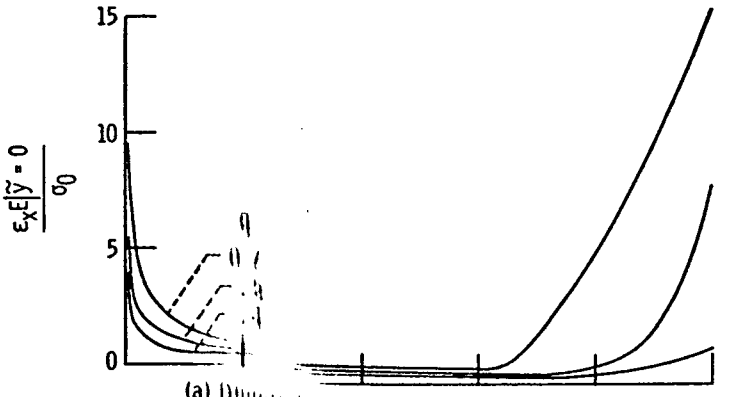

Fig. 52. Dimensionless x-directional and y-directional total strain distribution along x axis for a specimen with a 10^0 edge notch subjected to pure bending; plane strain, $\tilde{q} = 0.5$, $\alpha = 10^0$, $m = 0.05$, $\mu = 0.33$.

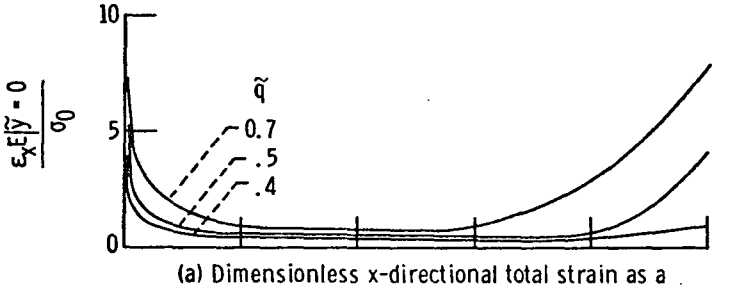

(a) Dimensionless x-directional total strain as a function of $\tilde{x}$

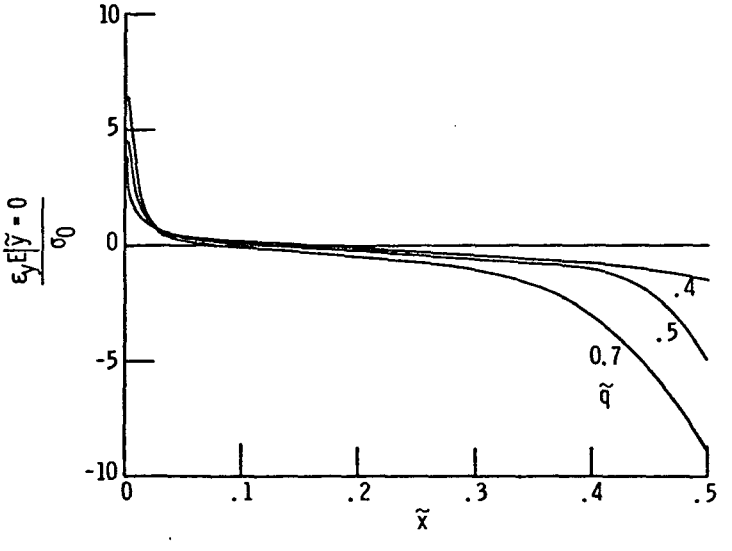

(b) Dimensionless y-directional total strain as a function of $\tilde{x}$

Fig. 53. Dimensionless x-directional and y-directional total strain distribution along x axis for a specimen with a 10^0 edge notch subjected to pure bending; plane strain, $\tilde{a} = 0.5$, $\alpha = 10^0$, $m = 0.10$, $\mu = 0.33$.

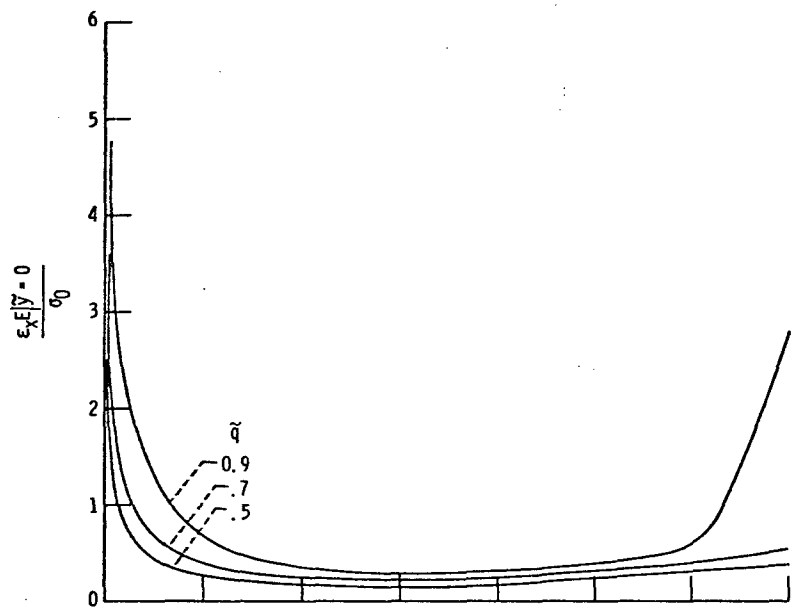

(a) Dimensionless x-directional total strain as a function of $\tilde{x}$.

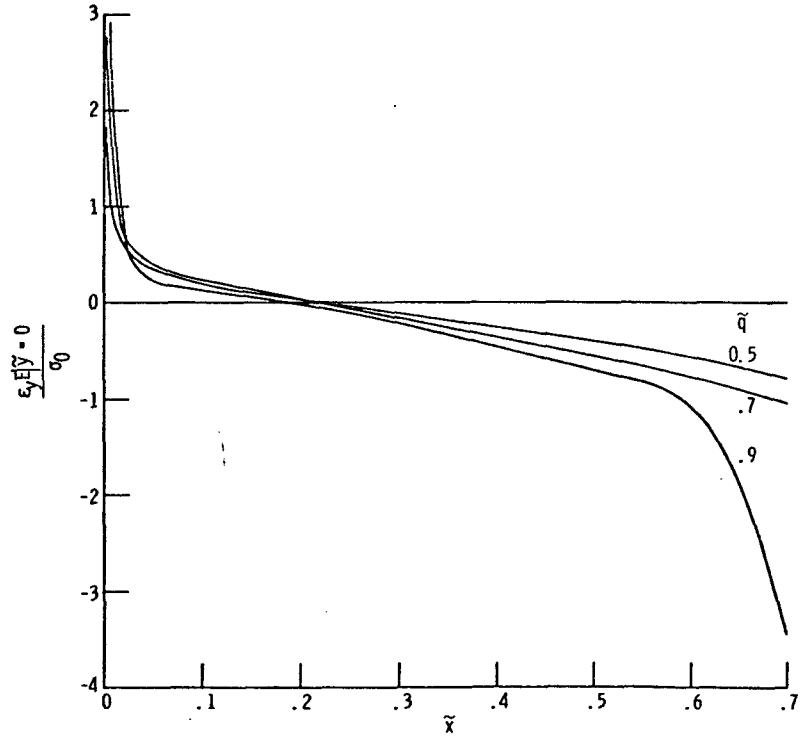

(b) Dimensionless y-directional total strain as a function of $\tilde{x}$.

Fig. 54. Dimensional x-directional and y-directional total strain distribution along x axis for a specimen with a 3^0 edge notch subjected to pure bending; plane strain, $\tilde{a} = 0.3$, $\alpha = 3^0$, $m = 0.10$, $\mu = 0.33$.

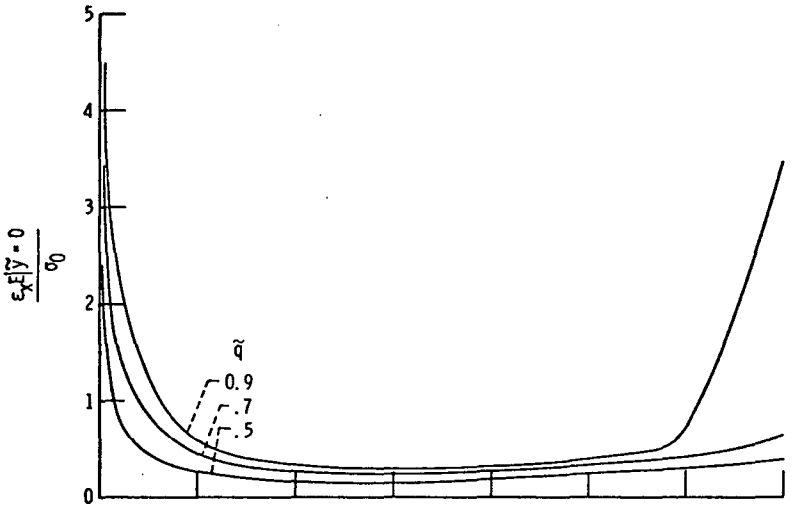

(a) Dimensionless x-directional total strain as a function of $\tilde{x}$.

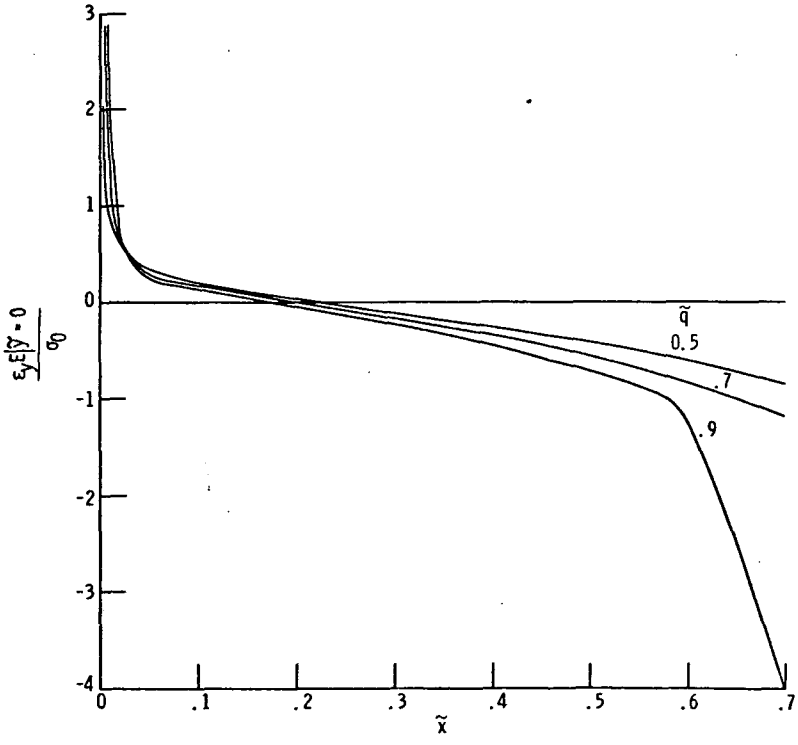

(b) Dimensionless y-directional total strain as a function of $\tilde{x}$.

Fig. 55. Dimensionless x-directional and y-directional total strain distribution along x axis for a specimen with a 10^0 edge notch subjected to pure bending; plane strain, $\tilde{a} = 0.3$, $\alpha = 10^0$, $m = 0.10$, $\mu = 0.33$.

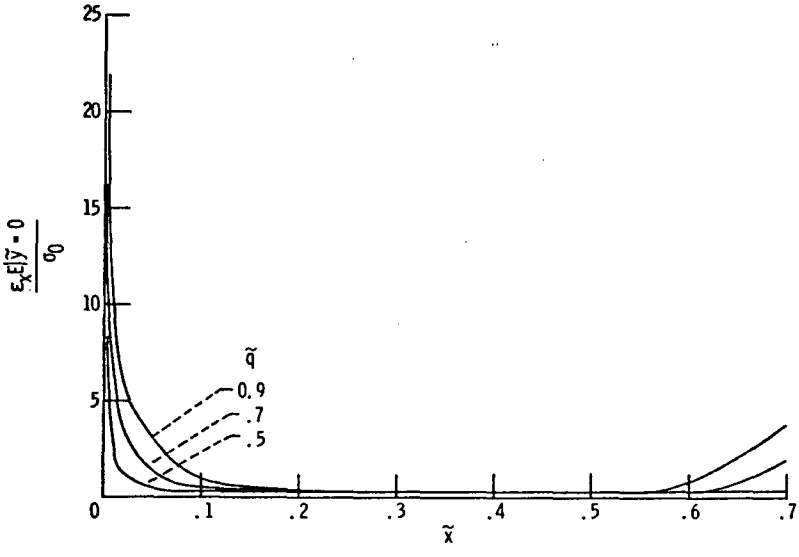

Fig. 56. Dimensionless x-directional total strain distribution along x axis for a specimen with a 10^0 edge notch subjected to pure bending; plane stress, $\tilde{a} = 0.3$, $\alpha = 10^0$, $m = 0.10$, $\mu = 0.33$.

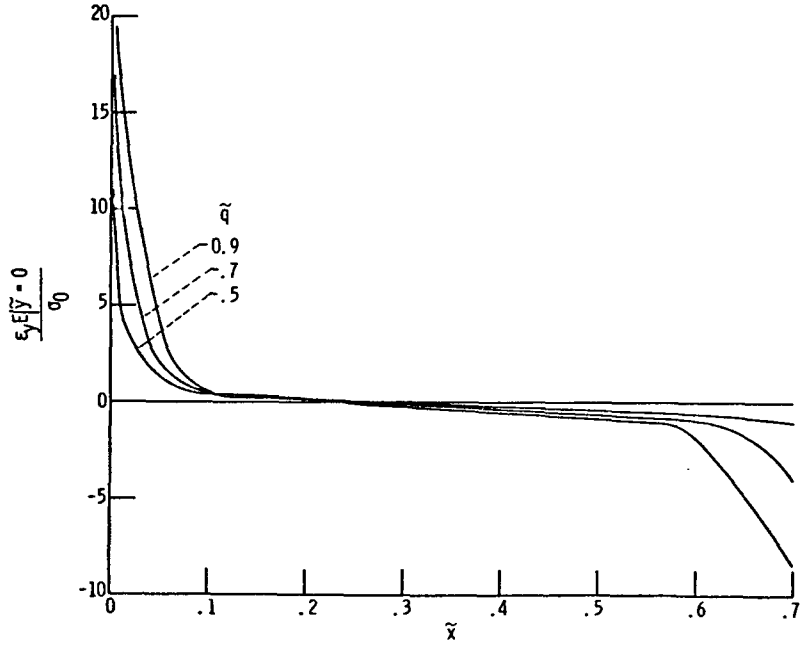

Fig. 57. Dimensionless y-directional total strain distribution along x axis for a specimen with a 10^0 edge notch subjected to pure bending; plane stress, $\tilde{a} = 0.3$, $\alpha = 10^0$, $m = 0.10$, $\mu = 0.33$.

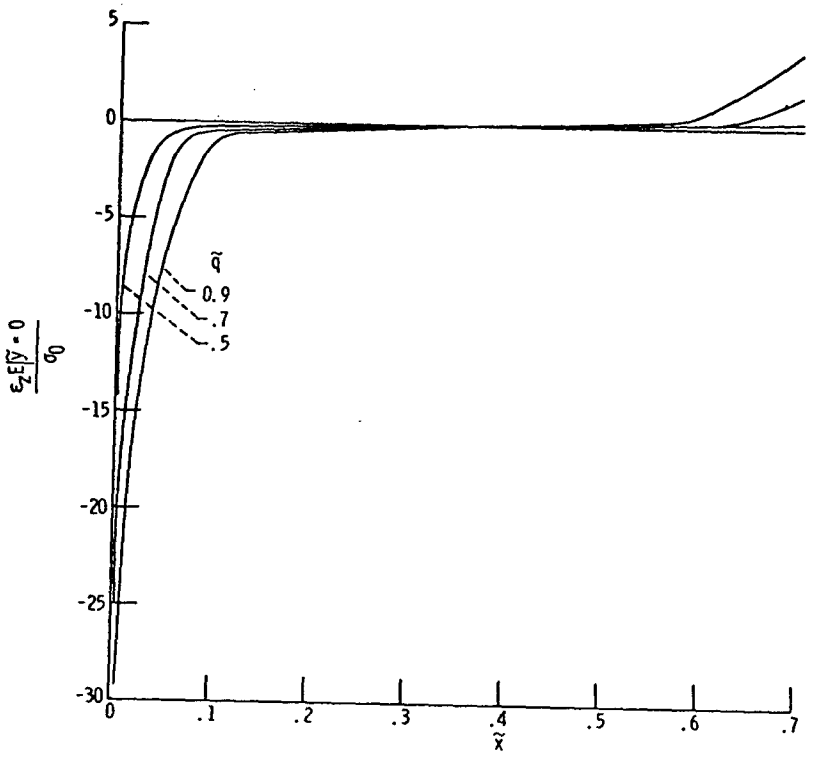

Fig. 58. Dimensionless z-directional total strain distribution along x axis for a specimen with a 10^0 edge notch subjected to pure bending; plane stress, $\tilde{a} = 0.3$, $\alpha = 10^0$, $m = 0.10$, $\mu = 0.33$.

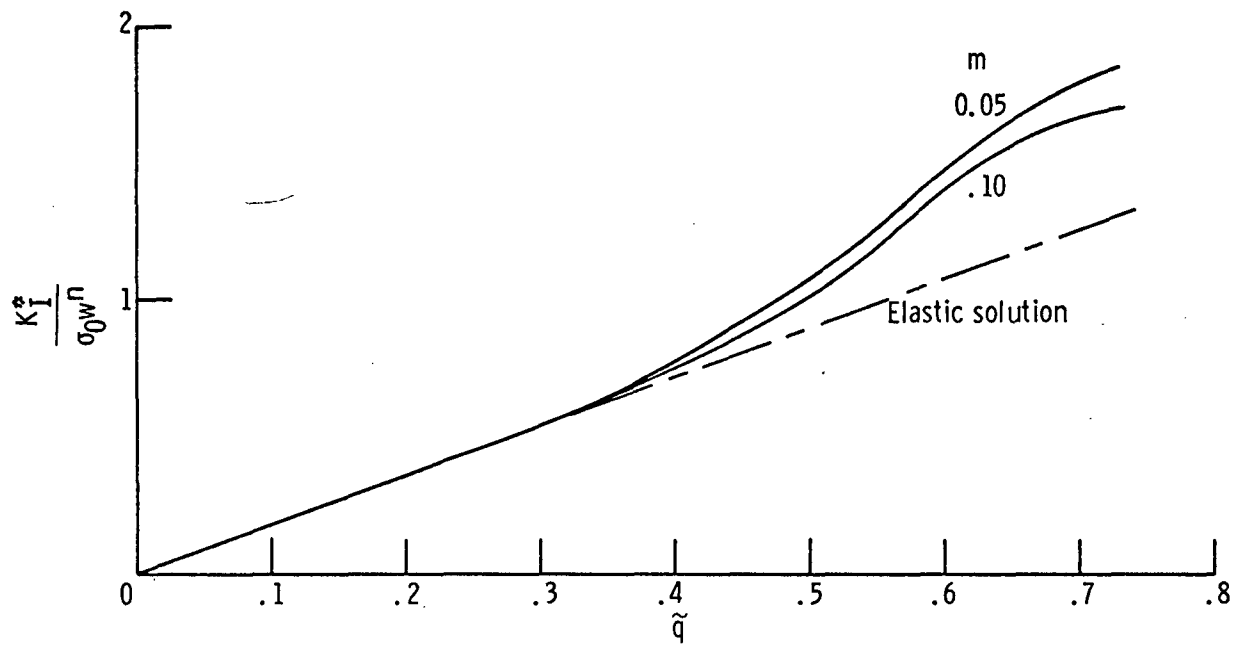

Fig. 59. Variation of dimensionless generalized stress intensity factor with load for a specimen with a 10^0 edge notch subjected to pure bending; plane strain, $\tilde{a} = 0.5$, $\alpha = 10^0$, $\mu = 0.33$.

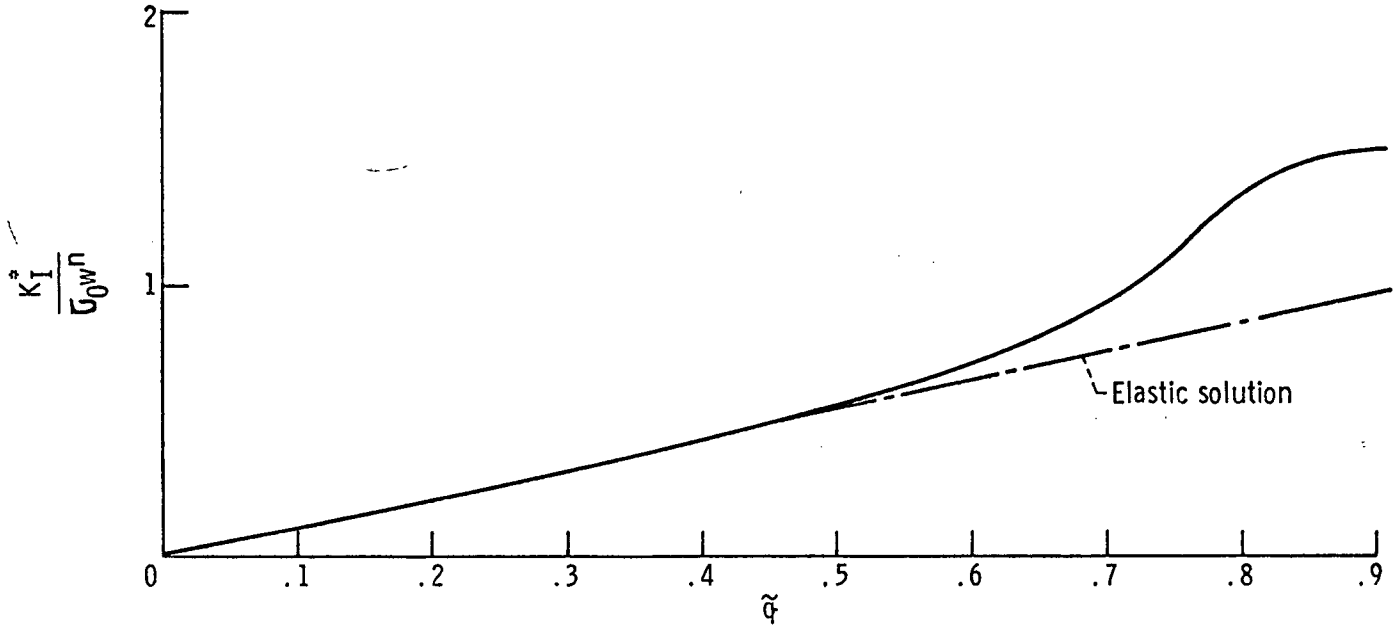

Fig. 60 Variation of dimensionless generalized stress intensity factor with load for a specimen with a 3^0 edge notch subjected to pure bending; plane strain, $\tilde{a} = 0.3$, $\alpha = 3^0$, $m = 0.10$, $\mu = 0.33$.

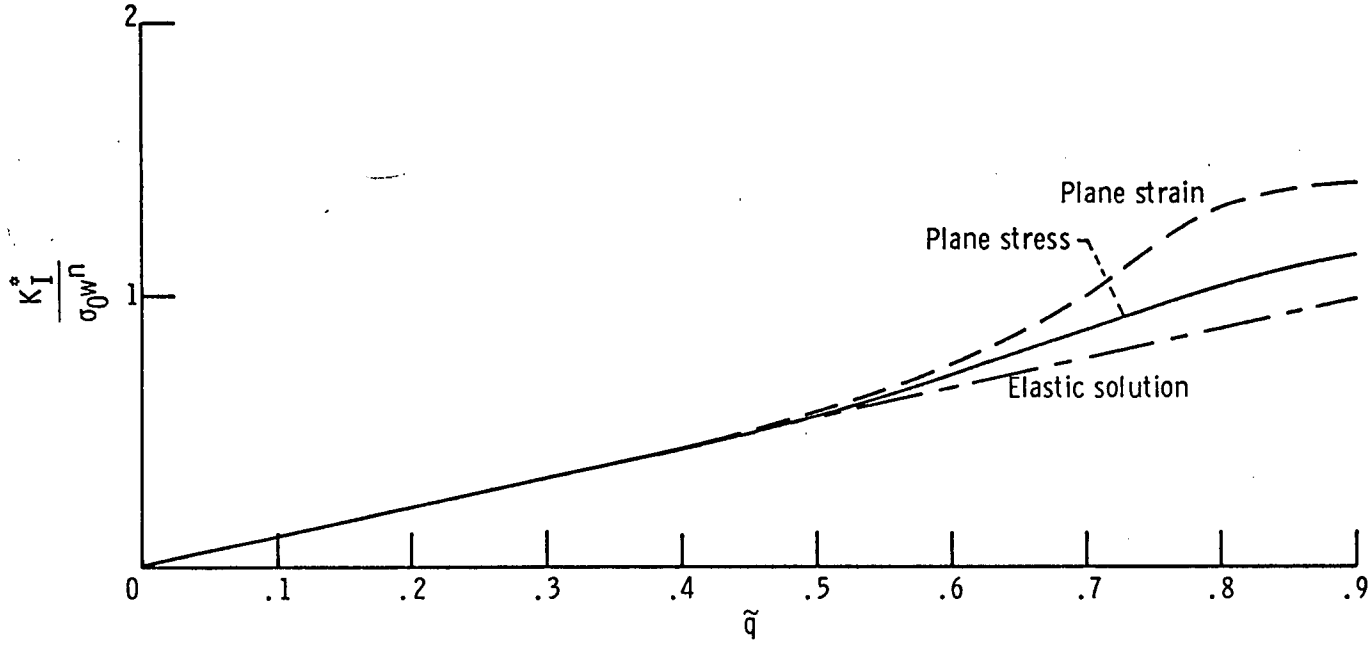

Fig. 61. Variation of dimensionless generalized stress intensity factor with load for a specimen with a 10^0 edge notch subjected to pure bending; $\tilde{a} = 0.3$, $\alpha = 10^0$, $m = 0.10$, $\mu = 0.33$.

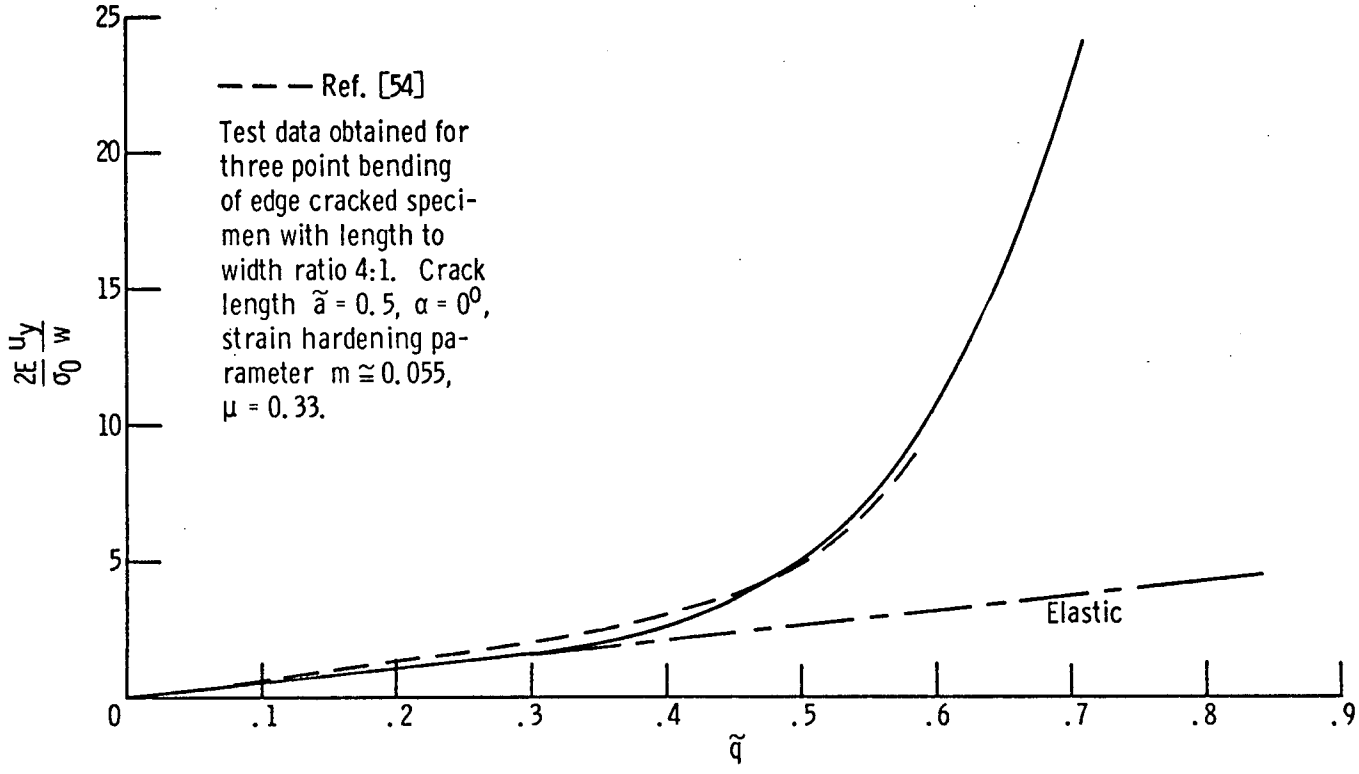

Fig. 62. Dimensionless plane strain y-directional notch opening displacement for a specimen with a 10^0 edge notch subjected to pure bending; $\tilde{a} = 0.5$, $\alpha = 10^0$, $m = 0.05$, $\mu = 0.33$.

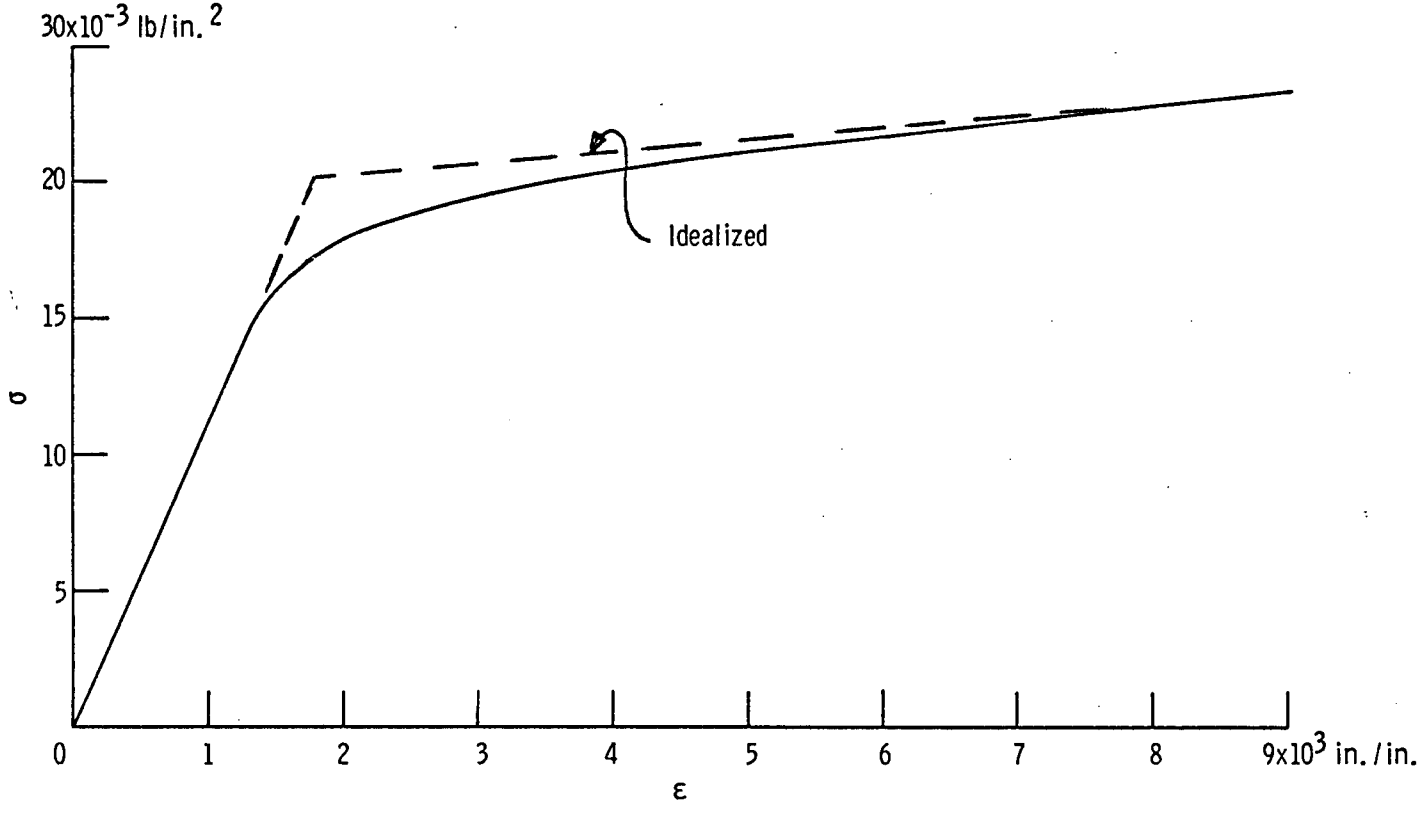

Fig. 63. Stress-strain curve for Al 5083-0 used in test Ref. [54]; E = 10.8 x 10^6 lb/in.^{2}, μ = 0.33.

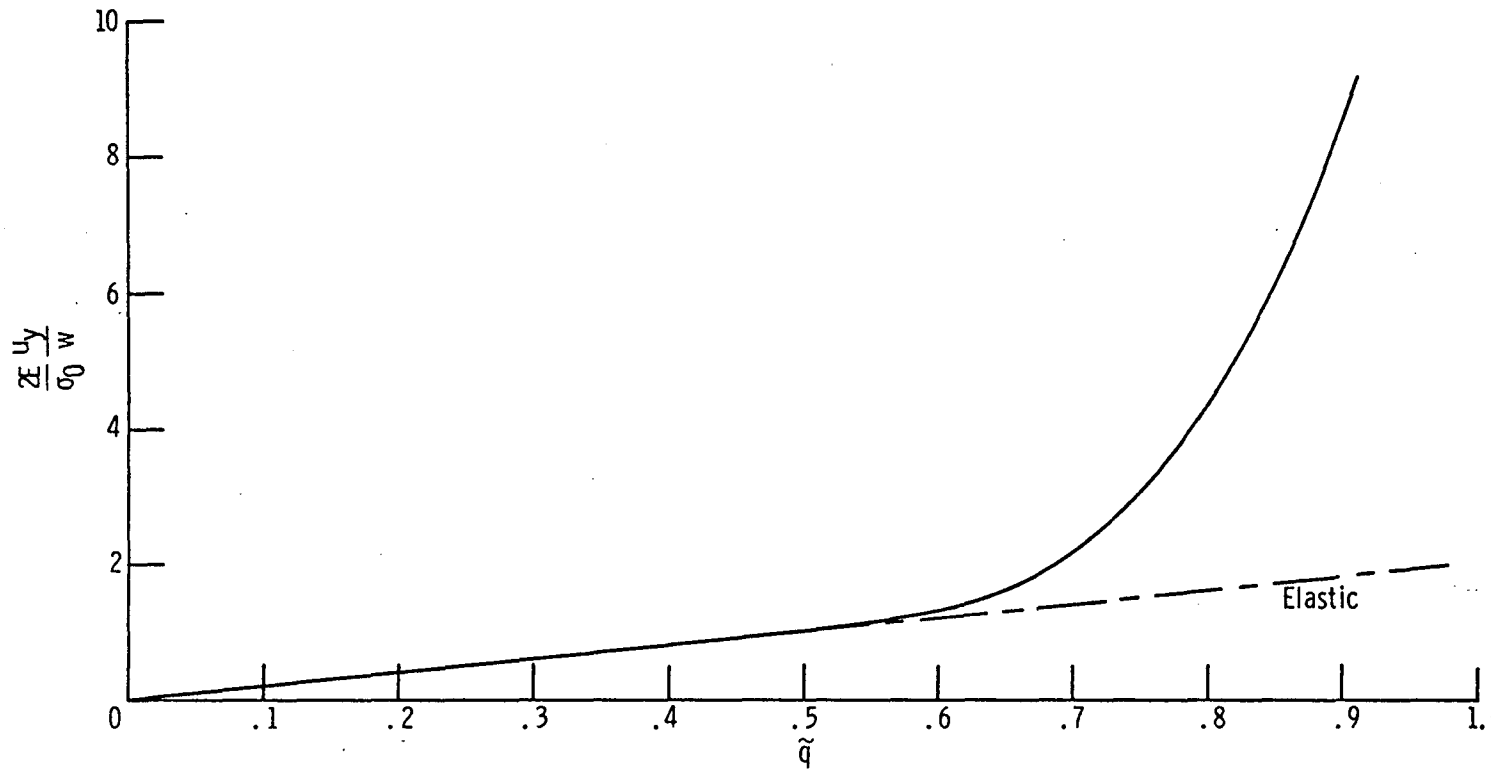

Fig. 64. Dimensionless plane strain y-directional notch opening displacement for a specimen with a 10^0 edge notch subjected to pure bending; $\tilde{a} = 0.3$, $\alpha = 10^0$, $m = 0.10$, $\mu = 0.33$.

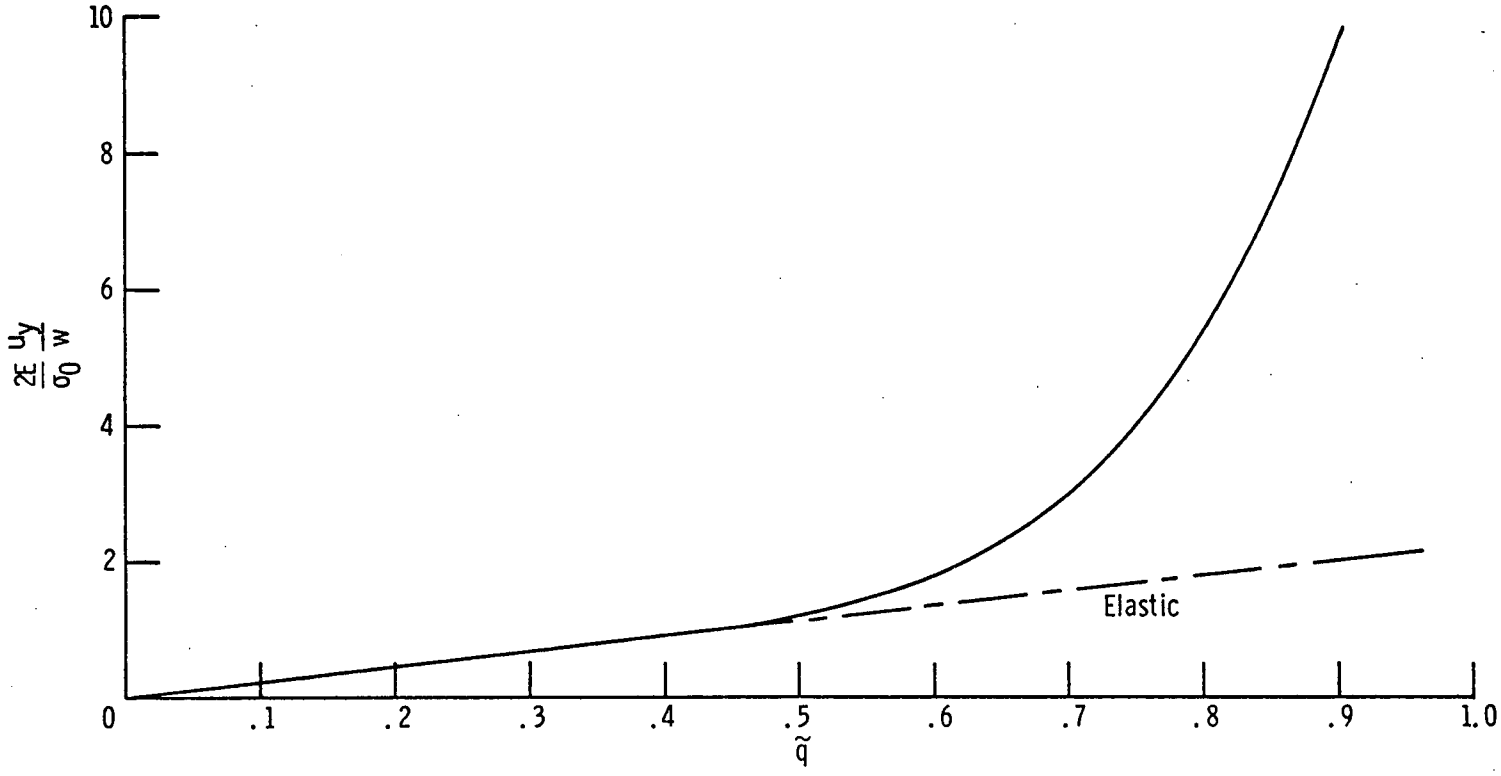

Fig. 65. Dimensionless plane stress y-directional notch opening displacement for a specimen with a 10^0 edge notch subjected to pure bending; $\tilde{a} = 0.3$, $\alpha = 10^0$, $m = 0.10$, $\mu = 0.33$.

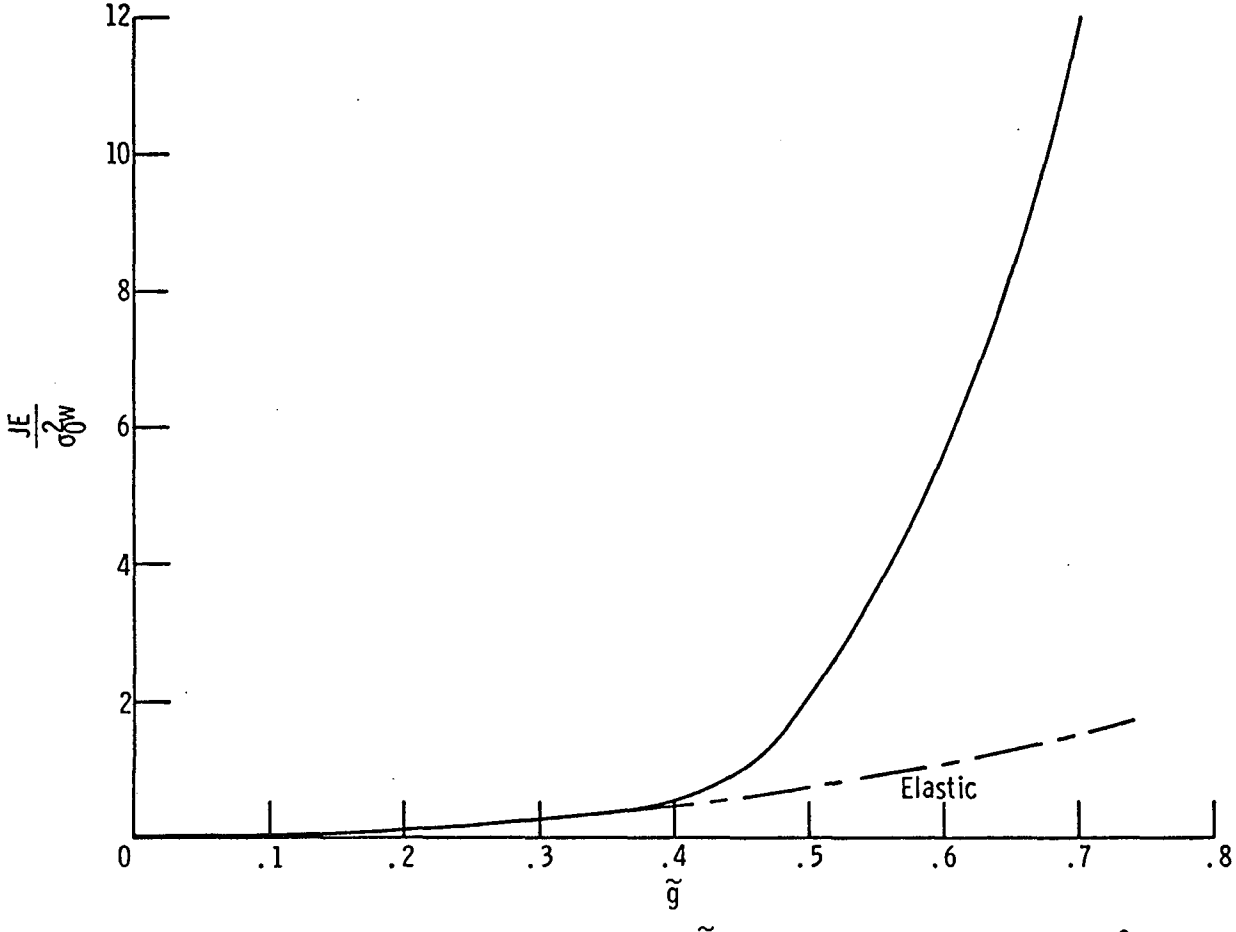

Fig. 66. Dimensionless plane strain Rice's $\tilde{J}$ integral for a specimen with a 10^0 edge notch subjected to pure bending; $\tilde{a} = 0.5$, $\alpha = 10^0$, $m = 0.05$, $\mu = 0.33$.

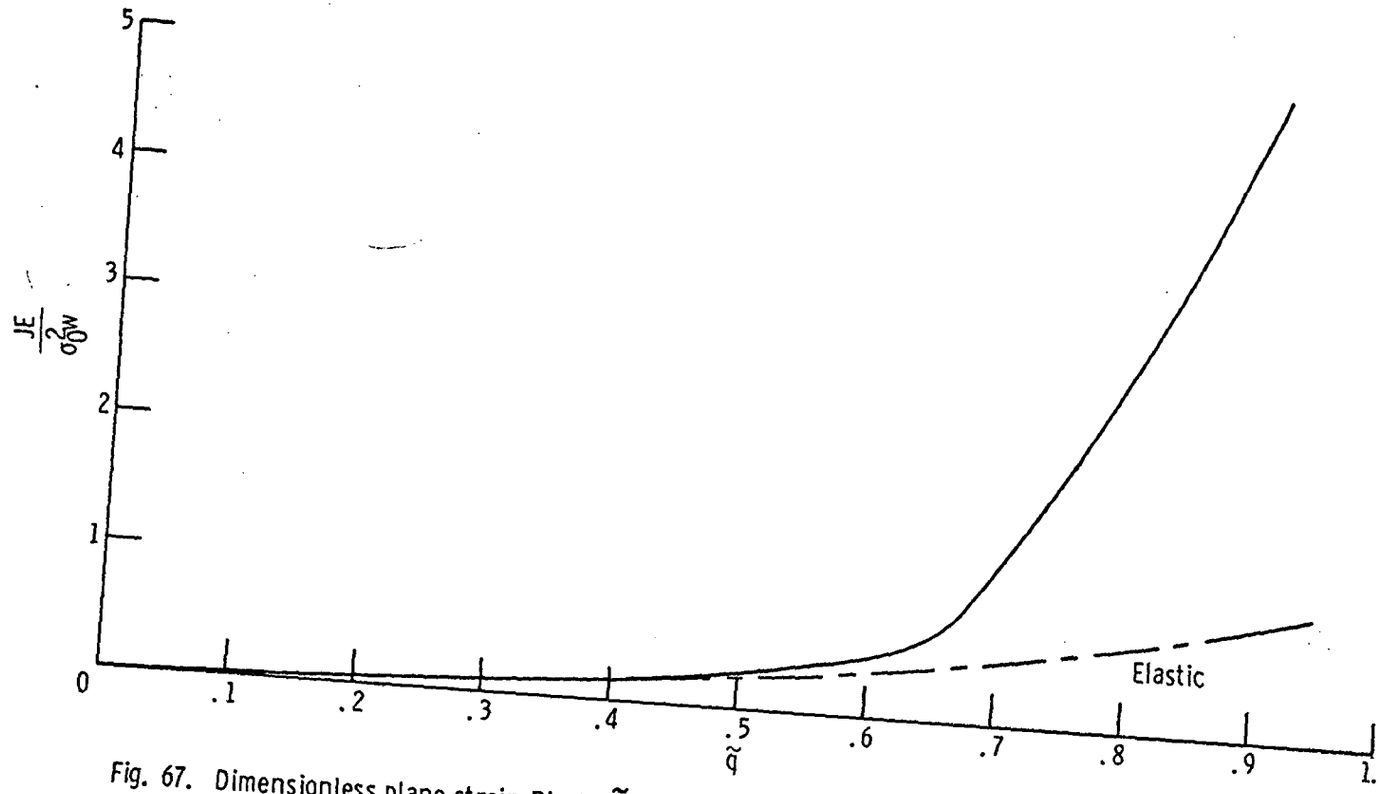

Fig. 67. Dimensionless plane strain Rice's $\tilde{J}$ integral for a specimen with a 10^0 edge notch subjected to pure bending; $\tilde{a} = 0.3$, $\alpha = 10^0$, $m = 0.10$, $\mu = 0.33$.

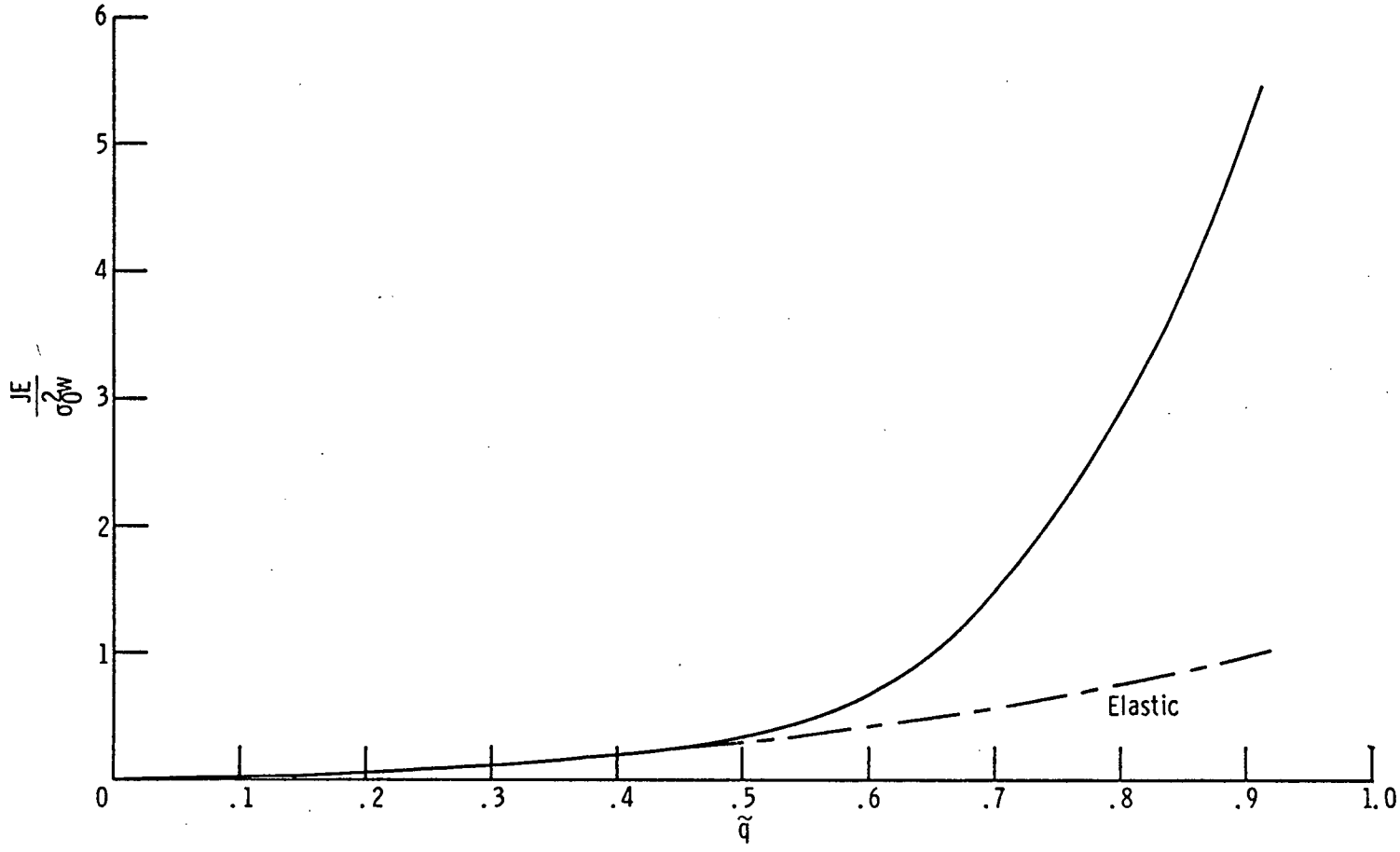

Fig. 68. Dimensionless plane stress Rice's $\tilde{J}$ integral for a specimen with a 10^0 edge notch subjected to pure bending; $\tilde{a} = 0.3$, $\alpha = 10^0$, $m = 0.10$, $\mu = 0.33$.

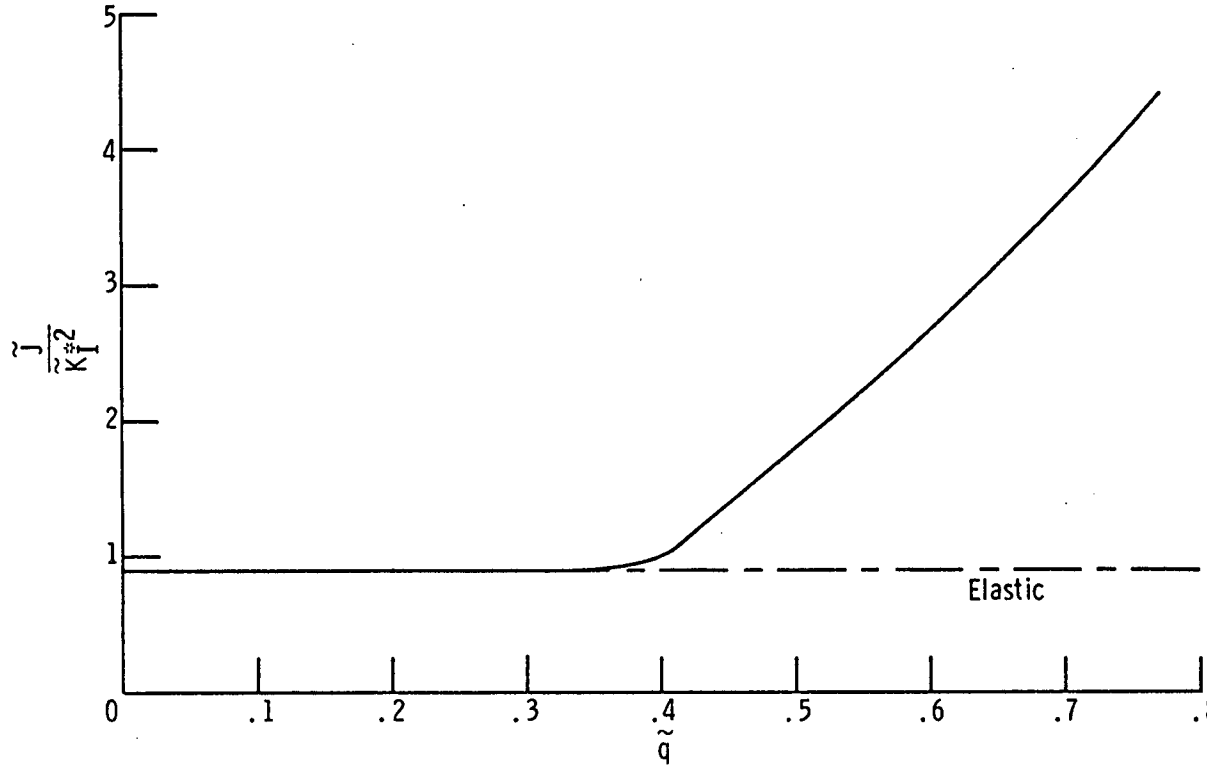

Fig. 69. Variation of the ratio of dimensionless Rice's $\tilde{J}$ integral to the square of dimensionless generalized stress intensity factor $\tilde{K}_I^{*2}$ with load for a specimen with a 10^0 edge notch subjected to pure bending; plane strain, $\tilde{a} = 0.5$, $\alpha = 10^0$, $m = 0.05$, $\mu = 0.33$.

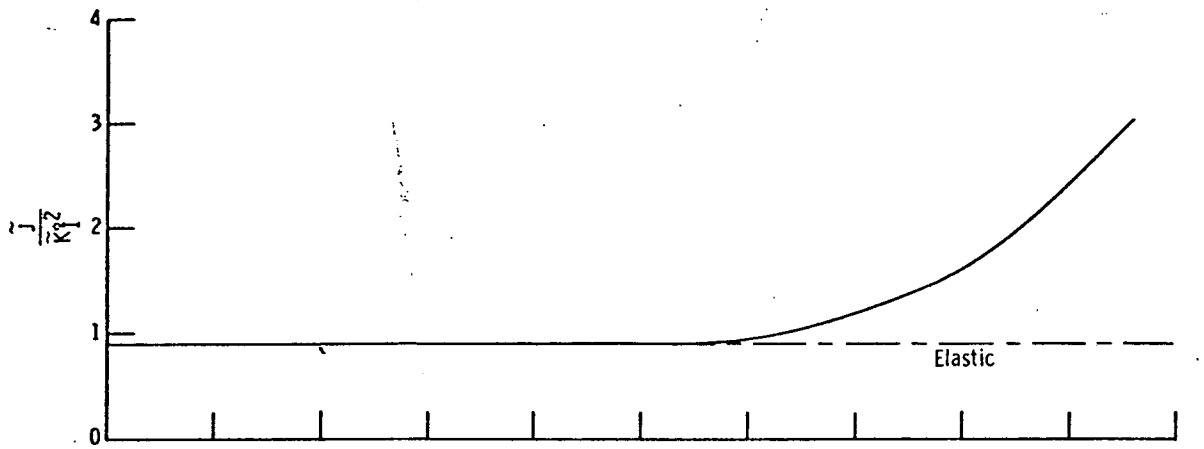

(a) Plane strain condition.

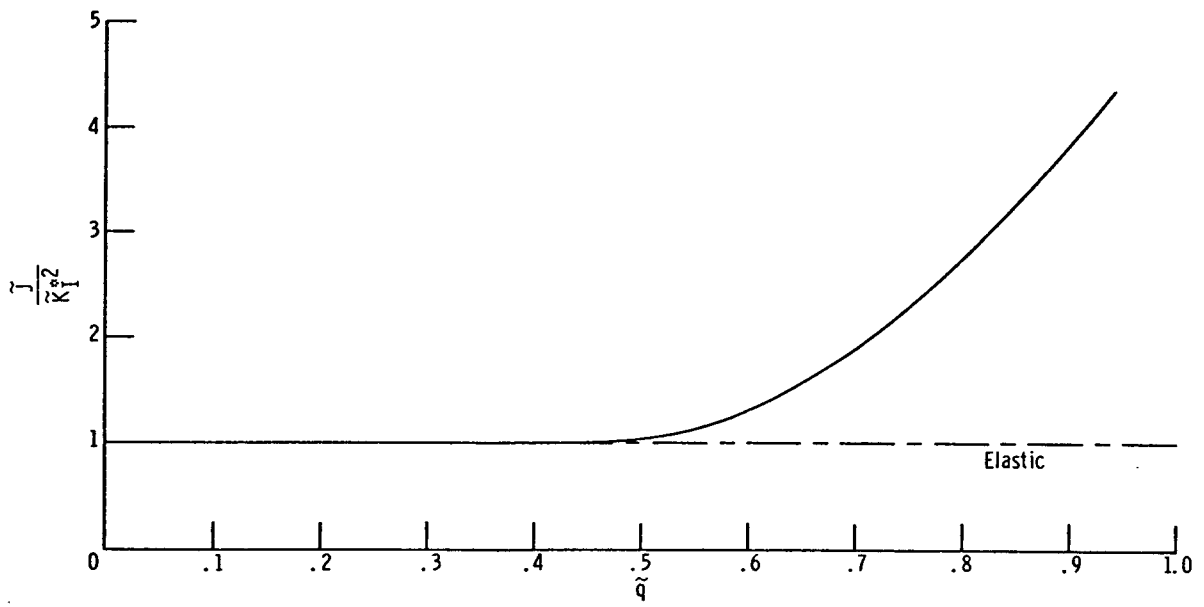

(b) Plane stress condition.

Fig. 70. Variation of the ratio of dimensionless Rice's $\tilde{J}$ integral to the square of dimensionless generalized stress intensity factor $\tilde{K}_I^{*2}$ with load for a specimen with a 10^0 edge notch subjected to pure bending; $\tilde{a} = 0.3$, $\alpha = 10^0$, $m = 0.10$, $\mu = 0.33$.

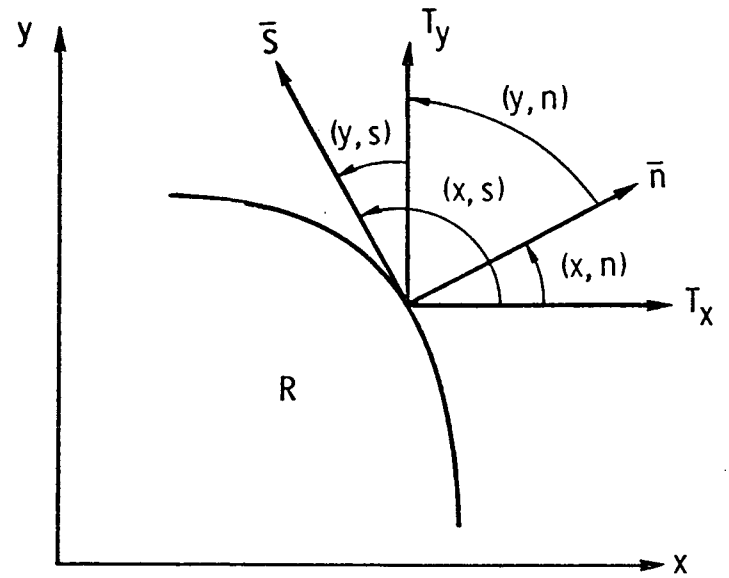

Fig. 71. Coordinate system describing directional cosines and boundary tractions.

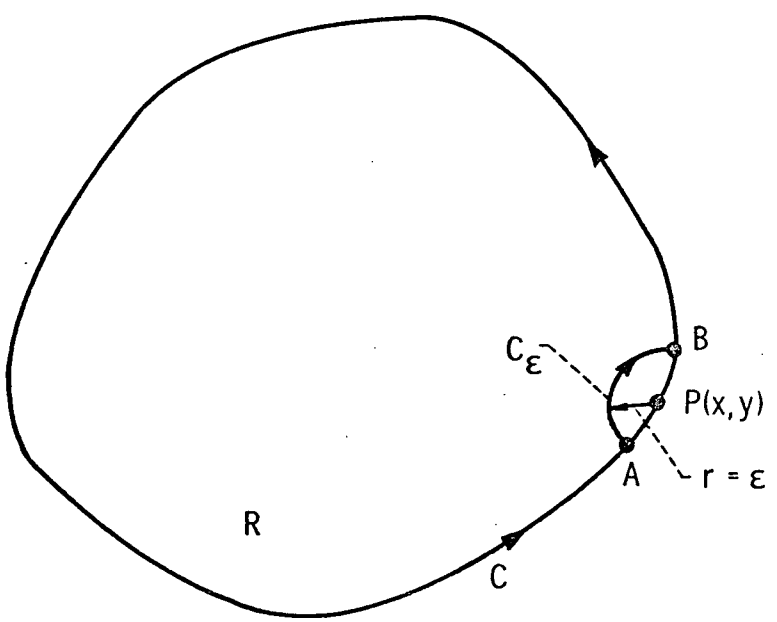

Fig. 72. Boundary contour excluding singular point $P(x,y) \subset C$.

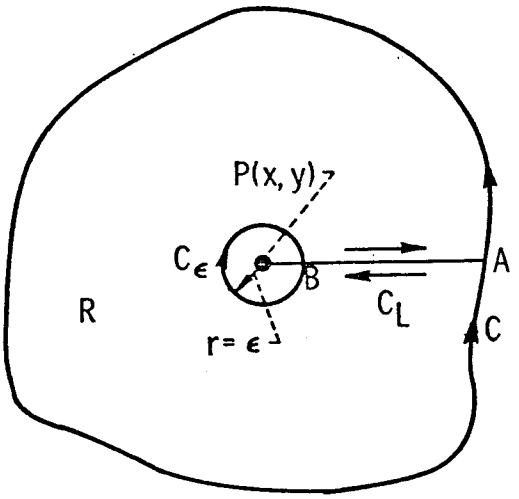

Fig. 73. Boundary contour excluding singular point $P(x,y) \subset R$.

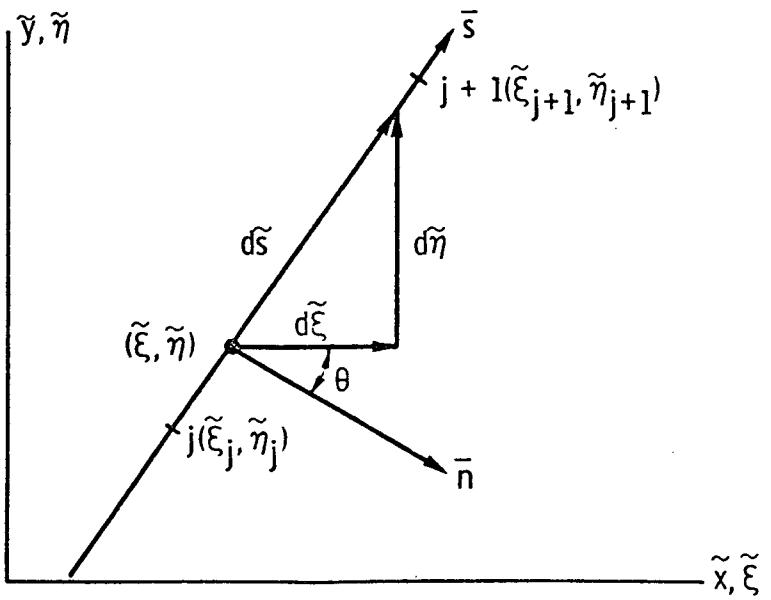

Fig. 74. Straight line boundary intervals.

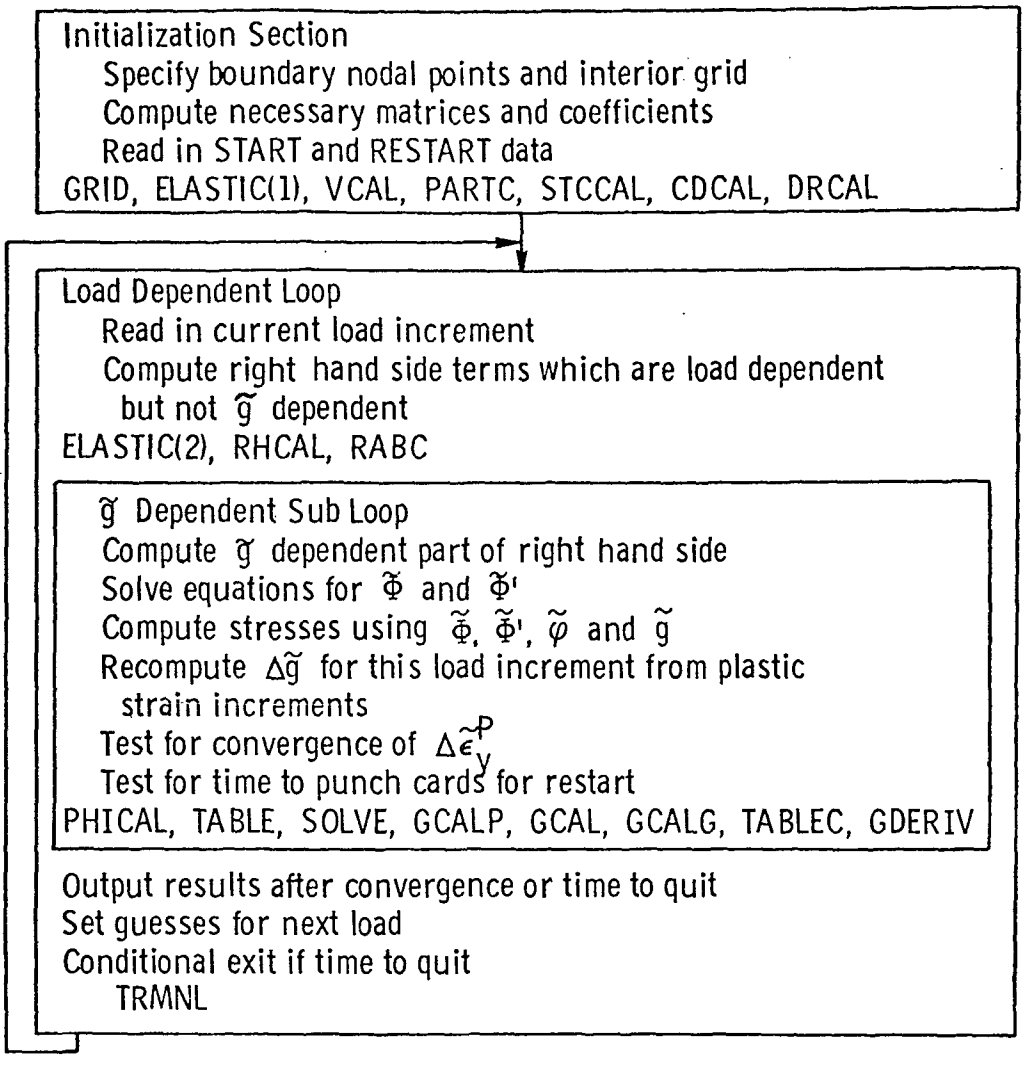

Fig. 75. Schematic representation of the computer program.